Exploring the activity of an inhibitory neurosteroid at $GABA_A$ receptors

Sandra Seljeset

A thesis submitted to University College London for the Degree of Doctor of Philosophy

November 2016

Department of Neuroscience, Physiology and Pharmacology

University College London

Gower Street

WC1E 6BT

Declaration

I, Sandra Seljeset, confirm that the work presented in this thesis is my own. Where information has been derived from other sources, I can confirm that this has been indicated in the thesis.

Abstract

The $GABA_A$ receptor is the main mediator of inhibitory neurotransmission in the central nervous system. Its activity is regulated by various endogenous molecules that act either by directly modulating the receptor or by affecting the presynaptic release of GABA. Neurosteroids are an important class of endogenous modulators, and can either potentiate or inhibit $GABA_A$ receptor function. Whereas the binding site and physiological roles of the potentiating neurosteroids are well characterised, less is known about the role of inhibitory neurosteroids in modulating $GABA_A$ receptors.

Using hippocampal cultures and recombinant $GABA_A$ receptors expressed in HEK cells, the binding and functional profile of the inhibitory neurosteroid pregnenolone sulphate (PS) were studied using whole-cell patch-clamp recordings.

In HEK cells, PS inhibited steady-state GABA currents more than peak currents. Receptor subtype selectivity was minimal, except that the ρ1 receptor was largely insensitive. PS showed state-dependence but little voltage-sensitivity and did not compete with the open-channel blocker picrotoxinin for binding, suggesting that the channel pore is an unlikely binding site. By using ρ1-α1/β2/γ2L receptor chimeras and point mutations, the binding site for PS was probed. All chimeras and mutants remained sensitive to PS, raising the question as to whether modulation could be due to indirect interactions between PS and the cell membrane. In hippocampal neurones, the major postsynaptic effect of PS was to increase the IPSC decay rate. However, PS also increased GABA release by activating presynaptic TRPM3 receptors. Upon block of TRPM3, GABA release was reduced by PS due to potentiation of presynaptic Kir2 channel activity.

In conclusion, PS directly modulates $GABA_A$ receptor kinetics by speeding up current decay at both neuronal and recombinant receptors. At inhibitory synapses, PS can enhance or inhibit GABA release by acting at TRPM3 or Kir2 channels respectively.

Acknowledgements

Firstly, I would like to thank my supervisor and mentor, Prof. Trevor Smart, whose enduring support and positivity have helped me complete this PhD. I would also like to thank the Wellcome Trust for providing the financial support to complete this project.

Many thanks goes to all the members of the Smart lab, past and present, for being a great source of support and entertainment for which I will always be grateful. I would especially like to thank Mike and Duncan for their help with the molecular biology work, and Phil for always being of assistance when my rig or U-tube misbehaved! I am also grateful to Laura for all her help and assistance with the hippocampal cultures. A special thanks goes to Damian for invaluable feedback, guidance and support, and for joining me in those daily tea breaks!

I would also like to thank my lovely friends and family. I will forever be grateful to my trumpet teacher Matt for turning my postgraduate student years into a musical adventure that I will never forget, and the members of UCLU Concert Band and SWON who have been like a family to me, providing a great source of support and fun over the past few years. Finally, the biggest of thanks are owed to my best friends Adam, Hazel, Liam and Sam for their love, encouragement and support, and for always being there for me.

Contents

List of figures

List of tables

List of equations

List of abbreviations

AChBP	Acetylcholine binding protein
Allopregnanolone	5α-pregnan-3α-ol-20-one
AMPA	α-amino-3-hydroxy-5-methyl-4-isoxazolepropionic acid
ANOVA	Analysis of Variance
AP	Action potential
AP2	Clathrin adaptor protein 2
AP5	(2*R*)-amino-5-phosphonovaleric acid
ATP	Adenosine triphosphate
Baclofen	β-(4-chloro-phenyl)-γ-aminobutyric acid
BAPTA-AM	1,2-bis(*o*-aminophenoxy)ethane-*N*,*N*,*N*′,*N*′-tetraacetic acid
BBB	Blood-brain barrier
BD-1063	BD-1063 dihydrochloride; 1-[2-(3,4-Dichlorophenyl)ethyl]-4-methylpiperazine dihydrochloride
BDZ	Benzodiazepine
BIC	Bicuculline
C3	Carbon 3
CA1	C*ornu ammonis* (CA) region1 of the hippocampus
CaMKII	Ca^{2+}/calmodulin-dependent kinase II
Ca_v	Voltage-gated Ca^{2+} channel
cDNA	Complementary deoxyribonucleic acid
C. elegans	*Caenorhabditis elegans*
CFU	Colony forming unit
CNQX	6-cyano-7-nitroquinoxaline-2,3-dione
CNS	Central nervous system
C-terminus	Carboxy-terminus
DBI	diazepam binding inhibitor
DIV	Days *in vitro*
dLGN	Dorsal lateral geniculate nucleus
DHA	Docosahexaenoic acid
DHEA	Dehydroepiandrosterone
DHEAS	Dehydroepiandrosterone sulphate
DMEM	Dulbecco's modified Eagle medium
DMSO	Dimethyl sulfoxide
DNA	Deoxyribonucleic acid
DOPE	Discrete Optimised Protein Energy
DPA	Dipicrylamine
E18	Embryonic day 18
EC_X	The concentration of substance eliciting X% of the maximal response
ECD	Extracellular domain
EDTA	Ethylene-diamine-tetra-acetic acid
EGTA	Ethylene glycol tetra-acetic acid

ELIC	Ligand-gated ion channel from *Erwinia chrysanthemi*
EM	Electron microscopy
Emax	The maximum response of an agonist
EPSCs	Excitatory postsynaptic currents
ER	Endoplasmic reticulum
FCS	Foetal calf serum
GA	General anaesthetic
GABA	γ-aminobutyric acid
$GABA_A$	γ-aminobutyric acid type-A
$GABA_AR$	γ-aminobutyric acid type-A receptor
$GABA_C$	γ-aminobutyric acid type-C
$GABA_BR$	γ-aminobutyric acid type-B receptor
GABARAP	$GABA_A$ receptor-associated protein
GAD65	Glutamic acid decarboxylase 65
γ2L	Long splice variant of the γ2 subunit
γ2S	Short splice variant of the γ2 subunit
GAT-1/2/3	GABA transporter 1, 2 and 3
GLIC	Ligand-gated ion channel from *Gleobacter violaceus*
GluCl	Glutamate-gated chloride channel from *Caenorhabditis elegans*
GlyR	Glycine Receptor
GPCR	G protein-coupled receptor
GTP	Guanosine triphosphate
HAP1	Huntingtin-Associated Protein-1
HBS	HEPES-buffered solution
HBSS	Hank's balanced salt solution
HEK293	Human embryonic kidney 293
HEPES	4-(2-hydroxyethyl)-1-piperazineethanesulfonic acid
3α/β-HSD	3α/β-hydroxysteroid-dehydrogenase
5-HT	5-hydroxytryptamine
$5\text{-}HT_3R$	Type-3 5-hydroxytryptamine receptor
IC_{50}	Concentration of antagonist producing 50% maximal inhibition
IPSCs	Inhibitory post-synaptic currents
I/V	Current-voltage
KCC2	K^+/Cl^- co-transporter 2
KI	Knock-in
KIF5	Kinesin motor protein 5
Kir	Inwardly-rectifying K^+ channel
LTP	Long-term potentiation
M1-M4	Transmembrane helices 1-4
MEM	Minimum essential media
mEPSCs	Miniature excitatory postsynaptic currents
MFA	Mefenamic acid
mIPSCs	Miniature inhibitory postsynaptic currents
ML133	ML133 hydrochloride; *N*-[(4-Methoxyphenyl)methyl]-1-naphthalenemethanamine hydrochloride

mRNA	Messenger ribonucleic acid
nAChR	Nicotinic acetylcholine receptor
Na_v	Voltage-gated Na^+ channel
n_H	Hill coefficient
NKCC1	$Na^+/K^+/Cl^-$ co-transporter 1
N-terminal	Amino-terminal
NMDA	*N*-Methyl-*D*-aspartate
NR1-2	NMDA receptor subunits 1 and 2
OATPs	Organic anion transporting proteins
OST α/β	Organic solute transporter α/β
P3-5	Postnatal day 3-5
P450	Cytochrome P450 enzyme
P450c17	microsomal 17-hydroxylase
P450c21	microsomal 21-hydroxylase
P450scc	Cytochrome P450 mitochondrial cholesterol side-chain cleavage
PB	Pentobarbitone
PBS	Phosphate buffered saline
PCR	Polymerase chain reaction
PDB	Protein data bank
pEGFP-C1	Enhanced green fluorescent protein
PKA, PKB, PKC, PKG	Protein kinase A, B, C and G
pLGICs	Pentameric ligand-gated ion channels
PLIC-1/2	Protein that Links Integrin-associated Protein with the Cytoskeleton-1 and 2
PKA, PKB, PKC, PKG	Protein kinase A, B, C and G
POPC	1-palmitoyl-2-oleoyl-*sn*-glycero-3-phosphocholine
PRIP1/2	Phospholipase-C Related Inactive Protein 1 and 2
PS	Pregnenolone sulphate
P4S	Piperidine-4-sulfonic acid
P/SS ratio	Peak current to steady-state current ratio
PTX	Picrotoxinin
Polyunsaturated fatty acids	PUFAs
RNA	Ribonucleic acid
RDL	Resistance to dieldrin; *Drosophila* ionotropic GABA receptor
RT-PCR	Reverse transcription polymerase chain reaction
SEM	Standard error of the mean
sIPSCs	Spontaneous inhibitory postsynaptic currents
SLC6	Solute carrier 6
SULT2A/B	Sulphotransferase 2A and 2B
TARPs	Transmembrane AMPA receptor regulatory proteins
TBPS	t-butylbicyclophosphorothionate
THDOC	tetrahydro-deoxycorticosterone; 5α-pregnan-3α,21-diol-20-one
TMD	Transmembrane domain
TPB	tetraphenylborate

TRP	Transient receptor potential
TRPM3	Transient receptor potential melastatin 3
TTX	Tetrodotoxin
UNC-49	*Caenorhabditis elegans* GABA receptor
vGAT	Vesicular GABA transporter
WT	Wild-type
ZAC	Zn^{2+}-activated cation channel

Chapter 1: Introduction

This introduction reviews the physiological role, structure, function and distribution of type A γ-aminobutyric acid receptors ($GABA_A$Rs) in the brain, and discusses the roles different types of neurosteroids can have in modulating inhibitory neurotransmission, with an emphasis on the inhibitory neurosteroids.

1.1. $GABA_A$ receptors

γ-aminobutyric acid (GABA) is the major inhibitory neurotransmitter in the brain, and exerts its actions via activation of two different classes of receptor: the pentameric ligand-gated ion channel (pLGIC) known as the $GABA_A$ receptor, and the G protein-coupled $GABA_B$ receptor (Olsen and Sieghart, 2008). The ionotropic $GABA_A$ receptor is the major inhibitory receptor in the central nervous system (CNS), and is a Cl^-- (and HCO_3^--) selective ion channel that generally allows the rapid influx of anions into the cell upon binding of and activation by GABA (Farrant and Kaila, 2007). The metabotropic $GABA_B$ receptor ($GABA_BR$) activates various effector systems depending on which G protein(s) it is coupled to, including inwardly-rectifying K^+ channels, voltage-gated Ca^{2+} channels and adenylate cyclase (Bowery et al., 2002; Bettler et al., 2004). The $GABA_AR$ family forms the main topic of this thesis, and its structural, physiological and pharmacological characteristics will be explored further below.

1.1.1. $GABA_A$ receptor structure and distribution

The $GABA_AR$ is part of the pLGIC family along with other mammalian Cys-loop receptors, including the nicotinic acetylcholine receptors (nAChRs) (Corringer et al., 2000), glycine receptors (GlyRs) (Breitinger and Becker, 2002), type-3 5-hydroxytryptamine receptors ($5\text{-}HT_3R$) (Davies et al., 1999; Thompson and Lummis, 2006) and the Zn^{2+}-activated cation channel (ZAC) (Davies et al., 2003). Cys-loop receptors are so termed because they contain a highly conserved structural motif in the extracellular domain (ECD) – a loop formed by a disulphide bridge (Smart and Paoletti, 2012). Invertebrate receptors activated by glutamate

and serotonin (anionic channels) or GABA (cationic channels) are also Cys-loop receptors, whilst the bacterial homologues, *Gleobacter violaceus* (GLIC) and *Erwinia chrysanthemi* (ELIC), lack the disulphide bridge and are therefore pLGICs but not Cys-loop receptors (Hilf and Dutzler, 2008; Bocquet et al., 2009).

The structure of pLGICs has in the recent years been elucidated by high-resolution structures from X-ray crystallography and electron microscopy of different members of the family. These include structures of the molluscan acetylcholine-binding protein (AChBP) (Brejc et al., 2001), the *Torpedo* nAChR transmembrane domain (TMD) and receptor (Miyazawa et al., 2003; Unwin, 2005), the human nACh α4β2 receptor (Morales-Perez et al., 2016), the *Caenorhabditis elegans* (*C. elegans*) glutamate-activated Cl^- channel α homopentamer (GluClα) (Hibbs and Gouaux, 2011; Althoff et al., 2014), the mouse 5-HT_3R (Hassaine et al., 2014), GLIC (Bocquet et al., 2009; Nury et al., 2011; Sauguet et al., 2014), ELIC (Pan et al., 2012; Ulens et al., 2014) and the human (α3) and zebrafish (α1) GlyRs (Du et al., 2015; Huang et al., 2015). The human $GABA_A$R β3 subunit has also been crystallised as a homomer bound to the agonist benzamidine in a presumably desensitised state (Miller and Aricescu, 2015). In addition to providing information about structure and topology, these crystal structures also provide insight into the molecular mechanisms of receptor activation, closure and desensitisation of the channels. Furthermore, some of these receptors have been co-crystallised with agonists, inhibitors and modulators, revealing the binding sites for these pharmacological agents. Crystal structures are also frequently used to form templates for receptor homology models, as explored in Chapter 4 (Fig. 4.2 and 4.10).

The amino acid sequences of eukaryotic and prokaryotic pLGICs show a sequence homology of about 18-20%, reflecting their phylogenetic distance (Corringer et al., 2012). The pLGICs show a common transmembrane topology, and many residues and motifs are conserved between members, demonstrating their essential roles in structure and function. Within the eukaryotic Cys-loop receptor superfamily, sequence homology can be up to 30%, but the similarity is even greater at the level of secondary and tertiary structures (Olsen and Sieghart, 2008). Each subunit contains a large hydrophilic amino (N)-terminal ECD, a TMD formed of four hydrophobic transmembrane α-helices (M1-M4) with a large

intracellular loop linking the M3 and M4 helices, and a relatively short extracellular carboxy (C)-terminus, as demonstrated for the $GABA_A$ receptor in Figure 1.1. The M2 helix of each subunit lines the channel pore, and the residues of this segment are named with prime numbers so that the residue at the N-terminal end is designated 0', corresponding to arginine 254 in the $GABA_AR$ α1 subunit.

There are 19 genes for $GABA_ARs$ identified in the human genome, including α1-6, β1-3, γ1-3, δ, ε, θ, π and ρ1-3 (the latter formerly known as the $GABA_C$ receptor) (Olsen and Tobin, 1990; Simon et al., 2004; Olsen and Sieghart, 2008). Additionally, some species, including birds, express β4 and γ4, but lack θ and ε subunits. These genes are probably orthologues, with the β4 subunit likely having evolved into the θ subunit in mammals, and the γ4 subunit having evolved into the ε subunit (Simon et al., 2004). Within a family of subunits (*e.g*. α1-6), there is about 70% sequence homology, and between members of different families, 20% sequence homology.

Some $GABA_AR$ subunits are expressed in two forms following alternative splicing, allowing for further subunit diversity (Simon et al., 2004; Olsen and Sieghart, 2008). Notably, the γ2 subunit can exist in a long (γ2L) and short (γ2S) version, the first containing an extra eight amino acid sequence in the M3-M4 intracellular loop with the consensus sequence for phosphorylation by protein kinase C (PKC) (Whiting et al., 1990). Thus, alternative RNA splicing allows for the generation of subunits that are differentially regulated in different types of tissue (Olsen and Sieghart, 2008). Alternative splice variants are also found for the α3-5, β2, ρ1, γ3 and ε subunits, though the functional significance of these variants remains unclear.

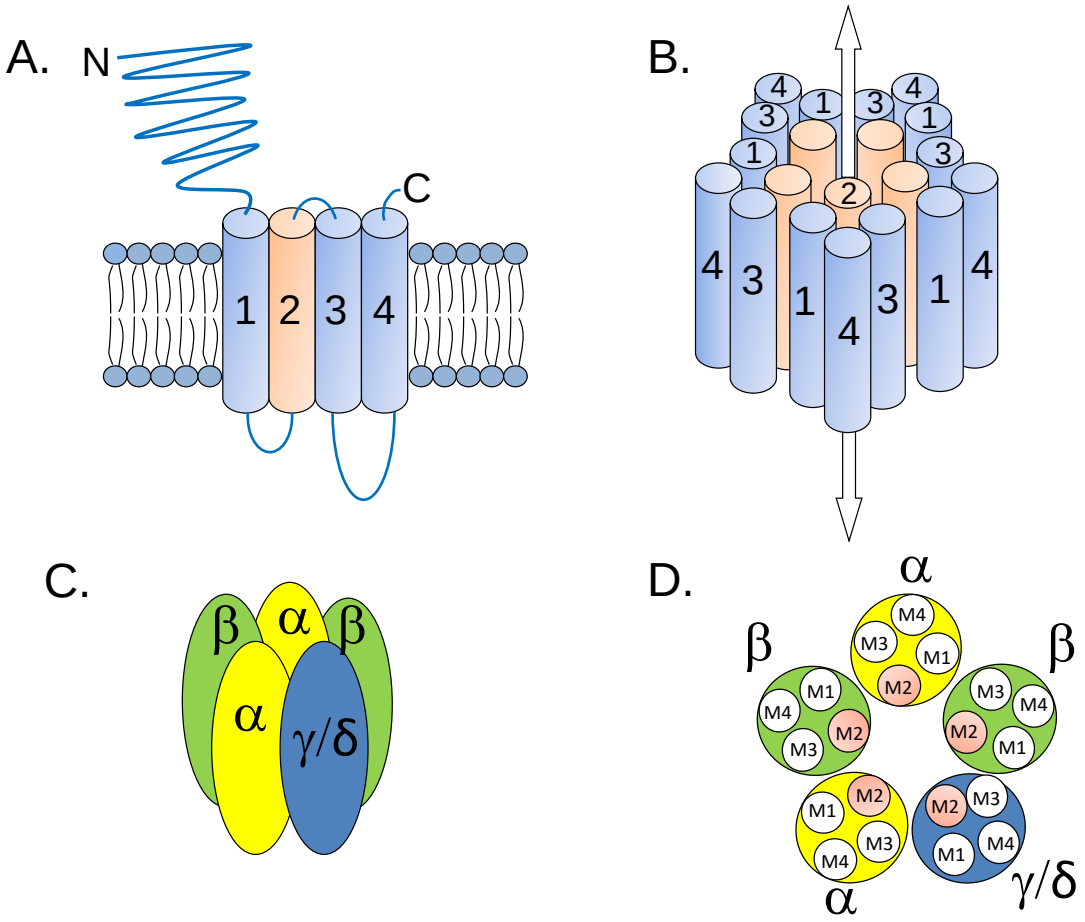

Figure 1.1 – The structure of the GABA$_A$ receptor.

A. The topology of a GABA$_A$R subunit: each GABA$_A$ receptor subunit has a large amino (N)-terminus, four transmembrane helices (M1-M4) forming the TMD, an intracellular M1-M2 linker, extracellular M2-M3 linker, large intracellular loop connecting the M3 and M4 helices and a short carboxy (C)-terminus. **B**. Transmembrane helices are arranged so that M2 lines the channel pore, with the more hydrophobic M1, M3 and M4 helices facing the lipid membrane. The channel can conduct Cl^- and HCO_3^- ions in either direction. **C**. The GABA$_A$ receptor is a pentameric assembly of subunits, the most common stoichiometry and arrangement likely being γ/δαβαβ in the clockwise direction viewed externally above the plane of the membrane. **D**. The arrangement of subunits and transmembrane helices within subunits, showing the M2 segment lining the central channel pore, and the γ/δαβαβ arrangement of the subunits.

Though some $GABA_A$ receptor subunits can express as homomeric functional receptors *in vitro* (*e.g*. β2/3) (Krishek et al., 1996b; Wooltorton et al., 1997), receptors are commonly comprised of more than one type of subunit under physiological conditions. The exception is ρ1-3, which expresses mostly as a homopentamer also *in vivo* (Enz and Cutting, 1999; Greka et al., 2000). The most likely subunit stoichiometry for heteromeric $GABA_A$ receptors is $(\alpha)_2(\beta)_2(\gamma)$, with γ sometimes being replaced with δ, π or ε (Tretter et al., 1997; Olsen and Sieghart, 2008; Fritschy and Panzanelli, 2014; Patel et al., 2014). The existence of receptors containing other subunit stoichiometries, or binary constructs of α and β subunits only, is also likely (Mortensen and Smart, 2006; Wagoner and Czajkowski, 2010; Fritschy et al., 2012; Fritschy and Panzanelli, 2014).

Although the availability of 19 different subunits could potentially allow for a huge diversity in $GABA_A$ receptor subunit combinations, a limited number of native subunit combinations appear to exist in the CNS, presumably as a result of rules for subunit assembly (Fritschy et al., 2012; Fritschy and Panzanelli, 2014). Studies using immunoprecipitation with extracts from specific brain regions, immunohistochemistry, immunocytochemistry and *in situ* hybridisation have shown that there are at least ~36 distinct $GABA_A$ receptor subtypes in CNS neurones. The distribution of subunits varies throughout development, between species, between brain regions and between neuronal compartments (Laurie et al., 1992a, 1992b; Wisden et al., 1992; Pirker et al., 2000; Hörtnagl et al., 2013). The α1-6 subunits largely participate in forming distinct receptor subtypes, each with distinct distribution patterns that only partially overlap with that of other α subunits. The majority of native $GABA_A$ receptors are composed of α1β2γ2 subunits (40-60%), with the other common subunit combinations being α2β2γ2 (15-20%), α4βδ/γ2 (<5%) and α6βδ/γ2 (<5%) (Fritschy and Mohler, 1995; McKernan and Whiting, 1996; Sieghart and Sperk, 2002). There is also evidence from co-immunoprecipitation studies that two α subunits can co-assemble to form a receptor, *e.g*. α1α6β2γ2L in adult rat cerebellum (Pollard et al., 1995) (Reviewed in Sieghart and Sperk 2002). The β2 and β3 subunits largely overlap with the α1 and α2 subunits, whereas the β1 subunit is expressed at much lower levels, but in multiple brain regions (Fritschy and Mohler, 1995; Hörtnagl et al., 2013). The γ2 subunit also has an almost ubiquitous expression pattern, and can

co-assemble with the vast majority of $GABA_AR$ subtypes (Fritschy et al., 2012; Fritschy and Panzanelli, 2014). Receptors in which the γ2 subunit is replaced by γ1, γ3, δ, or indeed π or ε, are less common (Sieghart and Sperk, 2002; Farrant and Nusser, 2005). The π and θ subunits may co-assemble with αβγ receptors to form receptors containing subunits from four families (Bonnert et al., 1999; Neelands and Macdonald, 1999).

The subunit combination of $GABA_ARs$ largely dictates their regional and subcellular distribution. Immunofluorescence and electron microscopy (EM) using immunogold embedding methods have shown that αxβxγ2L receptors are enriched in the postsynaptic membrane of GABA-containing synapses in many brain regions, including the cerebellum, globus pallidus, hippocampus and neocortex (Craig et al., 1994; Nusser et al., 1995, 1999; Farrant and Nusser, 2005). However, no receptors have been shown to have an exclusively synaptic location. Even the α1β2/3γ2L receptor, which is highly enriched at synapses, has a higher number outside than inside the synapse (Nusser et al., 1995).

In contrast, some receptors do not appear to accumulate at the synapse (Fig. 1.2). For instance, δ-containing receptors have been shown to exclusively exist in the extrasynaptic somatic and dendritic membranes of cerebellar granule cells (Nusser et al., 1998), and at extrasynaptic and perisynaptic sites in hippocampal CA1 pyramidal neurones and dentate gyrus granule cells (Wei et al., 2003; Scimemi et al., 2005). The δ subunit forms receptors with α6 and β2/3 in the cerebellum, and with α4 and βx in different forebrain structures, including the thalamus, neostriatum, CA1 and dentate gyrus of the hippocampus (Wei et al., 2003; Scimemi et al., 2005; Hörtnagl et al., 2013; Fritschy and Panzanelli, 2014).

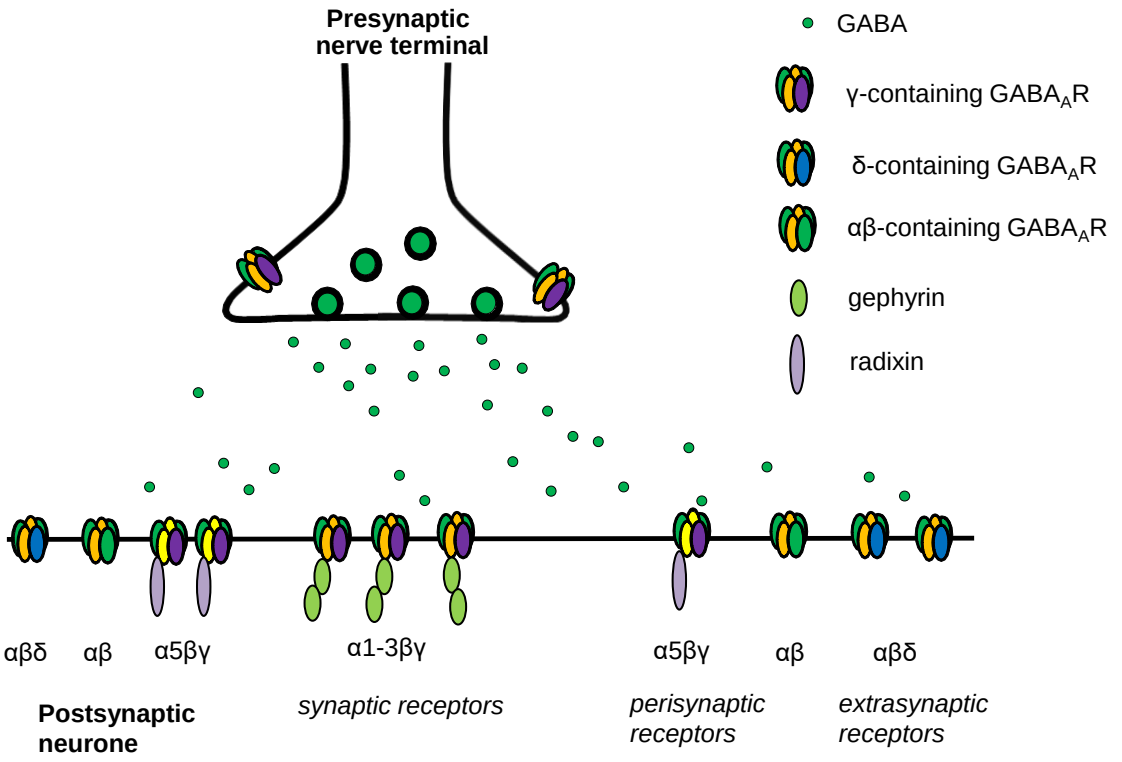

Figure 1.2 – Synaptic and extrasynaptic locations of GABA$_A$ receptors.

When GABA-containing synaptic vesicles fuse with the presynaptic membrane of a nerve terminal, GABA is released into the synaptic cleft. Synaptic receptors (α1-3βγ) experience the highest concentration of GABA (~1-3 mM) and are activated immediately following release to produce phasic currents. These receptors cluster at the postsynaptic density due to interactions with gephyrin (Luscher et al., 2011; Mukherjee et al., 2011). Peri- (α5βγ) and extrasynaptic (αβδ) receptors are exposed to a lower concentration of GABA (~100 nM), and produce a smaller and more persistent tonic current. α5-containing receptors cluster outside the synapse by interacting with phosphorylated radixin (Hausrat et al., 2015). When radixin is dephosphorylated, the α5-containing receptors can translocate to the postsynaptic density and contribute to synaptic currents.

Although the γ2 subunit targets GABA$_A$Rs to the postsynaptic density where the receptor is clustered and stabilised by the GABA$_A$R-associated protein gephyrin (Tyagarajan and Fritschy, 2014), α5β3γ2L receptors are predominantly found in peri- and extrasynaptic locations in hippocampal pyramidal neurones, showing that the α5 subunit can override the tendency of γ2 to promote synaptic clustering (Brünig et al., 2002; Glykys et al., 2008). Gephyrin interacts directly with the α1-3 subunits rather than the γ2 subunit (Mukherjee et al., 2011), which may in part explain why α5-containing receptors can cluster outside the synapse. Peri- and extrasynaptic clustering of α5-containing receptors is regulated by radixin, a

protein that interacts with the actin cytoskeleton (Luscher et al., 2011). In its phosphorylated state, radixin clusters these receptors in the extrasynaptic membrane, but if radixin is dephosphorylated, α5-containing receptors translocate to the postsynaptic density where they can contribute to synaptic currents (Hausrat et al., 2015). Furthermore, α3-containing receptors can also exist both synaptically and extrasynaptically (Brünig et al., 2002). α2-containing receptors are selectively enriched at the axon initial segment of hippocampal pyramidal neurones (Nusser et al., 1996; Panzanelli et al., 2011), but the composition of $GABA_A$Rs at the axon initial segment is likely to differ between brain regions (Gao and Heldt, 2016). In conclusion, receptors containing the γ2 subunit co-assembled with α1-3 and β2/3 predominantly exist at inhibitory synapses and mediate phasic inhibition, whereas receptors containing the α4-6 subunits (α4βxδ, α5βxγ2, α6βxδ) are predominantly or exclusively peri- and extrasynaptic, mediating tonic inhibition. Phasic and tonic modes of inhibition are further discussed in section 1.1.3.

$GABA_A$Rs also exist in the presynaptic membrane on distal axons and terminals, and play a role in regulating neuronal synchronisation and mediation of presynaptic afferent depolarisation (Fritschy and Panzanelli, 2014), and in regulating neurotransmitter release in some cell types (Bowery and Smart, 2006). These receptors are hardly detectable by immunohistochemistry, and the subunit composition of these is therefore not fully characterised (Kullmann et al., 2005).

1.1.2. Assembly and trafficking of $GABA_A$ receptors

The assembly of $GABA_A$Rs occurs in the endoplasmic reticulum (ER), and the specificity of this process limits the number of subunit combinations that become available in the plasma membrane (Luscher et al., 2011). This process is regulated by residues in the N-terminal domain in each subunit, and is aided by ER-associated chaperones such as calnexin. Regulating the cell surface expression of $GABA_A$Rs is a complex and important process that ultimately determines cell surface receptor numbers and regulates the efficacy of GABAergic neurotransmission. This process depends on the interaction of α and β subunits with PLIC-1 (protein that links integrin-associated protein with the

cytoskeleton-1) and PLIC-2, proteins that interfere with ubiquitination of substrates at the ER and prevent ER-associated degradation of subunits, leading to enhanced cell surface expression (Bedford et al., 2001). Other proteins that facilitate the delivery of $GABA_AR$s to the plasma membrane include the HAP1/KIF5 (huntingtin-associated protein-1/kinesin motor protein 5) complex and GABARAP ($GABA_AR$-associated protein). The KIF5/HAP1 complex is believed to be important for the fast delivery of $GABA_AR$s to synapses (Twelvetrees et al., 2010), along with GABARAP which also appears to promote the transport of $GABA_AR$s to the cell surface (Kittler et al., 2001; Leil et al., 2004).

The level of $GABA_AR$ surface expression is also regulated by clathrin-mediated endocytosis and receptor recycling, and the dynamics of these processes underlie both physiological and pathological adaptations of neuronal excitability (Luscher et al., 2011; Vithlani et al., 2011). The process of endocytosis is complex, and involves various adaptor proteins, *e.g*. clathrin adaptor protein AP2, with interacts directly with $GABA_AR$ β and γ subunits. This interaction is further regulated by phosphorylation of the subunits by various kinases, including Akt, protein kinase A (PKA) and PKC. Thus, various physiological processes can regulate $GABA_AR$ endocytosis and expression levels by activating kinases via G protein-coupled receptor (GPCR)- or receptor tyrosine kinase-mediated signalling.

Whether receptors get recycled or degraded following endocytosis, is, along with an array of other signalling molecules, regulated by interaction of the β subunit with HAP1, which interferes with the degradation of endocytosed $GABA_AR$s, thereby increasing recycling (reviewed in Luscher et al. 2011 and Vithlani et al. 2011). As endocytosis and exocytosis do not form part of this project, this will not be discussed any further here.

It is generally believed that $GABA_AR$s can only be removed from or inserted into the membrane at extrasynaptic sites, making lateral mobility of receptors essential for recruitment to the postsynaptic density (Thomas et al., 2005; Bogdanov et al., 2006). This allows receptors to move into and away from the synapse, and partly explains why a larger number of receptors that tend to cluster at the synapse (α1-3βxγ2) can exist outside than in the postsynaptic density. The

distribution of $GABA_A$Rs at synaptic and extrasynaptic locations depends on both the subunit composition of the receptor, and the interaction of subunits with the postsynaptic scaffold, including gephyrin and radixin (Luscher et al., 2011; Mukherjee et al., 2011; Tyagarajan and Fritschy, 2014; Hausrat et al., 2015).

1.1.3. Tonic and phasic inhibition mediated by $GABA_A$ receptors

As already discussed, the subunit composition of $GABA_A$Rs determines their localisation within a neurone, as well as between regions of the brain. Receptors that cluster in the postsynaptic density (α1-3βγ) take part in meditating a fast and transient form of inhibitory transmission known as phasic inhibition, and manifest as inhibitory postsynaptic currents (IPSCs). In contrast, receptors residing in the peri- and extrasynaptic membrane (α4βδ, α5βγ and α6βδ) mediate a less intense but more persistent form of tonic inhibition (Farrant and Nusser, 2005). Thus, $GABA_A$Rs can generate two spatially and functionally distinct modes of neuronal inhibition.

Receptors that typically mediate phasic currents have different biophysical properties compared to those involved in mediating tonic currents. In recombinant systems, changing the α subunit in an αβγ complex has the largest influence on the potency of GABA at the receptor, with α6 conferring the highest sensitivity to GABA and α3 conferring the lowest (Farrant and Nusser, 2005). Overall, the extrasynaptic-type receptors α6βδ and α4βδ have the lowest EC_{50} for GABA (~0.5 μM), whereas the α1-3βγ subtypes have EC_{50}s that are an order of magnitude higher. Thus, the receptors residing in the peri- and extrasynaptic space are better suited to respond to the lower concentrations of ambient GABA that can be experienced outside the synapse.

Receptors located in the postsynaptic density activate in response to action potential (AP)-induced and spontaneous quantal GABA release. Upon the arrival of an AP, the inflow of Ca^{2+} in the presynaptic membrane causes the membrane fusion of synaptic vesicles and release of tens of thousands of GABA molecules into the synaptic cleft, generating a peak GABA concentration in the millimolar range (Mody et al., 1994). Opposite the release site, a small number of receptors

(between ~10 and a few hundred) are located in the postsynaptic density (Edwards et al., 1990; Nusser et al., 1997). At a small synapse, the receptors will experience saturation upon neurotransmitter release even when only one vesicle of GABA is released. Hence, the amplitudes of IPSCs are more dependent on the number of receptors present for activation than the amount of GABA released following an AP. Whilst multiple vesicles are released in response to an AP to generate a spontaneous IPSC (sIPSC), single vesicles can be released spontaneously, generating a miniature IPSC (mIPSC). These are rapid GABA-mediated currents with a rise time of a few hundred microseconds, demonstrating the proximity of the postsynaptic receptors to the site of vesicle release (Farrant and Nusser, 2005). The response of a synapse to the release of a neurotransmitter from a single vesicle is termed quantal size, whereas quantal content is the number of vesicles released in response to an action potential (Del Castillo and Katz, 1954; Augustine and Kasai, 2007).

Although the high synaptic concentration of GABA following vesicle release rapidly drops due to diffusion, the most effective removal of GABA occurs through the uptake by active transporters into neurones and astrocytes (Glykys and Mody, 2007a). These transporters belong to the SLC6 family, and are high-affinity Na^+/Cl^--dependent membrane translocators of GABA, and an array of other amino acids (Chen et al., 2004). Three members of the family are GABA transporters (GATs): GAT-1 (SLC6A1), GAT-2 (SLC6A13) and GAT-3 (SLC6A11). Of these, GAT-1 is the most prevalent, and has a high density on the surface of neurones (Glykys and Mody, 2007a). Consequently, a large fraction of the released GABA will bind to a transporter, leading to its rapid removal from the synaptic cleft. The GAT transporters are also important regulators of the tonic conductance, being a highly effective regulator of ambient GABA concentrations.

Following repeated AP firing or simultaneous activation of multiple synapses, the large increase in GABA release can lead to its diffusion to adjacent perisynaptic and extrasynaptic receptors, or to receptors at neighbouring synapses (Barbour and Häusser, 1997; Kullmann, 2000; Farrant and Nusser, 2005). This is known as neurotransmitter ‘spillover’, and can be considered as a ‘phasic event’, as the increased GABA concentration is temporally related to synaptic release. This process leads to cross-talk between synapses, and can also lead to an increase

in the ambient concentration of GABA, which contributes to generating a tonic GABA current.

As GAT transporters are highly effective at removing GABA from the extracellular space following synaptic release (Chen et al., 2004), one might ask how a high enough concentration of GABA can be present for peri- and extrasynaptic receptors to generate a tonic current. Extracellular GABA concentrations have been estimated to be in the range of 100 nM - 2 μM (Lerma et al., 1986; Tossman et al., 1986). The source of extracellular GABA is uncertain, but could be due to spillover as described above, or it could be due to reversal of GATs. It has been shown that enhancing vesicular GABA release in hippocampal neurones in a slice preparation leads to an increase in both synaptic and tonic currents (Glykys and Mody, 2007b). Conversely, reducing GABA release by blocking APs or the vesicular GABA transporter (vGAT), leads to a decrease in phasic and tonic currents. Similarly, the tonic conductance of δ-containing $GABA_AR$s in thalamic relay neurons of the dorsal lateral geniculate nucleus (dLGN) is dependent on synaptic release of GABA, as blocking APs with tetrodotoxin or increasing the GABA release probability by elevating the extracellular concentration of Ca^{2+} led to a decrease or an increase in tonic conductance, respectively (Bright et al., 2007). Tonic GABA conductance in cerebellar granule cells also correlates with phasic $GABA_AR$ activity, and appears to result from GABA spillover (Brickley et al., 1996).

GABA release from astrocytes may also contribute to the ambient levels of the neurotransmitter: embryonic hippocampal neurones co-cultured with astrocytes exhibited a tonic $GABA_AR$ conductance that was absent in neurones cultured without astrocytes (Liu et al., 2000), and astrocytes have also been shown to release GABA in the rat olfactory bulb (Kozlov et al., 2006). Furthermore, there are conditions in which GABA transporters may reverse to cause release instead of uptake of extracellular GABA (Richerson and Wu, 2003). The reversal potential of GABA transporters is close to the resting potential of neurones under normal conditions, and the extracellular concentration of GABA is sufficiently high when the GABA transporter is at equilibrium to tonically activate high-affinity extrasynaptic $GABA_A$ receptors. As the transporter is driven by the electrochemical gradients of Na^+ and Cl^-, the direction of GABA transport will

depend on the membrane potential of the neurone. Therefore, as long as the membrane potential is more negative than the reversal potential, the transporter will operate in the inward direction and cells will take up GABA, and if the membrane potential is more positive than the reversal potential, the transporter will reverse and release GABA. Consequently, this can lead to an increased ambient GABA concentration, and an enhanced tonic conductance of peri- and extrasynaptic receptors. In cultured hippocampal neurones, GABAergic transmission has been shown to still occur when vesicular GABA release is blocked. This transmission was prevented when GAT-1 was blocked with tiagabine, and enhanced by agents that increased cytosolic GABA or Na^+, which would increase GAT-1 reversal (Wu et al., 2007). Thus, reversal of GAT-1 can lead to increased extracellular levels of GABA sufficient to activate high-affinity extrasynaptic $GABA_A$Rs.

Although the $GABA_A$Rs mostly mediate inhibitory signal transduction, this is not always the case (Fig. 1.3). The functional outcome of $GABA_A$R activation largely depends on the electrochemical gradient of Cl^- across the plasma membrane, as the receptor is about 5-fold more permeable to Cl^- than HCO_3^- (Bormann et al., 1987; Kaila, 1994). In most mature neurones, high expression of the K^+/Cl^- co-transporter 2 (KCC2) leads to extrusion of Cl^- to produce a Cl^- equilibrium potential (E_{Cl}) that is usually more negative than the resting membrane potential of the cell (Farrant and Kaila, 2007; Ben-Ari et al., 2012). Upon activation, the $GABA_A$Rs consequently produce a net influx of Cl^- ions, leading to membrane hyperpolarisation away from AP threshold. However, high expression of the $Na^+/K^+/Cl^-$ co-transporter (NKCC1) can, under some conditions, cause greater influx of Cl^-, leading to the generation of a depolarising Cl^- electrochemical gradient. When activated, the $GABA_A$Rs allow net Cl^- flux out of the cell, leading to membrane depolarisation. This occurs in most immature neurones, as well as in some mature neurones, *e.g*. cerebellar interneurones (Chavas and Marty, 2003; Ben-Ari et al., 2012).

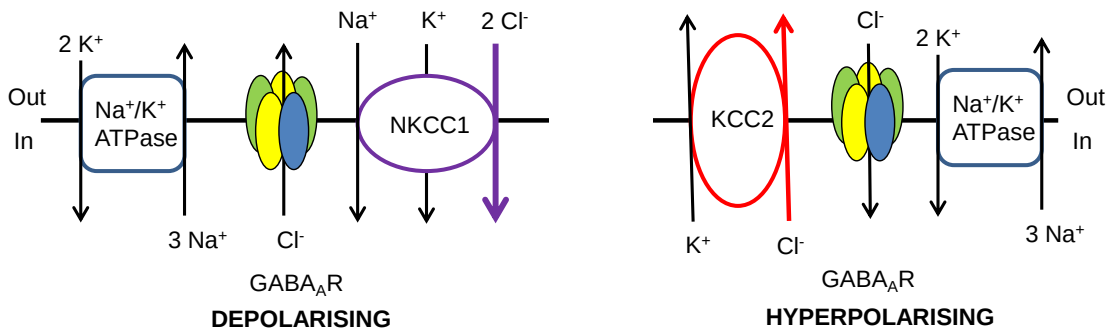

Figure 1.3 – The electrochemical gradient for Cl^- determines the direction of Cl^- flux through the channel pore of $GABA_A$ receptors.

In neurones expressing high levels of NKCC1 (*e.g*. immature neurones), the Cl^- equilibrium potential is positive to the resting membrane potential. Upon activation, $GABA_A$Rs will therefore allow a net Cl^- flux out of the cell and have a depolarising effect (left). In most mature neurones, NKCC1 is downregulated and KCC2 upregulated, resulting in a Cl^- equilibrium potential that is negative relative to the resting membrane potential. Consequently, activated $GABA_A$Rs will pass Cl^- into the cell resulting in hyperpolarisation of the neurone (right).

Extrasynaptic-type receptors can mediate a form for inhibition known as shunting inhibition (Farrant and Nusser, 2005). Tonically active $GABA_A$Rs increase the neurone's input conductance, and affect the magnitude and duration of the voltage response to an injected current, increasing the decrement of voltage with distance. The size and duration of excitatory postsynaptic potentials are therefore reduced by tonic GABA currents, and the temporal and spatial window over which signal integration can occur is consequently narrowed, reducing the likelihood of AP firing. Notably, tonically active $GABA_A$Rs can, even when the Cl^- gradient is depolarising, cause an increase in the membrane conductance giving rise to shunting of excitatory potentials, depending on the level of the tonic current conductance (Pavlov et al., 2014).

1.1.4. $GABA_A$ receptor pharmacology and modulation by endogenous ligands

The availability of 19 $GABA_AR$ subunits allows for the assembly of receptor subtypes with distinct biophysical and pharmacological profiles (Smart, 2015). This diversity in functional properties among different members of the $GABA_AR$ family is important for generating different physiological responses in different parts of the brain, cell types and between compartments of a neurone. Furthermore, different receptor subtypes are regulated by distinct endogenous modulators, including kinases, divalent cations and signalling molecules. This receptor diversity also allows for the targeting of specific receptor subtypes by pharmacological agents, and has implications for the use of drugs in research, health and disease.

All $GABA_ARs$ made up of αβγ/δ have a main conductance state of ~25-28 pS, though lower conductance states do also exist (Farrant and Nusser, 2005; Mortensen et al., 2010). Differences in the magnitude of the macroscopic response to GABA do, however, exist. GABA has a high affinity for δ-containing receptors, but its efficacy is lower than at the γ-containing receptors, meaning that it acts as a partial agonist at extrasynaptic δ-containing receptors (Brown et al., 2002; Mortensen et al., 2010). Consequently, δ-containing extrasynaptic receptors are capable of generating a low level of tonic inhibition at concentrations of GABA below those that would evoke IPSCs at synaptic receptors.

$GABA_ARs$ are modulated by various post-translational modifications that affect receptor function, number and localisation. Several phosphorylation sites have been identified in the M3-M4 intracellular loop of the α4, β1-3 and γ2 subunits (Kittler and Moss, 2003; Abramian et al., 2010; Luscher et al., 2011; Vithlani et al., 2011). Phosphorylation at these sites can differentially regulate the biophysical properties, pharmacology and trafficking of $GABA_ARs$. Various serine-threonine kinases (*e.g*. PKA and PKC) and tyrosine kinases (*e.g*. Src) can phosphorylate $GABA_ARs$ at specific residues (Moss and Smart, 1996). For instance, recombinant $GABA_ARs$ containing the β1 subunit are negatively modulated by phosphorylation of β1 serine residue 409 by PKA, whereas

phosphorylation of serines 408 and 409 in β3 potentiates GABA responses in HEK cells (McDonald et al., 1998). Similarly, Ca^{2+}/calmodulin-dependent kinase II (CaMKII) induces potentiation of α1β3 or α1β3γ2 $GABA_A$Rs expressed in a neuroblastoma (NG108-15) cell line, though this effect is not observed in HEK cells, suggesting post-translational modifications can be cell type specific (Houston and Smart, 2006; Houston et al., 2009).

Furthermore, phosphorylation can affect the modulation of the $GABA_A$R by other compounds. A good example of this is modulation by the endogenous potentiating neurosteroid tetrahydro-deoxycorticosterone (THDOC): enhancing the activity of PKC, and thus phosphorylation of $\beta3^{S408/S409}$, increases potentiation of synaptic-type α1β3γ2L receptors and extrasynaptic-type α4β3δ receptors in HEK cells, whereas inhibition of PKC activity reduced the level of potentiation by THDOC (Adams et al., 2015). This demonstrates how GABAergic inhibitory transmission can be fine-tuned by the interaction of two endogenous neuromodulators. Conversely, phosphorylation by PKC of $\beta2^{S410}$ in extrasynaptic δ-containing $GABA_A$Rs in dentate gyrus granule cells in the hippocampus and dorsal lateral geniculate relay neurons in the thalamus, downregulates tonic inhibition in these parts of the brain, likely by downregulating receptor surface expression (Bright and Smart, 2013). This shows how the effect of phosphorylation can be cell type- and context-specific, generating diverse responses under different conditions. In addition to modulating receptor activation, phosphorylation can also increase, reduce or stabilise receptor cell surface expression (Wang et al., 2003; Kittler et al., 2005).

Phosphorylation of $GABA_A$Rs by protein kinases is an example of endogenous modulation via post-translational modification of the receptors. Other modulators include the endogenous neurosteroids (Baulieu and Robel, 1990), which will be discussed in section 1.2., and endocannabinoids (Sigel et al., 2011). These agents interact directly with the $GABA_A$Rs to modulate their activity, as do a variety of other pharmacologically and clinically important drugs, including benzodiazepines, barbiturates, general anaesthetics and convulsants (Sieghart, 2015). All of these compounds allosterically modulate the $GABA_A$Rs via mostly distinct binding sites, resulting in a highly complex pharmacology for these receptors.

The $GABA_AR$ has two binding sites for GABA, located at the extracellular β^+-α^- interfaces (as indicated in Fig. 1.4) (Sigel et al., 1992; Smith and Olsen, 1994, 1995). Here, the (+)-side refers to the principal subunit (β), and the (-)-side refers to the complementary subunit (α). The benzodiazepine (BDZ) binding site is located at the extracellular α^+-γ^- interface (Pritchett et al., 1989; Sigel and Buhr, 1997; Sigel, 2002), although there is also some evidence that a BDZ binding site can exist in the α1-α1 interface of recombinant binary α1β3 receptors (assuming a subunit stoichiometry of $(\alpha1)_3(\beta3)_2$ (Che Has et al., 2016). BDZ-like anxiolytic compounds (*e.g*. pyrazoloquinoline 2-p-methoxyphenylpyrazolo [4,3–*c*] quinolin-3(5H)-one) may also bind at the $\alpha1^+$-$\beta3^-$ interface, a site that is homologous to the BDZ binding site at $\alpha1^+$-γ^- interface (Ramerstorfer et al., 2011). BDZs are the most described class of pharmacological agents acting at the $GABA_ARs$, and can exist as 'agonists', 'antagonists' and inverse agonists (Rudolph and Knoflach, 2011). In this case, 'agonist' refers to BDZs with positive allosteric modulatory activity at $GABA_AR$, *i.e.* positive allosteric modulators (*e.g*. diazepam and flunitrazepam), whereas 'antagonist' (*e.g*., flumazenil) refers to BDZs that have no effect when applied on their own, but can block potentiation by positive allosteric modulators and inverse agonists (Fig. 1.5). These modulators are known as neutral allosteric ligands. Inverse agonists are proconvulsant and anxiogenic compounds that can reduce the channel opening frequency of $GABA_ARs$ (*e.g*. methyl-β-carboline-3-carboxylate), and are also known as negative allosteric modulators. BDZ agonists represent the most widely prescribed class of drugs for the treatment of anxiety and insomnia disorders, and are used to treat seizures in epilepsy.

BDZs are selective for receptors incorporating the α1, α2, α3 and α5 subunits, and selectively abolishing diazepam binding from these subunits by introducing a histidine-to-arginine point mutation ($\alpha1^{H101R}$, $\alpha2^{H101R}$, $\alpha3^{H126R}$ or $\alpha5^{H105R}$) has contributed to elucidating the functions of individual $GABA_AR$ subtypes (Wieland et al., 1992; Rudolph and Knoflach, 2011). In α1 H101R knock-in (KI) mice, the sedative and anterograde amnesic actions of diazepam were absent and the anticonvulsant action reduced, whilst its anxiolytic actions were still present (Rudolph et al., 1999; McKernan et al., 2000). In α2 H101R KI mice, the anxiolytic action of diazepam was absent and the myorelaxant action was reduced, whilst

the sedative effect was still present (Löw et al., 2000; Crestani et al., 2001). For α3 H126R and α5 H105R KI mice, the animals still experienced the sedative and anxiolytic actions of diazepam, whereas the myorelaxant effect was reduced (Löw et al., 2000; Crestani et al., 2001, 2002). Taken together, these results show that the sedative, amnesic and some of the anticonvulsant actions of diazepam are mediated by α1-containing $GABA_AR$s, whilst the anxiolytic, and to a large extent, the myorelaxant actions are mediated by α2-containing receptors. The myorelaxant effect is also partly mediated by α3- and α5-containing receptors. Furthermore, the development of tolerance to the sedative effect of BDZs has been linked to α5-containing receptors (van Rijnsoever et al., 2004), whilst their addictive properties have been linked to α1-containing receptors (Tan et al., 2010). α5 H105R KI mice also show improved trace fear conditioning, *i.e*. associative learning (Crestani et al., 2002; Yee et al., 2004), and α5-containing receptors may therefore be a target for memory-enhancing drugs, including selective BDZ inverse agonists (Rudolph and Knoflach, 2011).

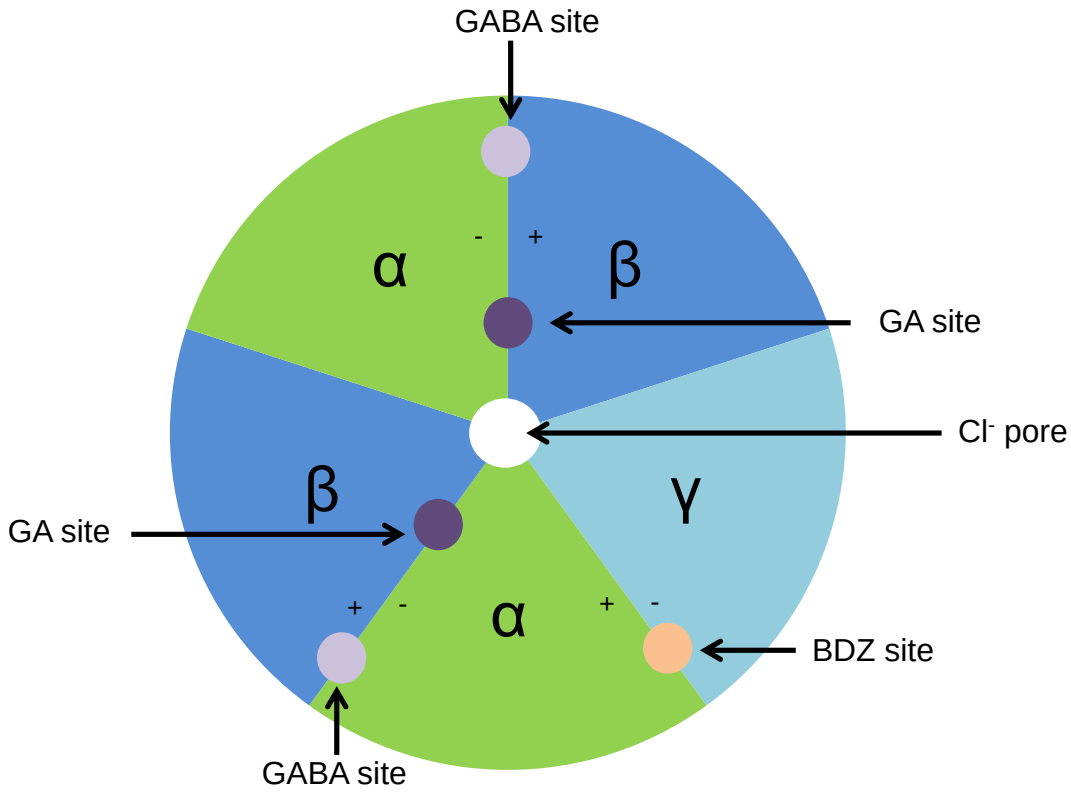

Fig. 1.4 – Interfacial binding sites for GABA, general anaesthetics and benzodiazepines at the $GABA_A$ receptor.

The orthosteric binding site for GABA is located in the ECD at the β^+-α^- subunit interfaces, and there are two sites in a heteromeric αβγ/δ receptor. GAs bind at the same interface, but in the TMD, located below the GABA binding sites. BDZs bind at the α^+-γ^- subunit interface, also in the ECD.

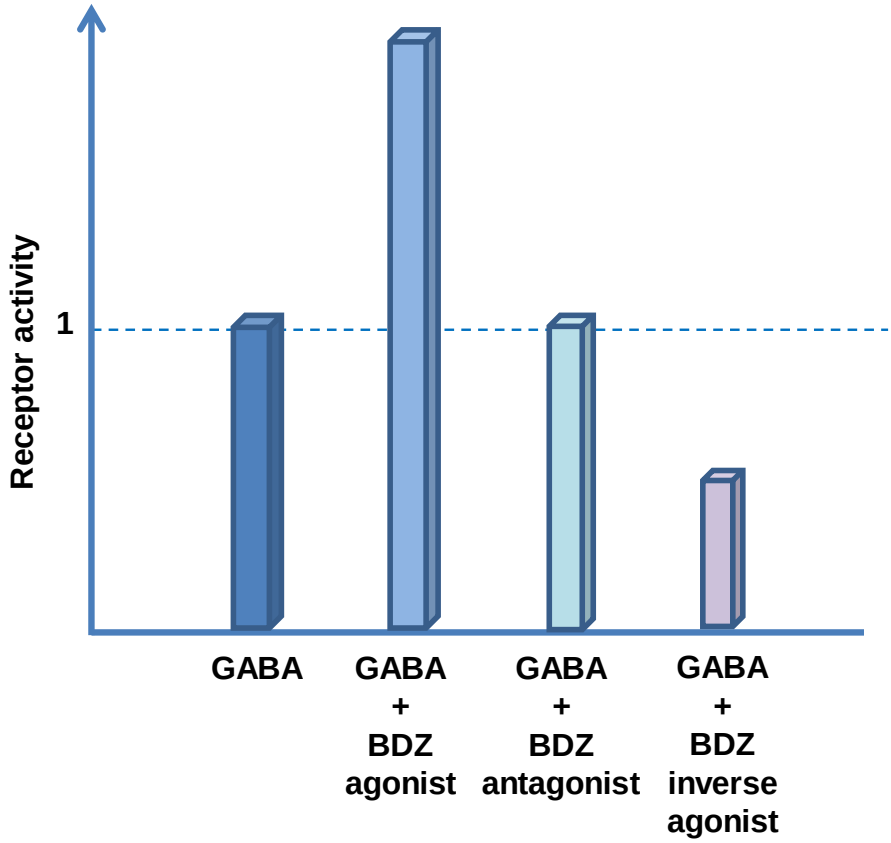

Figure 1.5 – Modulation of $GABA_A$ receptors by different types of benzodiazepines.

Whereas BDZ agonists act as positive allosteric modulators and increase $GABA_AR$ activity, BDZ antagonists have no effect on their own and when co-applied with GABA, but can block potentiation by BDZ agonists. BDZ inverse agonists are negative allosteric modulators, and can reduce the channel opening frequency of $GABA_ARs$ when co-applied with GABA.

This knowledge has aided the development of BDZs with selective actions by targeting specific receptor subtypes, *e.g*. anxiolysis without sedation by targeting α2-containing receptors. However, no such selective compounds have yet progressed beyond clinical trials (Rudolph and Knoflach, 2011).

Whereas BDZs represent a class of synthetic modulators of $GABA_ARs$, an array of endogenous modulators of these receptors also exists. There is evidence for an endogenous BDZ in the brain, an ‘endozepine’ known as diazepam binding inhibitor (DBI), that potentiates $GABA_AR$ currents (Christian et al., 2013). Other endogenous modulators include protons, which potentiate or inhibit the receptor depending on GABA concentration by binding to a residue in the M2 helix of β

subunits (Wilkins et al., 2002, 2005), and Zn^{2+}, which acts as a negative allosteric modulator of dimeric αβ receptors (and with lower potency at αβδ and much lower potency at αβγ receptors) (Smart et al., 1994; Hosie et al., 2003). There is also some evidence that endogenous endocannabinoids (*e.g*. 2-arachidonoyl glycerol) may potentiate $GABA_AR$s at low concentrations of GABA (Sigel et al., 2011).

The $GABA_AR$ is an important clinical target for an array of drugs in addition to the BDZs, including general anaesthetics (GAs) and barbiturates. Although now mostly replaced by more modern agents, barbiturates are a class of anti-convulsant, hypnotic and general anaesthetic that bind to $GABA_AR$s (Krasowski et al., 2001; Chiara et al., 2013). Unlike the BDZs, which increase $GABA_AR$ channel opening frequency, barbiturates (*e.g*. pentobarbitone) act by increasing the open time for $GABA_AR$ ion channels, and are thus highly toxic (Rudolph and Knoflach, 2011). Consequently, a newer generation of GAs have largely replaced barbiturates, including propofol, etomidate and volatile anaesthetics like isoflurane, all of which bind and act as positive allosteric modulators at the $GABA_AR$ (Olsen, 2015; Sieghart, 2015).

Mutagenesis studies and subsequent photoaffinity labelling led to the identification of key residues (N265 in M2 and M286 in M3 of the β2/3 subunit and M236 in M1 of the α subunit) that are thought to be essential for the binding of propofol and etomidate (Belelli et al., 1997, 1999; Krasowski et al., 2001; Li et al., 2006; Olsen, 2015). The site for GA binding is formed at the same β^+-α^- subunit interface as that for GABA, which has its binding site in the ECD about 50 Å above the GA site (Fig. 1.4). Thus, intersubunit binding pockets are likely to be common for both orthosteric and allosteric binding sites. Furthermore, the crystal structure of the Cys-loop receptor bacterial orthologue GLIC showed binding of the GAs propofol and desflurane to an intrasubunit binding pocket in a cavity accessible from the lipid bilayer (Nury et al., 2011). An intersubunit binding pocket was also identified when GluCl was crystallised bound to ivermectin, and is formed in the upper part of the TMD at each subunit interface, comprising residues contributed by M2 and M3 of one subunit, and of M1 from the adjacent subunit (Hibbs and Gouaux, 2011). A hydrogen bond is formed between ivermectin and serine 260 in M2, a residue that is homologous to a residue

thought to be important for binding of volatile anaesthetics (enflurane) and for ethanol action at glycine and $GABA_A$ receptors (M1 residues $\alpha1^{S270}$ and $\beta1^{S265}$, though M3 residues $\alpha1^{A291W}$ and $\beta1^{M286W}$ are also thought to be important) (Mihic et al., 1997). The same residue (S260 in GluCl) faces the intersubunit cavity in GLIC, which is bordered by the two residues that were thought to be important for etomidate binding at the $GABA_AR$ (M1 residue $\alpha1^{M236}$ and M3 residue $\beta3^{M286}$) (Li et al., 2006; Nury et al., 2011; Corringer et al., 2012). Note that the $\beta3^{M286}$ residue was also found to be involved in the action of enflurane (and ethanol) (Mihic et al., 1997). Taken together, these findings suggest that these inter- and intrasubunit binding pockets in a cavity accessible from the lipid bilayer are accessible to multiple pLGIC modulators.

Bicuculline (BIC) and picrotoxinin (PTX) are two commonly used $GABA_AR$ antagonists. Although widely accepted to be an open-channel blocker of $GABA_ARs$ (and GlyRs), multiple binding sites have been suggested for PTX in past studies (Olsen, 2015; Sieghart, 2015). The crystal structure of GluCl bound to PTX at M2 residues -2' to 2' corroborates the hypothesis that PTX (at least in GluCl) blocks the channel pore (Hibbs and Gouaux, 2011). The binding site of PTX is further discussed in Chapter 3, section 3.2.4. BIC is a selective competitive antagonist at the $GABA_AR$ (Andrews and Johnston, 1979), and is therefore suitable for use in neuronal recordings where GABAergic transmission needs to be blocked (Chapter 5). It may also have some negative allosteric properties as it reduces currents evoked by pentobarbitone (Ueno et al., 1997). A wide array of experimental $GABA_AR$ partial, full and inverse agonists and antagonists also exist that are important pharmacological tools in $GABA_AR$ research, but are not discussed further here.

1.2. Neurosteroids

Neurosteroids are an important class of neuromodulators. The term 'neurosteroid' was first coined to describe metabolites of sex and stress hormones that could modulate neuronal activity (Majewska et al., 1986; Baulieu and Robel, 1990; Lambert et al., 2003). Furthermore, neurosteroids are steroids that can be synthesised *de novo* within the nervous system, independent of the

activity of endocrine glands (Baulieu, 1981). Neurosteroids are synthesised in glial cells and neurones of the central and peripheral nervous systems, from cholesterol or steroid precursors imported from the periphery (Schumacher et al., 2000, 2008). Their action is non-genomic and involves rapid and direct interactions with receptors in the membrane.

Three classes of neurosteroids exist (Fig. 1.6): the 3α-hydroxypregnane steroids act as positive modulators of $GABA_AR$s (*e.g*. 5α-pregnan-3α-ol-20-one (allopregnanolone) and 5α-pregnan-3α,21-diol-20-one (THDOC)), whereas the naturally occurring diasteromers of these, the 3β-hydroxypregnane steroids (*e.g*. 5β-pregnan-3β-ol-20-one) act as negative allosteric modulators of the receptors along with the sulphated neurosteroids (*e.g*. pregnenolone sulphate and dehydroepiandrosterone sulphate (DHEAS)) (Akk et al., 2007; Wang et al., 2007; Wang, 2011). The sulphated neurosteroids are, due to their negative modulatory activity at $GABA_AR$s, commonly referred to as inhibitory neurosteroids, as opposed to the potentiating neurosteroids like allopregnanolone. Dehydroepiandrosterone (DHEA) is also an inhibitory neurosteroid at the $GABA_AR$s, despite not being sulphated at C3 of the A-ring (Fig. 1.6C). DHEA is, however, somewhat less potent than the sulphated neurosteroids at $GABA_AR$s (Park-Chung et al., 1999). The sulphated neurosteroids are the main focus of this project, with an emphasis on pregnenolone sulphate (PS).

1.2.1. Neurosteroid synthesis, metabolism and expression in the brain

The observations that steroids, including pregnenolone, DHEA and their sulphated esters, were present at higher concentrations in tissues from brain and peripheral nerves than in plasma, and that these steroids remained in the nervous system long after gonadectomy or adrenalectomy, led to the idea that these compounds might be synthesised *de novo* in the nervous system (Compagnone and Mellon, 2000; Mellon and Griffin, 2002). It has later been confirmed that steroidogenic enzymes are found within the nervous system, and that steroids are synthesised there to both modulate gene expression and neurotransmission through direct interaction with neurotransmitter receptors following their paracrine release.

Cholesterol acts as the main precursor of neurosteroid synthesis, and via a series of enzymatic reactions mediated by cytochrome P450 and non-P450 enzymes, different classes of neurosteroids can be generated (Fig. 1.7) (Mellon and Griffin, 2002). All enzymes required for the synthesis of potentiating neurosteroids have been identified in the CNS by mRNA and protein analysis in various species. In humans, hippocampal and temporal lobe expression and/or enzymatic activity have been demonstrated for cytochrome P450 mitochondrial cholesterol side-chain cleavage (P450scc), microsomal 21-hydroxylase (P450c21), 5α-reductase and 3α-hydroxysteroid-dehydrogenase (3α-HSD) (Stoffel-Wagner, 2003).

The concentration of potentiating neurosteroids in rodent brain has been estimated using radioimmunoassays and mass fragmentography, and is likely to be in a nanomolar range (<30 nM) in rodents (Uzunov et al., 1996; Bernardi et al., 1998). These nanomolar concentrations are sufficiently high to cause potentiation at $GABA_AR$s, and may, under some conditions, reach higher concentrations. For example, the concentrations of allopregnanolone and THDOC are increased by stress, fluctuate during the menstrual cycle, and increase during pregnancy and parturition (Concas et al., 1998; Mellon and Griffin, 2002; Reddy, 2003).

A.

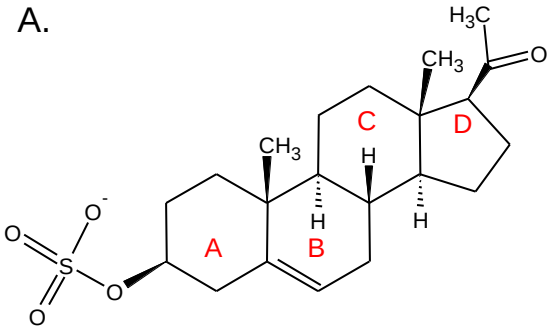

Pregnenolone sulphate

B.

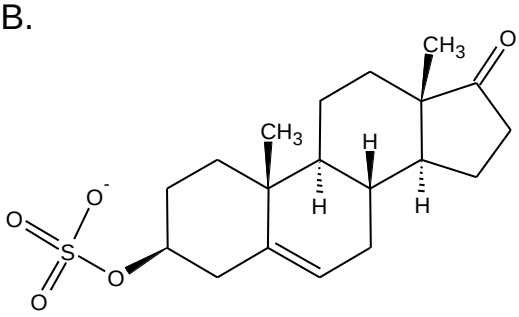

Dehydroepiandrosterone sulphate
(DHEAS)

C.

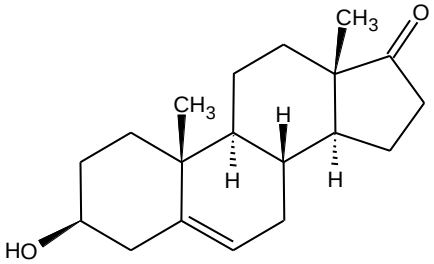

Dehydroepiandrosterone
(DHEA)

D.

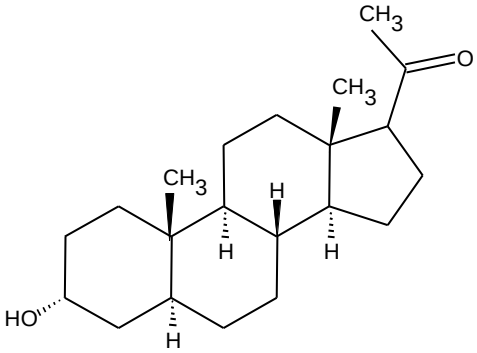

Allopregnanolone
(5α-pregnan-3α-ol-20-one)

E.

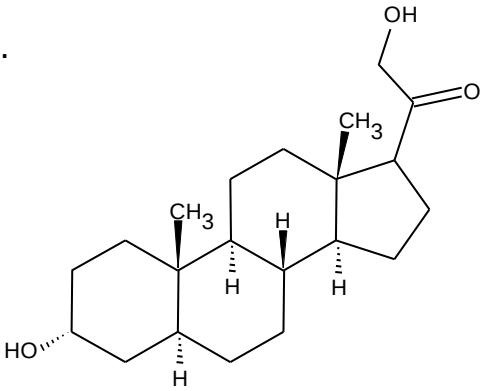

THDOC
(5α-pregnan-3α,21-diol-20-one)

Figure 1.6 – Chemical structures for selected potentiating and inhibitory neurosteroids.

Chemical structures for the sulphated neurosteroids pregnenolone sulphate (**A**) and DHEAS (**B**), the inhibitory neurosteroid DHEA (**C**) and potentiating neurosteroids allopregnanolone (**D**) and THDOC (**E**).

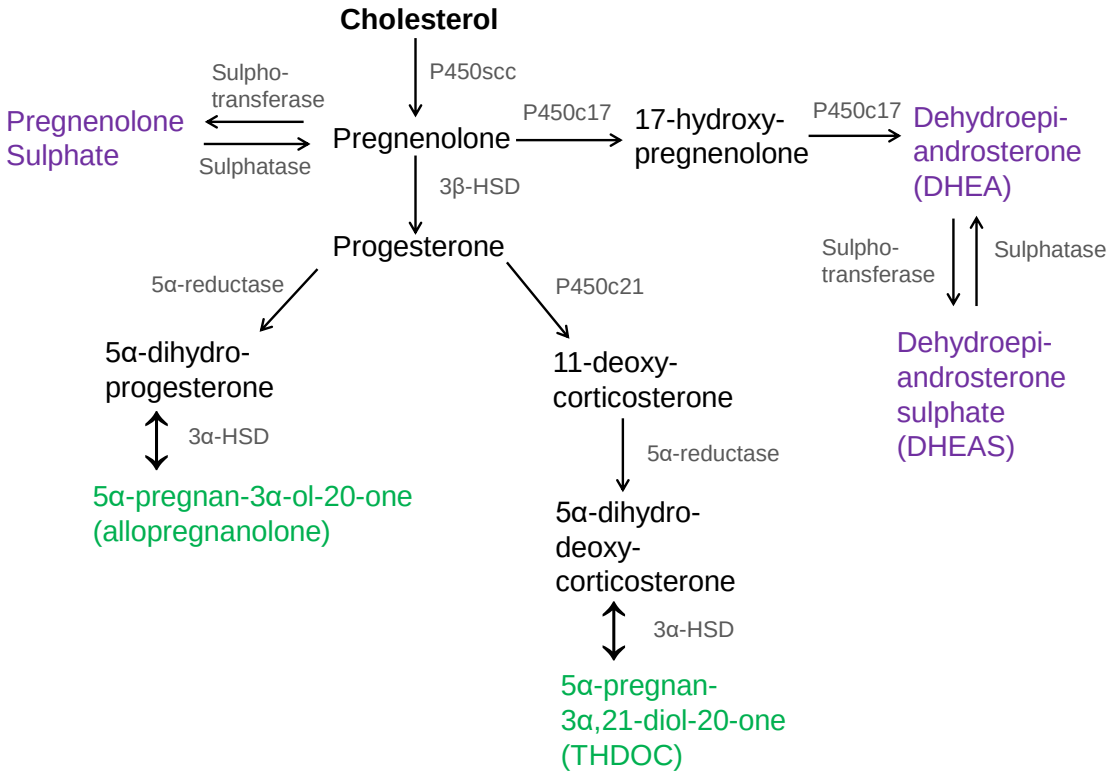

Figure 1.7 – Biosynthetic pathways for the neurosteroids.

The chart shows the pathways and enzymes involved in the synthesis of the major potentiating (green) and inhibitory neurosteroids (purple). Other neuroactive steroids can also be generated from the intermediates (black) via various enzymatic steps. The initial conversion of cholesterol into pregnenolone occurs in the mitochondria, whereas subsequent steps require relevant enzymes to be present in the cytosol. Abbreviations: 3β-HSD = 3β-hydroxysteroid-dehydrogenase, 3α-HSD = 3α-hydroxysteroid-dehydrogenase, P450scc = cytochrome P450 mitochondrial cholesterol side-chain cleavage, P450c17 = microsomal 17-hydroxylase, P450c21 = microsomal 21-hydroxylase. The diagram is modified from Mellon and Griffin (2002).

Sulphation of steroids is catalysed by cytosolic sulphotransferases, SULT2A and SULT2B (Schumacher et al., 2008). These transferases belong to the SULT2 family of 3β-hydroxy sulphotransferases. SULT2A mRNA has been documented in rat brain (Shimada et al., 2001), and SULT2B mRNA has been detected in rat and mouse brain (Schumacher et al., 2008). Immunohistochemistry confirmed the presence of hydroxysteroid sulphotransferases in pyramidal neurones and granule cells of the adult male rat hippocampus, whereas only weak staining was observed in astrocytes and oligodendrocytes (Kimoto et al., 2001). The presence

of sulphotransferases in hippocampal tissue was also confirmed with Western blotting. These findings suggest that sulphation of 3β-hydroxy steroids is likely to occur in neurones of the hippocampus.

In contrast to the potentiating neurosteroids, the presence of sulphated neurosteroids in the brain has been more difficult to confirm (Schumacher et al., 2008). The detection of pregnenolone sulphate was made difficult as only unconjugated steroids (non-sulphated) could be detected by radioimmunoassays and gas chromatography/mass spectrometry (Corpéchot et al., 1981, 1983; Schumacher et al., 2008). An improved protocol confirmed the presence of PS in the human brain (< 2 ng/g) and plasma (< 160 ng/g), but failed to detect its presence in rodent brains (Liere et al., 2004). Liquid chromatography-electrospray tandem mass spectrometry has recently allowed the direct quantitative determination of PS without hydrolysis in brain areas of 6-8 week-old rats, and confirmed the presence of PS in the cortex and hippocampus (Rustichelli et al., 2013). In homogenised tissue, the concentration of PS in the hippocampus was 10.3 ± 1.4 ng/g tissue compared to 4.5 ± 0.4 ng/g tissue in the cortex. The concentration of allopregnanolone was higher, at 38.4 ± 10.2 ng/g in hippocampal tissue, and 28.6 ± 5.8 ng/g in the cortex. These findings suggest that the presence of PS in both rodent and human brains is quite likely.

PS may exist at higher concentrations in local areas around neurones compared to those measured in tissue homogenates that effectively determine a mean value in a much larger volume. In fact, synaptic release via a retrograde mechanism has been described for a PS-like molecule following postsynaptic depolarisation in immature hippocampal neurones (P3-5), resulting in a synaptic concentration in the micromolar range (Mameli, 2005). Furthermore, blocking steroid sulphatases (Fig. 1.7) with a pharmacological agent (DU-14) in hippocampal slices from age-matched rats was shown to increase synaptic PS levels following exposure to ethanol, leading to an increase in presynaptic glutamate release (Mameli and Valenzuela, 2006). Inhibiting the P450scc enzyme, which converts cholesterol into pregnenolone (Fig. 1.7), with aminogluthetimide, prevented the ethanol-induced increase in PS release, as did an anti-PS antibody. These results provide strong evidence that synthesis of PS occurs in rodent brains. There is also immunohistochemical evidence that organic

solute transporters (OST α/β) for which PS and DHEAS have a high affinity are expressed in neurones of mouse and human cerebellum and hippocampus, and may be involved in clearing sulphated neurosteroids from the synapse (Fang et al., 2010). These are neurones that also express steroidogenic enzymes, and these findings further support a role for the inhibitory neurosteroids in modulating neurotransmission.

There is also some evidence that sulphated steroids can cross the blood-brain barrier (BBB) via active transport processes (reviewed in Schumacher et al. 2008). PS injected intravenously or intraperitoneally in rats can cross the BBB without being hydrolysed to pregnenolone (Wang et al., 1997; Higashi et al., 2003), and sulphoconjugated steroids have been shown to cross the sheep foetal BBB (Wood et al., 2003). Organic anion transporting proteins (OATPs) may provide a means for transporting sulphated steroids, and high levels of mRNA for these transporters have been detected in human white and grey matter (Steckelbroeck et al., 2004; Schumacher et al., 2008). OATPs have also been documented in the endothelial cells of brain capillaries, and in the BBB, and may thus participate in the uptake of sulphated steroids from plasma.

1.2.2. Molecular targets of inhibitory neurosteroids

Neurosteroids can directly modulate various receptors. The inhibitory neurosteroids are active at $GABA_A$Rs, other members of the Cys-loop family, other types of ligand-gated ion channels and voltage-gated ion channels (Gibbs et al., 2006; Smith et al., 2014).

By contrast, the $GABA_A$R is more sensitive to the potentiating neurosteroids (*e.g*. allopregnanolone and THDOC) than other members of the Cys-loop receptor family (Hosie et al., 2007). The homomeric ρ1 $GABA_A$R is, however, less sensitive to the potentiating neurosteroids than heteromeric $GABA_A$Rs (Morris et al., 1999), whereas the *Drosophila* Resistance to Dieldrin (RDL) $GABA_A$R is insensitive and was successfully used to find their binding site at mammalian $GABA_A$Rs (Hosie et al., 2006). GlyRs also show little or no sensitivity to

potentiating neurosteroids (Pistis et al., 1997; Belelli et al., 1999; Weir et al., 2004).

At the $GABA_AR$, potentiating neurosteroids are active in the nanomolar concentration range, and although the potency is similar amongst the different receptor subtypes, the efficacy of these steroids is greater at extrasynaptic-type δ-containing receptors (Belelli et al., 2002). At δ-containing receptors, allopregnanolone can potentiate the response to GABA EC_{10} beyond that produced by a saturating concentration of GABA, and the maximum effect (macroscopic efficacy) is greater than at γ2-containing receptors. A larger effect is thus likely to be observed at low concentrations of neurosteroid at extrasynaptic-type receptors, and potentiating neurosteroids are therefore likely to have a more significant effect on GABA tonic than synaptic currents.

Inhibitory neurosteroids (PS and DHEAS) are less selective than the potentiating neurosteroids. GlyRs are inhibited by PS and DHEAS in the low micromolar range (Maksay et al., 2001; Hong et al., 2013), whereas the GABA ρ1 receptor is only weakly sensitive to PS (IC_{50} > 300 μM) (Woodward et al., 1992; Li et al., 2007). There is also some evidence that PS inhibits nAChRs at micromolar concentrations in bovine adrenal chromaffin cells (Kudo et al., 2002), whilst it has been shown to activate homomeric α7 nAChRs (Chen and Sokabe, 2005; Yang et al., 2012). The *C. elegans* $GABA_AR$ homologue UNC-49B/C is antagonised by both PS and DHEAS at micromolar concentrations (Wardell et al., 2006; Twede et al., 2007). The activity of PS at GLIC, ELIC, GluCl and RDL are not reported in the literature, and will be discussed in Chapter 4, section 4.2.6.

Other receptor families have also been shown to be sensitive to modulation by PS. Recombinant *N*-methyl-*D*-aspartate (NMDA) receptors expressed in *Xenopus* oocytes can be positively and negatively modulated by PS depending on subunit composition (EC_{50}, IC_{50} > 10 μM): receptors comprising the GluN1 subunit expressed with GluN2A or GluN2B are potentiated by PS, whilst those comprising GluN1 with the GluN2C or GluN2D subunit are inhibited (Malayev et al., 2002; Jang et al., 2004; Kostakis et al., 2011). There is, however, some evidence that PS may increase glutamate release from presynaptic terminals via potentiation of receptors containing GluN2D subunits in hippocampal slices from

P3-4 rats (Mameli, 2005), suggesting the effect of PS on NMDA receptors may be dependent on various factors.

PS also acts as a non-competitive antagonist at α-amino-3-hydroxy-5-methyl-4-isoxazolepropionic acid (AMPA) and kainate receptors expressed in oocytes (IC_{50}s > 10 μM) (Wu et al., 1991; Yaghoubi et al., 1998). The transient receptor potential melastatin 3 (TRPM3) receptor is an example of a receptor that is directly activated by PS (EC_{50} ~ 20 μM) (Wagner et al., 2008). PS can also directly activate sigma1 (σ1) receptors in hippocampal neurones (Mtchedlishvili and Kapur, 2003). Morevoer, PS can potentiate currents through voltage-gated Ca^{2+} channels (Hige et al., 2006), and inwardly-rectifying K^+ channels containing the Kir2.3 subunit (Kobayashi et al., 2009). By contrast, voltage-gated Na^+ channels are inhibited by PS (Horishita et al., 2012). Thus, PS acts at multiple target proteins in the brain, though it has the highest potency at $GABA_A$Rs.

To complete this overview of PS target proteins, PS can act also at various receptors in the presynaptic terminal to increase or reduce neurotransmitter release, *e.g*. for acetylcholine (Darnaudéry et al., 2000, 2002), glutamate (Zamudio-Bulcock and Valenzuela, 2011; Zamudio-Bulcock et al., 2011), glycine (Hong et al., 2013) and GABA (Mtchedlishvili and Kapur, 2003; Zamudio-Bulcock and Valenzuela, 2011). The effects of PS on synaptic neurotransmitter release are discussed further in Chapter 5.

1.2.3. Inhibitory neurosteroids and the $GABA_A$ receptors

The molecular determinants necessary for the interaction with and inhibition by the inhibitory neurosteroids at the $GABA_A$Rs are not fully determined. The inhibitory neurosteroids are less potent than the potentiating neurosteroids (Akk et al., 2007), and these two classes of neurosteroids do not compete for common binding sites at $GABA_A$ receptors (Park-Chung et al., 1999; Akk et al., 2008; Seljeset et al., 2015). The inhibitory steroids are also non-competitive inhibitors at the $GABA_A$Rs with respect to GABA (Majewska et al., 1986, 1988), and exhibit state-dependent block with greater inhibition obtained with higher concentrations of agonist (Eisenman et al., 2003). Although the sulphated neurosteroids and the

3β-hydroxypregnane steroids show a similar profile of block at the $GABA_AR$s, including activation-dependence and sensitivity to a mutation in the M2 α-helix ($\alpha1^{V256S}$), these two classes of neurosteroid do not compete for a single binding site (Akk et al., 2001; Wang et al., 2006, 2007). Furthermore, inhibition by PS shows only weak voltage-dependence, suggesting that it is unlikely to be bound to a site (*e.g*. in the open channel) that experiences the membrane electric field (Majewska et al., 1988; Eisenman et al., 2003).

Single-channel recordings have shown that PS reduces the mean cluster duration of GABA single-channel currents (the average length of time between the first opening and the last closing transition of a channel during bursts occurring between sustained periods of desensitisation) without affecting intracluster open or closed time distributions (Akk et al., 2001). The block by PS develops slowly and occurs at similar rates for open or closed GABA channels. Whole-cell recordings have shown that PS has little effect on GABA peak currents, but manifests as an increased block of steady-state currents similar to an apparent increase in the rate of desensitisation (Shen et al., 2000). To further explore the profile of PS inhibition and its possible role in modulating desensitisation, the effect of PS on GABA whole-cell currents in cells expressing wild-type and mutant heteromeric $GABA_AR$s is assessed in this thesis (Chapters 3 and 4).

Block by PS does not depend on the presence of a γ2 subunit (Wang et al., 2006), although PS is more potent at receptors containing the γ2 rather than the δ subunit (Brown et al., 2002). The $GABA_AR$ subtype selectivity of PS is not fully characterised. Previous studies suggest the potency of PS is similar at recombinant α1β2γ2L and α5β2γ2L receptors expressed in oocytes (Rahman et al., 2006), but varies between α1, α2 and α3 containing αβγ receptors, with PS being 10-fold more potent at receptors containing α3 than α1 and 2.5-fold more potent than at receptors containing α2 (Zaman et al., 1992). However, the potency of PS at $GABA_A$ receptors containing all of the α1-6 subunits has not been assessed in one study using the same recording conditions and expression system. Thus, a complete profiling of the activity of PS at different $GABA_AR$ subtypes is required, and will provide insight as to whether PS is likely to be more important in regulating GABAergic transmission in some areas of the brain than

others, or if it plays a role within specific cellular compartments. $GABA_AR$ subtype selectivity of PS will be explored in Chapter 3, section 3.2.6.

Whereas potentiating neurosteroids can cross the membrane and access their binding site from within the cell (Akk et al., 2005, 2007), inhibitory neurosteroids carry a negatively charged sulphate group that render the molecules significantly less hydrophobic (Fig. 1.6). The inhibitory neurosteroids may therefore not be able to diffuse across lipid membranes. Whether PS can access its binding site at the $GABA_AR$ from within the cytosol is also not known, though work by others has shown that PS cannot access its binding site for TRPM3 (Wagner et al., 2008) and Kir2.3 from inside the cell (Kobayashi et al., 2009). Knowing whether PS can inhibit $GABA_ARs$ from the cytosolic face can help us determine where on the receptor PS is likely to bind, and is explored in Chapter 3, section 3.2.5.

The potentiating neurosteroids are active at $GABA_ARs$ at low nanomolar concentrations, and only cause direct activation at higher submicromolar to micromolar concentrations (Lambert et al., 2003; Hosie et al., 2006). The binding site for potentiation of $GABA_ARs$ by neurosteroids is located at glutamine (Q) 241 in the α subunit, and is conserved among the α1-6 subunits (Hosie et al., 2006, 2009). Mutating Q241 does not affect PS binding, making it unlikely that potentiating and inhibitory neurosteroids share a common binding site (Akk et al., 2008). Glutamine 241 is located at the base of a water-filled cavity between the M1-M4 interface, which is likely to increase in depth and volume following receptor activation, allowing the neurosteroid to bind and potentially keep the channel in an open state (Hosie et al., 2006). The binding site for the potentiating neurosteroids exists in the α subunits only, but moving M1 from α to β2 or γ2 subunits introduces sensitivity to neurosteroids in receptors in which the binding site is mutated (and removed) in the α subunit ($\alpha1^{Q241L}$) (Bracamontes et al., 2012). For inhibitory neurosteroids, it is not known whether the binding site is located on one or more subunits. To determine this, PS sensitivity will be studied using β3 homomers and $GABA_AR$ chimeras expressed in HEK cells (Chapter 3, section 3.2.8. and Chapter 4, section 4.2.7.).

1.2.4. Inhibitory neurosteroids in health and disease

The potentiating neurosteroids exert anxiolytic, anaesthetic and anticonvulsant actions, and multiple synthetic derivatives have been developed for potential clinical use (Reddy and Estes, 2016). These synthetic derivatives have been considered as potential treatments for several conditions, including epilepsy (including catamenial epilepsy and status epilepticus), infantile spasms, fragile X syndrome, premenstrual mood disorder, chronic pain and alcohol dependence, Alzheimer's disease, traumatic brain injury, bipolar disorder, smoking cessation and migraines (reviewed in Reddy & Estes 2016). Synthetic steroids have promising therapeutic aspects, as they are associated with few side effects with no development of tolerance, and appear to be well tolerated by patients. Metabolites of the synthetic steroids are also less likely to be active at intracellular steroid receptors than the naturally occurring counterparts, thereby reducing the likelihood of systemic side effects. To date, no synthetic neurosteroids have been approved for clinical use, but many clinical trials are ongoing. The exception is alphaxolone, which has been withdrawn from use in humans, but is still used in veterinary medicine.

Inhibitory neurosteroids may play various roles in health and disease. Reduced levels of PS in the hippocampus of aged rats are associated with cognitive deficits, possibly due to reduced PS-mediated acetylcholine release (Vallée et al., 1997). Experiments with DHEA and DHEAS have found conflicting effects on cognitive function in humans, though this might be due to the methods used to measure concentrations of sulphated steroid, as discussed in section 1.2.1. (Vallée et al., 2001a). PS has been shown to be memory-enhancing, and reverses scopolamine-induced amnesia in rats (Vallée et al., 2001b). Following administration into the hippocampus or amygdala, PS potently promotes memory enhancement in mice after having been trained using a foot-shock active avoidance paradigm (Flood et al., 1995). Various other studies also suggest that PS can promote memory and learning *in vivo*, and enhance long-term potentiation *in vitro* (Mayo et al., 1993; Sliwinski et al., 2004; Smith et al., 2014).

Furthermore, levels of PS (and DHEAS, along with some potentiating neurosteroids) measured by gas chromatography-mass spectrometry are reduced in parts of the human brain in patients suffering from Alzheimer's disease (Weill-Engerer et al., 2002). Interestingly, high levels of key proteins (β-amyloid and tau) implicated in the formation of plaques and neurofibrillary tangles are correlated with lower brain levels of PS and DHEAS, suggesting a possible neuroprotective role of these neurosteroids in Alzheimer's disease. PS can also reduce the loss of hippocampal pyramidal neurones following intracerebroventricular injection of β-amyloid in mice, ameliorating cognitive deficits (Yang et al., 2012). Antagonists of the σ1 receptor and the α7 nAChR blocked these effects of PS, suggesting that the neuroprotective effects of PS are mediated by these receptors. Furthermore, there is some evidence that sulfotransferase (SULT1A) activity is downregulated in patients with Alzheimer's disease (Vaňková et al., 2015), indicating that a loss of sulphated neurosteroids may play a role in disease progression. The complex effects of PS on memory and learning may implicate various neurotransmitter systems, and may involve modulation of neurotransmitter release as well as direct interaction with neurotransmitter receptors. Positive modulation of NMDA receptors may be involved, as well as negative modulation of $GABA_AR$s. The potential negative modulation of α5-containing $GABA_AR$s is interesting, as this subunit is abundant in the hippocampus (Pirker et al., 2000; Glykys et al., 2008; Hörtnagl et al., 2013), and inhibition of these receptors can promote memory and learning (Collinson et al., 2002).

In animal models of anxiety, PS has been shown to be anxiolytic, whereas DHEAS is anxiogenic (Reddy and Kulkarni, 1997). The effect of PS may however be biphasic, as one study observed anxiolytic effects of PS at low doses, and anxiogenic effects at higher doses (Melchior and Ritzmann, 1994; Strous et al., 2006). Both PS and DHEAS are proconvulsant following long-term subcutaneous administration in mice, though acute treatment has no such effect (Reddy and Kulkarni, 1998). Acute antidepressant effects of the inhibitory neurosteroids have also been observed on the Porsolt forced swim test of depression in mice, likely to occur via a σ1 or opioid δ receptor dependent mechanism (Reddy et al., 1998).

In a dopamine transporter knock-out mouse model of schizophrenia, PS normalised the schizophrenia-like behaviours, including the psychomotor agitation, stereotypy, prepulse inhibition deficits and cognitive impairments (Wong et al., 2015). These effects were shown to be NMDA receptor-dependent. Furthermore, the effects were mediated by PS rather than pregnenolone, as administration of the latter did not normalise the schizophrenia-like behaviours. This is important, as it shows that PS is not converted into pregnenolone following intraperitoneal injections. This also demonstrates that PS must be able to cross the BBB, and that it can reach the brain from the bloodstream. A separate study with schizophrenia patients did however show that pregnenolone can improve patients' functional capacity, likely after conversion to allopregnanolone and pregnenolone sulphate, as serum levels of these were increased (Marx et al., 2014). This indicates that modulation of $GABA_AR$s and NMDA receptors could be beneficial in schizophrenia. In an eight-week clinical trial, pregnenolone reduced cognitive deficits and negative symptoms when administered as an add-on treatment in patients with a recent onset of schizophrenia (Kreinin et al., 2014; Ritsner et al., 2014). A different study showed that pregnenolone decreased manic and depressive symptoms in patients with mono- or bipolar depression and a history of substance abuse (Osuji et al., 2010). These animal and clinical studies suggest that pregnenolone and its metabolites, including PS, may be beneficial in various CNS disorders. Some of these clinical trials are limited by sample size, and larger trials would be needed to verify the efficacy of pregnenolone or PS in patients with depression or schizophrenia.

Overall, these studies show that PS and DHEAS have multiple potentially therapeutic effects *in vivo*. As the inhibitory neurosteroids act at multiple receptors, it may be difficult to dissect out which receptors mediate which effects. Furthermore, effects may be occluded by systemic metabolism of the inhibitory neurosteroids, which can potentially convert them into a different class of neuroactive steroid. The study by Wong et al. (2015) shows that systemic metabolism of PS may not be a problem, though it is possible some conversion into other steroid molecules may still occur.

1.3. Project aims

As discussed in section 1.2.3., the binding site for the potentiating neurosteroids has been described and has helped to elucidate the mechanism by which this class of neurosteroids modulate the $GABA_AR$s (Hosie et al., 2006, 2007). In contrast, the binding site for the inhibitory neurosteroids is unknown, though some previous efforts have located a residue ($\alpha1^{V256}$; 2') in the M2 helix lining the channel pore (Akk et al., 2001) and various residues in the M1 helix and the M2-M3 linker of the *C. elegans* GABA UNC-49B/C receptor (Wardell et al., 2006; Twede et al., 2007). Knowing the binding site for the inhibitory neurosteroid can be helpful to gain more insight into how this group of compounds modulate $GABA_AR$s. Therefore, the aim of chapter 4 of this thesis is to assess whether any of the residues identified in previous studies could potentially be involved in forming a binding site for PS by introducing point mutations into $GABA_AR$ subunits and studying their effect on the efficacy and potency of PS (Chapter 4, sections 4.2.1-5.). Furthermore, finding a pLGIC that is insensitive to PS is useful in forming the basis for identifying subunit segments and residues important for PS binding. By introducing subunit segments from wild-type $GABA_AR$ subunits into an insensitive subunit to generate a chimera that is sensitive to PS, the residues necessary for binding may be identified. This chimera approach has successfully led to the identification of ligand binding sites in the past (Hosie et al., 2007), and is also used here to try and identify the binding site for the inhibitory neurosteroids (Chapter 4, section 4.2.6-7.).

Understanding the mechanism by which a ligand modulates a receptor may also gain insight into where on the receptor the ligand is likely to bind. As discussed in Chapter 3, previous studies of $GABA_AR$ modulation by PS have involved the use of various expression systems, DNA constructs from different species and different methods to measure current inhibition. The receptor subtype selectivity of PS has only been studied to a limited extent (Zaman et al., 1992; Zhu et al., 1996; Brown et al., 2002; Rahman et al., 2006), and a complete characterisation of modulation by PS of $GABA_AR$s incorporating each of the α1-6 subunits has not been carried out within the same heterologous expression system using consistent methods. As described in section 1.1.1., knowing whether a ligand is

receptor subtype selective can help us predict where in the brain and within which neuronal compartments the compound is likely to act. Therefore, one of the aims of Chapter 3 is to provide a full account of the $GABA_AR$ subtype selectivity of PS by studying inhibition at recombinant receptor subtypes incorporating each of the α1-6 subunits, and to determine whether the binding site for this steroid is likely to be present on one or more classes of subunit (sections 3.2.6-8.).

Furthermore, as different receptor subtypes participate in mediating phasic and tonic currents (section 1.1.3.), knowing whether PS is receptor subtype selective my help to predict whether PS is more active at typical synaptic-type or extrasynaptic-type receptors. The functional profile of PS inhibition is also further characterised in Chapter 3 by determining whether block by PS is activation- or voltage-dependent and assessing whether pre-application of the steroid increases inhibition (sections 3.2.1-3.). Inhibition by DHEA and DHEAS is also assessed and compared to inhibition by PS (section 3.2.1.). Understanding the functional profile of PS inhibition can predict where it binds on the receptor and whether phasic or tonic currents are likely to be more susceptible to block. As PS carries a negatively charged sulphate group (Fig. 1.6A), it is unlikely that this steroid can cross the lipid bilayer to access its binding site. This is assessed by applying PS via the intracellular solution through the patch pipette (section 3.2.5.). Due to similarities in the block induced by PS and the open-channel blocker PTX (Majewska and Schwartz, 1987; Eisenman et al., 2003), experiments are designed to determine whether these antagonists are likely to compete for a binding site, and if PS can block the $GABA_AR$ channel pore (section 3.2.4.). As PS is thought to act by increasing receptor desensitisation (Shen et al., 2000; Akk et al., 2001), inhibition by PS is also studied at mutated $GABA_ARs$ that desensitise faster or slower than the wild-type receptor to determine how desensitisation kinetics affect modulation by PS (section 3.2.9.).

The third results chapter, Chapter 5, aims to characterise modulation of fast GABAergic neurotransmission by PS in cultures of hippocampal neurones. Previous studies have shown that PS can reduce presynaptic GABA release, thereby reducing the frequency of IPSCs, but no direct modulatory effect on native $GABA_ARs$ has been reported (Teschemacher et al., 1997; Mtchedlishvili and Kapur, 2003) except under conditions in which $GABA_ARs$ are positively

modulated by allopregnanolone (Haage et al., 2005). As Mtchedlishvili and Kapur (2003) used nanomolar concentrations of PS, concentrations that do not inhibit whole-cell $GABA_AR$ currents (Chapter 3, section 3.2.1.), and Teschemacher et al. (1997) only observed delayed effects of PS, further experiments are needed to fully characterise the modulation of GABAergic transmission by PS. The aims of Chapter 5 are therefore to fully characterise the modulation of native postsynaptic $GABA_ARs$ by low micromolar concentrations of PS, particularly investigating any effects on IPSC peak amplitude and rate of decay (sections 5.2.1-3.). As discussed in section 1.2.2., PS is active at various neurotransmitter receptors. It is therefore not surprising that PS may act at more than one type of receptor in the synapse and regulate GABA release. By using pharmacological agents, two targets for PS are identified in the presynaptic membrane that serve to regulate GABA release (sections 5.2.3-8.).

Chapter 2: Methods

2.1. HEK293 cell culture

HEK293 cells (hereafter referred to as HEK cells) were cultured in 10 cm Petri dishes (Greiner Bio-One GmbH) using Dulbecco's modified Eagle medium (DMEM) supplemented with 10% v/v foetal calf serum (FCS), 100 U/mL Penicillin-G and 100 µg/mL streptomycin (Gibco by Life Technologies, Thermo Fisher Scientific). Cells were incubated at 37°C in humidified air with 5% CO_2 (BOC Healthcare). When reaching approximately 80% confluency, cells were passaged for maintenance. For passaging, cells were washed with 10 mL Ca^{2+}- and Mg^{2+}-free Hank's balanced salt solution (HBSS; Gibco) and detached from the dish using 2.5 mL 0.05% w/v trypsin-ethylene-diamine-tetra-acetic acid (trypsin-EDTA; Gibco). Cells were collected in 10 mL culture medium to inactivate the trypsin and centrifuged at 168 x *g* for 2 min (MSE Mistral 2000 centrifuge). The supernatant was aspirated, and the cell pellet was resuspended in 5 mL culture medium using a 1000P Gibson pipette. The cells were then plated at appropriate dilutions onto 10 cm Petri dishes. For electrophysiology, cells were plated onto 22 mm glass coverslips (VWR international) pre-coated with 100 µg/mL poly-L-lysine (Sigma).

2.2. HEK cell transfection

HEK cells plated onto coverslips for electrophysiology experiments were transfected with murine DNA (except GABA ρ1 subunit DNA which was human) following plating and allowed 16-40 h to express before each experiment. All subunits were expressed in a mammalian pRK5 vector to achieve high levels of expression. Using a calcium phosphate protocol, DNA encoding the individual receptor subunits (1 µg for each subunit) were mixed with 340 mM $CaCl_2$ (20 µL/coverslip) and 4-(2-hydroxyethyl)-1-piperazineethanesulfonic acid (HEPES)-buffered saline (HBS; 24 µL; 50 mM HEPES, 280 mM NaCl and 2.8 mM Na_2HPO_4, pH 7.2). Enhanced green fluorescent protein (pEGFP-C1) was used

as a marker for transfection. The total amount of DNA did not exceed 4 µg per coverslip. A transfection ratio of 1:1:1:1 was used for heteromeric receptors (*e.g*. α1β2γ2L with pEGFP-C1), whilst for homomeric receptors, a ratio of 2:1 (β3 or ρ1 with pEGFP-C1) provided improved expression.

2.3. Reagents

Compound	Supplier	Stock conc.	Solvent	Final conc.
Ba^{2+}	VWR	1 M	H_2O	3 mM
BD-1063 dihydrochloride	Tocris	10 mM	H_2O	0.3-10 µM
(+)-Bicuculline-methiodide	Sigma	50 mM	DMSO	20 µM
Cd^{2+}	VWR	1 M	H_2O	200 µM
CNQX	Abcam	10 mM	H_2O	10 µM
D-AP5	Tocris	20 mM	H_2O	20 µM
DHEA	Sigma	2 mM	Methanol	≤ 10 µM
DHEAS	Sigma	2 mM	Methanol	≤ 10 µM
Diazepam	Roche	10 mM	DMSO	500 nM
GABA	Sigma	1 M	H_2O	≤ 3 mM
Haloperidol	Sigma	25 mM	DMSO	50 µM
Kynurenic acid	Sigma	n/a	Krebs solution	1 mM
Mefenamic acid	Sigma	100 mM	DMSO	10 µM
ML133	Tocris	100 mM	DMSO	100 µM
Ononetin	Tocris	100 mM	DMSO	10 µM
Picrotoxin	Sigma	100 mM	DMSO	10 µM
Pregnenolone sulphate	Sigma	20 mM	DMSO	≤ 100 µM
Tetrodotoxin	Abcam	0.5 mM	H_2O	500 nM

***Table 2.1* – A complete list of pharmacological agents used in this project.**

The table lists all pharmacological agents used, including supplier, stock concentration, solvent and final concentration used in experiments.

2.4. Site-directed mutagenesis and DNA

All mutations were made using DNA from our own stocks as a template for PCR reactions. Point-mutations were generated using either the QuickChange kit

(QuickChange® II XL Site-Directed Mutagenesis Kit, Stratagene) or the Phusion kit (Phusion™ Site-Directed Mutagenesis Kit, Thermo Fisher Scientific) following standard molecular biology protocols. Colony forming units (CFUs) were selected for culturing, and grown in LB broth overnight for subsequent elution using the Plasmid Miniprep kit (GenElute™ Plasmid Miniprep Kit, Sigma-Aldrich). All DNA was sequenced using the Sanger Sequencing Service (Source Bioscience, Cambridge, UK). Following successful mutagenesis, larger cultures were grown and constructs were eluted for storage in TE buffer (1 µg/µl) using the Plasmid Maxi kit (HiSpeed® Plasmid Maxi Kit (25), Qiagen). Constructs were kept at -20°C for long-term storage. A table with all primers used for the mutagenesis PCR reactions is shown below (Table 2.2).

Other mutants that already existed in our laboratory and are not listed below include the 2' mutant $\alpha1^{V256C}$ (Thomas et al., 2005) and the desensitisation mutants, $\gamma2L^{V262F}$ and $\beta2^{L296V}$ (Gielen et al., 2015). All chimeras used in this study were prepared as described by Gielen et al. (2015).

Other subunits used for *Xenopus* oocyte expression studies include the *Drosophila* RDL (Resistance to dieldrin) isoform C receptor kindly provided by David Sattelle (Wolfson Institute for Biomedical Research, UCL), the glutamate-activated Cl^- channel construct $GluCl_{cryst}$ (Hibbs and Gouaux, 2011), the bacterial Cys-loop receptor homologs, *Erwinia chrysanthemi* GABA-gated ion channel (ELIC) and the *Gleobacter violaceus* proton-gated ion channel (GLIC), all provided by the Pasteur Institute, Paris.

Construct	Forward primer sequence (5' – 3')	Reverse primer sequence (5' – 3')
$\rho1^{P294S}$	TCCttaggtatcacaacggtgctgacc	gactctggcaggcacggc
$\rho1^{P294V}$	GTCttaggtatcacaacggtgctgacc	gactctggcaggcacggc
$\alpha1^{V256S*}$	cagtaccagcaagaactTCCtttggagt gacgactgttc	gaacagtcgtcactccaaaGGAagttcttgctggtac tg
$\alpha1^{Q228N}$	AACacatatctgccgtgcataatg	aataacaaagtagccaatttttctc
$\alpha1^{Q228N,Y230V}$	AACacaGTGctgccgtgcataatgacag	aataacaaagtagccaatttttctc
$\alpha1^{Y230V}$	caaacaGTGctgccgtgcataatgacag	aataacaaagtagccaatttttctc
$\alpha1^{Y230F}$	caaacaTTCctgccgtgcataatgacag	aataacaaagtagccaatttttctc
$\beta3^{A252S*}$	ctgctgctcgagttTCCcttgggattaccac	gtggtaatcccaagGGAaactcgagcagcag

Table 2.2 – Forward and reverse primer sequences used for point mutations.

*These point mutations were made using the QuickChange kit. The rest were produced with the Phusion kit. Codons introducing a point mutation are shown in capital letters.

2.5. Hippocampal cell culture

Hippocampal cultures were prepared from E18 Sprague-Dawley rat embryos in accordance with the *Animals (Scientific Procedures) Act, 1986*. Dissections were performed by Laura Fedele. Hemisected brains were stored in HBSS (with Ca^{2+} and Mg^{2+}; Gibco) on ice, and hippocampi were dissected out and cut in half. Working in a sterile hood, hippocampal tissue was transferred to a 35 mm Petri dish containing warmed (37 °C) trypsin solution (0.1% w/v; Gibco) for 10 min. The tissue was then transferred to a tube containing HBSS and washed over four cycles to remove any remaining trypsin. Dissociation of tissue into single cells was done in 2 mL plating medium (Minimum essential medium (MEM) supplemented with 2 mM L-glutamine, 10 U/mL Penicillin-G, 10 µg/mL streptomycin, 20 mM glucose, 5% (v/v) horse serum and 5% (v/v) heat-inactivated FCS; all from Gibco), using fire-polished glass Pasteur pipettes of increasingly smaller bore to triturate the tissue. The cell suspension was centrifuged for 10 min at 168 x *g*, and the pellet was resuspended in fresh plating

medium using a P1000 Gibson pipette. Per two hippocampi, 1 mL of plating medium was used. Cells (0.33 mL suspension per coverslip) were plated onto 22 mm coverslips coated in 500 µg/mL poly-L-ornithine (Sigma) made up in Borate buffer (50 mM boric acid and 12.5 mM sodium tetraborate in filtered water, pH 8.5; Sigma). The cells were left for at least one hour at 37 °C in humidified air with 5% CO_2 before the plating medium was replaced with maintenance medium (Neurobasal-A supplemented with 0.5% GlutaMAX, 50 U/mL Penicillin-G, 50 µg/mL streptomycin, 1% v/v B-27 supplement and 35 mM glucose; all from Gibco). The coverslips were topped up with 0.5 mL fresh medium every week, and electrophysiological recordings were carried out 10 to 16 days after plating.

2.6. Patch-clamp electrophysiology

Coverslips containing transfected HEK cells or hippocampal neurones were mounted into a recording chamber on the stage of a Nikon Eclipse TE300 microscope with differential interference contrast optics. Cells were continuously superfused with Krebs solution containing (in mM): 140 NaCl, 4.7 KCl, 1.2 $MgCl_2$, 2.52 $CaCl_2$, 11 glucose and 5 HEPES, adjusted to pH 7.4 with 1 M NaOH. For neuronal recordings, the Krebs solution was supplemented with 1 mM kynurenic acid (Sigma) to block excitatory glutamatergic transmission. Patch pipettes had resistances of 2.5-4 MΩ and were filled with one of two internal solutions. For HEK cell recordings, the internal solution was K^+-based, containing (in mM): 1 $MgCl_2$, 120 KCl, 11 EGTA, 10 HEPES, 1 $CaCl_2$ and 2 K_2ATP, adjusted to pH 7.2 with 1 M NaOH. For neurones, a Cs^+-based internal solution was used, containing (in mM): 140 CsCl, 2 NaCl, 10 HEPES, 5 EGTA, 2 $MgCl_2$, 0.5 $CaCl_2$, 2 NaATP and 0.5 NaGTP. The osmolarity of the internal solutions was measured using a vapour pressure osmometer (Wescor Inc.), and was in the range 300 ± 10 mOsm/L. All recordings were performed at room temperature.

Whole-cell membrane currents were recorded with an Axopatch 200B amplifier (Molecular Devices). HEK cells were voltage-clamped between -20 and -40 mV, and neurones were voltage-clamped at -60 mV. Data acquisition was performed with Clampex 10.3 (pCLAMP 10 software, Molecular Devices). Currents were filtered at 2 kHz and digitised at 20 kHz via a Digidata 1440A (Molecular Devices).

The series resistance was monitored and calculated throughout all recordings by measuring the membrane current responses to 10 mV hyperpolarising voltage steps of 50 ms duration at a frequency of 10 Hz. Recorded cells for which the series resistance varied by more than 30% were discarded. The series resistance was typically in the range 4-10 MΩ.

In HEK cells, a control response to ligand/agonist was obtained at regular intervals by applying GABA at a high concentration ($EC_{80\text{-}100}$) to obtain an estimate of membrane seal stability and any GABA current run-down over time. These responses were used to normalise subsequent responses that would be used as data points for creating concentration-response curves (described in section 2.8.1.). A U-tube application system was used for drug applications, as described in Fig.2.1. A wash-off period of 2-3 min was allowed between each application of drug to allow the receptors to recover from desensitisation and to minimise the run-down of currents.

In neuronal experiments, control responses or control recordings of synaptic currents were always obtained prior to drug application to optimise both cell holding current and series resistance stability. The wash-out of drug was also recorded to assess whether the effect of the drug washed out.

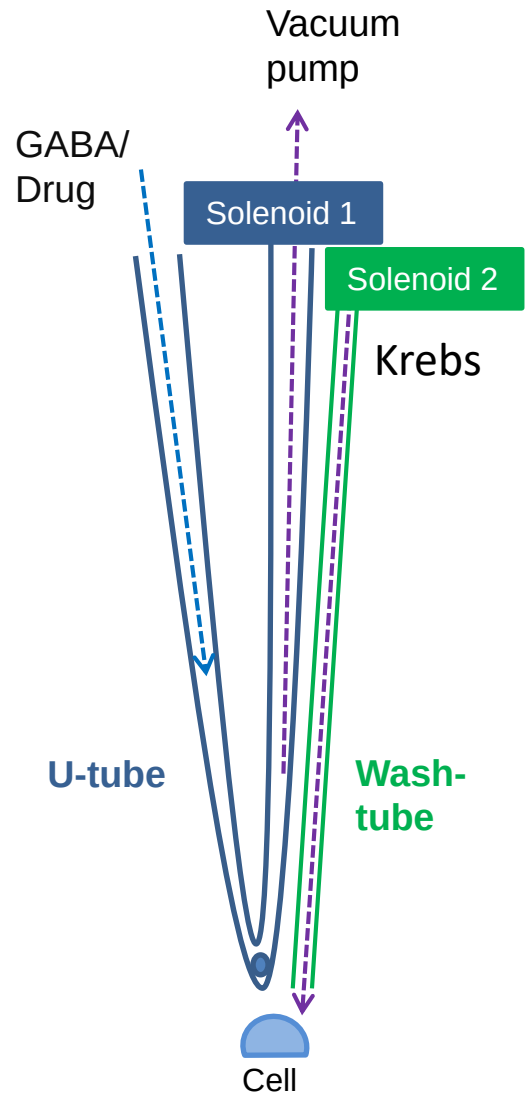

Figure 2.1 – Schematic diagram of the U-tube.

Drug solutions were applied through a U-tube (dark blue), and Krebs solution was applied through a wash-tube (green) to rapidly remove the drug solution following each application. Between drug applications solenoids remain open, allowing the solution that goes through the U-tube to pass through to waste via a vacuum pump, and the bath to be perfused with Krebs solution coming from the wash-tube. During drug application, solenoids are closed, stopping the flow of solution from the wash-tube, and allowing the drug solution to exit via a hole in the apex of the U-tube and superfuse over the recorded cell.

2.7. Homology modelling

Homology models of the mouse α1β2γ2L wild-type and 2' mutant receptors were created using the glutamate-activated Cl^- channel ($GluCl_{cryst}$) from *C. elegans* in complex with Fab and ivermectin (PDB 3rhw) as a template (Hibbs and Gouaux, 2011). A model of the *C. elegans* GABA-activated UNC-49B homomer was generated for both the wild-type and mutant receptor using the human GABA benzamidine-bound β3 homopentamer crystal structure as a template (PDB 4cof) (Miller and Aricescu, 2015). The amino acid sequences, with or without mutations, were aligned to the template sequences using the *align2d.py* script in Modeller 9.13 (Sali and Blundell, 1993). All five subunits of each receptor were aligned in the same file, and the final target-template alignment was used to build multiple 3D models using the automodel script in Modeller. The models with the lowest Discrete Optimised Protein Energy (DOPE) score were used, and optimal configurations of amino acid side-chains were determined with SCRWL4 (Krivov et al., 2009). All models were visualised in PyMOL version 1.3 (Schrödinger©).

2.8. Data analysis and statistics

2.8.1. Analysis of HEK cell recordings

The amplitudes of peak and steady-state agonist-activated currents were measured relative to the baseline holding current prior to agonist application using Clampfit 10.3.1.5 software (pClamp 10, Molecular Devices). To generate GABA concentration-response curves, the peak of each GABA response was normalised to the peak response to a saturating concentration of GABA (1 mM, unless otherwise stated) and expressed as a percentage,

$$Yn = \frac{Y}{Ymax} \times 100,$$

where Yn is the normalised response, Y is the response to any given concentration of GABA, and $Ymax$ is the response to a saturating concentration

of GABA. Likewise, steady-state currents were expressed as a percentage of the steady-state current measured at a given time point during the application of GABA.

For most experiments where inhibition of an agonist response was studied, the steady-state current was defined as the current measured at 10 s into drug application, *i.e*. at 10 s after the onset of the current. Agonists and antagonists were always co-applied, unless otherwise is stated. To study inhibition of a GABA response by PS, an EC_{80} concentration of GABA (the concentration at which 80% of maximal response is achieved) was co-applied with PS.

Normalised GABA concentration-response curves were fitted using the Hill Equation (equation 1),

$$Yn = Ymax\left[\frac{[A]^n}{EC_{50}^n + [A]^n}\right], \quad \text{.....(1)}$$

where Yn is the normalised response to GABA (percentage response), $Ymax$ is the control maximal response to GABA (100%), A is the concentration of GABA applied, EC_{50} is the concentration of GABA producing 50% of maximal response, and n is the Hill coefficient.

Inhibition curves were fitted using an inhibition model (equation 2),

$$Yn = Ymax\left(1 - \frac{[B]^n}{IC_{50}^n + [B]^n}\right), \quad \text{.....(2)}$$

where Yn is the normalised agonist response in the presence of antagonist, $Ymax$ is the maximal response in the absence of antagonist, B is the concentration of antagonist, n is the Hill coefficient and the IC_{50} is the concentration of antagonist producing 50% inhibition of the agonist response. All curves were fitted using a non-linear least squares algorithm in Origin 6.0 (Microcal™).

2.8.2. Analysis of hippocampal neurone recordings

For the analysis of GABA-mediated inhibitory postsynaptic currents (IPSCs), event detection was performed using the programme WinEDR (Version 3.5.2, John Dempster, Strathclyde University) by deploying an amplitude-threshold crossing method. All detected events were manually checked before further analysis was carried out in WinWCP (Version 4.8.6, John Dempster) to calculate event amplitudes and the frequency of IPSCs under different recording conditions. All validated IPSC events were included for the analyses of event amplitude and frequency, and were normalised to control IPSCs recorded over a control period of 2-5 min. Events that showed monotonic rises and uncontaminated decay phases were used for kinetic analysis (> 50 events in each condition). These were aligned on their initial rising phases and averaged synaptic waveforms were constructed from which current decays could be calculated by fitting a biexponential curve to the decay phase of the averaged waveform. Weighted tau (τ_w) values were calculated using the equation (equation 3),

$$\tau_w = \frac{A_1.\tau_1 + A_2.\tau_2}{A_1 + A_2}, \quad \text{.....(3)}$$

where τ_1 and τ_2 represent the time constants for each exponential component of the decay phase, and A_1 and A_2 are the relative amplitude contributions of τ_1 and τ_2 to the overall fit.

To assess any relative changes in the spontaneous IPSC (sIPSC) amplitudes, distributions of all sIPSC amplitudes were generated before and during drug application (*e.g*. 3-10 μM PS). The sIPSC amplitude distributions were fitted using a sum of Gaussians based on the function described below (equation 4),

$$y = y_0 + \sum_{i=1}^{n} A e^{\frac{-(X-Xc)^2}{2w^2}}, \quad \text{.....(4)}$$

where A is the peak amplitude of the distribution, Xc is the distribution mean amplitude, and w is the half-width of the distribution determined at $A/2$, and y_0 is

the baseline amplitude of the distribution. Fits were determined using a non-linear least squares Marquardt routine.

For the amplitude distributions of sIPSCs, equal numbers (200 per cell) of sIPSCs were sampled in each condition. In PS, sIPSCs were sampled 2 min after the onset of drug application to ensure the effect of the steroid had reached equilibrium.

Averaged IPSC waveforms were plotted using Microsoft Excel. Values for the average charge transfer for IPSCs were calculated by multiplying the area under the averaged waveform (charge transfer) by the frequency of IPSCs in each recording condition.

2.8.3. Statistics

Non-transformed data were used for the statistical analyses of neuronal data throughout, unless stated otherwise. For HEK cell data, transformed data (*e.g*. EC_{50}s and IC_{50}s) were used for the statistical analyses. The Kolmogorov and Smirnov test was used to check if data were normally distributed. For parametric data, pairwise comparisons were made using a paired one-tailed or two-tailed Student's t-test, as appropriate. The two-sample t-test (parametric) was used to compare data from different sets of experiments. Statistical comparisons between more than 2 groups were undertaken by one-way or repeated measures ANOVA (analysis of variance). ANOVA was followed by the Tukey post-hoc test. For non-parametric data, pairwise comparisons were made using the Wilcoxon matched pairs test. All statistical analyses were carried out in GraphPad InStat 3 (GraphPad Software, Inc.). The threshold for statistical significance was set at $p < 0.05$ (5%). Data are reported as mean ± standard error of the mean (SEM).

Chapter 3: Modulation by pregnenolone sulphate of recombinant $GABA_A$ receptors expressed in HEK cells

3.1. Introduction

In this chapter, I will study the functional profile of PS at recombinant $GABA_A$ receptors expressed HEK cells. These cells are widely used as an expression system for the study of the pharmacological and biophysical properties of recombinant proteins (Thomas and Smart, 2005). As the cells are of epithelial rather than neuronal origin, the HEK cell is considered a suitable expression system for studying proteins of neuronal origin in isolation, including the $GABA_A$ receptor. There is some evidence that HEK cells express low endogenous levels of the $GABA_A$ receptor β3, γ3 and ε subunits, but the functional impact of these following transfections with other subunits that should co-assemble to form functional receptors has been found to be minimal. Some evidence for the presence of an endogenous β3 subunit has however been confirmed both in untransfected cells and in cells transfected with α and γ subunits (Ueno et al., 1996; Davies et al., 2000; Thomas and Smart, 2005). Our laboratory has consistently been unable to detect GABA-activated currents in untransfected cells, and to detect β3 mRNA using reverse transcription (RT)-PCR (Thomas and Smart, 2005). As levels of these endogenous subunits appear to be below functional detection in our laboratory, the expression of $GABA_A$ receptor subunits in HEK cells can be controlled using cDNA transfection methods.

Although modulation of $GABA_A$ receptors by PS has been studied by various research groups in the past, clear interpretation of the published data is confounded by the use of various expression systems and procedures for analysing the data. Whereas some studies have exclusively looked at inhibition of GABA peak currents by PS despite the slowly developing block by the steroid (Park-Chung et al., 1999), other studies have been carried out in less physiologically relevant *Xenopus* oocytes or in neuronal cultures where individual GABA receptor subtypes cannot be studied in isolation (Zaman et al., 1992; Park-Chung et al., 1999; Shen et al., 2000; Eisenman et al., 2003).

The receptor subtype selectivity of PS has been studied to some extent (Zaman et al., 1992; Zhu et al., 1996; Rahman et al., 2006), but no complete profiling of inhibitory neurosteroid sensitivity at the most common $GABA_A$ receptor subtypes has yet been performed. Thus, a systematic study of the modulation of various $GABA_A$ receptor subtypes by PS using a single expression system (HEK cells), coupled to consistent methods and analytical techniques, is needed for a complete characterisation of PS inhibition. This allows for the acquisition of data that can be used for direct comparisons of the activity of PS at different receptor subtypes, and provides an indication as to whether modulation is likely to be more important in the synaptic or extrasynaptic membrane.

There are many benefits of using HEK cells compared to *Xenopus* oocytes. Whereas the oocytes are amphibian, the HEK cell allows for expression of recombinant neuronal proteins in a mammalian system where post-translational processing and other biochemical processes (*e.g*. signalling and modulatory pathways) are similar to those found in the proteins' native environment (Thomas and Smart, 2005; Goldin, 2006; Kvist et al., 2011). Furthermore, oocyte membranes have extensive invaginations and thus a large surface area, leading to lower apparent potencies and slower onsets of drug action compared to what would be observed in the native tissue of the protein. For these reasons, the modulation of $GABA_A$ receptors expressed in HEK cells are studied and discussed in detail in this chapter. Comparisons to findings in other expression systems and native tissue are made to build an extensive profile of inhibitory neurosteroid modulation of these receptors.

Different $GABA_A$ receptor subtypes were heterologously expressed in HEK cells and studied using whole-cell electrophysiology. Improved knowledge of how PS modulates $GABA_A$ receptors can increase our understanding of its role in physiology and pathophysiology, and assist us in building a hypothesis as to where PS is likely to bind at the receptor. In this chapter, the mode of inhibition by PS is investigated in order to determine if the compound displays properties such as voltage-sensitivity and use-dependence. Inhibition of $GABA_A$ receptors by the structurally similar inhibitory neurosteroids DHEA and DHEAS is also assessed, and their activity is compared to that of PS. To determine whether modulation by PS is likely to play a greater role within or outside the synapse, the

receptor subtype selectivity of PS is determined by expressing different receptor subtypes in HEK cells and comparing the potency and efficacy of the steroid at each receptor subtype.

3.2. Results

3.2.1. PS is a negative allosteric modulator of the α1β2γ2L receptor

The allosteric modulation of $GABA_A$ receptors by inhibitory neurosteroids was studied by recording whole-cell currents from HEK cells. Due to its high prevalence in the CNS (McKernan and Whiting, 1996; Pirker et al., 2000; Glykys et al., 2008; Hörtnagl et al., 2013), α1β2γ2L was chosen as the main receptor to be used in these initial characterisation studies. As the α1 and β2 subunits can assemble to form functional α1β2 receptors in HEK cells (Mortensen et al., 2012), the incorporation of the γ2L subunit was confirmed by applying diazepam, a γ-subunit selective benzodiazepine (Pritchett et al., 1989). At 500 nM, diazepam induced almost a doubling of the EC_5 GABA-activated current, confirming the presence of the γ2L subunit in the receptor complex (results not shown).

The inhibitory effect of PS at α1β2γ2L was confirmed by co-applying increasing concentrations of PS with GABA at an EC_{80} concentration (30 μM; Fig. 3.1A). Interestingly, co-applied PS was found to cause little reduction of GABA peak currents, but caused a more slowly developing block of steady-state currents that could be observed as an increased apparent rate of desensitisation (Fig. 3.1B and C). Current responses were measured 10 s after the start of drug application, *i.e*. 10 s from the onset of the GABA current. The current response measured at 10 s is here referred to as a steady-state current. The IC_{50} value for PS inhibition of the steady-state current at the α1β2γ2L receptor was found to be 0.4 ± 0.1 μM (n = 7). At 100 μM PS, the steady-state current had returned to baseline before the 10 s time point, showing that steady-state currents were completely blocked at this concentration of PS. Peak currents were only inhibited by about 40% at 100 μM PS, with little inhibition seen at lower PS concentrations (Fig. 3.1B). This indicates that PS more potently blocks steady-state than peak currents.

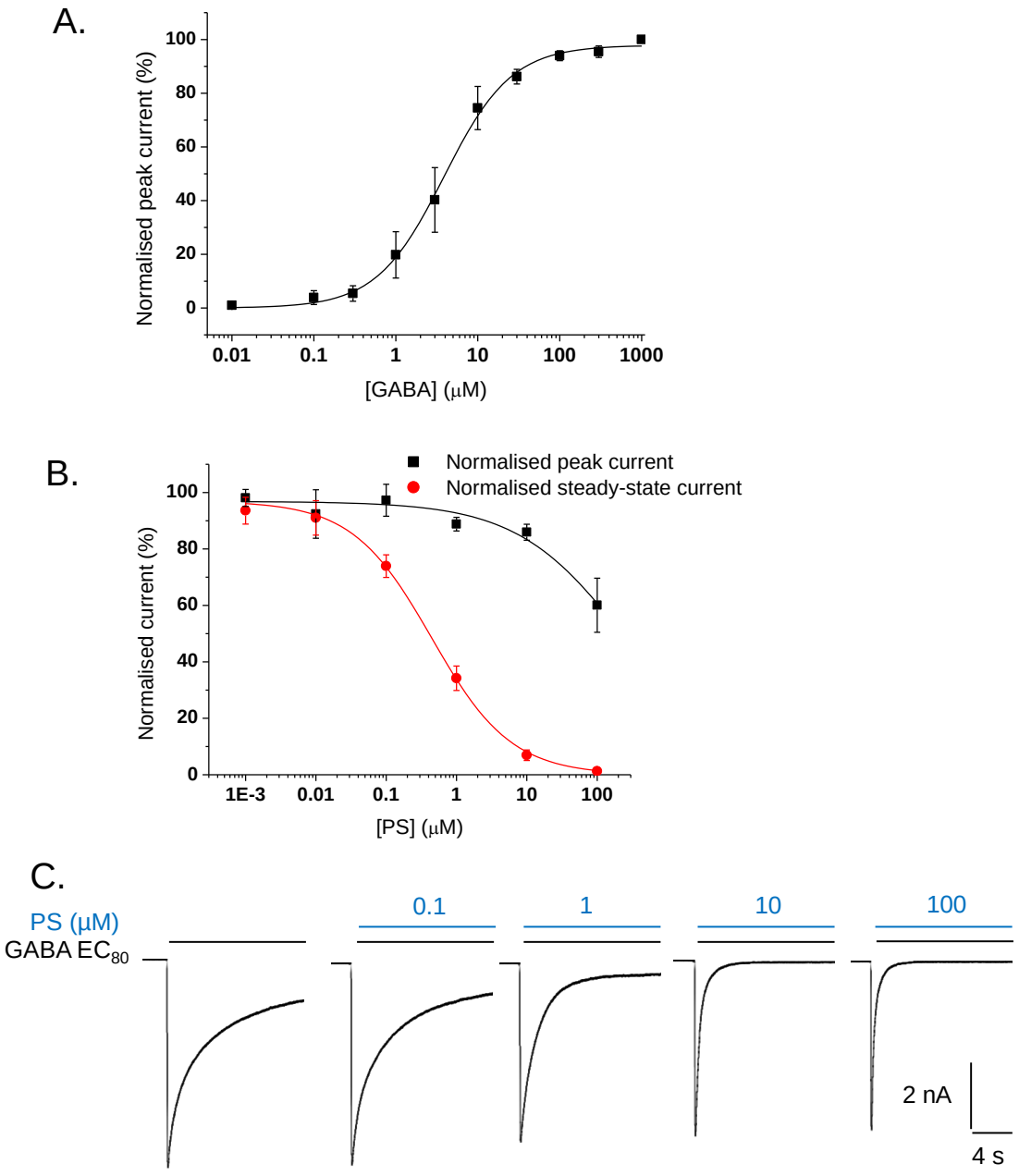

Figure 3.1 – GABA concentration-response curve and PS inhibition curve for the α1β2γ2L receptor.

A. Concentration-response curve for GABA at α1β2γ2L (n = 5). Current responses were normalised to the maximum response (E_{max}) evoked by 1 mM GABA. **B.** Inhibition curves for peak (black) and steady-state (red) currents in response to increasing concentrations of PS co-applied with GABA (EC_{80}) at α1β2γ2L (n = 7). Current responses with PS were normalised to the response evoked by GABA. Data are expressed as mean ± SEM. **C.** Example whole-cell currents for GABA EC_{80} and the inhibition caused by PS at increasing concentrations (0.1-100 μM PS).

To assess if the structurally similar inhibitory neurosteroids DHEA and DHEAS are acting similarly to PS, these steroids were co-applied with GABA at EC_{80} to the α1β2γ2L receptor (Fig. 3.2A-C). Similarly to PS, both DHEA and DHEAS caused little or no inhibition of the GABA peak current at concentrations up to 10 μM. Some inhibition of the steady-state current was observed, but only at 1 and 10 μM DHEA and DHEAS, indicating that they are less potent antagonists than PS at this receptor. At 10 μM, DHEA and DHEAS inhibited the steady-state GABA current to 48.6 ± 5.2% and 52.2 ± 7.1% of control, respectively.

Although both DHEA and DHEAS were found to be less potent than PS, some resemblance in their mechanism of action can be observed; all three compounds have little or no effect on peak currents, but cause a delayed inhibition of steady-state currents measured at 10 s. To determine if this delayed effect is due to a slowly developing block, or if it is state- or use-dependent, more experiments were carried out to further explore inhibitory neurosteroid activity. As PS is the most potent antagonist of the three inhibitory neurosteroids, the next studies focused solely on its activity.

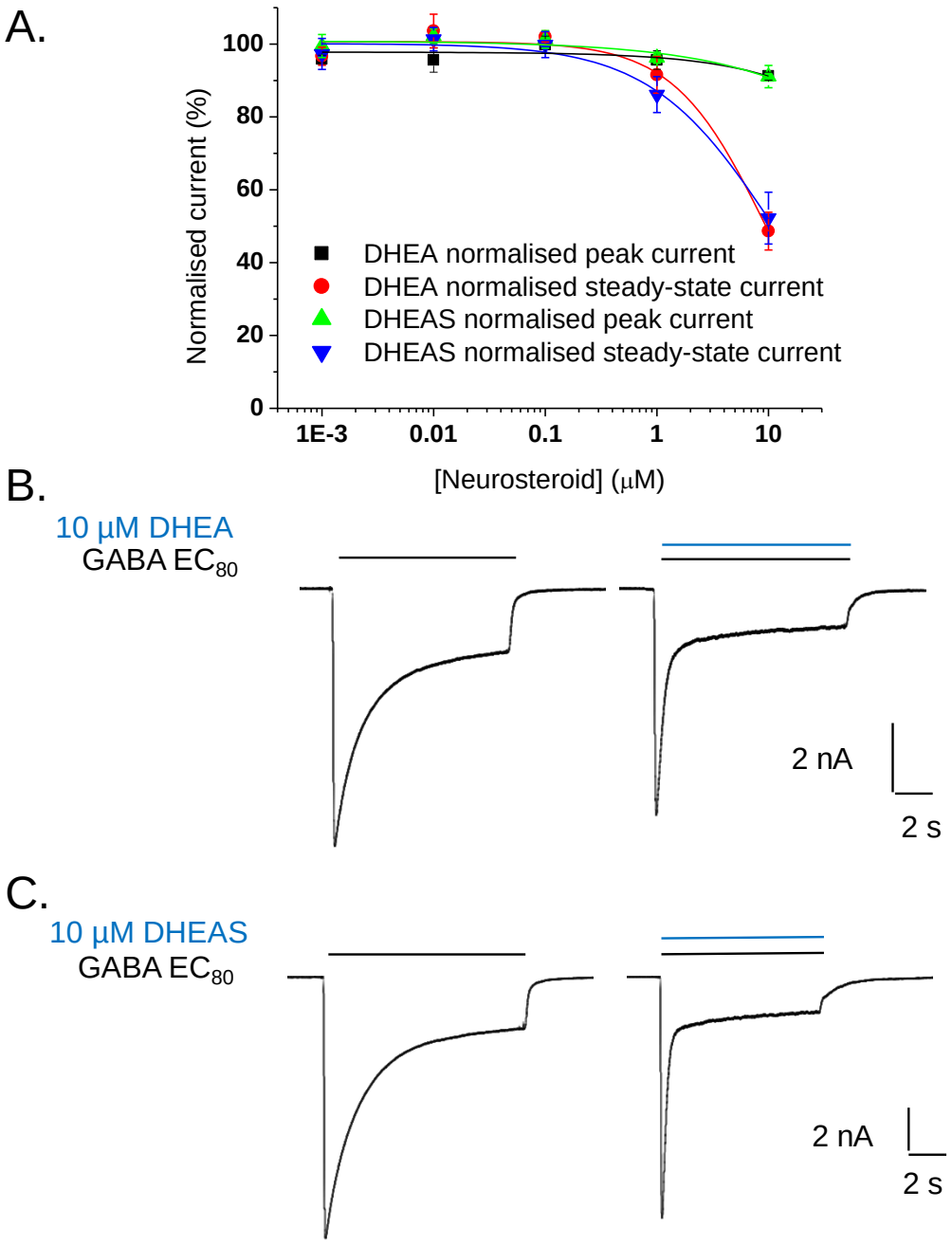

Figure 3.2 – Inhibition of GABA-evoked currents by DHEA and DHEAS at the α1β2γ2L receptor.

A. Inhibition curves for peak (DHEA in black, DHEAS in green) and steady-state (DHEA in red, DHEAS in blue) currents for increasing concentrations of DHEA and DHEAS co-applied with GABA (EC_{80}) at α1β2γ2L (n = 5). Current responses were normalised to the current response evoked by 30 μM GABA (EC_{80}). Data are expressed as mean ± SEM. **B, C.** Example traces showing whole-cell GABA EC_{80} current responses and the inhibition caused by DHEA (**B**) and DHEAS (**C**) at 10 μM.

3.2.2. Pre-applying PS does not increase inhibition

To determine if the delayed response to PS could be due to slow on-binding of the steroid to the receptor, *i.e*. that PS has a low association rate constant, PS was pre-applied to the recording chamber 20 s prior to co-application with GABA (Fig. 3.3A and B). If slow on-binding is causing the increased steady-state current inhibition, greater inhibition of the peak current would be expected following PS pre-application. Inhibition of steady-state currents was not increased by pre-application of PS; the IC_{50} for PS at α1β2γ2L is 0.4 ± 0.1 μM without pre-application, compared to 0.5 ± 0.1 μM with pre-application (n = 5; p = 0.3226). For peak current inhibition, the effect of PS was greater following pre-application. In co-application experiments without pre-application, the peak current in the presence of 100 μM PS was 60.1 ± 4.9% of the control response (GABA EC_{80}), compared with 20.9 ± 9.6% following PS pre-application, representing a doubling in inhibition (p = 0.0150). Thus, pre-application of PS increased GABA peak current inhibition at a high concentration of PS without altering the effect on steady-state currents.

A second experiment was designed to further clarify whether slow on-binding was causing the lag in PS inhibition. After achieving a stable response to successive applications of GABA EC_{80} at α1β2γ2L, 10 μM PS was pre-applied and kept in the recording chamber throughout three more subsequent co-applications of GABA and PS (Fig. 3.3C). The response to GABA and PS remained stable throughout the experiment, with only a small increase in the steady-state current at the third co-application (12.1 ± 3.5% for the first response compared with 15.1 ± 4.4% of GABA control for the third response; n = 5, p < 0.05). The peak current response remained stable throughout, and is similar to that achieved without pre-application; with pre-application, the peak response to the third application of GABA and 10 μM PS was 80.5 ± 2.9%, whereas without pre-application the response was 85.9 ± 2.8% of control (n = 5, p = 0.2230; Figs. 3.1B and 3.3C).

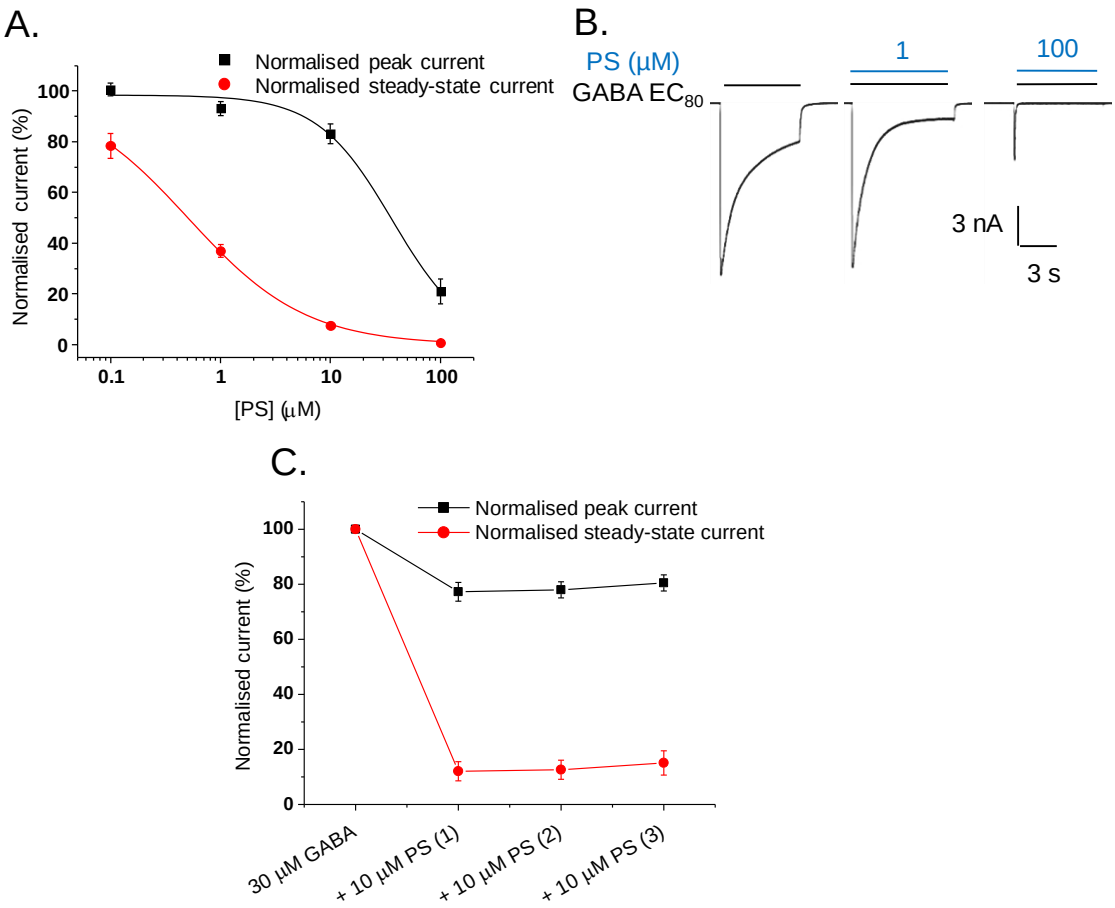

Figure 3.3 – Pre-application of PS at the α1β2γ2L receptor does not greatly increase inhibition of GABA currents.

A. Inhibition curves for peak (black) and steady-state (red) currents in response to co-applications of PS and GABA (EC_{80}) following PS pre-application at α1β2γ2L (n = 5). PS was pre-applied at the same concentration as that used in the subsequent co-application with GABA. **B.** Example traces showing the response to GABA and PS following steroid pre-application at α1β2γ2L. **C.** A graph showing the peak (black) and steady-state (red) current response to GABA (EC_{80}) before and after three repeated co-applications with 10 μM PS at α1β2γ2L (n = 5). PS was not washed out between the three co-applications to ensure PS remained bound to the receptor between GABA exposures. Data are expressed as mean ± SEM.

Thus, pre-application of PS does not increase inhibition of GABA peak currents, except at a high 100 μM concentration. In conclusion, pre-applying PS at the α1β2γ2L receptor makes little or no difference to the inhibition of GABA currents.

3.2.3. Antagonism by PS at α1β2γ2L is activation-dependent but only weakly voltage-sensitive

As pre-applying the antagonist only increased inhibition at a high concentration of PS (100 µM), it was assessed whether inhibition is state- or activation-dependent. By co-applying PS with different concentrations of GABA, it could be determined if modulation of the receptor is affected by factors like agonist occupancy and channel open probability. PS (1 µM) was co-applied with GABA at concentrations ranging between 1 µM (EC_{20}) and 1 mM (EC_{100}), and peak currents and steady-state currents were measured (Fig. 3.4A and B). Whereas inhibition of peak currents by PS was similar at all concentrations of GABA, a clear increase in steady-state current inhibition was observed at higher concentrations of GABA.

Increasing the GABA concentration from 1 to 3 µM increased the level of PS inhibition, with the normalised GABA response decreasing from 73.8 ± 4.3% at 1 µM to 61.8 ± 2.9% of control at 3 µM ($n = 7$, $p < 0.01$). Maximum inhibition was attained with 30 µM GABA, the normalised response being 33.6 ± 4.1% of control, which is significantly greater than at lower GABA concentrations ($p < 0.001$; Fig. 3.4A). Increasing GABA from 30 µM to 300 µM or 1 mM (EC_{100}) did not cause any further increase in PS block ($p > 0.05$). Accordingly, inhibition by PS has peaked when co-applied with GABA at its EC_{80} concentration (30 µM), making this the GABA concentration of choice to use in experiments regarding PS modulation of $GABA_A$ receptors.

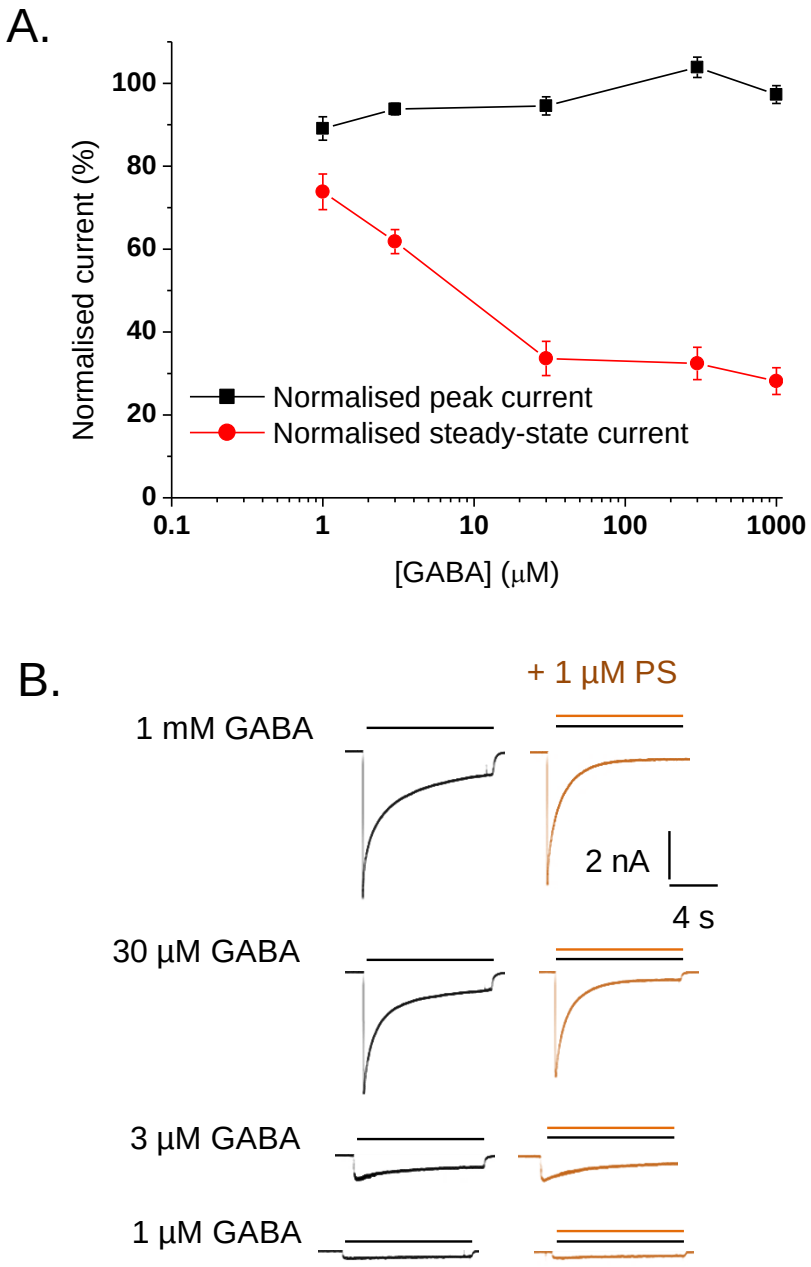

Figure 3.4 – Inhibition of GABA currents by 1 μM PS at α1β2γ2L is greater at higher concentrations of GABA.

A. Inhibition of GABA peak (black) and steady-state (red) currents in response to co-applications of 1 μM PS and increasing concentrations of GABA at α1β2γ2L (n = 7). Data are expressed as mean ± SEM. **B.** Example traces of GABA control currents (black) in the left-hand panel and after co-application with 1 μM PS in the right-hand panel (orange).

The observation that PS is more potent as an antagonist at higher GABA concentrations can mean one of three things: first, at a high concentration of agonist, the open probability of the channel is higher, meaning a channel binding

site is more accessible to PS. This observation could thus suggest that PS modulates the receptor by blocking the pore, its effect hence being use-dependent. Second, at higher concentrations of GABA, a larger proportion of receptors are bound to agonist. The increase in inhibition observed could be due to higher agonist occupancy at the receptor, arguing for the agonist needing to be bound to the receptor for PS to act as a negative modulator. Third, the increase in inhibition observed at high GABA could suggest that block by PS is state-dependent. In the presence of a high concentration of agonist, a larger proportion of receptors will be desensitised. It is possible that PS can only access its binding site and act as a negative modulator when the receptor is in a desensitised state.

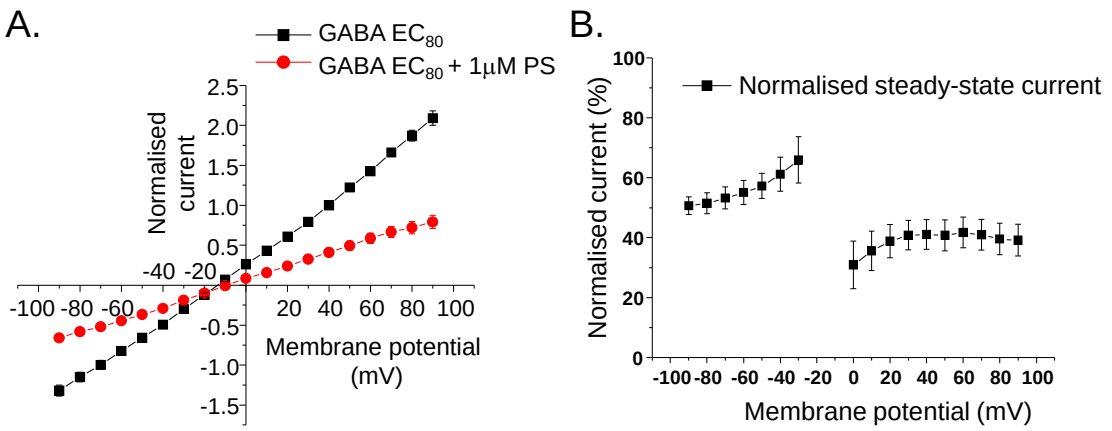

Figure 3.5 – Inhibition by PS is only weakly voltage-dependent.

A. An I/V-plot of steady-state currents for GABA (EC_{80}; black curve) and GABA co-applied with 1 µM PS (red curve) at α1β2γ2L (n = 8). The I/V-protocol was run 30 s into drug application, and currents were expressed so that the GABA response at 40 mV equals 1. **B.** The inhibition of the steady-state GABA current by PS is expressed as a percentage of the GABA control response at holding potentials between -90 and 90 mV, representing the same data as shown in A.

To investigate which one of these three scenarios is more likely to be true, a current-voltage (I/V) protocol was used to determine if antagonism by PS is voltage-sensitive. If inhibition by PS is greater at a high concentration of GABA because the open probability of the channel is high, voltage-sensitivity of PS block would be expected. As PS carries a negatively charged sulphate group on the C3 position of its A ring, greater block can be predicted to develop at depolarised holding potentials as this would attract PS towards the inside of the cell membrane. As shown in Fig. 3.5A and B, only a change in inhibition of about

12% was observed between hyperpolarised and depolarised membrane potentials, with the steady-state current in the presence of 1 µM PS being 50.7 ± 2.9% of control at -90 mV, compared to 39.1 ± 5.3% at 90 mV (n = 8, p = 0.0087). The weak voltage-sensitivity of PS suggests that binding is not strongly affected by the membrane electric field, arguing for the binding site to be located outside the channel pore. The activation-dependence of PS modulation is therefore more likely to be due to either higher agonist occupancy or state-dependence of block.

3.2.4. PS and PTX do not compete for binding at α1β2γ2L

To further examine if binding of PS within the channel pore is likely, an experiment was carried out to determine if PS competes for binding with PTX, which is a well-established open-channel blocker of $GABA_A$ receptors and other members of the pentameric ligand-gated ion channel family (Krishek et al., 1996a; Erkkila et al., 2008; Hibbs and Gouaux, 2011). GABA was applied at an EC_{100} concentration (1 mM) to obtain a stable control response prior to co-application with 10 µM PS at the α1β2γ2L receptor. PTX (10 µM) was then pre-applied to the recording chamber to expose the receptors to the blocker before it was co-applied with GABA. Due to block by PTX being use-dependent (Yoon et al., 1993), it was applied twice with GABA to achieve a steady-state inhibition, before GABA, PTX and PS were co-applied to determine if inhibition by the two antagonists is additive (Fig. 3.6A). As can be discerned from Fig. 3.6A and B, PS has very little effect on the peak current (95.2 ± 2.0% of control) whilst the steady-state current is greatly reduced, to 8.7 ± 1.5% of the control response. In contrast, PTX has a smaller inhibitory effect on the steady-state current (73.4 ± 1.8% of control after two applications), but did greatly reduce the peak current, to 37.3 ± 8.1% of control. When PS and PTX were both applied, however, profound block of both peak and steady-state currents was present: whilst the peak current was reduced to 24.5 ± 6.4% of control, the steady-state current was reduced to 6.5 ± 2.2%.

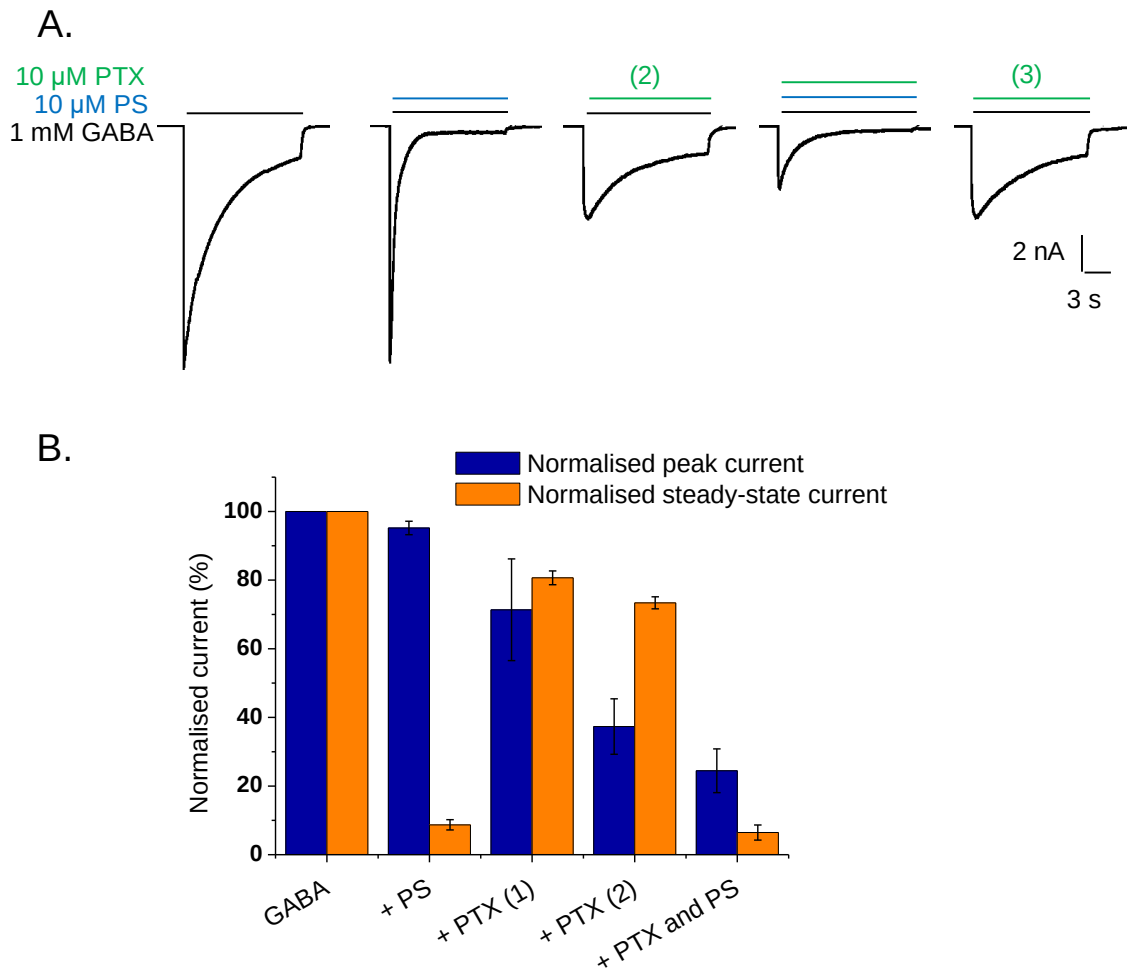

Figure 3.6 – PS and PTX do not compete for binding at α1β2γ2L.

A. Traces showing current responses of α1β2γ2L to GABA (EC_{100}: 1 mM), GABA co-applied with 10 μM PS, the response to GABA following pre-application of PTX in a second co-application (labelled (2)), the additive inhibitory effect of PS and PTX on the GABA current, and a control GABA response in the presence of PTX after PS wash-out (labelled (3)). PTX was continuously kept in the bath from the start of the PTX applications until the end of the experiment. **B.** The bar chart shows the responses of α1β2γ2L to GABA, PS and PTX as described in A. A third application of GABA with PTX only (PTX (3)) was applied as control for the added effect of PS in the presence of PTX, but this is not shown in the bar chart (n = 5). Data are expressed as mean ± SEM.

A control application of PTX following PS wash-out showed that this increased inhibition in the presence of PS was not due to greater block by PTX in its third application (Fig. 3.6B, trace labelled (3)). This observation shows that both PTX and PS are able to exert their inhibitory effect when co-applied, suggesting that there is unlikely to be an overlap in their binding sites. Put together with the low

voltage-sensitivity of PS, these two pieces of evidence argue for the binding site of the neurosteroid to be located outside the channel pore.

3.2.5. PS shows no antagonist activity when applied internally via the patch pipette

As PS has a lipophilic four-ring carbon backbone and is derived from cholesterol, it is possible that PS can partition into the membrane like other steroid molecules (Akk et al., 2009). Although potentiating neurosteroids can access their binding site from the cytoplasmic side of the membrane (Akk et al., 2005), this might not be the case for the inhibitory neurosteroids. The negatively charged sulphate group on the A ring of PS confers hydrophobicity to the molecule, which might render it incapable of crossing the membrane. PS may, however, still partition into the membrane.

To determine if PS can modulate the $GABA_A$ receptor from within the cell, 100 µM PS was applied internally through the solution in the patch pipette and the response to 1 mM GABA was recorded at 5 min intervals for 30 min. Control recordings were performed in cells with normal PS-free internal solution.

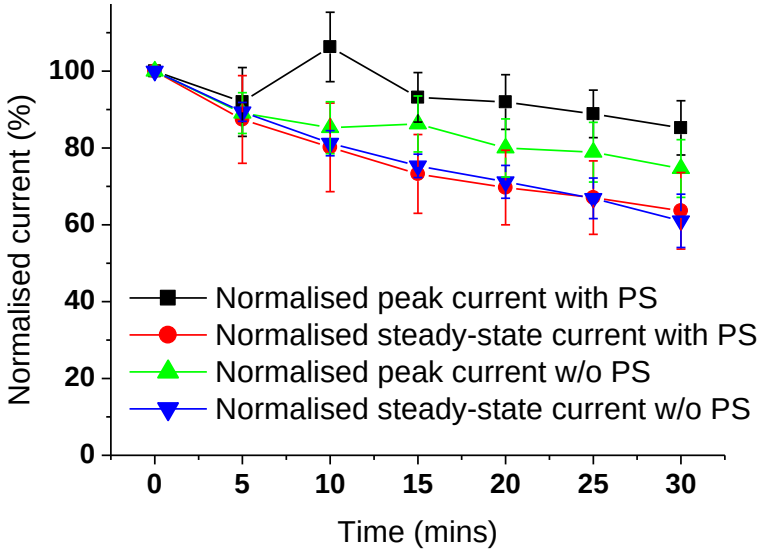

Figure 3.7 – PS does not inhibit GABA currents when applied through the patch pipette.

The graph shows the response of α1β2γ2L receptors to 1 mM GABA applied at 5 min intervals with and without 100 µM PS applied internally though the patch pipette solution (n = 7-8). The black (peak current) and the red (steady-state current) data points show the response to GABA with 100 µM PS applied through the patch pipette, whereas data points from cells with no PS are shown in green (peak current) and blue (steady-state current). Data are expressed as mean ± SEM.

As PS inhibits steady-state currents but has little effect on the peak current, a larger run-down of steady-state current is to be expected in cells containing PS in their internal solution if the steroid can still exert its action from within the cell. As demonstrated in Fig. 3.7, no greater run-down of the steady-state current was observed in cells with PS in the internal solution (63.6 ± 7.0% of initial GABA current) than in those with no steroid (61.0 ± 7.0% of initial GABA current) at the 30 min time point ($p = 0.8336$, $n = 7\text{-}8$). Likewise, peak current run-down was similar in the two populations of cells, with the current in cells exposed to no PS having reached 74.7 ± 7.0% of control compared with 85.2 ± 7.1% of control in cells with 100 µM PS in the internal solution ($p = 0.3244$). This finding implies that PS is not able to negatively modulate $GABA_A$ receptors from the cytosolic side of the cell, and suggests that its binding site is more likely to exist on the extracellular side of the protein.

3.2.6. Does PS show any receptor subtype selectivity?

As discussed in the introduction (Chapter 1), the $GABA_A$ receptor can form several receptor subtypes that comprise different subunit combinations. These receptor subtypes can display distinct pharmacological profiles, with varying sensitivities to pharmacologically active agents. Whereas only γ-containing receptors are modulated by the benzodiazepines (Pritchett et al., 1989), extra-synaptic δ-containing receptors show a greater sensitivity to potentiating neurosteroids than synaptic receptors (Belelli et al., 2002; Akk et al., 2007). To determine if PS shows any receptor subtype selectivity like the potentiating neurosteroids, various $GABA_A$ receptor subtypes incorporating each of the α1-6 subunits, β2/3 and γ2L/δ were expressed in HEK cells. The aim was to provide an indication as to whether PS is more likely to play a role in modulating synaptic or extrasynaptic receptors in a neuronal environment.

GABA concentration-response curves were first constructed for each receptor subtype in order to find their respective EC_{80} values (Fig. 3.8A and B). As inhibition by PS is affected by the co-applied concentration of GABA (see section 3.2.3), it is important to keep the 'functional concentration' of GABA the same between experiments (*i.e*. matched responses). Inhibition experiments were therefore conducted using an EC_{80} concentration of GABA, co-applied with PS (0.001-100 μM) without pre-application. A summary of GABA EC_{50} values, the Hill coefficients and approximate EC_{80} values for each receptor subtype is shown in Table 3.1.

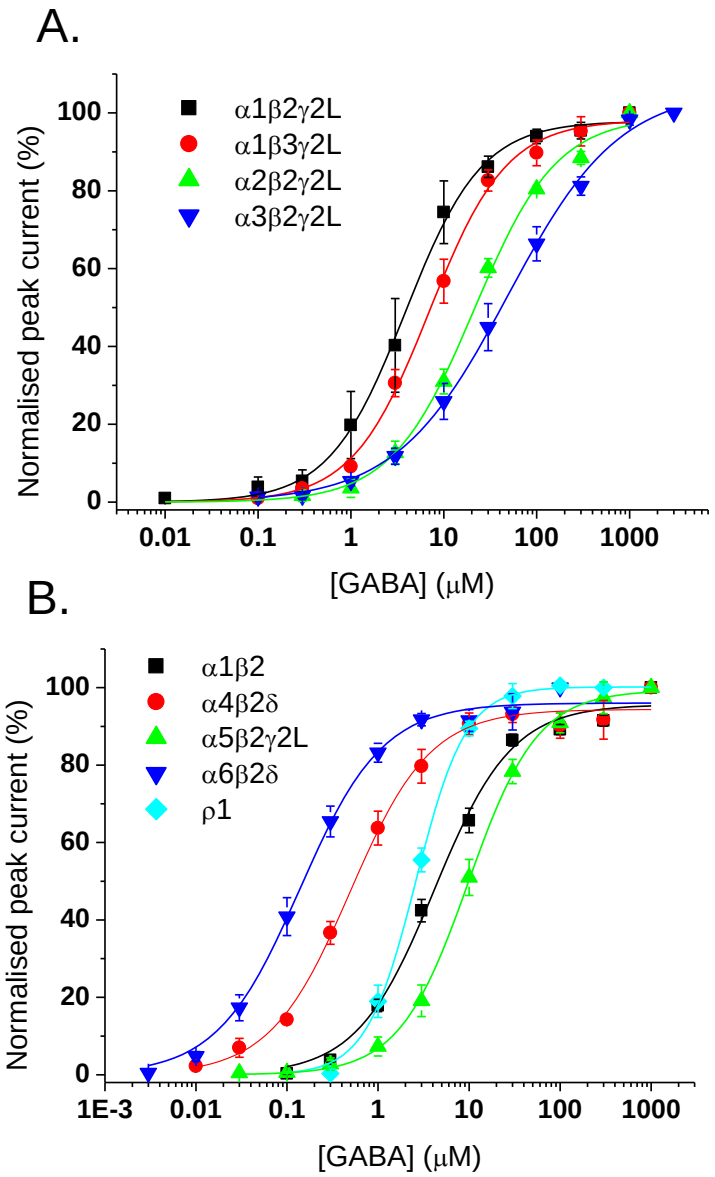

Figure 3.8 – GABA concentration-response curves for $GABA_A$ receptor subtypes.

A. GABA concentration-response curves for receptors typically present at the synapse, including α1β2γ2L (black), α1β3γ2L (red), α2β2γ2L (green) and α3β2γ2L (blue) (n = 5-8). Currents are expressed as a percentage of the maximal current in response to EC_{100} (1 mM, except for α3β2γ2L which peaks at 3 mM). **B.** GABA concentration-response curves for receptors that typically reside outside the synapse, including α1β2 (black), α4β2δ (red), α5β2γ2L (green), α6β2δ (blue) and ρ1 (cyan) (n = 5-8). Currents are expressed as a percentage of the maximal current in response to EC_{100} (300 μM - 1 mM). All data are expressed as mean ± SEM.

Receptor	GABA EC_{50} (μM)	n_H	GABA EC_{80} (μM)
α1β2γ2L	4.9 ± 1.4	1.3 ± 0.1	30
α1β3γ2L	7.5 ± 1.2	1.1 ± 0.1	30
α2β2γ2L	21.1 ± 2.1	1.0 ± 0.1	100
α3β2γ2L	64.6 ± 14.3	0.8 ± 0.1	300
α1β2	4.4 ± 0.6	1.0 ± 0.0	20
α4β2δ	0.5 ± 0.1	1.0 ± 0.1	3
α5β2γ2L	10.3 ± 1.5	1.2 ± 0.1	30
α6β2δ	0.2 ± 0.0	1.1 ± 0.1	1
p1	2.6 ± 0.3	1.7 ± 0.1	10

Table 3.1 – GABA concentration-response parameters for $GABA_A$ receptor subtypes.

Data are derived from the GABA concentration-response curves shown in Figure 3.8 (n = 5-7). All values are mean ± SEM.

As shown in Fig. 3.9A-D, PS exhibits a similar profile of block at each receptor subtype studied, except at the ρ1 receptor which was notably less sensitive. At this receptor, inhibition of both peak and steady-state currents was only present at 100 μM PS (see traces in Fig. 3.10C). For the heteromeric αβγ/δ receptors, PS inhibition of steady-state currents yielded IC_{50} values ranging between 0.4 and 1.3 μM, as summarised in Table 3.2. All receptors containing β2 and γ2 expressed with α1,2,3 or 5 had similar IC_{50} values ($p > 0.05$), whereas the α1β2 heteromer was somewhat less sensitive to PS than the receptors containing γ2L ($p < 0.001$). Similarly, replacing β2 with β3 made the α1βγ2L receptor less sensitive to the effect of PS on steady-state current ($p < 0.001$). The δ-containing receptors, α4β2δ and α6β2δ, were also less sensitive to PS than the γ2L-containing heteromers, but were not different from α1β2. Taken together, these results suggest that the β and γ/δ subunits are more important in determining the potency of PS than the α subunit isoform (α1-6). However, the observed

differences in IC_{50} values between the receptor subtypes are relatively small (Table 3.2).

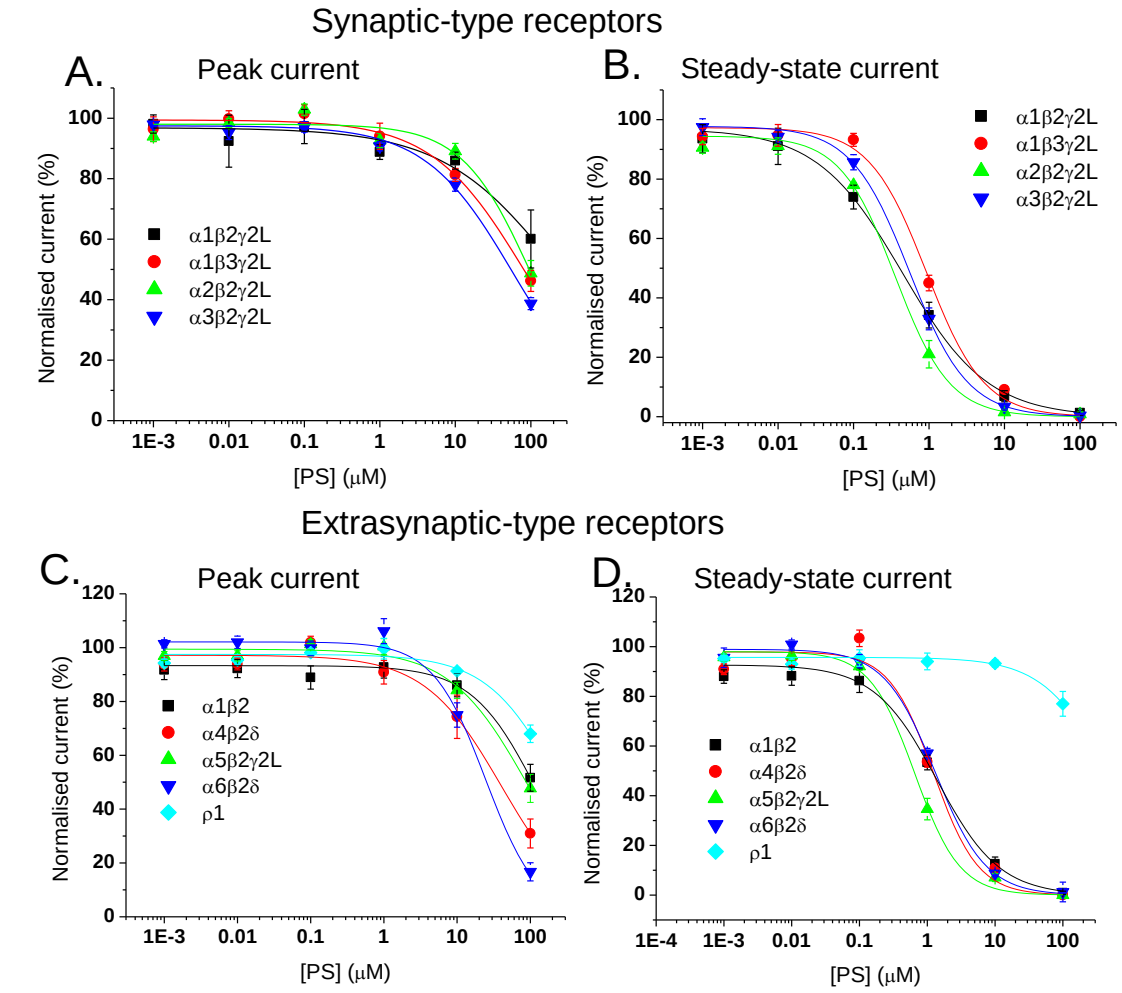

E. **α1β2γ2L** – a synaptic-type receptor

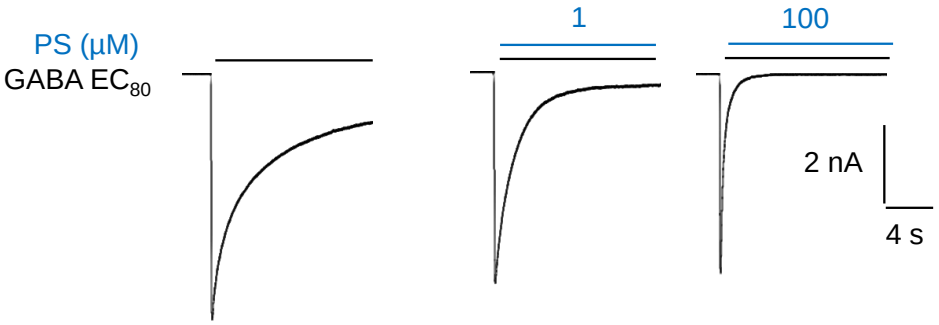

F. **α4β2δ** – an extrasynaptic-type receptor

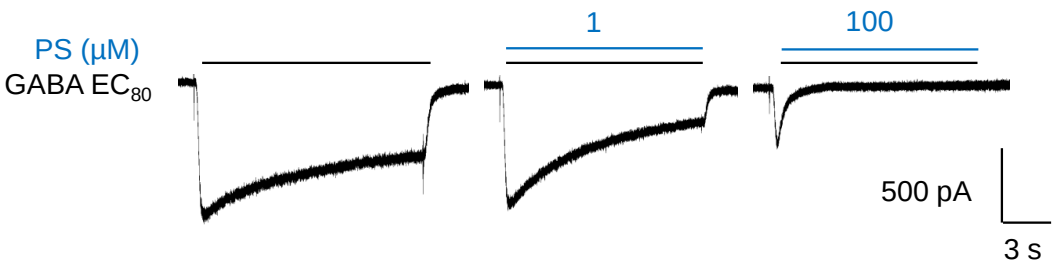

Figure 3.9 – Inhibition of GABA currents by PS at various $GABA_A$ receptor subtypes.

A. Inhibition of GABA EC_{80} peak currents by PS at typical synaptic receptors, including α1β2γ2L (black), α1β3γ2L (red), α2β2γ2L (green) and α3β2γ2L (blue) (n = 5-7). **B.** Inhibition of GABA EC_{80} steady-state currents by PS at typical synaptic receptors, including α1β2γ2L (colour-coded as in A.), α1β3γ2L, α2β2γ2L and α3β2γ2L (n = 5-7). **C.** Inhibition of GABA EC_{80} peak currents by PS at receptors that typically exist outside the synapse, including α1β2 (black), α4β2δ (red), α5β2γ2L (green), α6β2δ (blue) and ρ1 (cyan) (n = 5-6). **D.** Inhibition of GABA EC_{80} steady-state currents by PS at receptors that typically exist outside the synapse, including α1β2 (colour-coded as in C.), α4β2δ, α5β2γ2L, α6β2δ and ρ1 (n = 5-6). Data are expressed as mean ± SEM. **E.** Example traces for a GABA EC_{80} response and the effect of co-application with 1 and 100 μM PS at α1β2γ2L, a typical synaptic-type receptor. **F.** Example traces for the GABA EC_{80} and PS responses at a typical extrasynaptic-type receptor, α4β2δ.

The differences observed in the block of peak currents by a high concentration of PS (100 μM) at the different receptor subtypes were larger than the differences in the block of steady-state current (Fig. 3.9A and C, example traces in E and F). Compared with inhibition of the α1β2γ2L GABA peak current (60.1 ± 9.6% of GABA control current), inhibition by 100 μM PS was 43.3% greater at α6β2δ (16.7 ± 3.4% of control; $p < 0.001$) and 29.1% greater at α4β2δ (31.0 ± 5.4% of control; $p < 0.01$). The least inhibition of peak current by PS was observed at ρ1 (68.0 ± 3.3% of GABA control current), but this block was not statistically different from that observed at the synaptic-type $GABA_A$ receptors ($p > 0.05$).

As inhibition of the ρ1 receptor by PS was distinctly different from the rest of the $GABA_A$ receptor subtypes, a further set of experiments was undertaken to characterise the pharmacological profile of PS at this receptor. If it was found to be largely insensitive to modulation by PS, ρ1 could potentially be used to dissect the location of the binding site for PS by using site-directed mutagenesis and receptor chimeras. As inhibition of α1β2γ2L by PS was found to depend on the concentration of GABA, it was investigated whether this also applied to the ρ1 receptor. As shown in Fig. 3.10A, 30 μM PS was co-applied with GABA at concentrations between 1 μM (EC_{20}) and 300 μM (EC_{100}). For both peak and steady-state currents, the normalised response to PS was 80-90% of the GABA control response at all concentrations of GABA, suggesting that there is no activation-dependent block at this receptor.

To determine whether PS caused greater inhibition of ρ1 receptor-mediated GABA currents if allowed more time to bind, PS was pre-applied at least 20 s prior to each co-application of GABA and PS. Inhibition was not greater following pre-application for peak or steady-state GABA currents at 100 µM PS ($p > 0.05$), indicating that allowing PS more time to bind to the receptor does not increase inhibition at the ρ1 receptor (Fig. 3.10B). Taken together, these results indicate that the ρ1 receptor is largely insensitive to modulation by PS at concentrations ranging between 0.001 and 10 µM, but some inhibition is evident at 100 µM (Fig. 3.10C).

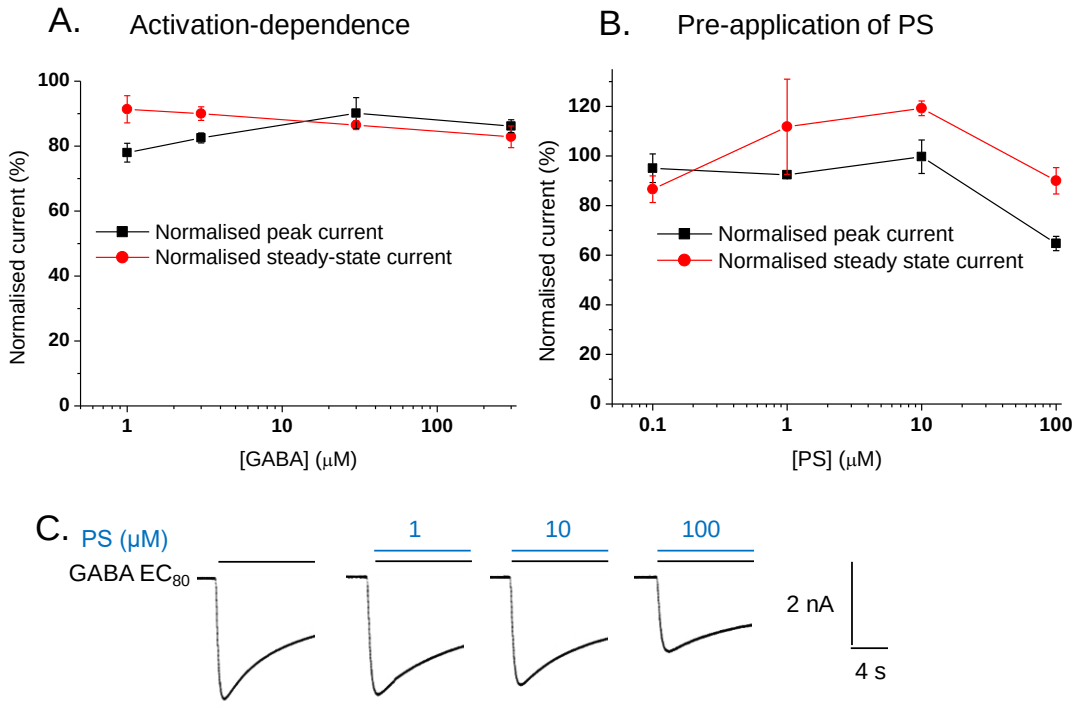

Figure 3.10 – Characterisation of the activity of PS at the ρ1 receptor.

A. Co-application of 30 µM PS with various concentrations of GABA to determine if inhibition of ρ1 by PS is activation-dependent (n = 7). **B.** The response of ρ1 to GABA EC_{80} (10 µM) and PS at various concentrations following PS pre-application (n = 3). PS was pre-applied at the same concentration as that used in the subsequent co-application. Data are expressed as mean ± SEM. **C.** Example traces for the response of the ρ1 receptor to GABA EC_{80} and PS (1-100 µM) co-applications.

Receptor	PS IC_{50} (μM)	n_H
α1β2γ2L	0.4 ± 0.05	0.8 ± 0.1
α1β3γ2L	1.0 ± 0.08	1.3 ± 0.2
α2β2γ2L	0.4 ± 0.05	1.3 ± 0.2
α3β2γ2L	0.6 ± 0.05	1.2 ± 0.1
α1β2	1.3 ± 0.07	0.9 ± 0.1
α4β2δ	1.3 ± 0.1	1.4 ± 0.1
α5β2γ2L	0.7 ± 0.1	1.3 ± 0.1
α6β2δ	1.3 ± 0.1	1.1 ± 0.03
p1	> 300	-

Table 3.2 – Functional parameters for PS derived from inhibition curves.
Data are derived from the curves shown in Figure 3.9 for inhibition of GABA EC_{80} steady-state currents by PS (n = 5-7). All values are mean ± SEM.

3.2.7. Does PS act as a negative allosteric modulator at receptors that typically exist outside the synapse?

Due to the fact that extrasynaptic receptors residing outside the synapse are unlikely to experience concentrations of GABA as high as those used in the PS inhibition experiments described above (Farrant and Nusser, 2005; Glykys and Mody, 2007b), more experiments were carried out to see if PS can inhibit α4β2δ GABA currents when lower concentrations of ambient GABA are used to reproduce the conditions of tonic inhibition.

To determine if PS acts as an activation- or state-dependent antagonist at α4β2δ, or if inhibition can occur at lower concentrations of agonist, the neurosteroid was co-applied with GABA at concentrations ranging between 0.1 μM (EC_{15}) and 3 μM (EC_{80}). As with α1β2γ2L, 1 μM PS produced greater inhibition at the relatively higher (1-3 μM) concentrations of GABA at the α4β2δ receptor (Fig. 3.11A and

C), with maximal block being reached at 1 µM GABA or higher (> EC_{50}). Whereas the peak current in the presence of PS was around 90% of the GABA control current at all agonist concentrations, the steady-state current was reduced to approximately 55% of control when GABA was applied at 1 µM (EC_{70}) or higher concentrations. This shows that PS acts as a state-dependent antagonist also at α4β2δ receptors, which raises the question as to whether inhibition is likely to occur at receptors located outside the synapse where ambient GABA concentrations are likely to be lower.

To investigate whether inhibition of a tonic GABA current is likely to occur, HEK cells were kept in a Krebs solution containing 100 nM GABA for a few minutes to let the 'tonic' GABA current reach steady state, before PS was applied at increasing concentrations to estimate the extent of inhibition of this emulated tonic current. As 100 nM is near the GABA EC_{15} concentration for the α4β2δ receptor (Fig. 3.8B), a small 'tonic' current (50-300 pA) was present. GABA is thought to exist at high nanomolar concentrations in the extracellular space of the CNS, making this a suitable concentration to use in this experiment (Lerma et al., 1986; Tossman et al., 1986). The amplitude of the 'tonic' current was estimated by washing out GABA after the steroid applications, and inhibition was expressed as a percentage of this current. Inhibition was present at concentrations of PS higher than 0.1 µM (Fig. 3.11B and D), with full block reached at 100 µM. Interestingly, 100 µM PS caused an outward current that was greater than the GABA current, suggesting that the steroid might also be acting at a receptor that is endogenously expressed in HEK cells. As a control, 100 µM PTX was applied and was found to cause a smaller outward current than PS (traces in Fig. 3.11D). Whereas PTX seems to fully inhibit the 'tonic' current, PS produced an outward current that was larger than the GABA current. This can either be due to block of a small standing current present in HEK cells or activation of an endogenously expressed receptor by PS (see section 3.2.8).

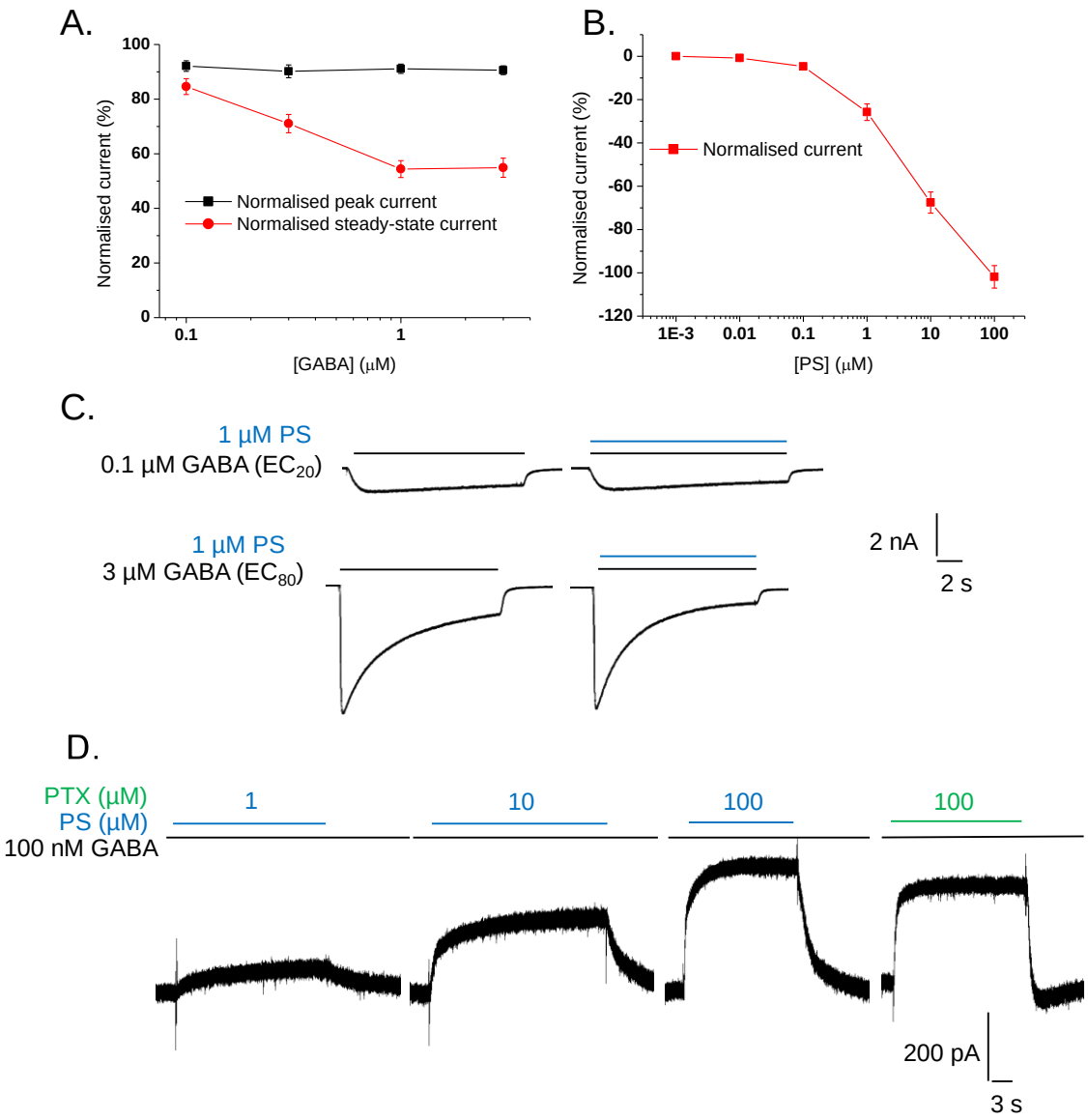

Figure 3.11 – Characterisation of PS modulation of the α4β2δ receptor.

A. PS (1 μM) was co-applied with GABA at various concentrations to determine if inhibition of α4β2δ GABA currents is activation-dependent (n = 6). **B.** To mimic a tonic GABA current at the α4β2δ receptor, 100 nM GABA was kept permanently present in the recording chamber. The plotted data illustrate the inhibition of this current caused by PS at increasing concentrations (n = 7). Data are expressed as mean ± SEM. **C.** Example traces demonstrating the greater inhibition caused by PS at higher concentrations of GABA. **D.** Example traces showing inhibition of a 100 nM GABA current by PS, mimicking the potential effect of PS on a tonic GABA current. Also illustrated is the greater outward current caused by application of 100 μM PS compared with 100 μM PTX.

3.2.8. PS acts as an antagonist at β3 homomers

As the α subunit seemed less important for determining the potency of PS at $GABA_A$ receptors, β3 was expressed as a homomer in HEK cells to determine whether this subunit carried a binding site for PS. All three β subunits can form homomeric receptors, but of these the one formed by the β3 subunit gives the largest current and is thus the most robust to study (Krishek et al., 1996b; Wooltorton et al., 1997). Although the β3 homomer is insensitive to GABA, it can be activated by pentobarbitone (PB), which creates a slowly activating current that is followed by a rebound current upon wash-off (Wooltorton et al., 1997). For the purpose of determining whether PS can bind to the β3 subunit, PB (500 μM) was used as an agonist, and was co-applied with PS (1 – 10 μM; Fig. 3.12A and B). The neurosteroid caused a concentration-dependent block of the PB-induced β3 homomer peak current measured at 5 s, and seemed to also reduce (though to a lesser extent) the magnitude of the rebound current upon wash-off.

This observation argues that a binding site for PS must exist on the β3 subunit, raising the question as to whether the steroid binds to more than one type of subunit at the $GABA_A$ receptor.

PB (500 μM) also activates the α1β2γ2L receptor, inducing a current that could be inhibited by PS in a concentration-dependent manner (1-100 μM; data not shown). Interestingly, the rate of onset of PS inhibition was faster at the PB-activated β3 homomer and α1β2γ2L receptor compared with the GABA-activated α1β2γ2L receptor. This raised the question as to whether the binding site for PS is more accessible at a receptor complex activated by PB than by GABA, or whether PB makes the $GABA_A$ receptor enter a state that is preferable for PS inhibition. The IC_{50} values for PS-mediated inhibition of PB-activated currents both at the β3 homomer and α1β2γ2L receptor were, however, nearer 10 μM than 1 μM, making PS a less potent antagonist at a receptor activated by PB than GABA.

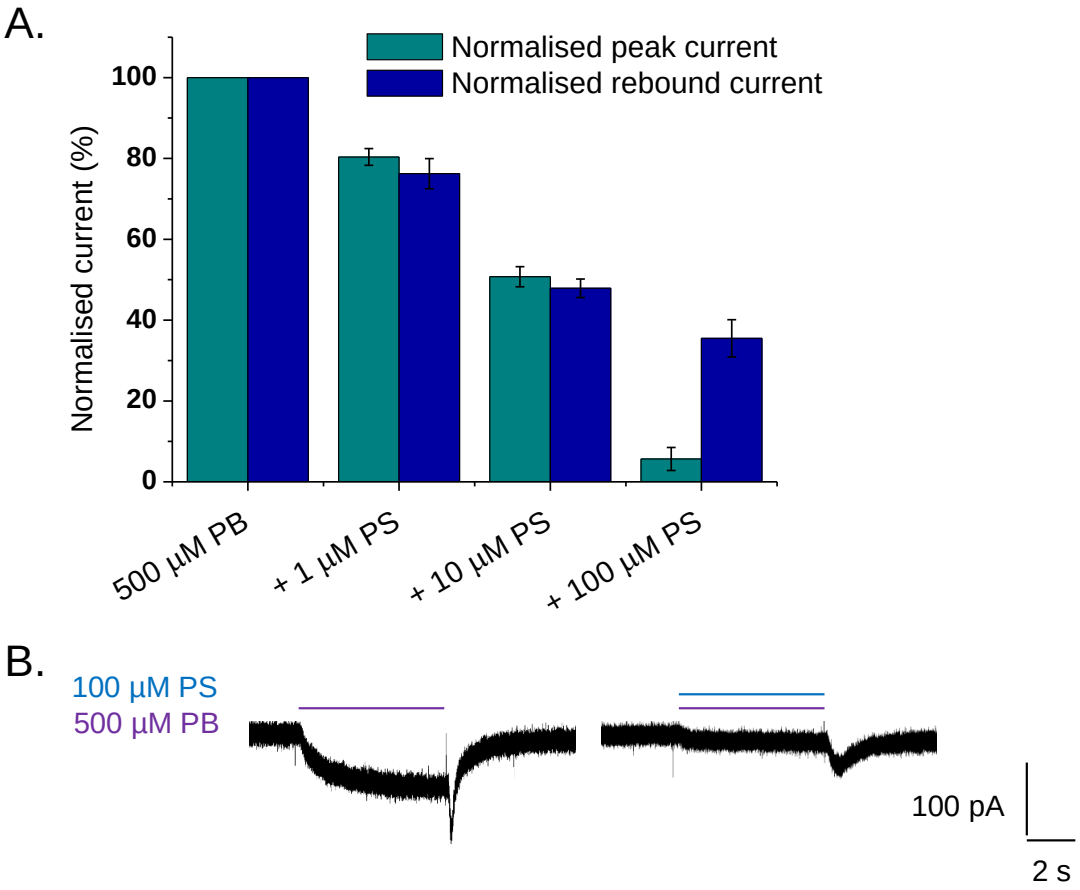

Figure 3.12 – Pentobarbitone-activated β3 homomers are antagonised by PS.

A. β3 homomers were activated by 500 µM PB and inhibition by PS (1-100 µM) was assessed following co-application. The bar chart shows how PS inhibits both the peak current (measured at 5 s) and the rebound current induced by PB (n = 8). Data are expressed as mean ± SEM. **B.** Example traces showing the β3 homomer response to 500 µM PB and inhibition by 100 µM PS.

Due to the observation that 100 µM PS seemed to cause an outward current larger than the GABA-induced current at the α4β2δ receptor and the block produced by 100 µM PTX (section 3.2.7), PS was applied on its own in untransfected cells to see if the outward current could be due to the presence of spontaneously active β homomers formed from endogenously expressed subunits (Ueno et al., 1996; Geiger et al., 2012), or another type of endogenous ion channel. For this purpose, a CsCl-based internal solution was used to remove any possible currents from endogenously expressed K^+ channels. In most untransfected cells, 100 µM PS induced a notable transient fast outward current (representative trace shown in Fig. 3.13) that could be as large as 100 pA. This

current quickly diminished and reached a plateau of 5 to 25 pA which was followed by a small rebound current upon wash-off. The transient peak differs from the current that was observed in the cells transfected with α4β2δ receptors, and is unlikely to be due to a transient block of β homomer currents. Furthermore, Krebs solution did not induce any current when applied through the U-tube, suggesting that the PS-mediated current is not an artefact. The cause of the current consequently remains unidentified. Nevertheless, its small amplitude and transient nature suggests it is unlikely to interfere with the inhibition caused by PS of extrasynaptic-type $GABA_A$ receptors.

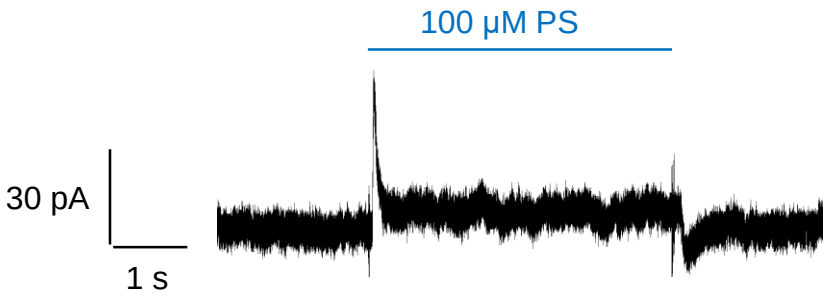

Figure 3.13 – A representative trace for the response of an untransfected HEK cell to 100 µM PS.

The cell was held at -60 mV and PS applied for the duration indicated by the bar.

3.2.9. Inhibition by PS at slower- and faster-desensitising $GABA_A$ receptor mutants

As PS causes greater inhibition at higher concentrations of GABA but does not appear to act as a classical open-channel blocker, receptors might be more susceptible to block when they are in a desensitised state. To investigate if the desensitisation kinetics of a receptor affects its sensitivity to PS, two point mutations were introduced into α1β2γ2L: a valine to phenylalanine substitution was made at residue 262 at the -3' position on the intracellular side of the M2 helix of the γ2L subunit ($\gamma2L^{V262F}$), making the heteromeric receptor desensitise faster, and a leucine to valine substitution at residue 296 in the M3 helix of the β2 subunit ($\beta2^{L296V}$) was made to slow down the rate of desensitisation of the

receptor (Gielen et al., 2015). These mutations minimally affected GABA potency compared to wild-type α1β2γ2L, and 1 mM GABA could still be used as the EC_{100}.

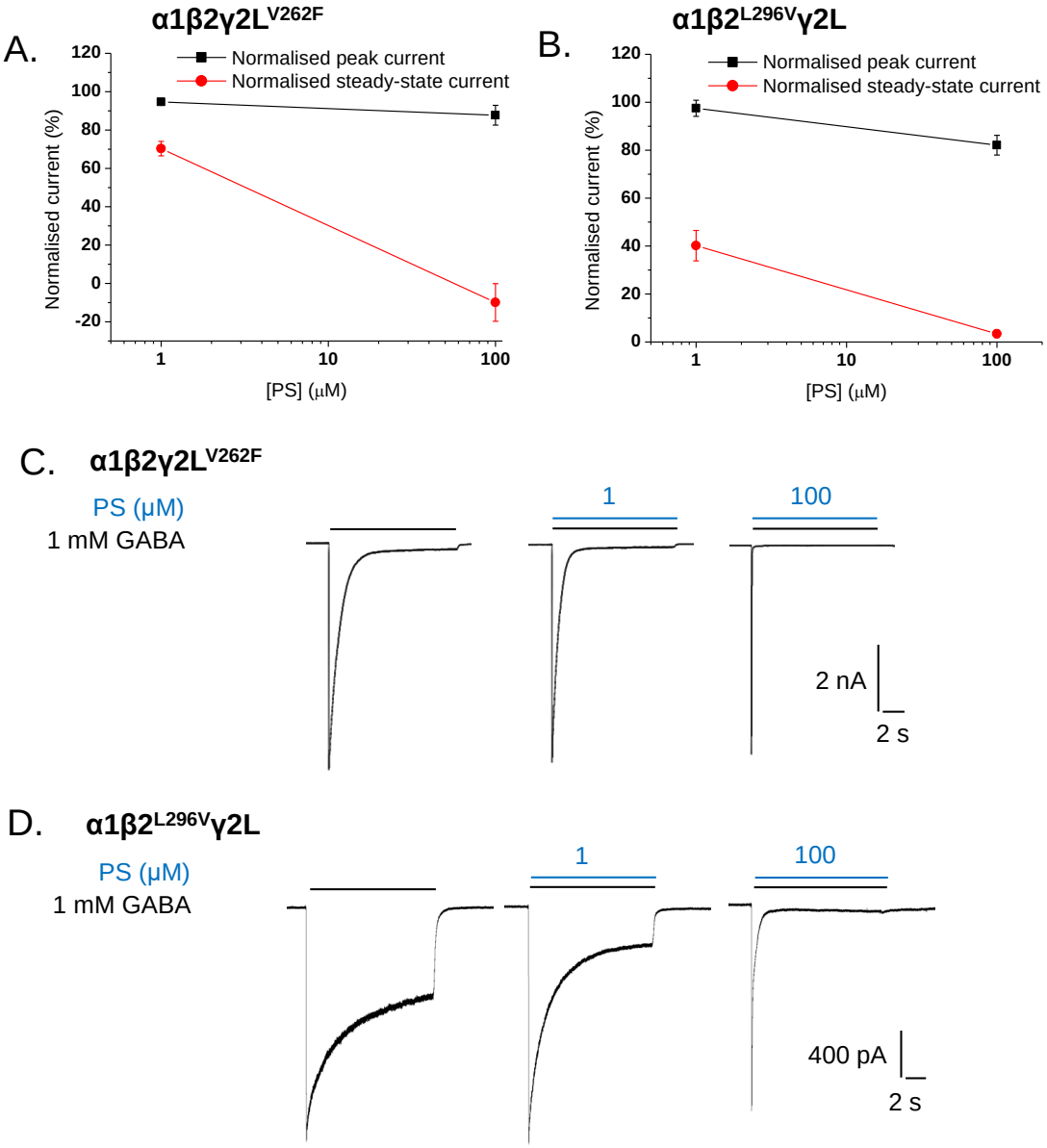

Figure 3.14 – PS antagonises GABA-mediated currents at the desensitisation mutants α1β2γ2L^{V262F} and α1β2^{L296V}γ2L

A. The graph shows inhibition of peak (black) and steady-state (red) currents caused by 1 μM and 100 μM PS during a co-application with 1 mM GABA at α1β2γ2L^{V262F} (n = 5). **B.** The graph shows inhibition of peak (black) and steady-state (red) currents caused by 1 μM and 100 μM PS during a co-application with 1 mM GABA at α1β2^{L296V}γ2L (n = 4). Data are expressed as mean ± SEM. **C, D.** Example traces for PS inhibition of GABA-mediated currents at α1β2γ2L^{V262F} (**C**), and α1β2^{L296V}γ2L (**D**).

There is a considerable difference in the desensitisation kinetics of these mutant receptors compared to wild-type. The faster-desensitising receptor mutant, α1β2γ2L^{V262F}, exhibited a very small steady-state current 10 s into GABA (1 mM) application, having reached 4.8 ± 2.3% (n = 5) of the peak current, compared to 20.1 ± 2.7% (n = 7) for the wild-type receptor (Fig. 3.14C). The steady-state current of the slower-desensitising receptor mutant, α1β2^{L296V}γ2L, reached 37.8 ± 4.1% (n = 4) of the peak current, meaning a smaller proportion of receptors were in a desensitised state compared to wild-type (Fig. 3.14D).

Both receptor mutants were sensitive to PS. As with the wild-type receptor, peak currents were minimally inhibited by the steroid, whereas marked inhibition of the steady-state current was present. For 1 μM PS, the slower-desensitising mutant, α1β2^{L296V}γ2L, was similar in profile to wild-type, with the steady-state current having reached 40.2 ± 6.3% of control at 10 s (compared with 28.1 ± 8.6% at wild-type, $p = 0.045$), suggesting its IC_{50} value is below 1 μM and similar to the wild-type receptor. At 100 μM PS, virtually full block of the steady-state current was achieved. The faster-desensitising receptor mutant, α1β2γ2L^{V262F}, was less sensitive to 1 μM PS than wild-type as steady-state currents reached only 70.3 ± 3.8% of control at 10 s ($p < 0.0001$). At 100 μM PS, a full block was however achieved, as well as block of a small standing current caused by the constitutive channel activity for this mutant. Taken together, these findings show that PS is equally efficacious at the wild-type and mutant receptors, but is less potent at the mutant that desensitises faster. Whether this difference in potency is due to the decay kinetics of the mutant receptor being different from the wild-type, or if the mutation has affected the binding or signal transduction of PS, remains elusive. It is not unexpected that PS is less potent at the faster-desensitising receptor mutant. If PS acts to promote the desensitised state, either by speeding up entry into this state or by stabilising it, there will be less scope for inhibition by PS if the mutation itself has already promoted this state. Conversely, PS would be expected to have more of an effect at the slower-desensitising receptor mutant.

3.3. Discussion

This chapter has examined the modulation by PS of recombinant $GABA_A$ receptors expressed in HEK cells. The steroid acts as a negative allosteric modulator of $GABA_A$ receptors and is significantly more potent than the structurally similar inhibitory neurosteroids DHEA and DHEAS. The onset of inhibition by PS appeared to be slow, with little effect on the peak current and a considerable effect on the steady-state current, leading to an increase in the apparent rate of desensitisation. Pre-applying PS before receptor activation did not increase inhibition of GABA currents, suggesting that slow on-binding was not the reason for the lack of peak current inhibition. The effect of PS was, however, greater at higher concentrations of GABA, which could be interpreted as activation- or state-dependence of block. Block by PS is only weakly voltage-sensitive and the steroid does not compete with the open-channel blocker PTX for binding, suggesting that the channel pore is an unlikely binding site. When applied through the internal solution of the patch pipette, GABA currents were not inhibited by PS, which shows that the steroid can only access its binding site from the extracellular side of the receptor. PS only showed a low degree of receptor subtype selectivity, although the ρ1 receptor was notably less sensitive than the heteromeric αβγ and αβδ receptors.

3.3.1. The mode of inhibition by PS of $GABA_A$ receptors

Understanding the mechanism by which inhibitory neurosteroids modulate the $GABA_A$ receptors is important for understanding the conditions under which the steroids modulate these receptors in the brain, and can also help us in building a profile of potential binding sites for the compounds. In this chapter, we have seen that PS is a significantly more potent inhibitor of the α1β2γ2L receptor than the structurally similar steroids DHEA and DHEAS, and PS was therefore chosen to be the main compound of interest. This was perhaps a bit surprising, as PS and DHEAS have previously been reported to have similar potency at the $GABA_A$ receptor, with DHEA being less potent than the other two (Park-Chung et al., 1999). Such differences may arise due to different experimental conditions,

including that the study by Park-Chung et al. used chick primary spinal cord neurones and assessed inhibition of whole-cell GABA peak currents as opposed to steady-state currents.

Inhibition by PS was greater at higher concentrations of GABA, which could suggest activation- or use-dependence of block. Inhibition appeared to develop slowly, leading to greater block of steady-state currents than peak currents. Furthermore, applying PS before GABA application and activation of the receptors did not increase inhibition, indicating that the slowly developing block is not due to slow association of PS to the receptors. Similar kinetics of PS block following pre-application compared to no pre-application have previously been reported for rat hippocampal neurones (Eisenman et al., 2003). These results are entirely consistent with the idea that receptors have to be activated before PS can modulate the response. However, contrary results have also been reported in *Xenopus* oocytes expressing bovine α1β2γ2L receptors, where greater inhibition of GABA currents was observed following PS pre-application (Zaman et al., 1992). This discrepancy may reflect the access of PS to the different cell membranes in HEK cells and oocytes, with molecules needing more time to access the receptors expressed in oocytes.

If inhibition by PS is use-dependent, repeated applications of GABA with PS permanently present in the extracellular solution would lead to a gradual increase in inhibition upon each exposure to agonist. As no such increase was observed, the greater block gained at high GABA is likely to be due to state- rather than use-dependence of block, raising the question as to whether higher inhibition at high GABA is due to high receptor occupancy or to a conformation of the receptor caused by high activity, *e.g*. desensitisation. A previous study addressed this question by assessing PS potency in the presence of a saturating concentration of a partial agonist, piperidine-4-sulfonic acid (P4S), which only produces 30-40% of the maximal GABA current (Eisenman et al., 2003; Mortensen et al., 2004). At this concentration, the potency of PS was more than threefold lower compared with a maximal concentration of GABA. When comparing the fractional block by PS of currents produced by functionally equivalent concentrations of GABA and P4S, *i.e*. concentrations activating a similar proportion of receptors, the inhibition by PS of the α1β2γ2L receptor expressed in oocytes was similar. This shows that

level of receptor activity rather than agonist occupancy is likely to be a key determinant for PS potency.

The concept of activation-dependent block can be indicative of the antagonist needing to access the channel pore to reach its binding site. For many pharmacological agents, this mode of block coincides with voltage-dependence (Newland and Cull-Candy, 1992; Cui et al., 2006). Despite its negatively charged sulphate moiety, PS (1 μM) was not found to exhibit much voltage-dependence, with block being only 12% greater at depolarised than hyperpolarised membrane potentials. Similar findings on the rate and extent of block have been reported by others in oocytes, HEK cells and rat cortical neurones (Majewska et al., 1988; Akk et al., 2001; Eisenman et al., 2003), and again strongly suggest that PS does not act as an open-channel blocker and that its binding site is likely to be located outside the channel pore. Also, the sulphate moiety of PS may not be essential for $GABA_A$ receptor inhibition (Seljeset et al., 2015). These findings suggest that the binding by PS is hardly influenced by the membrane electric field.

The profile of block by PS has previously been shown to be similar to that of PTX at low GABA concentrations (Eisenman et al., 2003). In early studies, PTX was found to displace PS in rat brain membranes (Majewska et al., 1990), and PS was found to competitively inhibit the binding of the PTX-like blocker and convulsant, t-butylbicyclophosphorothionate (TBPS) in rat synaptosomes (Majewska and Schwartz, 1987). Radioligand displacement is often interpreted as competition by two compounds for binding to the same site, but for allosteric proteins like the $GABA_A$ receptor, this is not always the case. Furthermore, mutating the 2' residue of the M2 helix of $GABA_A$ receptor α and/or β subunits led to the identification of a possible binding site for PTX in the channel pore (Zhang et al., 1994; Xu et al., 1995), which is supported by the crystal structure of GluCl bound to PTX at this site (Hibbs and Gouaux, 2011). Due to these similarities and possible overlap in binding sites for PS and PTX, an experiment was conducted to try and determine if the two antagonists compete for binding at α1β2γ2L. As shown in Fig. 3.6, PS and PTX did not appear to compete for binding as their inhibitory effect on GABA currents were shown to be almost additive. Moreover, the effects of PS and PTX have been described as distinctly different at high GABA concentrations by others, with PTX having little or no effect on steady-

state currents (Eisenman et al., 2003). As PS markedly attenuates steady-state currents at high GABA concentrations, this result strengthens the hypothesis that the mechanism of block by PS and PTX are distinct and hence the compounds are likely to have separate binding sites.

As potentiating neurosteroids have been found to partition into the plasma membrane and can exert their effect from the cytosol (Akk et al., 2007, 2009), it was important to determine if PS can also modulate the α1β2γ2L receptor from within the cytosol. As the response to extracellular GABA was no different in cells with 100 µM intracellular PS compared with no PS, it is likely that PS can only reach its binding site from the extracellular side of the membrane. This result also suggests PS has a defined binding site rather than affects the receptor protein in a non-specific manner. This is also supported by the finding that TRPM3 channels can be activated by extracellular but not intracellular PS (Wagner et al., 2008).

3.3.2. PS exhibits little receptor subtype selectivity at recombinant $GABA_A$ receptors expressed in HEK cells

Knowing whether an endogenous molecule exhibits any $GABA_A$ receptor subtype selectivity can help us predict in which regions of the brain and subcellular locations the compound is likely to have an effect. To determine whether PS is receptor subtype selective, its potency was determined at α1-3β2γ2L, α5β2γ2L, α4β2δ and α6β2δ receptors heterologously expressed in HEK cells. When co-applied with GABA at an EC_{80} concentration at these receptor subtypes, PS IC_{50}s for the block of steady-state current were in the range of 0.4 to 1.3 µM. Although the differences in potency at some of the subtypes are statistically different, the small difference observed suggests that not much subtype selectivity is likely to exist under physiological conditions. A somewhat higher efficacy of PS for block of peak current was, however, observed at the δ-containing receptors, and could imply a potential role for PS in modulating GABA-mediated tonic currents.

The potency of PS has previously been shown to be similar at α1β2γ2L and α5β2γ2L receptors expressed in *Xenopus* oocytes when co-applied with GABA at an EC_{80} concentration (Rahman et al., 2006), which supports the findings

presented here. Furthermore, Rahman et al. found that the potency and efficacy of PS were increased in the presence of the potentiating neurosteroid THDOC, which corroborates the hypothesis that high receptor activation or increased channel open probability promotes inhibition by PS. Contrasting results have also been reported: a study of bovine α1/3β2γ2 receptors expressed in *Xenopus* oocytes showed that the α3-containing receptor was tenfold more sensitive to PS than the α1β2γ2 receptor when co-applied with GABA at an EC_{50} concentration. Another study showed that PS was more potent at α6β3γ2 than at α6β3δ expressed in HEK cells, suggesting that the potency of PS is reduced by the δ subunit (Zhu et al., 1996). It should be noted, however, that they also reported a lower potency and efficacy of THDOC at the δ-containing receptor, a finding that has later been disputed (Belelli et al., 2002). Furthermore, PS was found to be twofold more potent at the α4β3γ2 receptor than the α4β3δ receptor expressed in mouse L(-tk) fibroblast cells, suggesting that the γ2 subunit confers increased sensitivity to PS (Brown et al., 2002).

Similarly to that noted for PS, the α subunit (1-6) does not influence the potency of potentiating neurosteroids to a great extent when co-expressed with the β1 and γ2L subunits in oocytes, with EC_{50} values being in the range of 74 to 317 nM when co-applied with GABA EC_{10} (Belelli et al., 2002). The β subunit isoform did not influence the modulatory actions of allopregnanolone (Hadingham et al., 1993; Belelli et al., 2002), which is different from what was observed for PS, as replacing β2 with β3 in the α1βγ2L complex reduced its potency. The efficacy of the potentiating neurosteroids does, however, vary greatly between receptor subtypes at physiological concentrations (3-100 nM) of the compounds, allowing for receptor selectivity under physiological conditions. At δ-containing receptors, allopregnanolone can potentiate the response to GABA EC_{10} beyond that produced by a saturating concentration of GABA (Belelli et al., 2002). This shows that for potentiating neurosteroids, δ-containing receptors are not necessarily sensitive to lower concentrations of the steroids, but the maximum effect (macroscopic efficacy) is greater than at γ2-containing receptors, and a larger effect is thus likely to be observed at low concentrations of steroid at these receptors (Belelli et al., 2002; Wohlfarth et al., 2002; Akk et al., 2007). The potentiating neurosteroids are therefore more likely to show selective receptor

modulation than PS as the inhibitory neurosteroid shows similar potency and efficacy at all receptor subtypes studied. To determine whether the lower potency of PS observed at α4/6β2δ compared with the α1-3β2γ2L receptors is due to the α4/6 subunit or the δ subunit, a control experiment replacing the δ subunit with γ2L is required. However, PS was found to be twofold more potent at the α4β3γ2 receptor than the α4β3δ receptor expressed in mouse L(-tk) fibroblast cells, suggesting that the γ2 subunit confers increased sensitivity to PS (Brown et al., 2002).

The receptor subtype that did stand out from the crowd was the ρ1 receptor, which showed little or no sensitivity to PS at concentrations below 100 μM. This is different from the potentiating neurosteroids, which can act as positive and negative allosteric modulators of GABA currents at the ρ1 receptor, though the concentrations needed are higher than at heteromeric receptors (> 1 μM) (Morris et al., 1999). PS has also been shown to be a very weak blocker of the human ρ1 receptor expressed in oocytes (Li et al., 2007), which corroborates the present findings. As the ρ1 subunit forms a homomeric pentamer in HEK cells, the receptor is ideal for use in structure-function studies. Due to its low sensitivity to PS, chimeras of ρ1 and other $GABA_A$ receptor subunits, as well as point mutations, were used to further study and characterise the mechanism of inhibition by PS at these receptors. Using ρ1 as a 'null' receptor, the aim was to identify the binding site for PS (see Chapter 4).

Whether the binding site for PS is present at one or more subunits, is not clear. As α1β2 heteromers were modulated by PS, the binding of the steroid does not depend on the presence of the γ2L subunit. As the β subunits can form homomeric complexes activated by PB (Krishek et al., 1996b; Wooltorton et al., 1997), this was exploited to determine if PS can antagonise PB-induced currents at the β3 homomer in HEK cells. Inhibition of the PB-mediated currents confirmed the presence of a binding site for PS at the β3 subunit, but does not exclude the possibility that the steroid can also bind to the α1-6 and γ2L subunits.

3.3.3. PS can antagonise a 'tonic' GABA current at the α4β2δ receptor in HEK cells

Due to the enhanced block of $GABA_A$ receptor-mediated steady-state current by PS, the steroid might play a more significant role in modulating the persistent low level of tonic currents that exist outside synapses than in antagonising the fast and transient currents occurring within the synapse. However, as modulation of the α4β2δ receptor by PS was also shown to be activation- or state-dependent, it is uncertain whether the steroid will be active at the low concentrations of GABA that are likely to exist outside the synapse. To investigate whether PS is likely to modulate tonic currents under physiological conditions, a tonic GABA current was mimicked by applying 100 nM GABA to α4β2δ receptors. The concentration of GABA that is likely to exist outside the synapse has been under considerable debate, and is likely to be below 1 µM (Glykys and Mody, 2007b; Wlodarczyk et al., 2013), making 100 nM a suitable concentration to use. At concentrations of 0.1-100 µM, PS inhibited these GABA 'tonic' currents. This suggests that inhibition of tonic currents may occur despite the activation-dependent mechanism of block by PS, and this is explored further in hippocampal cultures (see Chapter 5). The inhibition by 100 µM PS was greater than that caused by 100 µM PTX, a concentration that should cause full inhibition of a GABA current (Krishek et al., 1996a). As the outward current induced by 100 µM PS also appeared to be larger than the 100 nM GABA-induced current, PS might activate or inhibit receptors that are endogenously expressed in HEK cells. One possibility is that endogenously expressed β subunits form homomers in these cells and produce a spontaneous current that is antagonised by PS (Ueno et al., 1996; Thomas and Smart, 2005). Another possibility is that an endogenously expressed K^+ channel is potentiated by PS, mediating an outward current. These aspects are discussed further in Chapter 5.

3.3.4. The potency of PS may be affected by the kinetics of the $GABA_A$ receptor

As PS is less potent at δ-containing receptors and is almost inactive at ρ1 homopentamers compared with the γ2L-containing receptors, one factor that may be influential is the kinetics of the receptor. Whereas ρ1 desensitises very little,

δ-containing receptors that typically reside outside the synapse desensitise less than the γ-containing receptors that are found at the synapse (Saxena and Macdonald, 1994; Bianchi and Macdonald, 2002; Brown et al., 2002; Yang et al., 2006). Previous studies have also suggested a role for PS in modulating desensitisation. PS increases the rate and extent of macroscopic GABA receptor desensitisation at hippocampal autapses and in nucleated patches, and appears to slow the rate of recovery from desensitisation (Shen et al., 2000). Thus, the apparent slow onset of inhibition and increased rate of decay of GABA whole-cell currents in HEK cells might be explained by PS promoting entry of the receptors into one or more desensitised states and stabilising these states. This was also supported by the observation that PS was less effective under conditions in which receptors desensitise less, as no effect on deactivation was observed when the low affinity and less desensitising agonists taurine and β-alanine were applied to nucleated patches (Shen et al., 2000). Only after longer applications of β-alanine, when some degree of desensitisation was present, did PS have an effect. These findings suggest that PS is most effective as an inhibitor under conditions in which the $GABA_A$ receptors desensitise.

To investigate this, two $GABA_A$ receptor mutants with altered desensitisation kinetics were employed. A point-mutation in the γ2L subunit, $\gamma2L^{V262F}$, makes the α1β2γ2L receptor desensitise faster, whereas a mutation in the β2 subunit, $\beta2^{L296V}$, reduces the rate of desensitisation (Gielen et al., 2015). If PS acts to promote the desensitised state of receptors, increased levels of block would be expected at the slower-desensitising $\alpha1\beta2^{L296V}\gamma2L$ receptor than at the wild-type, whereas the opposite would be predicted for the faster desensitising $\alpha1\beta2\gamma2L^{V262F}$ receptor. As predicted, lower levels of inhibition were achieved at the faster desensitising mutant in response to 1 mM GABA co-applied with 1 μM PS, whereas the slower desensitising mutant was similar to wild-type. The efficacy of PS was not affected by the mutations, as full block of the steady-state current was achieved by 100 μM PS at both receptors. The reduced potency of PS at the faster desensitising mutant may, however, be due to the mutation interfering with the signal transduction of PS, and does not in itself show that PS is less effective when desensitisation is increased. A simplified linear gating scheme for the modulation of $GABA_A$ receptors by PS is shown in Fig. 3.15.

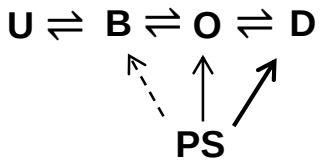

Figure 3.15 – A gating scheme for PS modulation.

This gating scheme shows that PS is likely to bind to one or more of three receptor states, which is supported by four observations. First, PS in unlikely to bind to the unbound state of the receptor (U), as pre-applying the steroid does not increase inhibition at most concentrations of PS. Second, PS might be able to bind to the occupied receptor (bound state; B), as inhibition is greater at high agonist concentrations. Third, PS probably binds to the open (O) and desensitised (D) states of the receptor since inhibition seems to be strongly dependent on receptor activation. Fourth, the overall effect of PS inhibition is to increase the proportion of receptors that enter a desensitised state, which is observed as an increase in steady-state current inhibition with increasing concentrations of PS.

3.4. Conclusion

This chapter has discussed the mechanism of block by PS at different subtypes of the $GABA_A$ receptor expressed in HEK cells. It has been shown that PS is more potent than the other two inhibitory neurosteroids that are commonly found in the brain, namely DHEA and DHEAS. Furthermore, PS exhibits a slowly-developing block of GABA currents that is not increased by pre-application or repeated receptor activation, but is greater at higher concentrations of GABA. These findings suggest that block by PS is state-dependent, which is also supported by the observation that the steroid is less potent at wild-type receptors with slower desensitisation kinetics. The greater block of steady-state than peak currents argues for PS to have a role in modulating desensitisation, possibly by promoting entry into a desensitised state or by stabilising receptors in this state.

In the pursuit of finding a binding site for PS, this chapter has shown that the steroid is unlikely to act as an open-channel blocker as it only exhibits weak voltage-dependence and does not appear to compete for binding with PTX. Furthermore, PS does not act from within the cytosol, suggesting that it needs to access the receptor from its exterior face to act as an antagonist.

PS displays little receptor subtype selectivity, although the ρ1 receptor is distinctively different from the heteromeric αβγ/δ receptor and could potentially act as a ‘null’ receptor for further structure-function studies, an aspect that is discussed in Chapter 4. Due to the effect of PS on emulated tonic currents in α4β2δ expressing cells, the steroid might have a role in modulating tonic currents under physiological conditions. This will be further discussed in Chapter 5.

Chapter 4: Searching for the pregnenolone sulphate binding site: structure-function studies on recombinant $GABA_A$ receptors

4.1. Introduction

This chapter considers the structural basis for PS inhibition of $GABA_A$ receptors through the use of the chimera approach and site-directed mutagenesis. Previous attempts have been made to find the binding site for PS. One study identified a residue located near the bottom of the second transmembrane segment (M2) of the $GABA_AR$ α1 subunit to be important for modulation by PS (Akk et al., 2001), whereas a separate group identified up to six residues in M1 and one at the top of M2 that were critical for PS and DHEAS inhibition at the *C. elegans* GABA receptor, UNC-49B/C (Wardell et al., 2006; Twede et al., 2007). To determine if the residues identified in these studies are important for modulation of murine $GABA_A$ receptors by PS, the homologous residues near the intracellular end of M2 (at 2') and those identified in the UNC-49B/C are studied in murine $GABA_A$ receptors through the use of site-directed mutagenesis. The binding site is also further probed by using ρ1-α1/β2/γ2 chimeras in an attempt to find the residue(s) that makes the heteromeric $GABA_A$ receptors more sensitive to PS compared to the ρ1 receptor.

The involvement of the $GABA_A$ receptor 2' residue, which is near the cytoplasmic end of the M2 α-helix, was first discovered by Akk et al. (2001) when carrying out single-channel recordings in HEK cells expressing recombinant $\alpha_1\beta_2\gamma_{2L}$ receptors. This residue was chosen because it had previously been shown to be involved in the block by PTX at the *Drosophila* GABA receptor RDL (Ffrench-Constant et al., 1993), as well as the mammalian $GABA_A$ ρ_1 receptor (Wang et al., 1995). Substituting the 2' valine residue of α1 (V256) and homologous alanine residue of β2 (A252) for a serine residue, the apparent association rate for PS inhibition was reduced 30-fold in cells expressing $\alpha1^{V256S}\beta2\gamma2L$ but not $\alpha1\beta2^{A252S}\gamma2L$ (Akk et al., 2001). Single channel analysis showed that the cluster duration in the presence of PS was also increased compared to the wild-type receptor, suggesting that the mutation in the α_1 subunit reduces the known ability

of PS to shorten cluster duration. Similar 2' mutations in β2 and γ2L subunits had no such effect. Despite these findings, studies of whole-cell GABA currents have shown that the inhibitory effect of PS is reduced or abolished in *Xenopus* oocytes recombinantly expressing α1β2^{A252S}γ2L or α1^{V256S}β2γ2L (Wang et al., 2006, 2007), showing that the mutation in either the α1 or β2 subunit can affect PS sensitivity.

To further explore whether the 2' residue can be involved in PS binding, the α1^{V256S} and β3^{A252S} mutations were studied here in HEK cells by recording whole-cell currents. The β3 subunit was chosen as this can also form a homomer to aid the investigation. Furthermore, the 2' residue of the ρ1 subunit was also mutated to investigate whether this residue could affect (and increase) the ρ1 receptor's sensitivity to PS.

The *C. elegans* $GABA_A$ receptor UNC-49 is a close homologue of the mammalian $GABA_A$ receptor, and is encoded by one gene, *unc-49*, that generates three different splice variants containing a shared N-terminus and three different C-termini: UNC-49A, UNC-49B and UNC-49C (Bamber et al., 1999, 2003). These are structurally and pharmacologically closely related to the mammalian $GABA_A$ receptor. Whereas UNC-49A is only expressed at low levels, high levels of UNC-49B and UNC-49C are found at the neuromuscular junction of the nematode (Bamber et al., 1999, 2005). The UNC-49B subunit can form a pentameric homomer *in vitro* and *in vivo*, whereas the UNC-49C subunit can only co-assemble with UNC-49B to form functional receptors (Bamber et al., 2005).

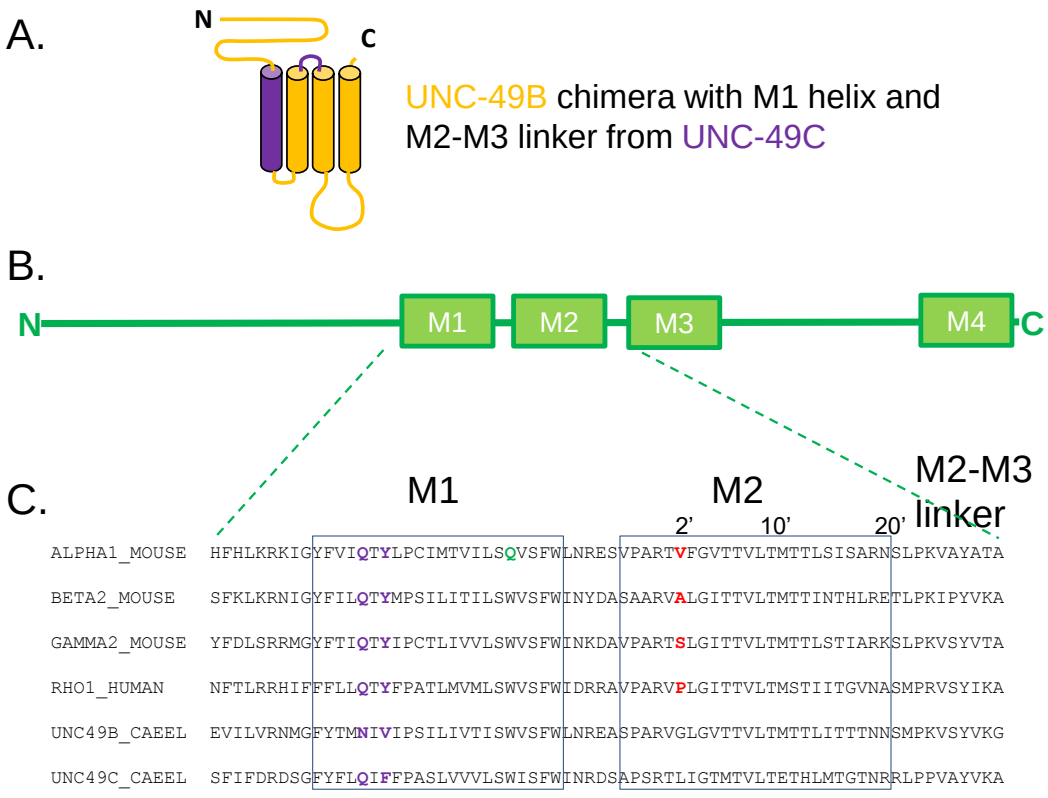

Figure 4.1 – UNC-49B/C chimera, linear transmembrane topology of a $GABA_A$ receptor subunit and sequence alignments for the mouse α1, β2 and γ2 subunits, human ρ1 and C. elegans UNC-49B and C.

A. Schematic diagram of the transmembrane topology of an UNC-49B/C chimera in which residues from UNC-49B are shown in orange and residues from UNC-49C are shown in purple. The M1 helix and the M2-M3 linker are from UNC-49C, whereas the rest of the chimera sequence is from UNC-49B. **B**. The linear transmembrane topology of a $GABA_AR$ subunit is shown, with amino acid sequence alignments for the mouse α1, β2 and γ2L subunits, human ρ1 and *C. elegans* UNC-49B and **C**. Residues discussed and mutated in this study are shown in colour: 2' residues are shown in red, $\alpha1^{Q241}$ involved in potentiating neurosteroid binding is shown in green and residues identified as important for inhibitory neurosteroid binding in the UNC-49B/C studies are shown in purple. The figure is adapted from Seljeset et al. 2015.

The finding that PS inhibits the UNC-49B/C heteromer more strongly than the UNC-49B homomer (with IC_{50}s of 2.3 µM and estimated 191 µM, respectively), suggested that the UNC-49C subunit contains residues or sequences that are important for PS modulation (Wardell et al., 2006). By introducing amino acid sequences from UNC-49C to UNC-49B, residues were identified that could convert UNC-49B into a PS-sensitive receptor. A chimera formed between UNC-49B and C, with the M1 segment and M2-M3 linker of UNC-49C and remaining

sequences from UNC-49B, showed that these two regions fully accounted for the sensitivity of UNC-49C to PS (Fig. 4.1A). Specifically, six specific residues in M1 and one residue on the top of M2 were found to increase the sensitivity of UNC-49B 57-fold, *i.e*. to the same level as the UNC-49B/C receptor complex. Mutating a neutral asparagine on top of M2 in UNC-49B to a positively charged arginine, N305R, increased the sensitivity of the receptor to PS to the same extent as the whole of the M2-M3 linker.

Two residues in M1 were identified that are conserved among the mammalian PS-sensitive $GABA_A$ receptor subunits and UNC-49C, but are different in UNC-49B (Wardell et al., 2006). These, residues 259 and 261, are a glutamine and an aromatic residue, respectively, in the PS-sensitive subunits, but are asparagine and valine in UNC-49B (Fig. 4.1B). The UNC-49B receptor with the N305R, N259Q and V261F mutations was still 6.7-fold less sensitive to PS than the chimera that contained the whole of M1, and twofold more sensitive than the UNC-49B receptor containing only the N305R mutation. Another five residues in M1 of UNC-49C were then identified, and when introduced into UNC-49B, increased the sensitivity to PS: T257F, M258L, I262F, S264A and I265S. An UNC-49B receptor with all these mutations was maximally inhibited by PS. However, reverting the V261F mutation by re-introducing the valine residue to UNC-49B did not reduce the potency of PS, suggesting that this residue was not necessary for inhibition. Consequently, a UNC-49B receptor with six M1 mutations and one M2-M3 linker mutation was found to be 57-fold more sensitive to PS than wild-type, and only 1.4-fold less sensitive than the UNC-49B/C receptor complex. However, in a later study, the N259Q and V261F mutations were found to fully account for the ability of the UNC-49C M1 domain to confer DHEAS sensitivity to UNC-49B (Twede et al., 2007).

As the N259Q and V261F mutations conferred PS sensitivity to UNC-49B and the glutamine and an aromatic residue (tyrosine) are conserved among the mammalian $GABA_A$ receptor subunits (Fig. 4.1B), these residues were explored as a potential binding site for PS in the $GABA_A$ receptor in this study. Although the UNC-49B^{N305R} mutation was found to confer PS sensitivity (Wardell et al., 2006), this residue was not explored further here as the murine α1 subunit shares the asparagine residue with UNC-49B at this position. A homology model of UNC-

49B with the N259Q and V261F mutations in the M1 segment and the N305R mutation in the M2-M3 linker is shown in Fig. 4.10 (section 4.3.4).

Finally, the chimera approach was used to probe for the binding site of PS. As the ρ1 receptor is largely insensitive to PS, chimeras between this subunit and other murine $GABA_A$ receptor subunits were used to determine if increased sensitivity to PS can be conferred by introducing amino acid sequences from other subunits to ρ1.

4.2. Results

4.2.1. $GABA_A$ receptor α1 and β3 2' mutations do not ablate inhibition by PS

Although block by PS is only weakly voltage-sensitive, the ion channel pore has repeatedly been proposed as a potential binding site. A serine mutation at the 2' position in the M2 transmembrane segment of the α1 subunit ($\alpha1^{V256S}$) was observed to cause a 30-fold decrease in the rate of block for PS (Akk et al., 2001), and subsequent whole-cell recordings in *Xenopus* oocytes also showed that inhibition by PS could be reduced or even ablated by this mutation (Wang et al., 2006, 2007). To evaluate whether this residue near the intracellular side of the channel pore is involved in PS binding or if it is just necessary for signal transduction, 2' mutations were introduced into the α1 and β3 subunit. Figure 4.2 shows the position of the 2' residues of the α and β subunits, and the amino acid side chain positions in a receptor with the $\alpha1^{V256S}$ mutation. An α^{V256C} mutation was also studied as the point mutant already existed in the lab, and due to the structural similarity of a serine and a cysteine residue.

Three 2' mutations were studied by recording GABA-evoked whole-cell currents in HEK cells expressing either $\alpha1^{V256S}$ or $\alpha1^{V256C}$ with β2 and γ2L, and $\beta3^{A252S}$ with α1 and γ2L. To assess whether these mutations affected GABA potency and the gating of the receptors, GABA concentration-response curves were derived for each mutant (Fig. 4.3). Whereas the $\beta3^{A252S}$ mutation minimally affected the EC_{50} of the $\alpha1\beta3^{A252S}\gamma2L$ receptor (6.1 ± 0.6 μM compared with 7.5 ± 1.2 μM for wild-type α1β3γ2L, $p = 0.300$, $n = 5$-6), the concentration-response curves for $\alpha1^{V256S}\beta2\gamma2L$ and $\alpha1^{V256C}\beta2\gamma2L$ were shifted to the left compared with the wild-type α1β2γ2L receptor (Fig. 4.3, Table 4.1). The $\alpha1^{V256S}\beta2\gamma2L$ receptor was about 6-fold more sensitive to GABA, with the EC_{50} reduced from 4.9 ± 1.4 μM for wild-type to 0.8 ± 0.2 μM for the mutant ($p = 0.0104$, $n = 5$-6). Similarly, the $\alpha1^{V256C}\beta2\gamma2L$ receptor had an EC_{50} of 1.1 ± 0.2 μM, representing a 4.5-fold increase in GABA sensitivity compared with wild-type ($p = 0.0145$, $n = 5$). Thus, the α1 2' mutations appear to increase GABA potency by 4-5 fold, whilst the β3 2' mutation had no effect.

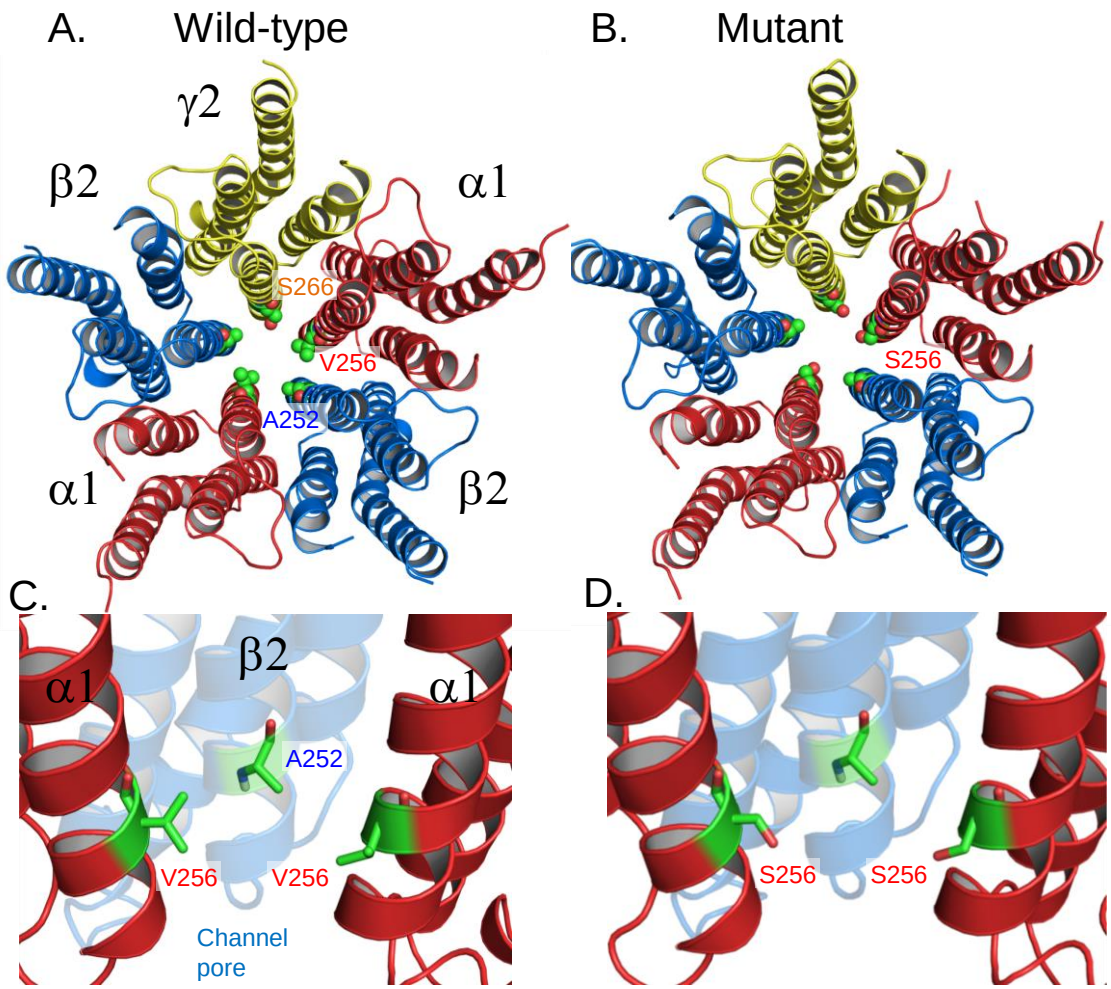

Figure 4.2 – $GABA_A$ receptor homology models showing the position of the 2' residue in the wild-type and mutant receptor.

A. The model shows a plan view of the wild-type murine α1β2γ2L receptor with the extracellular domain removed. The transmembrane domains and the ion channel lining formed by the M2 helix of each subunit are shown, as well as the wild-type 2' residues, $\alpha1^{V256}$, $\beta2^{A252}$ and $\gamma2^{S266}$. **B**. The model shows the same view as in A, but with $\alpha1^{V256}$ replaced with $\alpha1^{S256}$. **C**. Side view for the wild-type α1β2γ2L receptor at the 2' position, depicting the residues for two α1 subunits and a β2 subunit. **D**. A similar view to that in C, showing a mutant $GABA_A$ receptor with the 2' mutation $\alpha1^{V256S}$. The figure is taken and modified from Seljeset et al. 2015.

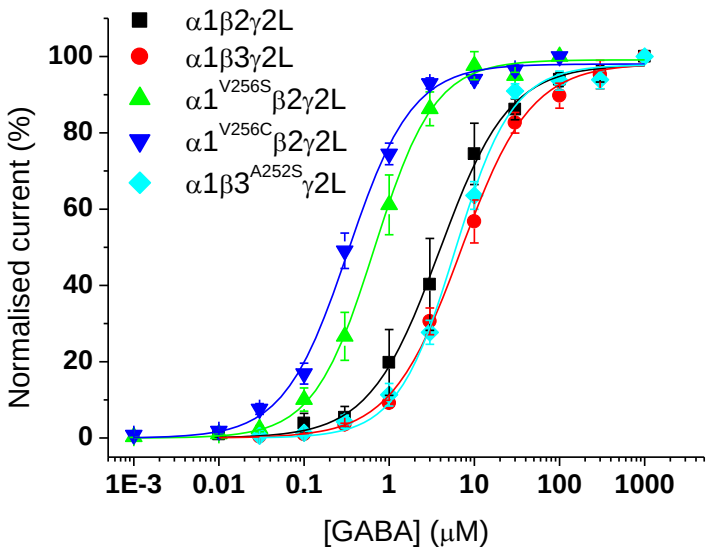

Figure 4.3 – A 2' mutation in the α1 subunit shifts the GABA concentration-response curve to the left but has no effect in the β3 subunit.

Concentration-response curves for α1β2γ2L (black), α1β3γ2L (red), $\alpha1^{V256S}\beta2\gamma2L$ (green), $\alpha1^{V256C}\beta2\gamma2L$ (blue) and $\alpha1\beta3^{A252S}\gamma2L$ (cyan) (n = 5-8). Current responses were normalised to the maximum response (E_{max}) evoked by 1 mM GABA. Data are expressed as mean ± SEM.

Receptor	GABA EC_{50} (μM)	n_H	GABA EC_{80} (μM)
α1β2γ2L	4.9 ± 1.4	1.3 ± 0.1	30
α1β3γ2L	7.5 ± 1.2	1.1 ± 0.1	30
$\alpha1^{V256S}\beta2\gamma2L$	0.8 ± 0.2	1.3 ± 0.0	2
$\alpha1^{V256C}\beta2\gamma2L$	1.1 ± 0.2	1.2 ± 0.0	3
$\alpha1\beta3^{A252S}\gamma2L$	6.1 ± 0.6	1.3 ± 0.1	30

Table 4.1 – GABA concentration-response parameters for wild-type $GABA_A$ receptors and 2' mutants.

Data were determined from the GABA concentration-response curves shown in Figure 4.3 (n = 5-8). All values are mean ± SEM.

To assess the PS-sensitivity of the 2' mutants, whole-cell currents in response to GABA EC_{80} with PS at increasing concentrations were recorded, as previously described for wild-type receptors (Chapter 3). Despite the previously reported reduction or ablation of PS sensitivity in these mutants, all three receptors were antagonised by PS at higher concentrations (Fig. 4.4 and 4.5). Whereas the inhibition curves for inhibition of steady-state currents were shifted to the right for all three mutants, greater inhibition of the GABA peak current was observed for the $\alpha1^{V256S}\beta2\gamma2L$ and $\alpha1^{V256C}\beta2\gamma2L$ receptor mutants. A rebound current was also present upon wash-out of 100 µM PS at all three mutants, meaning that channels re-entered an open state before closure.

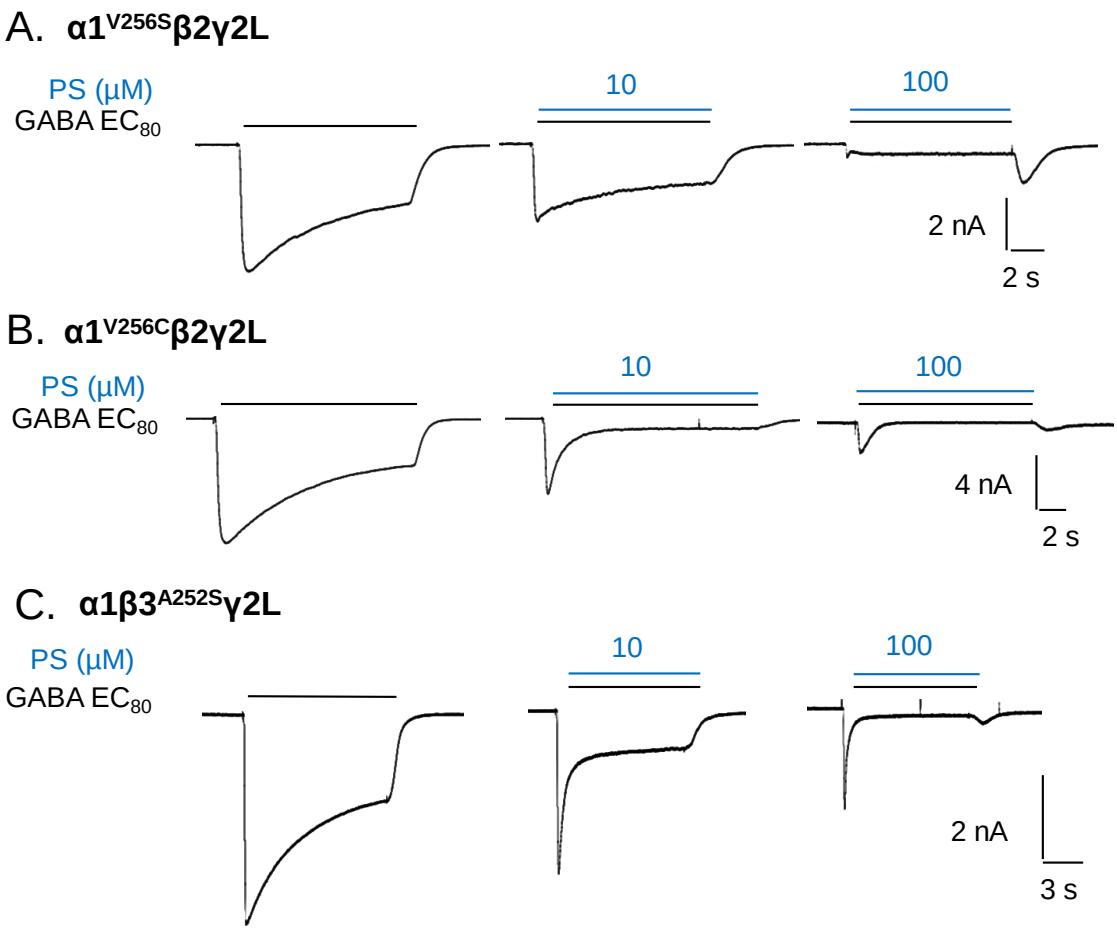

Figure 4.4 – Inhibition of GABA currents for $\alpha1^{V256S}\beta2\gamma2L$, $\alpha1^{V256C}\beta2\gamma2L$ and $\alpha1\beta3^{A252S}\gamma2L$ receptor mutants.

The current traces show the response of $\alpha1^{V256S}\beta2\gamma2L$ (**A**), $\alpha1^{V256C}\beta2\gamma2L$ (**B**) and $\alpha1\beta3^{A252S}\gamma2L$ (**C**) to GABA EC_{80} and 10-100 µM PS. PS was co-applied with GABA.

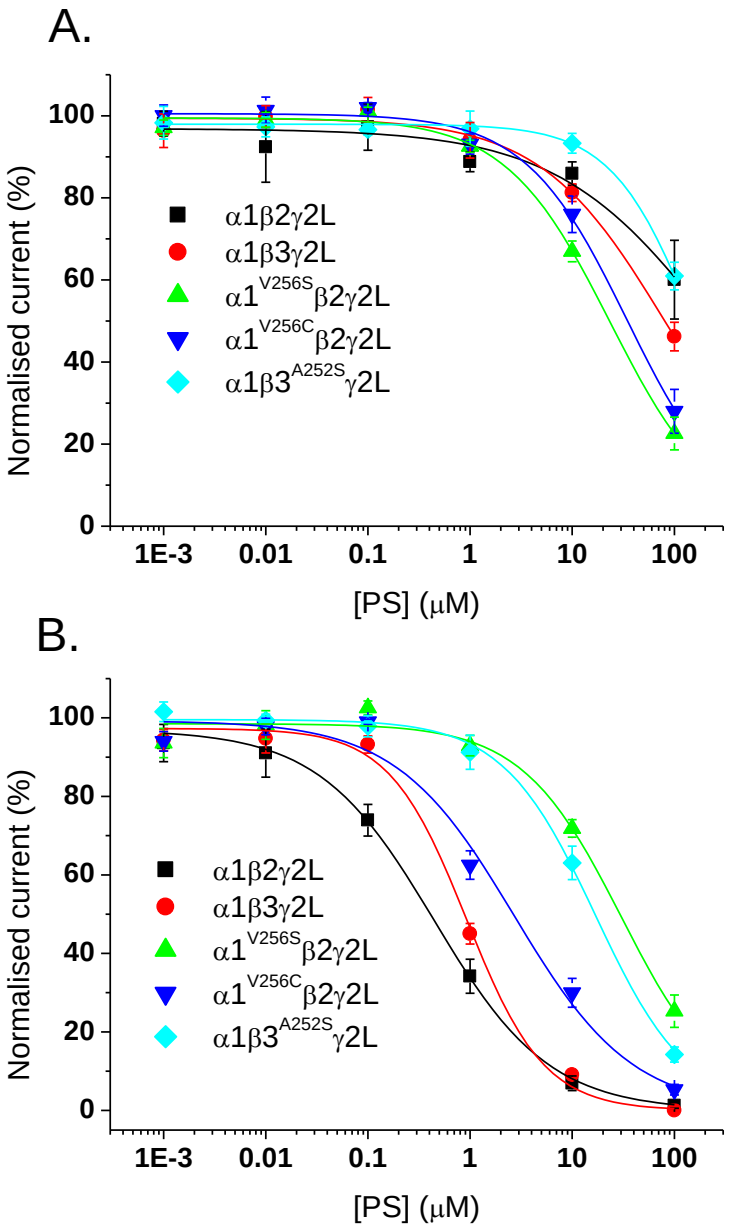

Figure 4.5 – PS inhibition curves for α1β2γ2L, α1β3γ2L, α1^{V256S}β2γ2L, α1^{V256C}β2γ2L and α1β3^{A252S}γ2L receptors.

A. Inhibition of GABA EC_{80} peak current responses by PS at α1β2γ2L (black), α1β3γ2L (red), α1^{V256S}β2γ2L (green), α1^{V256C}β2γ2L (blue) and α1β3^{A252S}γ2L (cyan) (n = 7-8). **B**. Inhibition of GABA EC_{80} steady-state current responses by PS at α1β2γ2L, α1β3γ2L, α1^{V256S}β2γ2L, α1^{V256C}β2γ2L and α1β3^{A252S}γ2L (colour coded as in A; n = 7-8). Data are expressed as mean ± SEM.

As demonstrated in Fig. 4.4 and 4.5, inhibition of GABA peak currents was notably larger at the α1^{V256S}β2γ2L and α1^{V256C}β2γ2L receptor mutants than at the

wild-type α1β2γ2L receptor at high PS concentrations (10 and 100 μM). At the wild-type receptor, 100 μM PS inhibited the GABA EC_{80}-induced peak current to 60.1 ± 9.6% of control, which increased to 22.6 ± 4.0% at $\alpha1^{V256S}\beta2\gamma2L$ (p = 0.0014, n = 6-7) and 28.0 ± 5.3% at $\alpha1^{V256C}\beta2\gamma2L$ (p = 0.0076, n = 6). In contrast, peak current inhibition was reduced by the $\beta3^{A252S}$ mutation: 100 μM PS inhibited the peak current to 46.2 ± 3.5% of control at the wild-type α1β3γ2L receptor, compared to 61.0 ± 3.4% at $\alpha1\beta3^{A252S}\gamma2L$ (p = 0.0109, n = 6-8). Thus, introducing a 2' mutation to the α1 subunit increased GABA peak current inhibition, whereas the homologous mutation at the β3 subunit reduced inhibition.

Receptor	**Peak IC_{50} (μM)**	**Peak n_H**	**Steady-state IC_{50} (μM)**	**Steady-state n_H**
α1β2γ2L	n/a	n/a	0.4 ± 0.1	0.8 ± 0.1
α1β3γ2L	n/a	n/a	1.0 ± 0.1	1.3 ± 0.2
$\alpha1^{V256S}\beta2\gamma2L$	27.8 ± 6.6	0.9 ± 0.1	35.5 ± 8.2	0.9 ± 0.0
$\alpha1^{V256C}\beta2\gamma2L$	30.0 ± 6.1	0.9 ± 0.1	2.8 ± 0.6	0.8 ± 0.1
$\alpha1\beta3^{A252S}\gamma2L$	n/a	n/a	17.7 ± 2.5	1.1 ± 0.1

Table 4.2 – PS concentration-response parameters derived from inhibition curves for wild-type and 2' mutant α1β2/3γ2L receptors.

Data are derived from the curves shown in Figure 4.5 for inhibition of GABA EC_{80} peak and steady-state currents by PS (n = 7-8). IC_{50} and n_H values derived for PS from curves of GABA peak currents are called Peak IC_{50} and Peak n_H, whereas Steady-state IC_{50} and Steady-state n_H refer to values derived from the inhibition curves for steady-state currents. All values are mean ± SEM.

All three mutations made the receptors less susceptible to steady-state current inhibition by PS. As summarised in Table 4.2, the IC_{50} for PS was shifted from 0.4 ± 0.1 μM for the wild-type α1β2γ2L receptor to 2.8 ± 0.6 μM for the $\alpha1^{V256C}\beta2\gamma2L$ receptor mutant (p = 0.0005, n = 5-7) and 35.5 ± 8.2 μM for the $\alpha1^{V256S}\beta2\gamma2L$ receptor mutant (p = 0.0005, n = 7; Fig. 4.5B). The $\beta3^{A252S}$ mutation shifted the IC_{50} from 1.0 ± 0.1 μM for wild-type α1β3γ2L to 17.7 ± 2.5 μM for $\alpha1\beta3^{A252S}\gamma2L$ (p < 0.0001, n = 7-8). Due to the increased peak current inhibition by PS of the $\alpha1^{V256S}\beta2\gamma2L$ and $\alpha1^{V256C}\beta2\gamma2L$ receptor mutants, IC_{50}s for peak

current inhibition were found to be 27.8 ± 6.6 µM and 30.0 ± 6.1 µM, respectively. The IC_{50}s for peak current inhibition at the wild-type α1β2/3γ2L receptors were not found as inhibition was only present at 100 µM PS, but are likely to be in the range of 100-300 µM.

In conclusion, all three 2' mutations shifted the steady-state PS inhibition curves to the right. Substituting the 2' Val of α1 for Ser caused the largest shift, but both α1 2' mutants were more susceptible to peak current inhibition by PS. The $\beta3^{A252S}$ mutation, by contrast, reduced peak current inhibition by PS. This was an unexpected result, and as a consequence, PS was investigated on a 'simpler' homomeric receptor formed from β3 subunits.

4.2.2. The $\beta3^{A252S}$ homomer is inhibited by PS

As the binding site for PS might be present on more than one subunit, or indeed be interfacial with residues contributed from more than one subunit, the $\beta3^{A252S}$ subunit was expressed as a homomer and studied using PB as an agonist. This eliminates the possibility of PS being able to cause inhibition by binding to other wild-type subunits in the heteromeric receptors that were studied above (section 4.2.1.). The $\beta3^{A252S}$ subunit formed a homomer that was slowly activated by 500 µM PB (Fig. 4.6). Due to the slow kinetics of the homomer, the 'peak' current induced by PB was measured at 30 s. When co-applied with PS, inhibition of the peak current was obtained, and a rebound current was present upon wash-off, especially at 100 µM where the rebound current was similar in magnitude to the PB control current.

Compared to the wild-type β3 homomer, PS was less potent at the 2' mutant. At 10 µM PS, the PB-induced peak current was inhibited to about 40% of control at the wild-type homomer, compared to about 80% of control at the mutant. Whereas full block was observed at 100 µM PS at the wild-type homomer (Chapter 3, Fig. 3.12), the current was still approximately 30% of control at the $\beta3^{A252S}$ homomer. Furthermore, the ability of PS to inhibit the rebound current at the β3 homomer was ablated by the 2' mutation. In conclusion, PS is still able to bind to and inhibit PB-induced currents at the $\beta3^{A252S}$ homomer, suggesting that

the 2' residue does not form the binding site for PS. Note that 500 µM PB was used to activate both the wild-type and mutant homomer, a concentration that might not produce the same open probability at the two complexes. This might also have affected the level of block attained at these homomers, due to the activation-dependence of inhibition by PS.

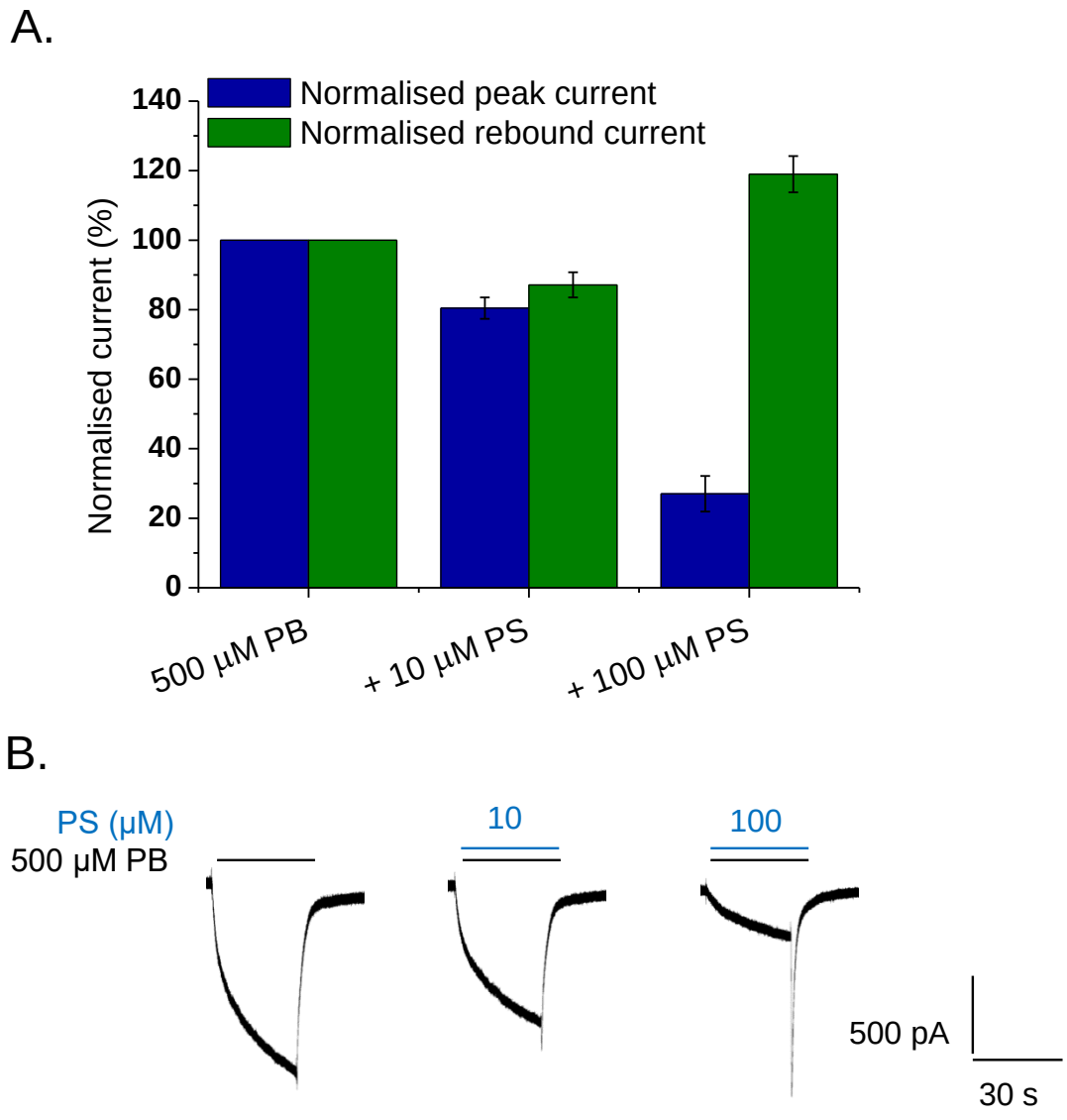

Figure 4.6 – The β3^{A252S} homomer is sensitive to PS.

A. The bar chart shows the normalised peak current (blue) and rebound current (green) response of the β3^{A252S} homomer to 500 µM PB and inhibition by 10 and 100 µM PS following co-applications (n = 5). Data are expressed as mean ± SEM. **B**. Representative traces for the response of the β3^{A252S} homomer to PB and inhibition of this current by 10-100 µM PS.

4.2.3. PTX blocks GABA-induced currents at α1^{V256S}β2γ2L

Previous studies have shown that PTX acts by blocking the $GABA_A$ receptor channel pore. In particular, the 2' residue has been shown to be necessary for PTX block through mutation studies (Ffrench-Constant et al., 1993; Zhang et al., 1994; Xu et al., 1995), and by the crystal structure of the Cys-loop receptor homologue GluCl bound to picrotoxin (Hibbs and Gouaux, 2011). The α1^{V256S}β2γ2L receptor mutant would therefore be expected to be insensitive to block by PTX.

To test this, receptors were activated by GABA EC_{80} (2 μM) and 10 μM PTX was pre-applied to the recording chamber for 20 s before GABA and PTX were co-applied twice. PTX was an efficacious blocker of α1^{V256S}β2γ2L (Fig. 4.7). The GABA peak current was 9.3 ± 2.3% of control at the second co-application with PTX, whereas the steady-state current was down to 24.9 ± 8.8% of control. This suggests that the 2' mutant might be more sensitive to PTX than the wild-type α1β2γ2L receptor, as an EC_{100} GABA peak current was inhibited to 37.3 ± 8.1% of control at the second co-application with PTX, and the steady-state current was inhibited to 73.4 ± 1.8% of control. This suggests that the 2' residue may not form the binding site for PTX, or that mutating the α1 subunit only is insufficient to remove the binding site from a heteromeric αβγ receptor.

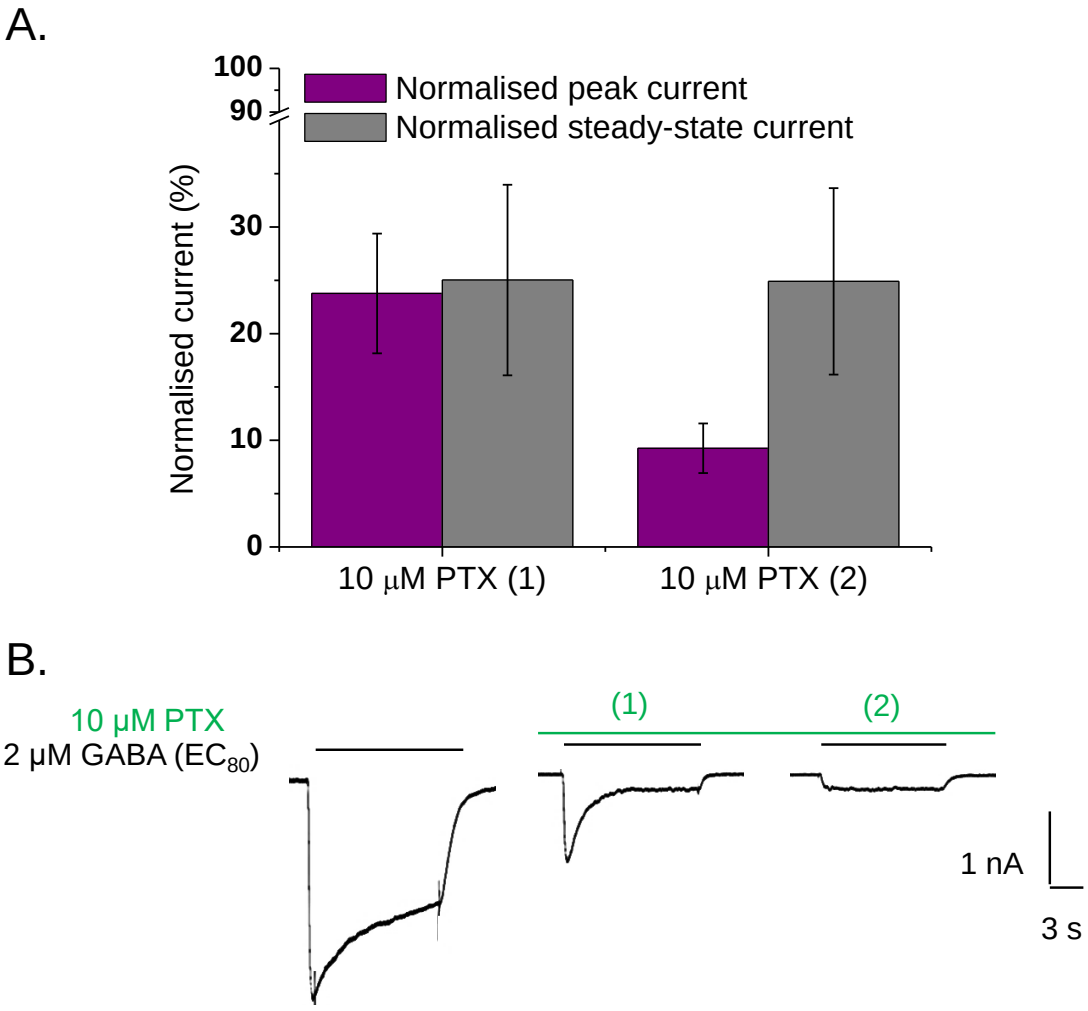

Figure 4.7 – The α1^{V256S}β2γ2L receptor is sensitive to PTX.

A. The bar chart shows the normalised GABA EC_{80} peak (purple) and steady-state (grey) current response in the presence of 10 μM PTX following two repeated co-applications (labelled (1) and (2)). PTX was applied to the recording chamber prior to receptor activation and kept in the chamber throughout the experiment (n = 4). Data are expressed as mean ± SEM. **B**. Representative traces showing the current responses of α1^{V256S}β2γ2L to 2 μM GABA (EC_{80}) and the inhibition caused by 10 μM PTX following two repeated co-applications preceded by a pre-application.

4.2.4. The 2' P294V mutation renders the ρ1 receptor sensitive to PS

As inhibition by PS is only weakly voltage-sensitive and block does not increase after repeated receptor activation in the presence of PS, it is not likely that the steroid acts by blocking the open channel pore. As mutating the 2' residue located near the intracellular side of the channel affects the modulation of $GABA_A$ receptors by PS, a plausible explanation is that this residue is essential in the coupling of PS binding to inhibition. As the ρ1 receptor is largely insensitive to PS (Chapter 3, Fig. 3.9-10), it is possible that this receptor lacks the machinery that is necessary to couple the binding of PS to inhibition. Whereas α1 has a valine residue at the 2' position, ρ1 has a proline (Fig. 4.1). If the 2' valine residue is essential for signal transduction, swapping the 2' proline of ρ1 for a valine residue might confer increased PS sensitivity. To test this hypothesis, two different ρ1 2' mutations were generated to see if the potency of PS at this receptor could be increased. If the $\alpha1^{V256}$ residue is necessary for PS signal transduction, mutating the 2' proline residue of ρ1 to valine ($\rho1^{P294V}$) would be expected to increase the potency of PS at the receptor. As a negative control, proline was also mutated to a serine ($\rho1^{P294S}$), as this amino acid reduced PS potency at the α1β2γ2L receptor. This mutation was not expected to increase the potency of PS at ρ1.

Both mutations shifted the GABA concentration-response curve to the right: the EC_{50} for wild-type ρ1 was 2.6 ± 0.3 μM, compared with 24.2 ± 1.1 μM for $\rho1^{P294V}$ ($p < 0.0001$, n = 4-8) and 9.7 ± 1.2 μM for $\rho1^{P294S}$ ($p = 0.0009$, n = 6-8; Fig. 4.8; Table 4.3). This shows that the 2' mutation affects the potency of GABA and possibly the gating kinetics of ρ1.

To assess the PS sensitivity of the mutants, GABA at EC_{80} was co-applied with PS at increasing concentrations (Fig. 4.9). The $\rho1^{P294S}$ behaved similarly to wild-type ρ1, with no greater inhibition of the peak or steady-state currents observed. In contrast, the $\rho1^{P294V}$ receptor mutant was notably more sensitive to PS, with clear inhibition of the steady-state current being present at concentrations higher than 1 μM (Fig. 4.9B and D). The IC_{50} for steady-state current inhibition by PS at $\rho1^{P294V}$ was 6.0 ± 0.6 μM, about 6-fold higher than at wild-type heteromeric αβγ/δ

receptors. This result supports a role for 2' valine in the signal transduction of PS at $GABA_A$ receptors.

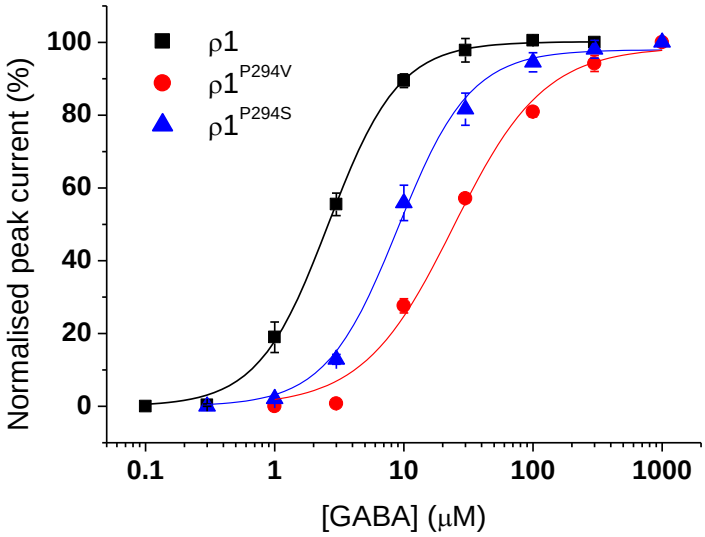

Figure 4.8 – GABA concentration-response curves for the wild-type ρ1 receptor and the 2' mutant receptors $\rho1^{P294V}$ and $\rho1^{P294S}$.

For the wild-type receptor, current responses were normalised to the 300 μM GABA (EC_{100}) response. Mutant receptor currents were normalised to the 1 mM GABA response (n = 4-12). Data are expressed as mean ± SEM.

Receptor	GABA EC_{50} (μM)	n_H	GABA EC_{80} (μM)
ρ1	2.6 ± 0.3	1.7 ± 0.1	10
$\rho1^{P294V}$	24.2 ± 1.1	1.3 ± 0.1	100
$\rho1^{P294S}$	9.7 ± 1.2	1.6 ± 0.1	30

Table 4.3 – GABA concentration-response parameters for the wild-type ρ1 receptor and the 2' mutants $\rho1^{P294V}$ and $\rho1^{P294S}$.

Values are derived from the data shown in Figure 4.8 and are expressed as mean ± SEM (n = 4-12).

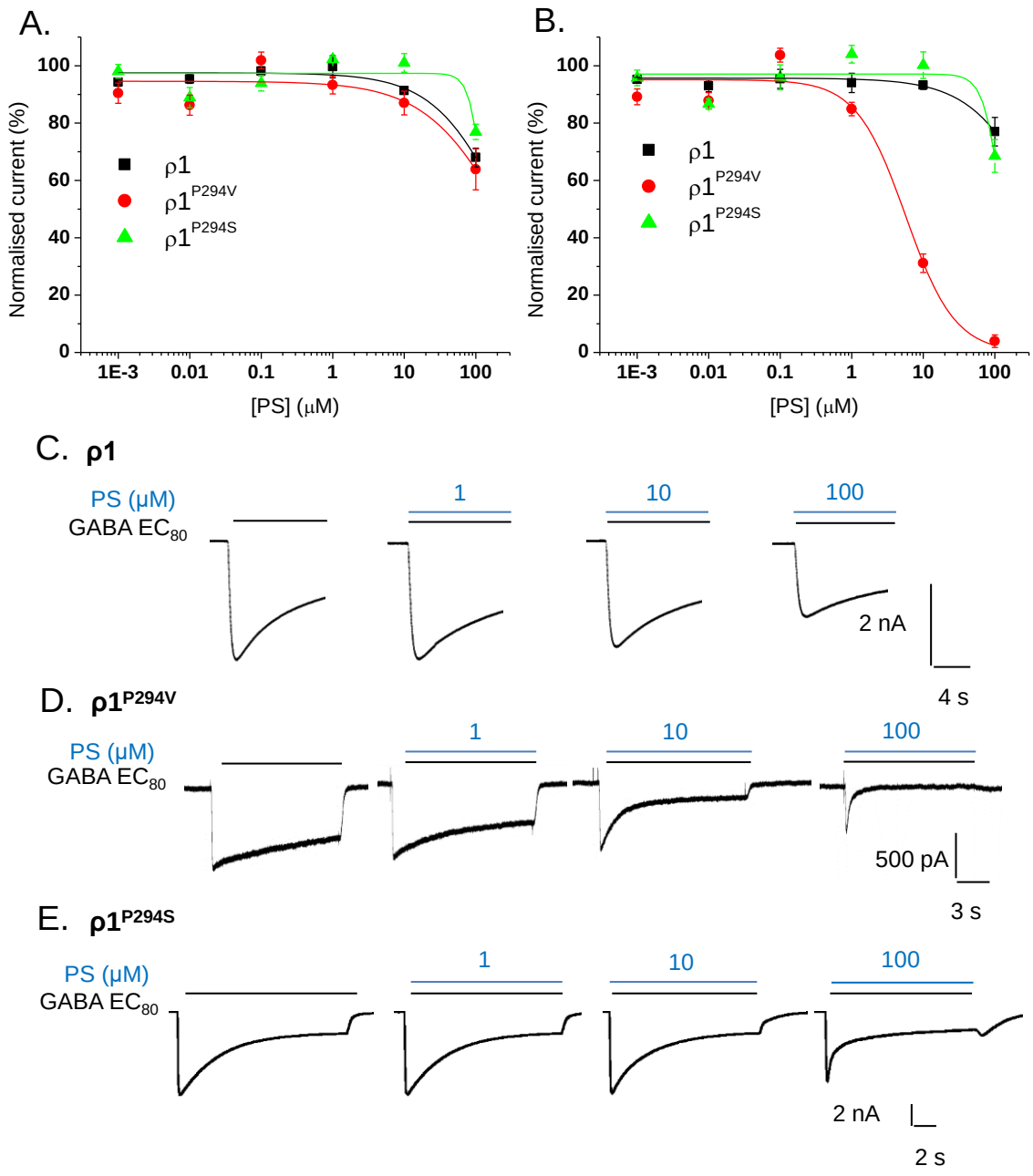

Figure 4.9 – PS inhibition curves for ρ1 wild-type and mutant receptors with representative traces.

A. Inhibition by PS of GABA-mediated peak currents at wild-type ρ1 (black), $\rho1^{P294V}$ (red) and $\rho1^{P294S}$ receptors (green) (n = 6-12). **B**. Inhibition by PS of GABA-mediated steady-state currents at wild-type ρ1 (black), $\rho1^{P294V}$ (red) and $\rho1^{P294S}$ receptors (green) (n = 6-12). Data are expressed as mean ± SEM. **C-E**. Representative traces for wild-type ρ1 (**C**), $\rho1^{P294V}$ (**D**) and $\rho1^{P294S}$ (**E**) in response to GABA EC_{80} and co-applications with 1, 10 and 100 μM PS.

4.2.5. Residues identified in UNC-49B/C studies are not important for PS binding at the murine $GABA_A$ receptor

Studies carried out using the *C. elegans* UNC-49 receptor identified an array of residues that were thought to be important in inhibitory neurosteroid binding. As PS is 80-fold more potent as an inhibitor at UNC-49B/C heteromers compared to UNC-49B homomers (with IC_{50}s of 2.3 µM and 191 µM, respectively), residues found in UNC-49C, but not UNC-49B, may be involved in forming a binding site for PS (Wardell et al., 2006). Chimeras formed between UNC-49B and UNC-49C implied a key role for M1 and the extracellular M2-M3 linker of UNC-49C, as these regions fully accounted for the sensitivity to PS inhibition. As described in the introduction, two residues were found to be conserved among UNC-49C and other PS-sensitive mammalian $GABA_A$ receptor subunits: where UNC-49C and other PS-sensitive subunits have a glutamine and an aromatic residue (phenylalanine in UNC-49C, tyrosine in other $GABA_A$ receptor subunits), UNC-49B has an asparagine (N259) and valine (V261; Fig. 4.1 and 4.10). N259 in UNC-49B is homologous to Q228 in the α1 subunit, whereas V261 is homologous to Y230. My hypothesis was that substituting the residues at positions 228 and 230 of the α1 subunit with the homologous residues in UNC-49B would make the mammalian $GABA_A$ receptor less sensitive to PS, whereas introducing a residue from UNC-49C would not affect, or possibly increase, the potency of PS. Thus, four different mutant α1 subunits were generated: $\alpha1^{Q228N}$ to replace glutamine (in α1) with asparagine from UNC-49B, $\alpha1^{Y230F}$ to replace tyrosine (in α1) with the structurally similar phenylalanine from UNC-49C, $\alpha1^{Y230V}$ to introduce the hydrophobic valine of UNC-49B to α1, and a double mutant, $\alpha1^{Q228V/Y230V}$, introducing both residues of interest from UNC-49B into the α1 subunit. Whereas the $\alpha1^{Y230F}$ mutant was expected to be approximately similar in PS sensitivity to wild-type α1, reduced sensitivities were expected for receptors containing the $\alpha1^{Q228N}$, $\alpha1^{Y230V}$ and $\alpha1^{Q228V/Y230V}$ mutations.

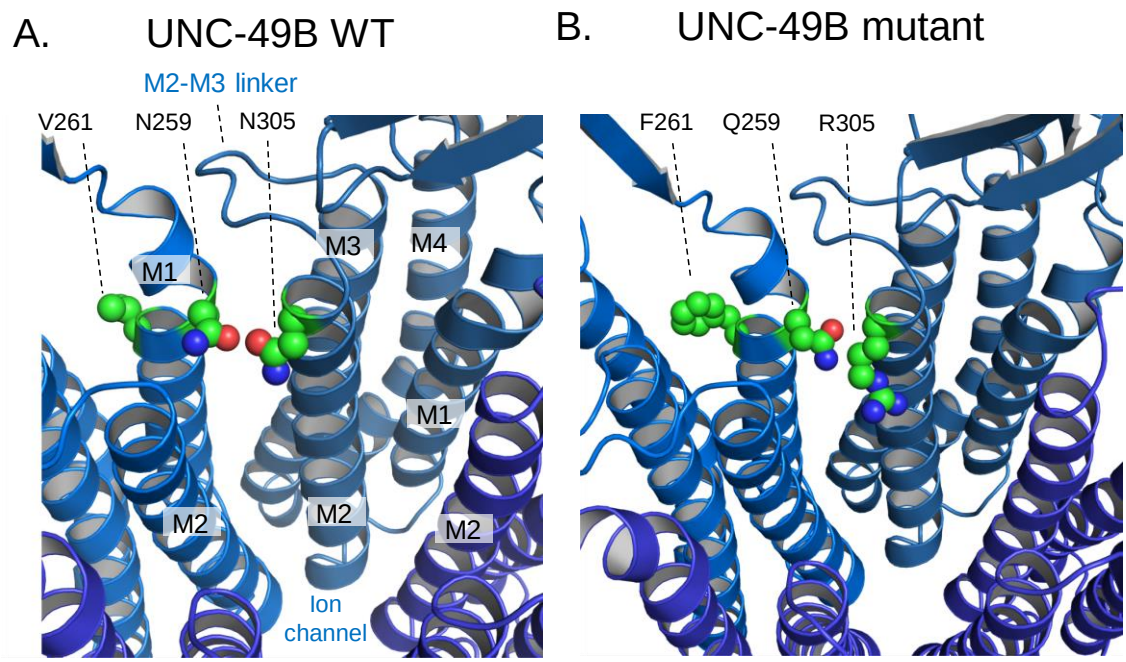

Figure 4.10 – UNC-49B homology models showing the position of the M1 residues mutated in this study as well as a residue implicated in PS binding on the top of M2.

A. A homology model of the wild-type (WT) UNC-49B receptor showing the M1 residues that are implicated in PS binding, N259 and V261, as well as N305 at the top of M2. **B**. A homology model of the mutant UNC-49B receptor, where the three residues highlighted in A have been substituted for Q259, F261 and R305, rendering the homomer more sensitive to PS. The extracellular domains are removed, showing the transmembrane domains and the channel lining formed by M2. The *C. elegans* UNC-49B models are based on the crystal structure of the $GABA_A$ receptor β3 subunit homomer (PDB 4cof). The figure is taken and modified from Seljeset et al. 2015.

To determine if the mutations affected GABA activation of the receptor, each mutant α1 subunit was co-expressed with β2 and γ2L and the GABA concentration-response relationship studied (Fig. 4.11). As summarised in Table 4.4, the mutations only caused small changes to the GABA EC_{50}s (up to 3-fold), with all curves shifted to the right. Whereas GABA EC_{50} is 4.9 ± 1.4 μM for the wild-type receptor, the EC_{50} was increased to 11.2 ± 1.3 μM for $\alpha1^{Q228N}\beta2\gamma2L$ ($p = 0.0055$, $n = 5$), 15.1 ± 2.2 μM for $\alpha1^{Y230F}\beta2\gamma2L$ ($p = 0.0024$, $n = 5$-6), 7.5 ± 2.0 μM for $\alpha1^{Y230V}\beta2\gamma2L$ ($p = 0.1547$, $n = 5$) and 9.1 ± 2.1 μM for $\alpha1^{Q228N/Y230F}\beta2\gamma2L$ ($p = 0.0649$, $n = 5$). The effect of the mutations on GABA potency and potentially gating was therefore minimal.

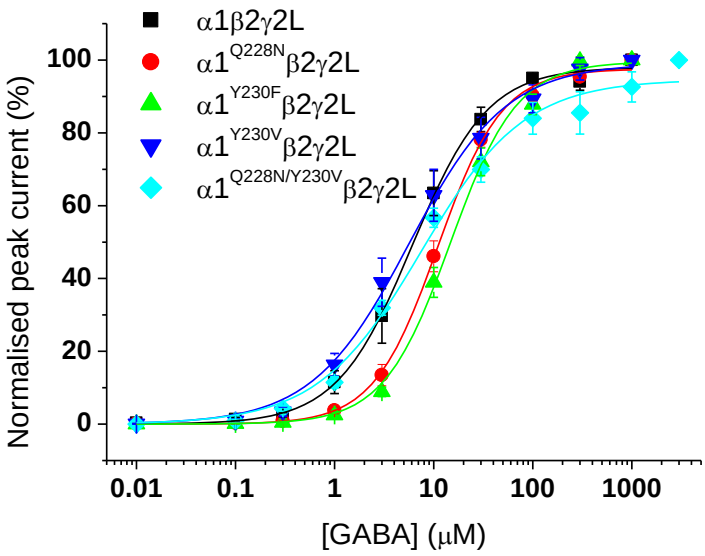

Figure 4.11 – GABA concentration-response curves for α1β2γ2L and M1 mutants.

GABA concentration-response curves for α1β2γ2L (black), $\alpha1^{Q228N}\beta2\gamma2L$ (red), $\alpha1^{Y230F}\beta2\gamma2L$ (green), $\alpha1^{Y230V}\beta2\gamma2L$ (blue) and $\alpha1^{Q228N/Y230V}\beta2\gamma2L$ (cyan) (n = 5-6). Peak current responses were normalised to the 1 mM GABA response (EC_{100}), except for $\alpha1^{Q228N/Y230V}\beta2\gamma2L$ current responses which were normalised to the current evoked by 3 mM GABA. Data are expressed as mean ± SEM.

Receptor	GABA EC_{50} (μM)	n_H	GABA EC_{80} (μM)
α1β2γ2L	4.9 ± 1.4	1.3 ± 0.1	30
$\alpha1^{Q228N}\beta2\gamma2L$	11.2 ± 1.3	1.4 ± 0.1	30
$\alpha1^{Y230F}\beta2\gamma2L$	15.1 ± 2.2	1.4 ± 0.0	50
$\alpha1^{Y230V}\beta2\gamma2L$	7.5 ± 2.0	1.0 ± 0.1	30
$\alpha1^{Q228N/Y230V}\beta2\gamma2L$	9.1 ± 2.1	0.9 ± 0.1	30

Table 4.4 – GABA concentration-response parameters for the α1β2γ2L M1 mutant receptors.

Values are derived from the data shown in Figure 4.11 and are expressed as mean ± SEM (n = 5-6).

The sensitivity of the mutant receptors to PS was assessed by measuring whole-cell current responses to co-applications of GABA EC_{80} and increasing concentrations of PS. All mutants were sensitive to PS (Fig. 4.12 and 4.13, Table 4.5), and current responses were similar in profile to the wild-type response. The PS IC_{50} for steady-state current inhibition at α1β2γ2L is 0.4 ± 0.1 μM, compared to 0.4 ± 0.1 μM at $\alpha1^{Q228N}\beta2\gamma2L$ ($p = 0.1812$, $n = 7\text{-}8$), 0.8 ± 0.2 μM at $\alpha1^{Y230F}\beta2\gamma2L$ ($p = 0.0096$, $n = 6\text{-}7$), 0.2 ± 0.0 μM at $\alpha1^{Y230V}\beta2\gamma2L$ ($p = 0.0010$, $n = 5\text{-}7$) and 0.4 ± 0.0 μM at $\alpha1^{Q228N/Y230F}\beta2\gamma2L$ ($p = 0.2901$, $n = 7$). Thus, for only two of the mutants was the PS IC_{50} different from that for wild-type: it was doubled for $\alpha1^{Y230F}\beta2\gamma2L$, where no change was expected, and it was halved for $\alpha1^{Y230V}\beta2\gamma2L$, which was expected to be less sensitive to PS. However, these are small changes, and as the mutations had little effect on PS sensitivity, the residues identified in the UNC-49B/C studies are unlikely to be essential for PS modulation of mammalian $GABA_A$ receptors. However, it should be noted that in the original UNC-49B/C chimera studies (Wardell et al., 2006; Twede et al., 2007), the potency of PS was studied in a homomeric complex. This could be important because all subunits then carried the mutation, a situation that does not occur when only the α subunit is mutated in an αβγ heteromer.

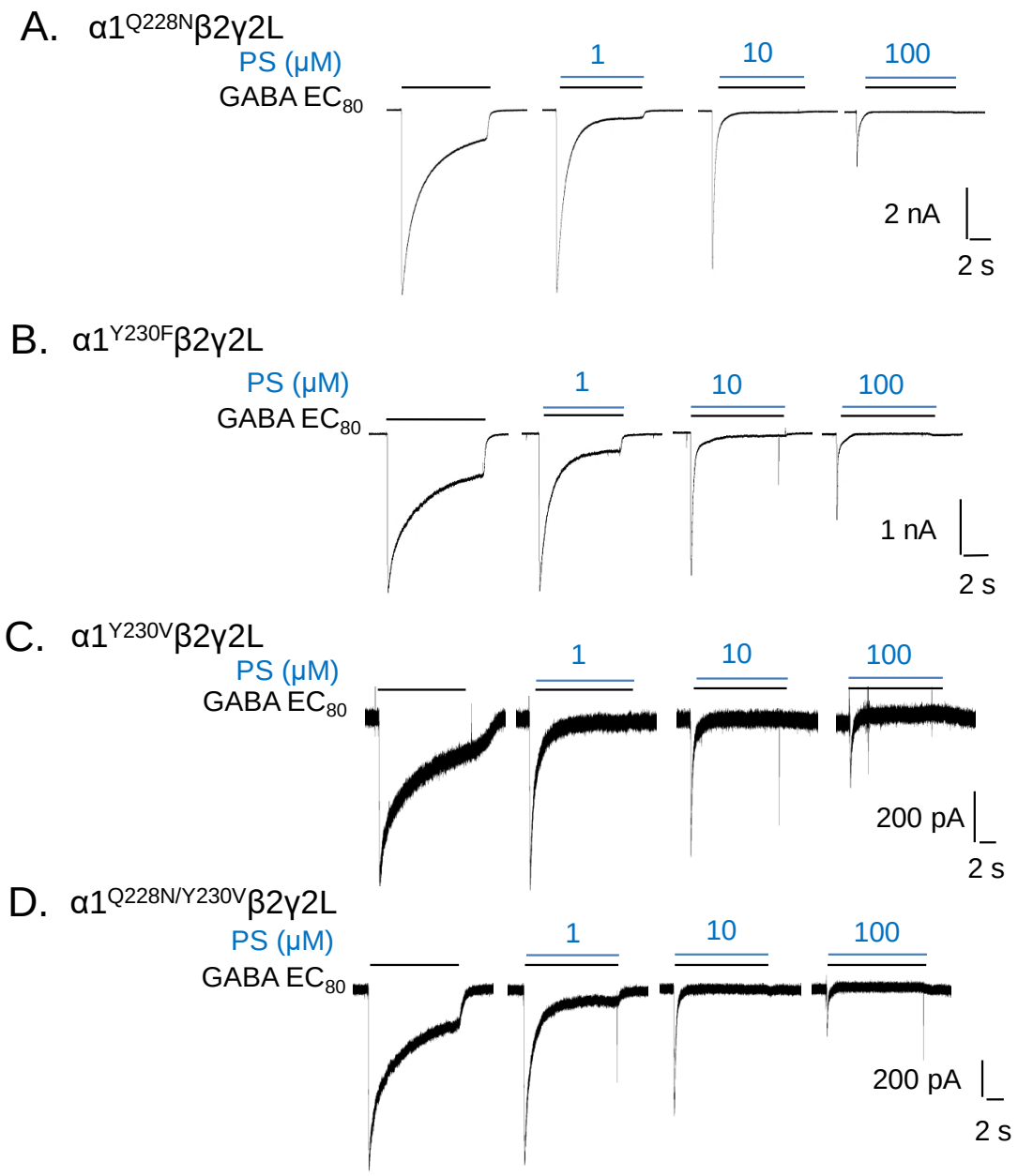

Figure 4.12 – Representative traces for α1^{Q228N}β2γ2L, α1^{Y230F}β2γ2L, α1^{Y230V}β2γ2L and α1$^{Q228N/Y230V}$β2γ2L.

A-D. Traces for the current response to GABA EC_{80} and GABA EC_{80} co-applied with 1, 10 and 100 μM PS at α1^{Q228N}β2γ2L (**A**), α1^{Y230F}β2γ2L (**B**), α1^{Y230V}β2γ2L (**C**) and α1$^{Q228N/Y230V}$β2γ2L (**D**).

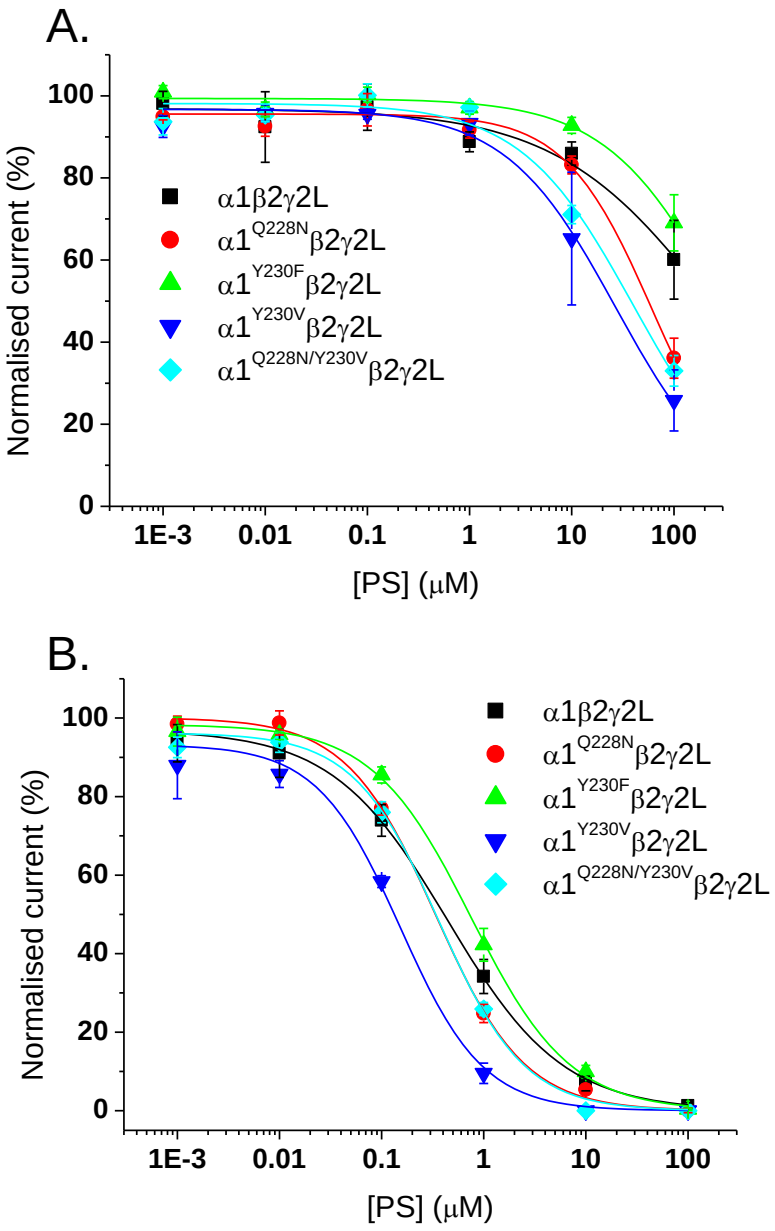

Figure 4.13 – PS inhibition curves for α1β2γ2L and M1 mutants.

A. Inhibition of GABA EC_{80} peak currents by PS at α1β2γ2L (black), $α1^{Q228N}β2γ2L$ (red), $α1^{Y230F}β2γ2L$ (green), $α1^{Y230V}β2γ2L$ (blue) and $α1^{Q228N/Y230V}β2γ2L$ (cyan) (n = 5-7). **B**. Inhibition of GABA EC_{80} steady-state currents by PS for the same receptors as in A. The colour coding is the same in both panels. Data are expressed as mean ± SEM.

At 100 μM PS, peak current inhibition was, however, greater at three of the mutants than at the wild-type receptor: whereas the peak current reached 60.1 ± 9.6% of control at α1β2γ2L, it attained 36.1 ± 4.9% at $α1^{Q228N}β2γ2L$ ($p = 0.0250$, n = 6), 25.8 ± 7.4% at $α1^{Y230V}β2γ2L$ ($p = 0.0116$, n = 5-6) and 33.0 ± 3.7% at

$\alpha1^{Q228N/Y230F}\beta2\gamma2L$ ($p = 0.0088$, $n = 6\text{-}7$). Again, these are the mutations that were predicted to reduce the sensitivity of the α1β2γ2L receptor to PS. The residues identified in the UNC-49B/C studies are therefore more likely to be involved in signal transduction than the binding of PS.

Receptor	**Steady-state IC_{50} (μM)**	**n_H**
α1β2γ2L	0.4 ± 0.1	0.8 ± 0.1
$\alpha1^{Q228N}\beta2\gamma2L$	0.4 ± 0.0	1.0 ± 0.0
$\alpha1^{Y230F}\beta2\gamma2L$	0.8 ± 0.2	0.9 ± 0.1
$\alpha1^{Y230V}\beta2\gamma2L$	0.2 ± 0.0	1.2 ± 0.2
$\alpha1^{Q228N/Y230V}\beta2\gamma2L$	0.4 ± 0.0	1.1 ± 0.1

Table 4.5 – PS concentration-response parameters for the α1β2γ2L M1 mutant receptors.

Values are derived from the data shown in Figure 4.13B and are expressed as mean ± SEM. IC_{50}s are for steady-state current inhibition by PS.

4.2.6. Finding a 'null' receptor for PS

As discussed in the main introduction (Chapter 1), a range of receptors are sensitive to PS, and can either be directly activated or negatively or positively modulated by the steroid. To further investigate the effects of PS and identify its binding site, a panel of pLGICs were screened for sensitivity to PS, aiming to find a receptor that is insensitive to PS for use in chimera studies with $GABA_A$Rs. For screening, one concentration of the receptor agonist and of PS was applied to each construct (Fig. 4.14). Although sensitivity of the GlyR to PS has been confirmed in primary cultures (Wu et al., 1997; Hong et al., 2013), the GlyR α1 subunit was expressed in HEK cells and was found to be inhibited by 100 μM PS (Fig. 4.14A). GLIC, $GluCl_{cryst}$, ELIC and RDL were expressed in *Xenopus* oocytes and studied using two-electrode voltage clamp (Fig. 4.14B-E). These recordings were performed by Dr Duncan Laverty.

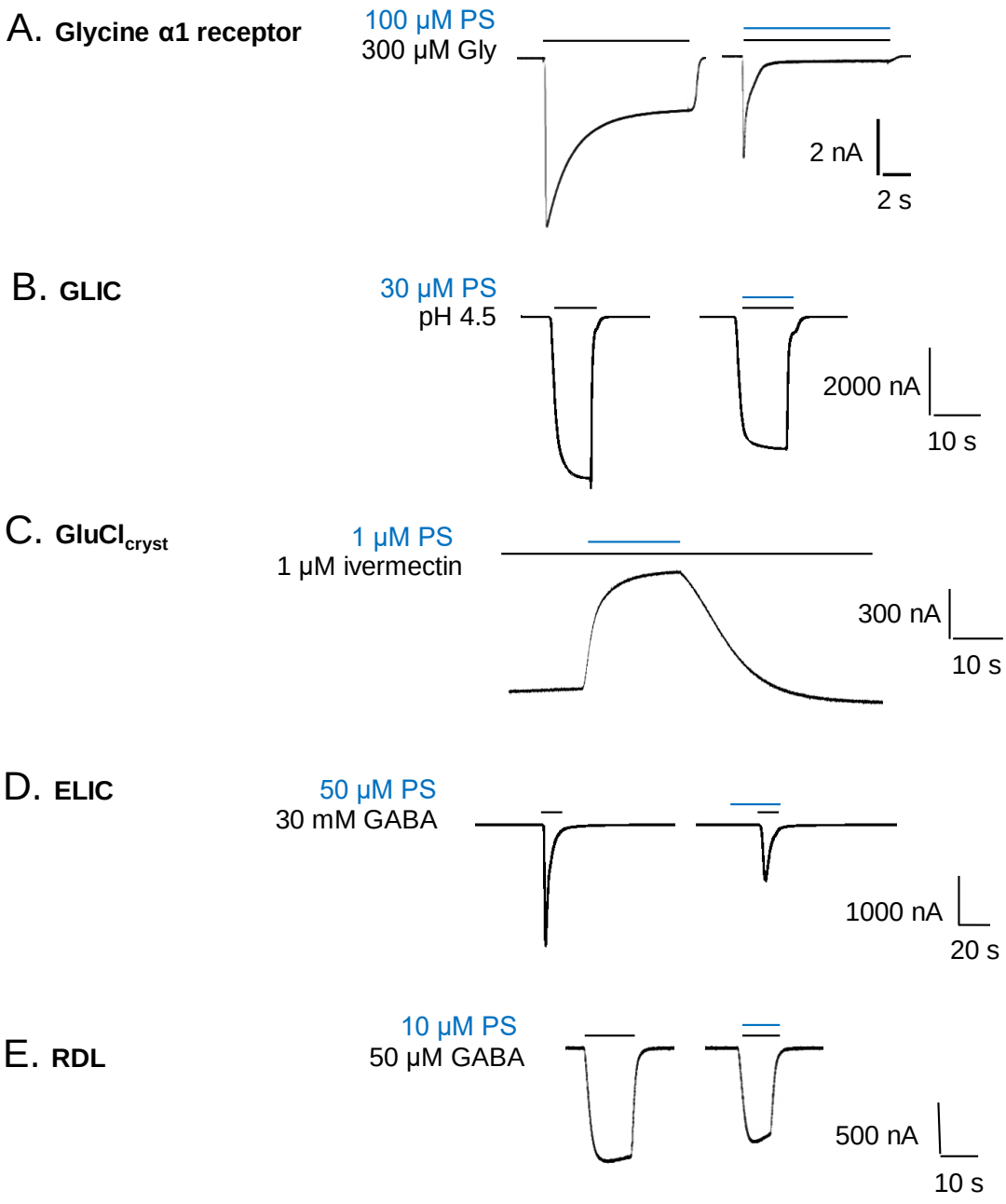

Figure 4.14 – The inhibitory effect of PS at a selection of ionotropic homomeric receptors.

The traces show the responses of a selection of potential 'null' receptors to agonist as indicated with and without PS. The GlyR α1 subunit (**A**) was expressed in HEK cells and whole-cell currents recorded using patch clamping. GLIC (**B**), $GluCl_{cryst}$ (**C**), ELIC (**D**) and RDL (**E**) were expressed in *Xenopus* oocytes and whole-cell currents were recorded using two-electrode voltage clamp. Currents were measured in response to co-applications of agonist and PS at GlyR α1, GLIC and RDL. For ELIC, PS was pre-applied, and $GluCl_{cryst}$ was activated by ivermectin prior to PS application.

As can be observed from the traces, all receptors were antagonised by PS, though GLIC and RDL were notably less sensitive than the other receptors. The mammalian $GABA_AR$ ρ1 subunit was concluded to be the best option for chimera studies as it is closely related to the other $GABA_ARs$ and displays low sensitivity to PS, as discussed below.

4.2.7. Probing the binding site for PS using ρ1-α1/β2/γ2 chimeras

The chimera approach has frequently been used in the past to locate domains involved in forming the binding sites for pharmacological agents (Corringer et al., 1998; Quiram and Sine, 1998; Wardell et al., 2006; Hosie et al., 2007, 2009). Using a receptor that is insensitive to modulation by the compound of interest, ligand-sensitivity can be introduced by creating chimeras between the 'null' receptor and the receptor subunit that is ligand-sensitive. By determining which receptor segments confer sensitivity on the 'null' receptor, the residues involved in the binding of the compound can eventually be determined by site-directed mutagenesis.

Due to the low sensitivity of the $GABA_A$ ρ1 subunit to PS, this subunit could potentially be used as a 'null' receptor. By studying the activity of PS at chimeras formed of ρ1 and α1, β2 or γ2, the aim was to find the residues that render the heteromeric αβγ receptor more sensitive to PS than the homomeric ρ1 receptor.

The chimeras used were previously created (Gielen et al., 2015), and are named such that the N-terminal end of the chimera appears first in the name, followed by a number which cites the position in the mature protein at which the residues from the second subunit starts to form part of the chimera. For example, for the first chimera studied, ρ1-260-α1, all residues from the N-terminus up to residue 260 are from ρ1, and the residues after position 260 are from α1. Chimeras were expressed in HEK cells, and whole-cell currents in response to GABA and GABA EC_{80} co-applied with PS were recorded.

The chimera ρ1-260-α1 contains the ECD of ρ1 and the TMD of α1 (Fig. 4.15A). TMD is here defined as all four transmembrane segments with intracellular and

extracellular linkers. This chimera was designed to determine whether PS is likely to bind to the ECD or TMD of α1. If the chimera was found to be sensitive, this would suggest that PS is likely to bind in the TMD of α1. A lack of sensitivity would argue for the ECD of α1 to be important in PS binding.

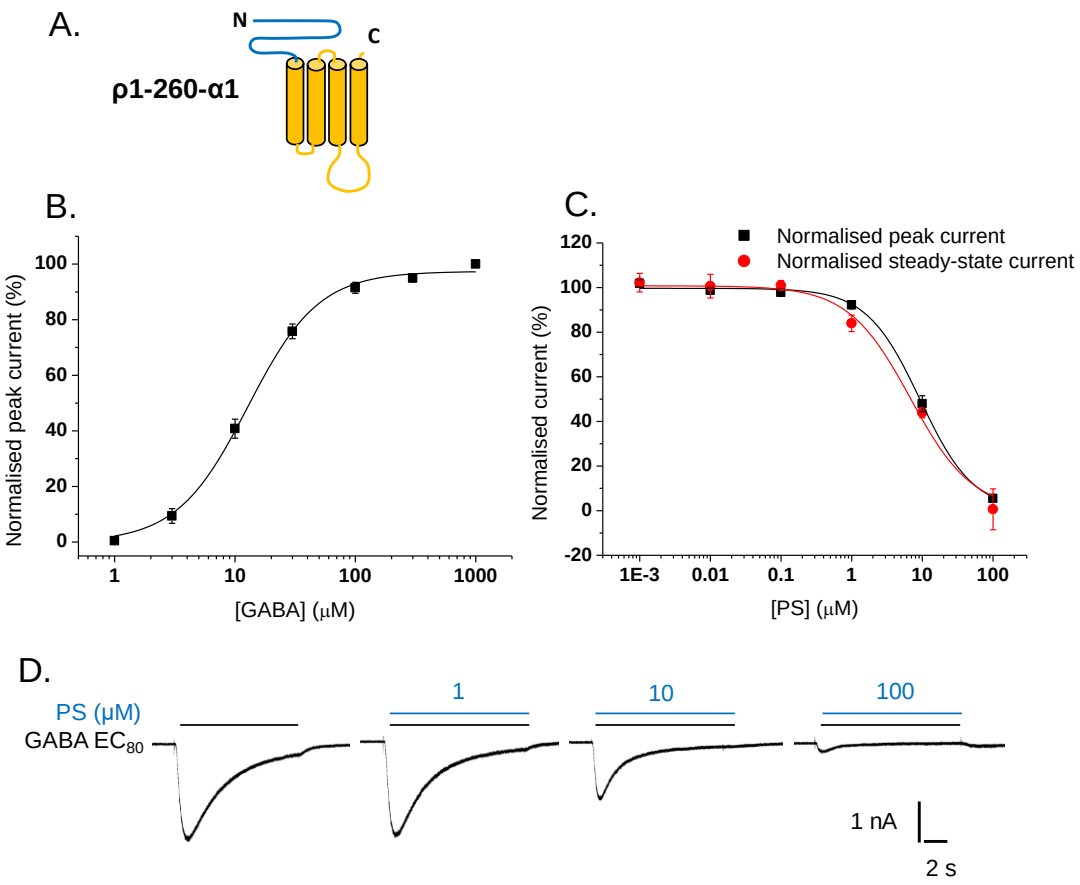

Figure 4.15 – Profiling the ρ1-260-α1 chimera.

A. Schematic diagram of the transmembrane topology of a ρ1-260-α1 chimera in which the ECD is from ρ1 (blue) and the TMD is from α1 (orange). **B**. GABA concentration-response curve for the ρ1-260-α1 chimera (n = 6). Peak current responses were normalised to the 1 mM GABA (EC_{100}) response. **C**. Inhibition of GABA EC_{80} (30 μM) peak and steady-state currents (measured at 10 s) by PS at the ρ1-260-α1 chimera (n = 5). Current responses were normalised to the GABA EC_{80} response. Data are expressed as mean ± SEM. **D**. Representative traces showing the response of ρ1-260-α1 to GABA EC_{80} and co-applications with 1, 10 and 100 μM PS.

PS inhibited the GABA EC_{80} currents at ρ1-260-α1 (Fig. 4.15C and D). The potency of PS was lower than at heteromeric wild-type receptors (0.4-1.3 μM), but prominent inhibition of both peak and steady-state GABA currents was still observed. Peak and steady-state currents were antagonised to a similar extent, with IC_{50}s of 9.5 ± 1.1 μM and 7.9 ± 1.7 μM, respectively. As shown in the graph and traces (Fig. 4.15C and D), virtually full inhibition of the GABA peak and steady-state current was obtained at 100 μM PS. These results show that PS can antagonise a chimera where the ECD is from the largely PS-insensitive ρ1 subunit, and suggested that the steroid is more likely to bind to the TMD of α1. Another possibility is that PS can bind in the ECD of ρ1, but that residues found in the TMD of α1 are necessary for signal transduction.

A similar chimera was studied, substituting α1 for γ2S. The ρ1-260-γ2S chimera constituted the ECD of ρ1 and the TMD of γ2S (Fig. 4.16A). GABA-induced currents for this chimera tended to escalate throughout the recording (Fig. 4.16E), and responses were therefore harder to interpret. Clear inhibition was however observed at concentrations of PS higher than 1 μM, and full inhibition of the steady-state current was attained at 100 μM PS (Fig. 4.16C and D). A rebound current was present on wash-out of 100 μM PS, showing that the chimera re-opened before closure. The peak current was also inhibited by PS, and reached 39.2 ± 5.1% of control at 100 μM PS. At concentrations below 1 μM, inhibition by PS might have been masked by the increase in GABA current observed throughout the recording. These results suggested that PS might also have a binding site in the TMD of the γ2S subunit. As for the ρ1-260-α1 chimera, an alternative explanation is that PS binds in the ECD of ρ1, and that residues in the TMD of γ2S are sufficient and necessary for signal transduction. PS appears to be somewhat less potent at this chimera compared to the ρ1-260-α1 chimera as less than 50% inhibition is reached at 10 μM PS, but this reduced potency might be due to the escalating GABA-induced current throughout the recording.

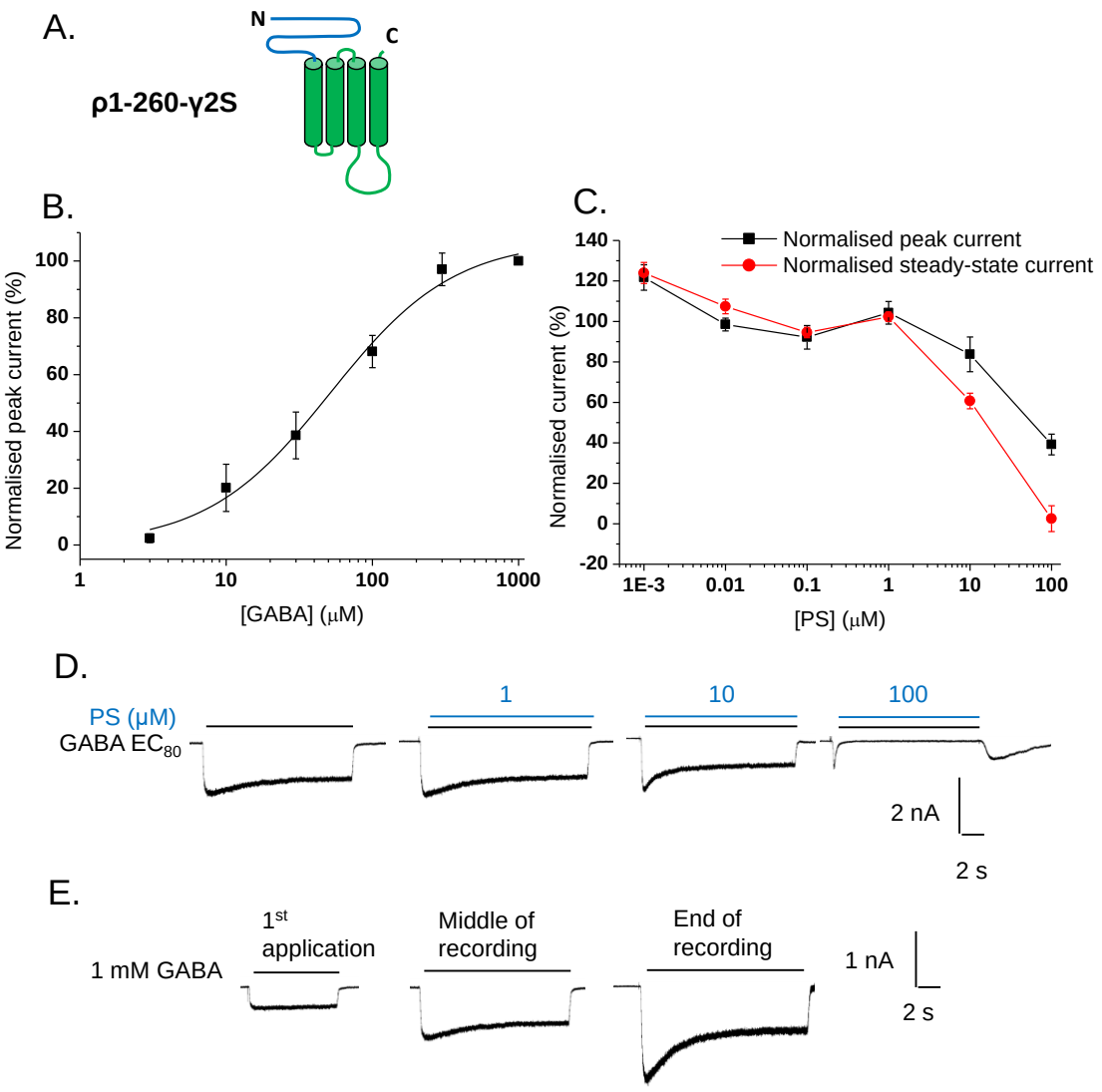

Figure 4.16 – Profiling the ρ1-260-γ2S chimera.

A. Schematic diagram of the transmembrane topology of the ρ1-260-γ2S chimera in which the ECD is from ρ1 (blue) and the TMD is from γ2S (green). **B**. GABA concentration-response curve for ρ1-260-γ2S (n = 6). **C**. Inhibition of GABA EC_{80} (200 μM) peak (black) and steady-state (red) currents by PS at ρ1-260-γ2S (n = 5). **D**. Representative traces for the current responses of ρ1-260-γ2S to GABA EC_{80} with and without 1-100 μM PS. Note the rebound current visible at 100 μM PS. **E**. Traces showing the increased current response of ρ1-260-γ2S to GABA (1 mM) throughout the experiment.

A heteromeric chimera was also studied where three chimeric subunits were used. Each subunit constituted the TMD of ρ1 and the ECD of α1 (α1-222-ρ1), β2 (β2-218-ρ1) and γ2 (γ2-235-ρ1; Fig. 4.17A). As PS was hypothesised to bind in the TMD of α1, β2 and γ2, inhibition by PS was not expected with this chimera. Surprisingly, PS appeared to inhibit the GABA-induced current, as well as a standing current that was caused by constitutive channel activity of the heteromeric chimera. Clear inhibition was only present at 10 μM and 100 μM PS, steady-state current having reached 39.0 ± 5.1% and -258.4 ± 35.7% of the control GABA EC_{80} current, respectively. Similarly, the peak current had reached 63.1 ± 3.6% and -227.4 ± 33.8% at 10 μM and 100 μM PS, respectively. The negative percentage inhibition describes inhibition by 100 μM PS of constitutive channel activity. This constitutive current had an amplitude that could be more than three times that of the GABA control current, and was susceptible to inhibition by PS also when it was applied without GABA (Fig. 4.18). These results show that PS can bind and induce inhibition also in a complex where the TMD is solely from ρ1. Whether the ECDs from α1, β2 and γ2 conferred increased potency of PS at a chimera where the whole of the TMD is from ρ1 (compared to ρ1 wild-type) is uncertain.

As the concentration-response plots for PS in Fig. 4.17 and 4.18 show, PS showed a similar profile of block of both GABA-mediated and spontaneous currents. Whereas no inhibition was observed at 1 μM PS, 10 and 100 μM PS caused inhibition of the current both when co-applied with GABA and when applied on its own. It cannot be excluded that PS only mediated block of the spontaneous current rather than the GABA-mediated current, especially as the outward current was greater when 100 μM PS was applied in the absence of GABA. If this is the case, these results would argue for residues in the TMD of α1, β2 and γ2 to be essential for PS inhibition of GABA-induced currents.

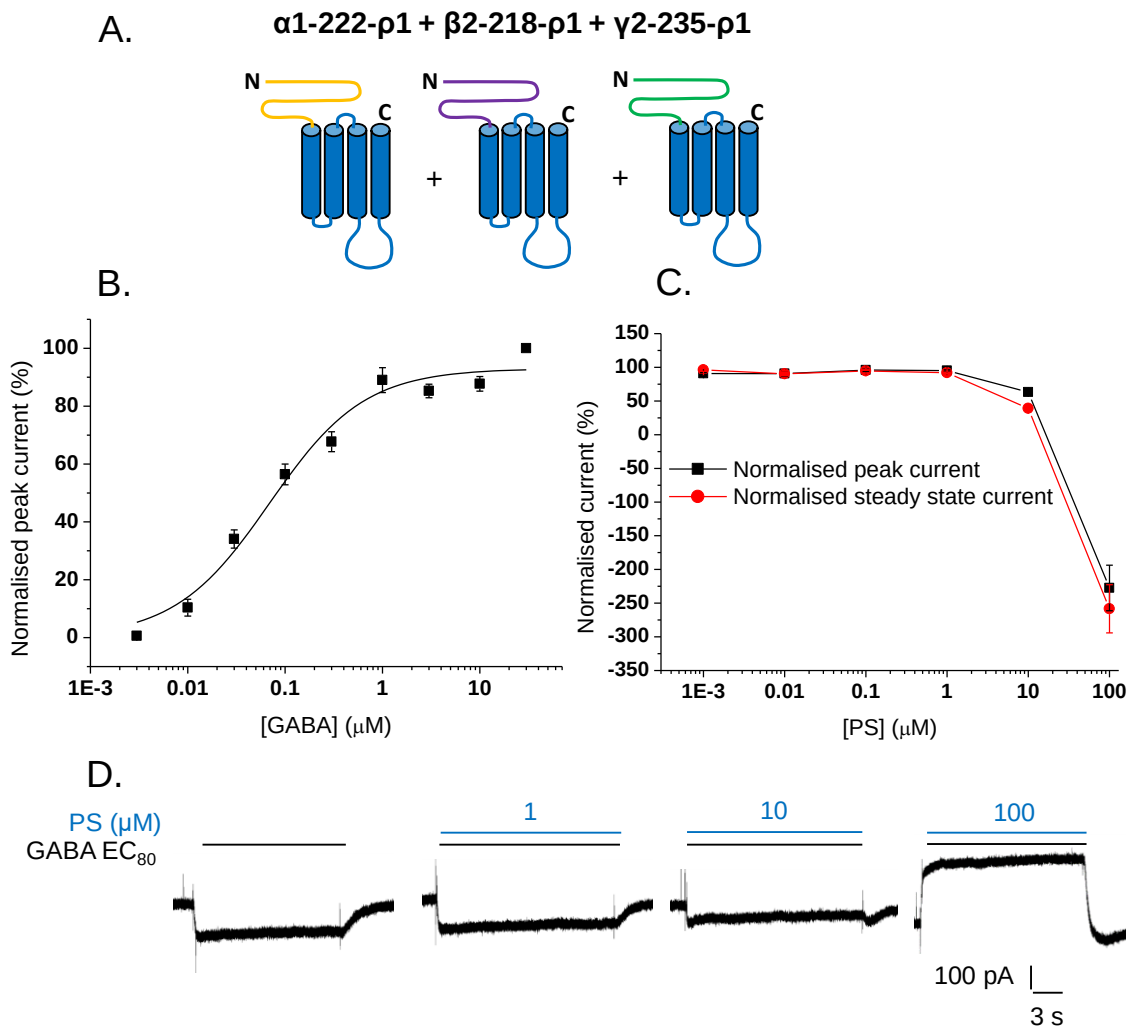

Figure 4.17 – Profiling the α1-222-ρ1 + β2-218-ρ1 + γ2-235-ρ1 chimera.

A. Schematic diagram of the transmembrane topology of the heteromeric α1-222-ρ1 + β2-218-ρ1 + γ2-235-ρ1 chimeric receptor. ECDs are from α1 (orange), β2 (purple) and γ2 (green), and the TMD is from ρ1 (blue). **B**. GABA concentration-response curve for the α1-222-ρ1 + β2-218-ρ1 + γ2-235-ρ1 chimera (n = 7). **C**. Inhibition of GABA EC_{80} (1 μM) peak (black) and steady-state (red) currents by PS at the α1-222-ρ1 + β2-218-ρ1 + γ2-235-ρ1 chimera (n = 9). Data are expressed as mean ± SEM. **D**. Representative traces for activation of α1-222-ρ1 + β2-218-ρ1 + γ2-235-ρ1 by GABA (EC_{80}) and inhibition by PS (1-100 μM) following co-application. Note the large constitutive current evident with 100 μM PS.

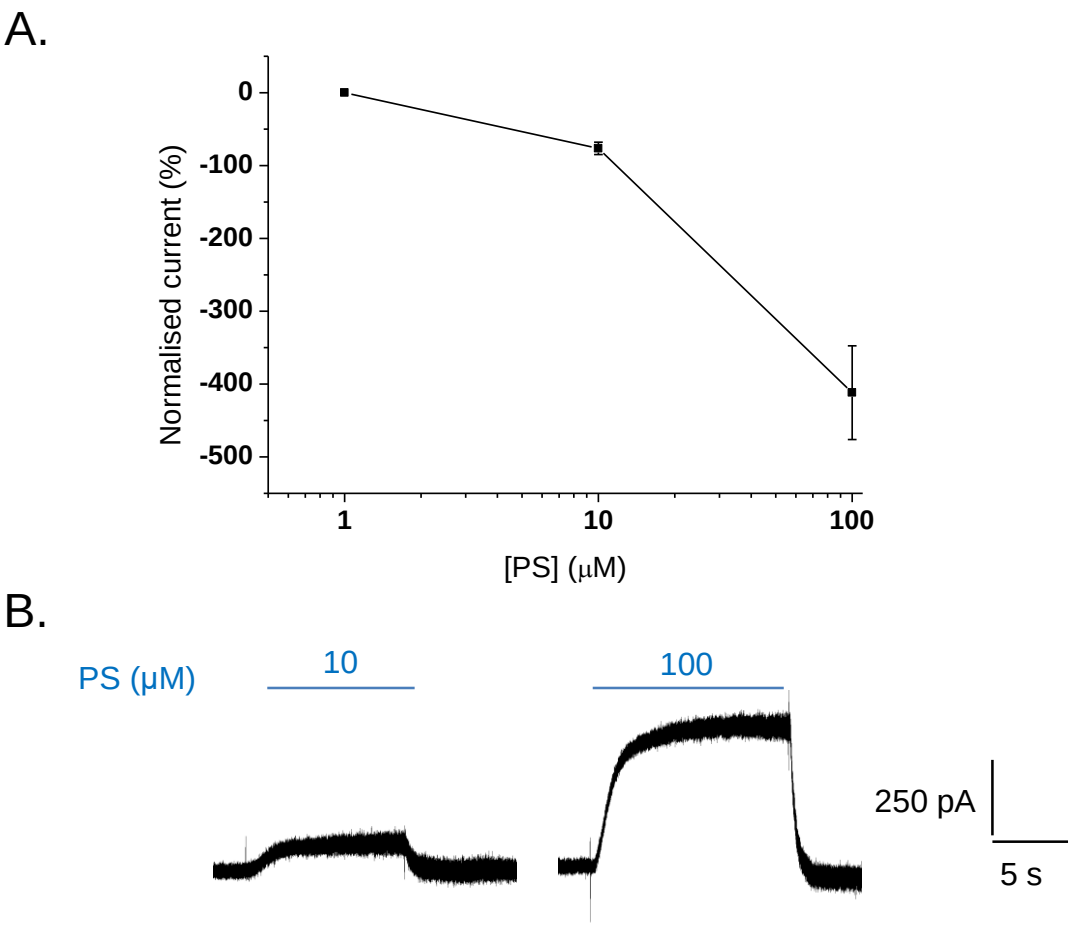

Figure 4.18 – Inhibition of constitutive α1-222-ρ1 + β2-218-ρ1 + γ2-235-ρ1 chimera channel activity by PS.

A. The graph shows the concentration-response relationship of PS (1-100 μM) for inhibition of the constitutive current of the α1-222-ρ1 + β2-218-ρ1 + γ2-235-ρ1 chimera. The current is normalised to the GABA EC_{80} (1 μM) current. Data are expressed as mean ± SEM (n = 6). **B**. Representative traces showing the outward current induced by PS (10-100 μM) when it is applied in the absence of GABA. This shows that PS can block a constitutively active channel.

As a next step, another chimera was used comprising ρ1 from the N-terminal up until the start of M4: ρ1-433-α1 (Fig. 4.19). This chimera showed that PS can cause inhibition of GABA currents at a chimera that is mostly ρ1: at this chimera, where only M4 and the C-terminal are from α1, PS inhibited both the peak and steady-state GABA EC_{80} currents at concentrations higher than 1 μM. At 10 μM PS, peak and steady-state currents were inhibited to 64.9 ± 2.4% and 61.8 ± 4.4% of control, respectively, whereas at 100 μM PS, currents reached 5.5 ± 1.5% and 0.6 ± 9.2% of control, respectively. Large rebound currents were also present upon the wash-out of GABA and PS.

These findings suggest that ρ1 is probably not an ideal 'null' receptor for PS, and that the binding site for the steroid is likely to exist at this subunit. It is possible that PS binds to the wild-type ρ1 receptor, but causes little inhibition of GABA currents due to a missing signal transduction 'machinery'. Introducing residues from α1, β2 or γ2 appears to be sufficient to provide the improved coupling of PS binding to inhibition at the ρ1 chimera complexes.

Another four chimera complexes were also screened for sensitivity to PS, using a simpler experimental design. ρ1-284-α1 (Fig. 4.20A; ρ1 up to the end of M1), ρ1-352-α1 (Fig. 4.20B; ρ1 up to start of the M3-M4 linker), α1-285-ρ1 with β1-281-ρ1 (Fig. 4.20C; α1 or β2 up to start of M3) and α1-308-ρ1 with β2-304-ρ1 (Fig. 4.20D; α1 or β2 up to start of the M3-M4 linker) were all inhibited by 100 μM PS co-applied with 1 mM GABA (Fig. 4.21). Large rebound currents were observed on wash-out of GABA and PS, suggesting the receptor chimeras were re-entering an open state before closure.

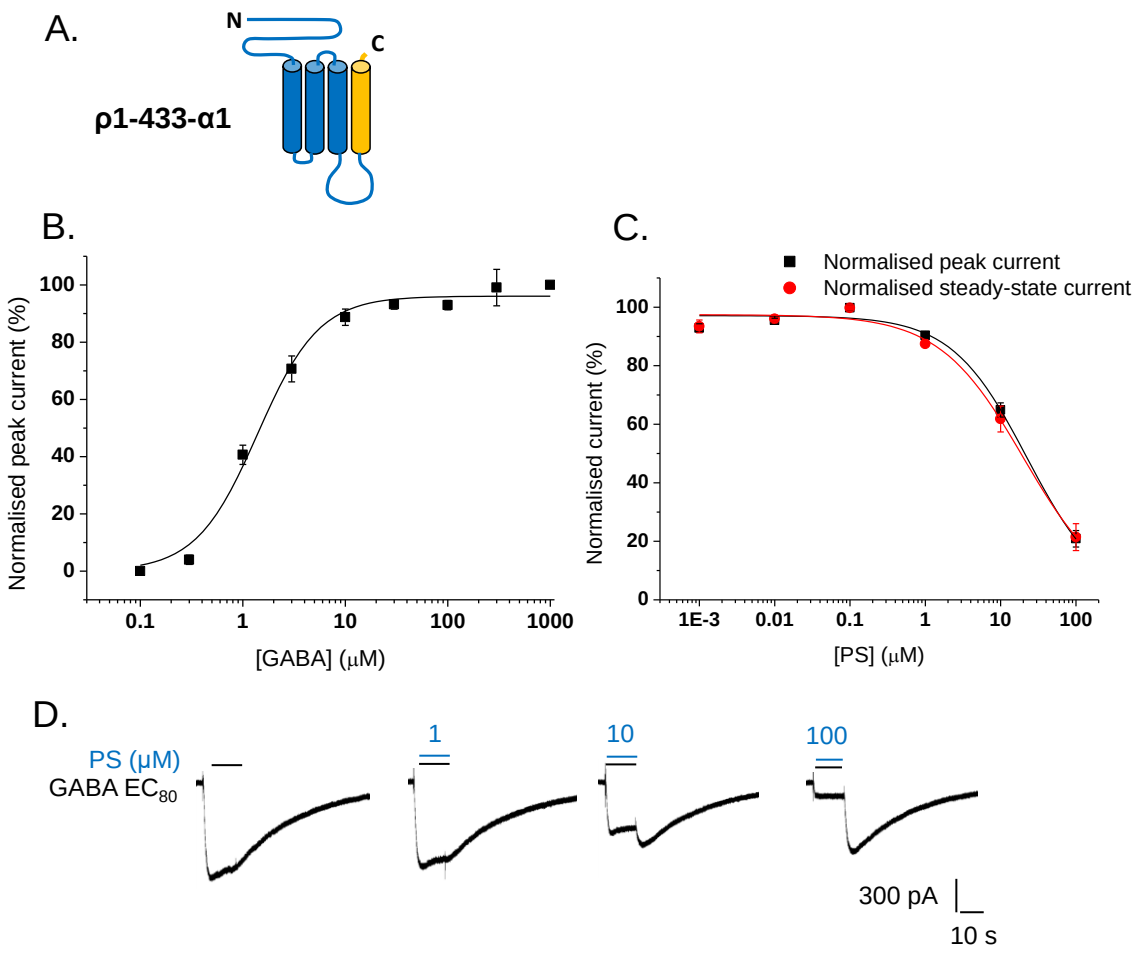

Figure 4.19 – Profiling the ρ1-433-α1 chimera.

A. Schematic diagram of the transmembrane topology of the ρ1-433-α1 chimera. The ECD, M1-M3 and the intracellular M1-M2 and M3-M4 linkers are from ρ1 (blue), whereas M4 and the C-terminal are from the α1 subunit (orange). **B**. GABA concentration-response curve for ρ1-433-α1 (n = 5). **C**. Inhibition of GABA EC_{80} (10 μM) peak (black) and steady-state (red) currents by PS at the ρ1-433-α1 chimera (n = 7). **D**. Representative traces for GABA (EC_{80}) activation and PS (1-100μM) inhibition at the ρ1-433-α1 chimera.

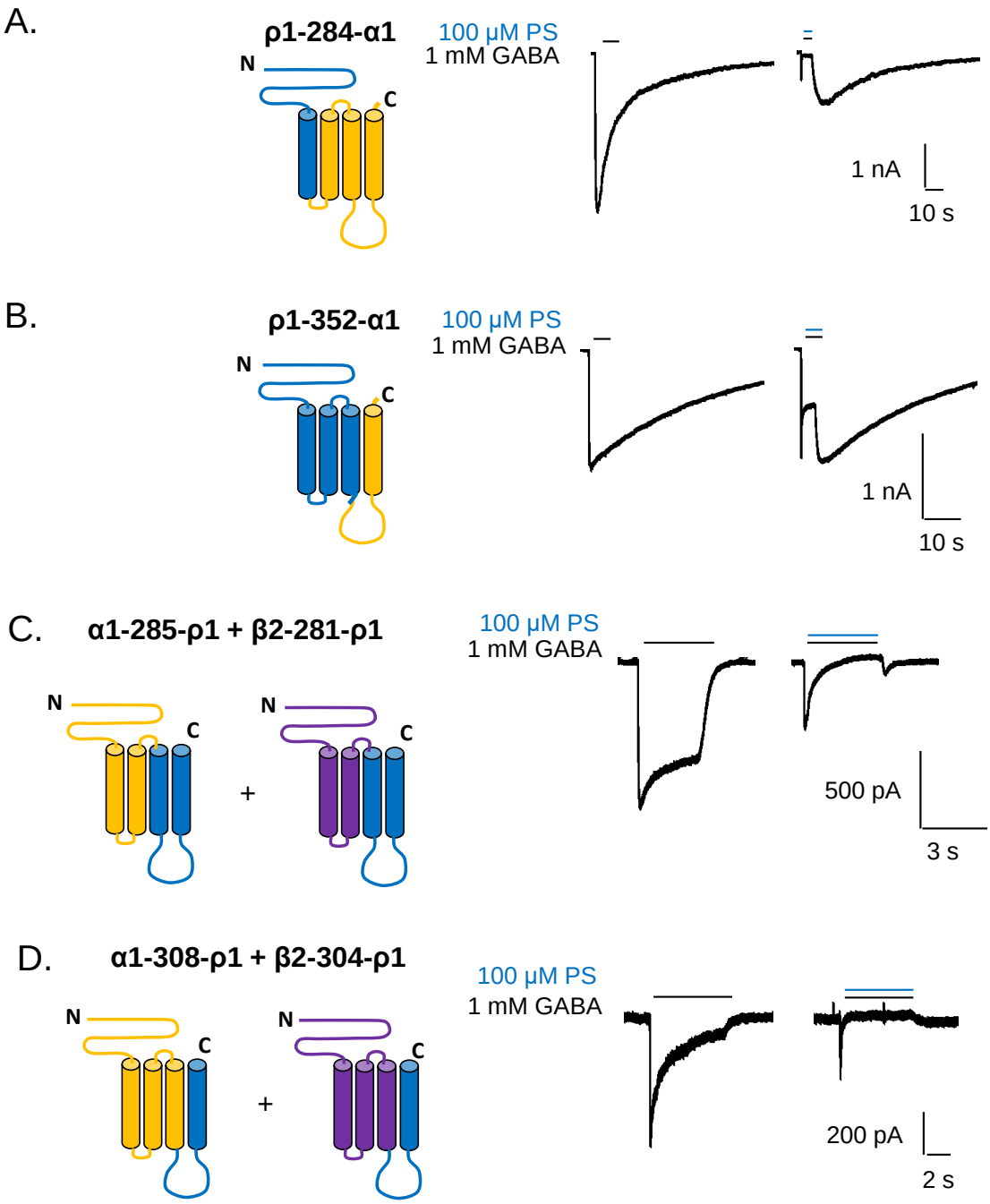

Figure 4.20 – Inhibition of 1 mM GABA currents by 100 μM PS at four chimeras.

A. A schematic of the transmembrane topology of ρ1-284-α1 chimera with representative traces for 100 μM PS inhibition of a 1 mM GABA current. The ECD, M1 and the M1-M2 linker are from ρ1 (blue), whilst the rest of the chimera is from α1 (orange). **B**. A schematic of the transmembrane topology of ρ1-352-α1 chimera with representative traces showing 100 μM PS inhibition of a 1 mM GABA current. The ECD and all residues up until the end of M3 are from ρ1 (blue), whereas the rest of the chimera is from α1. **C**. A schematic of the transmembrane topology of α1-285-ρ1

+ β2-281-ρ1 chimera with representative traces for 100 μM PS inhibition of a 1 mM GABA current. The N-terminus and all residues up until the start of M3 are from α1 (orange) or β2 (purple), with the rest of the chimera being formed from ρ1 residues (blue). **D**. A schematic of the transmembrane topology of α1-308-ρ1 + β2-304-ρ1 chimera with representative traces for 100 μM PS inhibition of a 1 mM GABA current. The N-terminus and all residues up until the end of M3 are from α1 (orange) or β2 (purple), with the rest of the chimera being formed from ρ1 residues (blue).

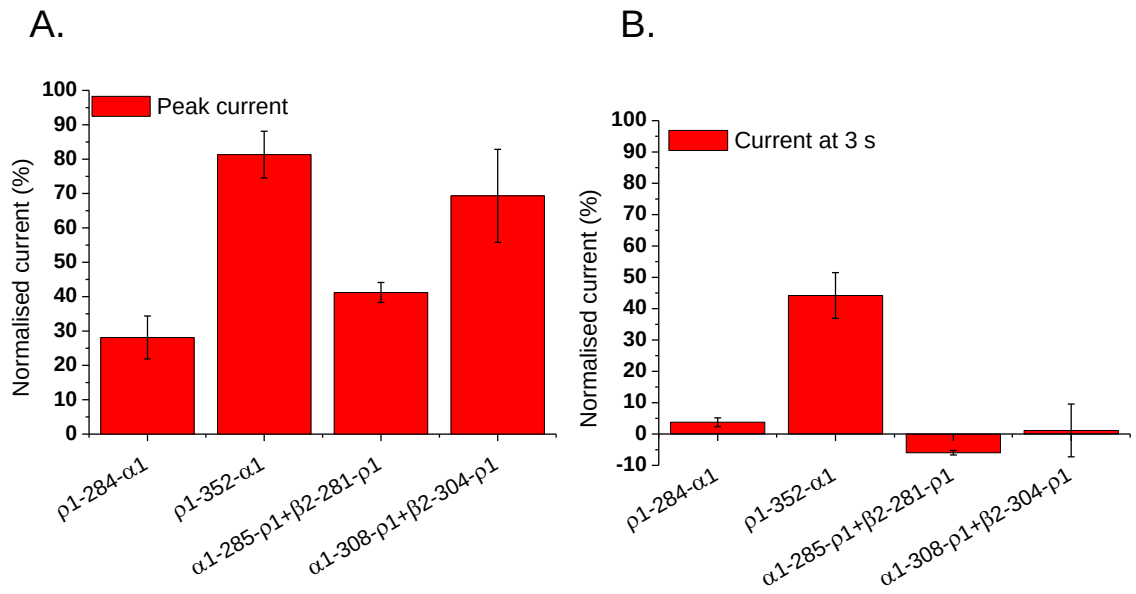

Figure 4.21 – Inhibition of 1 mM GABA currents by 100 μM PS at four chimeras.

A. Inhibition by 100 μM PS of a 1 mM GABA peak current at ρ1-284-α1, ρ1-352-α1, α1-285-ρ1 + β2-281-ρ1 and α1-308-ρ1 + β2-304-ρ1 (n = 3). **B**. Inhibition by 100 μM PS of a 1 mM GABA current measured at 3 s at ρ1-284-α1, ρ1-352-α1, α1-285-ρ1 + β2-281-ρ1 and α1-308-ρ1 + β2-304-ρ1 (n = 3). Data are expressed as mean ± SEM.

As can be discerned from the traces in Fig. 4.20 and the bar charts in Fig. 4.21, clear inhibition was present at all chimeras. Full steady-state current inhibition was obtained at thee of the chimeras, the exception being ρ1-352-α1 where inhibition only just exceeded 50%. Notably the peak current was also less affected by PS in the ρ1-352-α1 chimera, approaching the sensitivity of the WT ρ1 receptor. Nevertheless, these findings demonstrate that a variety of chimeras formed between ρ1 and α1 (or β2 and γ2) exhibit some sensitivity to PS. This

means it is difficult to envisage using the ρ1 subunit as a background 'null' receptor to find the binding site for PS.

4.3. Discussion

This chapter aimed to bring us closer to finding the binding site for PS at mammalian $GABA_A$ receptors. It has been shown that the 2' mutants $\alpha1^{V256S/C}\beta2\gamma2L$ and $\alpha1\beta3^{A252S}\gamma2L$ remain sensitive to PS, though curves for inhibition of the steady-state current were shifted to the right and, surprisingly, peak current inhibition was increased at the α1 2' mutants. The receptors also remained sensitive to PTX, despite the 2' residue's likely involvement in forming a binding site for this $GABA_AR$ channel blocker. Introducing the 2' valine of α1 to ρ1, $\rho1^{P294V}$, did however increase the sensitivity of the homomeric receptor to PS which supports a role for this residue in the signal transduction pathway of PS.

The UNC-49B/C residues that were identified as important for PS and DHEAS modulation are unlikely to be important for the inhibition of murine $GABA_A$ receptors. When a homologous residue in the α1 subunit was mutated to an UNC-49B residue that was predicted to reduce PS inhibition ($\alpha1^{Y230V}$), the IC_{50} for steady-state current inhibition was halved. Conversely, introducing a UNC-49C residue into the α1 subunit that was predicted to promote inhibition ($\alpha1^{Y230F}$), actually increased the IC_{50}. Peak current inhibition was also increased at all the mutants that were predicted to reduce PS sensitivity. These findings suggest that these residues are also involved in the signal transduction rather than the binding of PS.

The ρ1 chimera studies showed that all the combinations of subunit sequences yielded receptors that were sensitive to PS. These findings argue for the binding site of PS being present on the wild-type ρ1 subunit, but that an efficient transduction machinery is absent.

4.3.1. The 2' residue is unlikely to form a binding site for PS at ρ1 and α1β2/3γ2L receptors

Early work suggested an essential role for the 2' residue in PTX block of the RDL (Ffrench-Constant et al., 1993) and ρ receptors (Wang et al., 1995), and mutating either the α and/or β subunit at this position removed PTX block from $GABA_A$ receptors (Xu et al., 1995). This finding was later supported by the crystal structure of GluCl bound to PTX in the ion channel at 2' (Hibbs and Gouaux, 2011). Due to similarities in the block produced by PS and PTX, Akk et al. (2001) set out to determine if this residue was also essential for inhibition by PS. Single channel recordings showed that the α1 2' mutation, $\alpha1^{V256S}$, reduced the apparent association rate of PS 30-fold and the cluster duration in the presence of PS was no longer reduced. The homologous mutations in the β2 and γ2L subunits had no such effect.

The present study has shown that for macroscopic GABA currents, the inhibition curve for PS is shifted to the right also when the β3 subunit is mutated at 2'. Replacing the 2' residue with serine did, however, have a greater effect on PS sensitivity at the α1 than the β3 subunit. Compared to the wild-type receptors, the IC_{50}s for steady-state current inhibition for $\alpha1^{V256S}\beta2\gamma2L$ and $\alpha1\beta3^{A252S}\gamma2L$ were increased 89-fold and 18-fold, respectively. In contrast to the findings of Akk et al. (2001), other studies have shown that the inhibitory effect of PS on whole-cell currents is reduced or abolished in *Xenopus* oocytes expressing either $\alpha1^{V256S}\beta2\gamma2L$ or $\alpha1\beta2^{A252S}\gamma2L$ (Wang et al., 2006, 2007). This supports the notion that by mutating either the α1 or β2/3 subunits, the potency and efficacy of PS is reduced. However, taken together with the low voltage-dependence of PS, it is likely that the 2' mutation alters an allosteric mechanism and interferes with the signal transduction rather than directly affecting the binding of PS. It should be noted that in the studies by Wang et al. (2006, 2007), PS was only used at concentrations up to 2 μM, which could explain why they reported a complete loss of PS sensitivity at the 2' mutants.

Interestingly, the $\alpha1^{V256S}$, but not the $\beta2^{A252S}$ mutation, eliminates $GABA_A$ receptor antagonism by the 3β-hydroxypregnane steroids (Wang et al., 2002, 2007;

Seljeset et al., 2015). These are diastereomers of the potentiating 3α-hydroxypregnane steroids, but are similar to the sulphated neurosteroids in that they non-competitively inhibit the $GABA_A$ receptor in an activity- or state-dependent manner. In the study by Wang et al. (2007), desensitisation kinetics were characterised by finding the ratio between the peak current and the steady-state current at 20 seconds (P/SS ratio). In wild-type receptors, PS increases the P/SS ratio in a concentration-dependent manner, but the ratio remains unchanged at increasing concentrations of PS when the 2' mutation is introduced to the α1 or β2 subunit. This suggests that PS promotes desensitisation of wild-type receptors, or keeps them in a desensitised state, whereas this effect is removed in the mutant receptors. An alternative explanation is that as the mutation increases the susceptibility to peak current inhibition by PS (or rather, that it makes the peak and steady-state currents equally susceptible to inhibition), as shown in section 4.2.1, the P/SS ratio remains unchanged at increasing concentrations of PS. Block by the 3β-hydroxypregnane steroid did not cause a concentration-dependent increase in the P/SS ratio in wild-type or mutant receptors, suggesting that the mechanism of block by sulphated steroids and 3β-hydroxypregnane steroid is not shared (Wang et al., 2007). It also implies that the 2' residue is unlikely to be the common binding site for either group of steroids, and corroborates the hypothesis that this is likely to be a residue important for an allosteric mechanism (Seljeset et al., 2015). The increased sensitivity of the ρ1 receptor to PS upon the introduction of the α1 2' residue ($ρ1^{P294V}$) also agrees with this hypothesis, and suggests that the binding site for PS is already present at the ρ1 subunit.

As the 2' residue has been shown to be a likely binding site for PTX in mutational studies (Wang et al., 1995; Xu et al., 1995; Ueno et al., 2000), and the crystal structure of GluCl shows the molecule interacting with the 2' threonine and -2' proline at the cytosolic end on the M2 helix (Hibbs and Gouaux, 2011), it was surprising to find that the $α1^{V256S}β2γ2L$ receptor was at least as sensitive to PTX as the wild-type receptor. However, other studies have also shown that the $α1^{V256S}β2γ2L$ and $α1β2^{A252S}γ2L$ remain sensitive to PTX (Wang et al., 2002, 2006; Chisari et al., 2011). Replacing the 2' valine of the α2 subunit with tryptophan ($α2^{V257W}$) does however remove the PTX sensitivity of α2β2 receptors

expressed in *Xenopus* oocytes (Ueno et al., 2000). This could be because the PTX binding site is removed or because tryptophan sterically blocks access to the binding site. Thus, the serine residue might not be disruptive enough to prevent block by PTX.

Taken together, the effect of the 2' mutations in ρ1 and α1β2/3γ2L on PS sensitivity suggest that this residue is involved in the allosteric mechanism or signal transduction that occurs following binding. This is corroborated by the observation that PS block is only weakly voltage-sensitive, and the finding that the 3β-hydroxypregnane steroids, which likely inhibit the receptor via a different mechanism, are also affected by the 2' mutation.

4.3.2. Residues identified in UNC-49B/C studies are unlikely to form a binding site for PS

Introducing residues from the M1 segment of UNC-49B, which are thought not to define the binding site for PS (Wardell et al., 2006), were found to either increase ($\alpha1^{Y230V}$) or have no effect ($\alpha1^{Q228N}$) on the inhibition by PS at the α1β2γ2L receptor. By contrast, introducing a residue from UNC-49C which was predicted to promote inhibition or have no effect ($\alpha1^{Y230F}$), reduced inhibition at the α1β2γ2L receptor. These findings suggest that the residues identified are, like the 2' residue, likely to be involved in the allosteric signalling mechanism that occurs following PS binding rather than forming a binding site for PS *per se*. This finding is corroborated by another study where the M1 segment of UNC-49B was swapped into mammalian α1, β2, and γ2 subunits to determine if this could remove PS sensitivity (Baker et al., 2010). None of the chimaeras containing M1 of UNC-49B showed any (predicted) loss of sensitivity to PS, suggesting that the residues identified in UNC-49C, although important for modulation by sulphated neurosteroids, cannot form a binding site that is conserved among different species. These studies show that individual point mutations can often disrupt the activity of a pharmacological agent by interfering with receptor behaviour rather than ligand binding. Thus, single point mutations do not, by themselves, identify ligand binding sites, and corroborating evidence is always necessary (Colquhoun, 1998).

4.3.3. Probing the binding site for PS using ρ1 chimeras

Various chimeras between ρ1 and α1, β2 or γ2 subunits were studied to try and determine which residues are important for the binding of PS. Surprisingly, all sequences from α1, β2 or γ2 that were swapped into ρ1 increased the potency of PS at the receptor. Even the chimeric receptor complex containing the TMD of ρ1 and ECD of α1, β2 and γ2 (α1-222-ρ1 + β2-218-ρ1 + γ2-235-ρ1) was sensitive to PS, which shows that the 2' $\rho1^{P294V}$ mutation may not be essential for PS inhibition of ρ1 receptor currents. However, it might be that only the constitutive current, rather than the GABA-mediated current, was inhibited by PS at the α1-222-ρ1 + β2-218-ρ1 + γ2-235-ρ1 chimera. This would imply that residues in the TMDs of the α1, β2 and γ2 subunits are necessary for the ability of PS to block GABA-mediated currents. Moreover, chimeras containing the ECD of ρ1 and the TMDs of α1 or γ2 (ρ1-260-α1/γ2) were sensitive to PS. Taken together, these results suggest that PS is likely to bind to all of the subunits included in this study, as the chimera studies showed that inhibition occurs in chimeras containing sequences from ρ1 and α1 or γ2, and experiments with the β3 homomer showed that PS can inhibit PB-induced currents. The homomeric wild-type ρ1 receptor likely fails to respond efficiently to the binding of PS because of an absent signalling mechanism. The residues necessary for this allosteric mechanism are likely to be present in α1, β2 and γ2 subunits, and absent in the wild-type ρ1 receptor.

4.3.4. Is inhibition by PS due to effects on lipids in the plasma membrane?

The question that arises is where is PS binding? The lack of enantioselectivity of a pharmacological agent at a receptor is sometimes used as evidence that no specific binding site is present, and that modulation occurs through indirect interaction between the modulator and the receptor (Twede et al., 2007; Seljeset et al., 2015). This could be through the partitioning of the ligand into the membrane, leading to a change in the properties of the lipid bilayer around the receptor. Whereas the potency of DHEAS and its enantiomer differs 7-fold in inhibiting $GABA_A$ receptor currents, PS was found to show no enantioselectivity for inhibition of GABA whole-cell currents in rat hippocampal neurones (Nilsson

et al., 1998). However, the opposite result was obtained in a study using the UNC-49B/C receptor: the natural enantiomer of PS was three times more potent than its enantiomeric counterpart, whilst DHEAS showed no enantioselectivity (Twede et al., 2007). The selectivity of various $GABA_A$ receptors for neurosteroid enantiomers may, however, depend on the specific way that the molecule contacts its binding site at the receptor, and the absence of enantioselectivity does not unequivocally distinguish direct ligand-receptor interactions from indirect membrane interactions. However, some specificity in engaging with a binding site is suggested from the structure-activity studies of PS at native $GABA_A$ receptors (Park-Chung et al., 1999; Seljeset et al., 2015).

Previous studies have investigated whether PS may act by indirectly modulating $GABA_A$ receptors through partitioning into the lipid layer of the plasma membrane (Mennerick et al., 2008; Akk et al., 2009; Chisari et al., 2010, 2011). PS increases membrane capacitance, whereas potentiating neurosteroids do not, and this increased capacitance has been suggested to mediate the inhibitory effect of PS on the $GABA_A$ receptor (Mennerick et al., 2008). The level of inhibition caused by PS and structurally similar sulphated steroids also correlates with the degree of capacitance change the steroids produce. It has also been shown that structurally diverse detergents and amphiphiles, *e.g*. triton X-100 and docosahexaenoic acid, perturb the lipid membrane and antagonise $GABA_A$ receptors in a manner that is similar to PS, with antagonism that is promoted by receptor activation and manifests as an apparent increase in desensitisation (Søgaard et al., 2006; Chisari et al., 2010). Interestingly, negative modulation by these amphiphiles was also almost abolished by the $\alpha1^{V256S}$ mutation. The same characteristics apply to the hydrophobic anions, *e.g*. dipicrylamine (DPA) and tetraphenylborate (TPB), both of which antagonise $GABA_A$ receptors in a manner similar to PS and are affected by the 2' mutation (Chisari et al., 2011). However, one important factor not in accord with a membrane perturbation effect is that I have shown that PS cannot inhibit $GABA_A$ receptors from within the cell (Chapter 3, section 3.2.5.). If disruption of the membrane is enough to cause inhibition, without any specific ligand-receptor interaction, some inhibition would also be expected when PS is applied inside the plasma membrane. However, as all $GABA_A$ receptor subunits,

including ρ1, appear to have a binding site for PS, it is possible that the interactions are not very specific.

4.4. Conclusion

This chapter has shown that PS can inhibit GABA-induced currents at $\alpha1^{V256S/C}\beta2\gamma2L$ and $\alpha1\beta3^{A252S}\gamma2L$ receptors as well as the receptors with residues introduced from UNC-49B. These results suggest that the residues identified previously by Akk et al. (2001), Wardell et al. (2006) and Twede et al. (2007) are unlikely to be involved in forming a binding site in the mammalian $GABA_A$ receptor. Furthermore, the ρ1 chimera work suggested that this subunit is likely to also contain a binding site for PS, but the transduction machinery necessary for allosteric modulation is most probably absent.

Chapter 5: Modulation of GABAergic transmission in hippocampal neurones by PS

5.1. Introduction

The two previous results chapters have discussed the mechanism by which PS modulates recombinant $GABA_A$ receptors in HEK cells, and explored potential binding sites for the inhibitory neurosteroid at these receptors. To investigate the effect of PS on GABAergic transmission under physiological conditions, dissociated hippocampal neurones from E18 rats were used in electrophysiological experiments after 10 to 16 days in culture. As PS was found to have a greater inhibitory effect on GABA steady-state than peak currents in HEK cells, the study was designed to explore whether PS might have a role in modulating the decay phase of synaptic GABA currents, and if current amplitudes can be affected. Previously, PS was observed to inhibit an emulated tonic GABA current in HEK cells (see section 3.2.7.), and it would therefore be interesting to determine if inhibition of a tonic GABA current can occur in the more physiological environment of a hippocampal neurone where ambient GABA exists, primarily due to synaptic release.

Modulation of GABAergic IPSCs by PS has been studied previously. PS has been reported to have no direct modulatory effect on $GABA_A$ receptors in dissociated hippocampal neurones, as the amplitude of IPSCs was not diminished (Teschemacher et al., 1997; Mtchedlishvili and Kapur, 2003). A presynaptic effect of PS was however observed, as the steroid appeared to reduce the frequency of GABA-mediated IPSCs.

In hippocampal neurones from P1 rats that had been in culture for 3 to 9 weeks, PS was shown to reduce the frequency of miniature IPSCs (mIPSCs) (Teschemacher et al., 1997). PS was applied at concentrations ranging between 1 and 50 μM, at which 1 μM had the greatest effect on the mIPSC frequency. Furthermore, PS did not directly modulate postsynaptic $GABA_A$ receptors, as no reduction in IPSC amplitude was observed until after wash-out of the steroid. The

reduction in mIPSC frequency induced by 1 μM PS (to 70% of control) was observed after 10 to 15 min of exposure to PS, and was irreversible as the frequency did not recover following wash-out.

A later study using hippocampal neurones from E18 rats after 2-3 weeks in culture reported a decrease in the frequency of mIPSCs and spontaneous IPSCs (sIPSCs) of 40-60% (Mtchedlishvili and Kapur, 2003). This effect was observed at a much lower concentration of PS (30 nM), was more immediate in onset and reversible. The effect of PS could also be mimicked by a σ1 receptor agonist and blocked by σ1 receptor antagonists, implicating a role of this receptor in regulating GABA release in the presynaptic membrane. Unsurprisingly for such a low concentration, 30 nM PS did not appear to modulate postsynaptic $GABA_A$ receptors, as no effect was observed on peak amplitudes or decay time constants.

Whereas the study by Teschemacher et al. (1997) only studied mIPSCs and observed a rather delayed effect of PS, the study by Mtchedlishvili and Kapur (2003) only used concentrations of PS too low to have a direct effect on $GABA_A$ receptors. Therefore, I decided to study the effect of PS on IPSCs in rat hippocampal neurones (embryonic day (E) 18 + 10-16 days *in vitro* (DIV)) using micromolar concentrations of PS to increase the likelihood of observing a direct effect on postsynaptic $GABA_A$ receptors, as observed in HEK cell recordings. As PS affects the decay phase of whole-cell GABA currents in HEK cells, I was interested to find out if PS might also affect the rate of decay of IPSCs. As described below, PS was found to have both presynaptic and postsynaptic effects, most likely caused by acting at multiple receptors that exist in or close to the inhibitory synapse.

5.2. Results

5.2.1. PS inhibits GABA whole-cell currents in hippocampal neurones

For electrophysiological recordings in hippocampal neurones, fast glutamatergic transmission was blocked with 1 mM kynurenic acid. The addition of 20 µM bicuculline (BIC) abolished all synaptic currents, demonstrating that all IPSCs were mediated by $GABA_A$ receptors (Johnston, 2013).

To demonstrate that PS can antagonise GABA-mediated whole-cell currents in hippocampal neurones, like in HEK cells, GABA at EC_{80} (30 µM) was co-applied with PS at increasing concentrations. As neurones express various subtypes of the $GABA_A$ receptor, the IC_{50} will be influenced by the composition of receptors present in the cells and might be different from the values derived from HEK cell recordings.

Similarly to the inhibition produced at recombinant $GABA_A$ receptors, GABA peak currents were weakly inhibited in neurones, to 71.4 ± 5.3% of control at 100 µM PS (Fig. 5.1B and C). The steady-state current was inhibited in a concentration-dependent manner by PS, with an IC_{50} of 3.3 ± 0.5 µM (Fig. 5.1C). This value is somewhat higher than the IC_{50}s for the individual subtypes of the recombinant receptors, which ranged between 0.4 and 1.3 µM PS in HEK cells (see section 3.2.6.). These results show that native $GABA_A$ receptor-mediated whole-cell currents are inhibited by PS in hippocampal neurones.

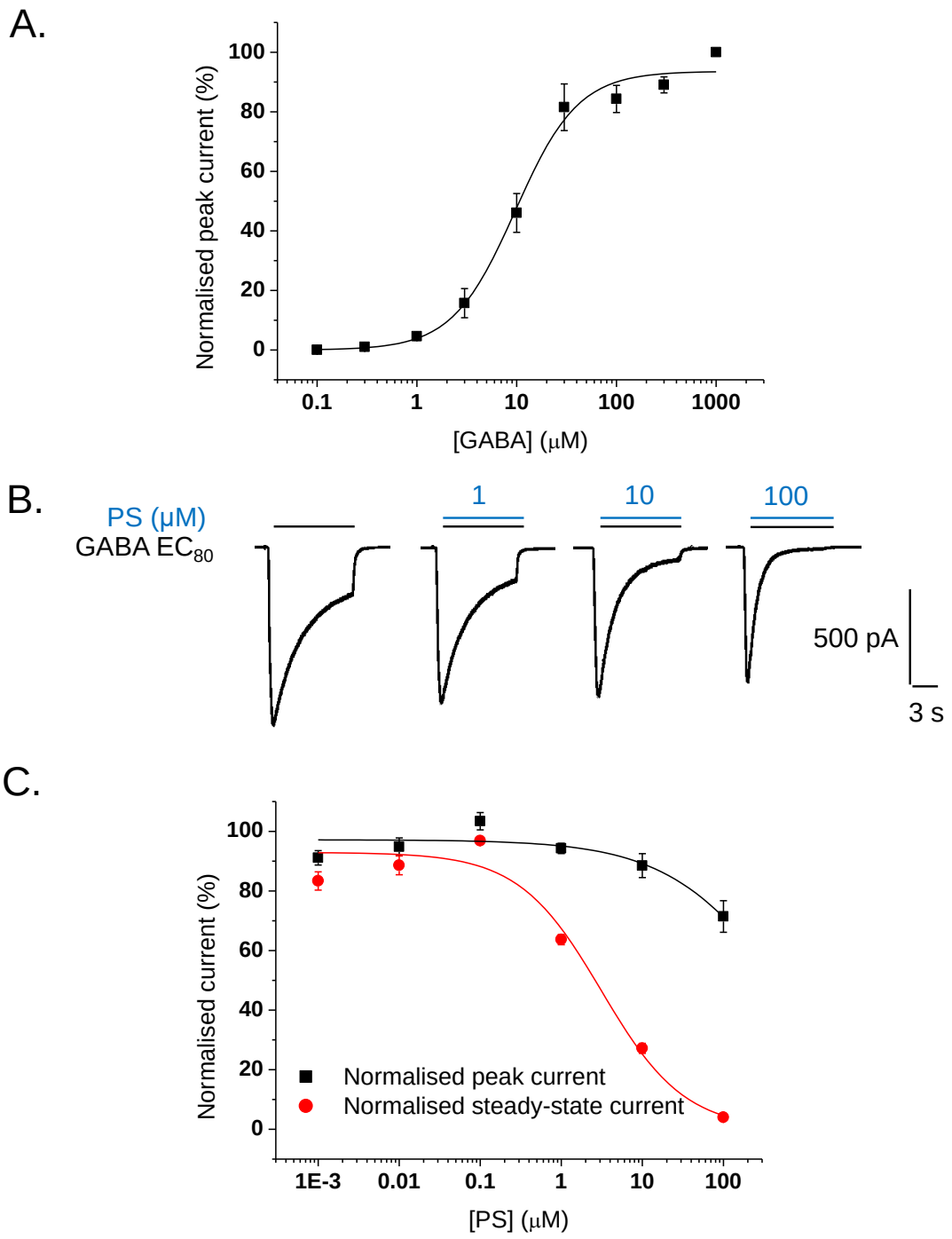

Figure 5.1 – PS inhibits whole-cell GABA currents in hippocampal neurones.

A. GABA concentration-response curve for whole-cell currents in hippocampal neurones (n = 5). Currents were normalised to the GABA EC_{100} (1 mM) response. **B**. Representative traces for inhibition of GABA EC_{80} currents by PS (1-100 μM) in hippocampal neurones. **C**. Inhibition curves for the inhibition of GABA EC_{80} peak (black) and steady-state (red) currents by PS in hippocampal neurones (n = 8). Data are expressed as mean ± SEM.

5.2.2. PS increases presynaptic GABA release in hippocampal neurones

To determine if PS can also inhibit synaptic $GABA_A$ receptor currents (IPSCs), neurones were exposed to PS with no exogenously applied GABA. IPSCs are kinetically very different from GABA whole-cell currents; whereas whole-cell currents are slow in onset and can last for seconds, IPSCs are very fast and transient events lasting milliseconds. Due to the slow onset of inhibition by PS, which in HEK cells was measured 10 s into drug application, it is not certain whether PS can inhibit the peak amplitude of IPSCs. The delayed inhibition that was measured at 10 s in HEK cells is more likely to manifest as an effect on the decay phase of an IPSC.

As shown for 3 µM PS in Fig. 5.2, the frequency of IPSCs went up dramatically when neurones were exposed to PS. The effect on frequency was concentration-dependent (Fig. 5.4 and 5.5A), and reversible, as washing out PS brought the frequency back to baseline level (Fig. 5.2 and 5.3B).

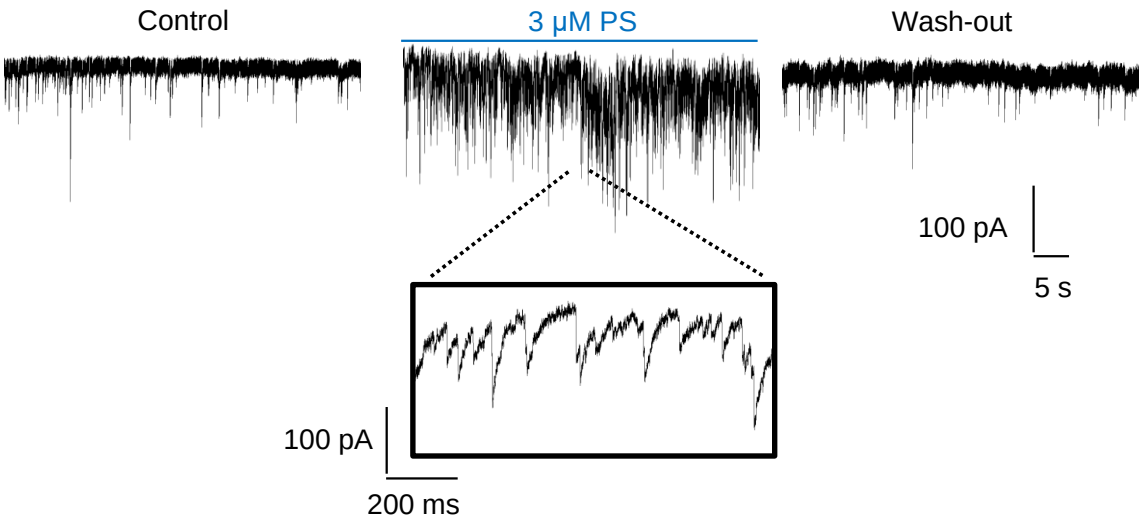

Figure 5.2 – Representative traces demonstrating the increase in IPSC frequency induced by PS.

The traces show recorded IPSCs under control conditions (left), in the presence of 3 µM PS (middle) and upon wash-out of PS (right). The zoomed in trace in the box shows 1 s of recording, increasing the resolution of individual IPSCs.

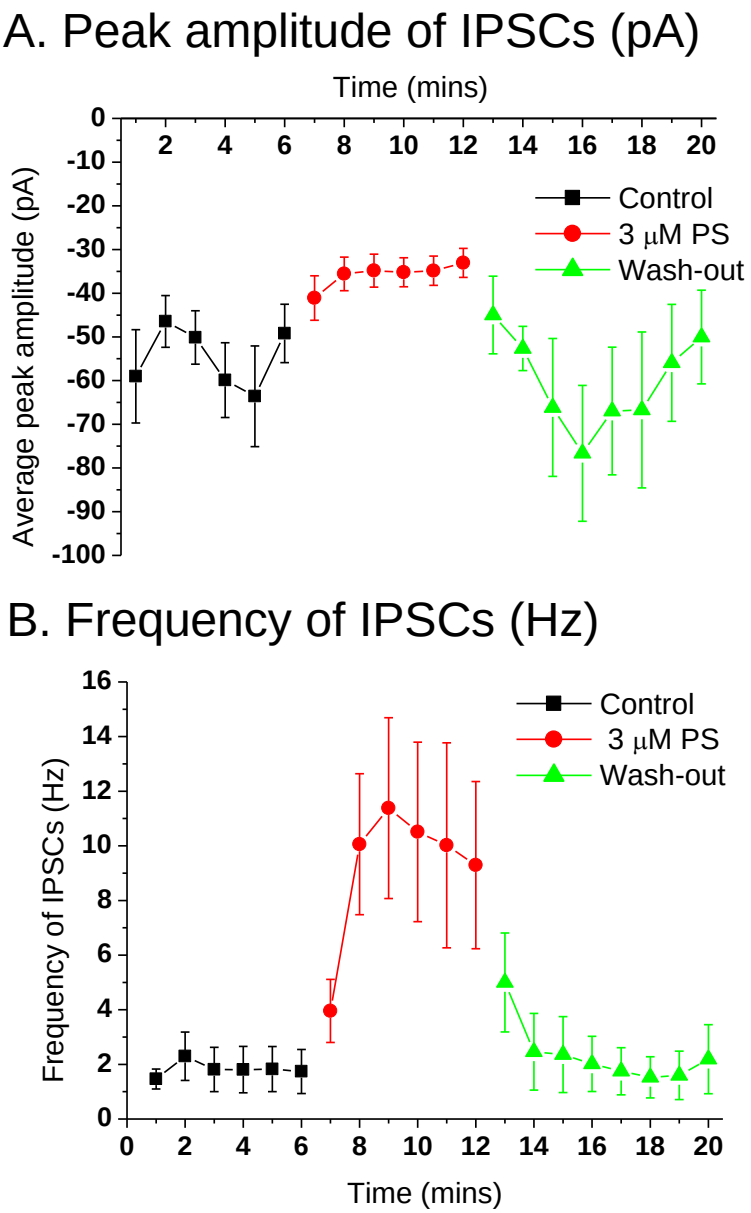

Figure 5.3 – Time courses for the effects of PS on IPSCs in hippocampal neurones.

A. Plot of peak amplitude of IPSCs before, during and after PS, with mean amplitudes in control (black), 3 μM PS (red) and wash-out (green) shown. All events within each minute of recording were averaged (n = 8). **B**. Plot of mean frequency of IPSCs over time in control (black), 3 μM PS (red) and wash-out (green) (n = 8). Data are plotted as mean ± SEM.

The increase in presynaptic GABA release was gradual in onset, and peaked within ~2 min of exposure to PS (for 3 μM PS, see Fig. 5.3B). The inhibitory effect of PS on IPSC amplitude was faster in onset and showed little time-dependence (Fig. 5.3A).

The presynaptic effect of PS on GABA release was concentration-dependent (Fig. 5.4 and 5.5). Compared to control, the fold increase in frequency was 1.78 ± 0.97 at 30 nM PS ($p = 0.249$, $n = 6$), 2.53 ± 1.08 at 1 µM ($p = 0.0741$, $n = 6$), 8.72 ± 2.30 at 3 µM ($p = 0.0039$, $n = 8$) and 12.93 ± 4.11 at 10 µM PS ($p = 0.0005$, $n = 8$). Although all values are normalised for presentation, statistical analyses were undertaken by comparing non-normalised data in control and PS in paired datasets, both for frequency and amplitude. All statistical analyses of PS modulation in neurones were performed comparing raw data from paired datasets, unless otherwise is stated.

A postsynaptic effect of PS may have been masked by the PS-induced increase in presynaptic GABA release. However, as demonstrated by the time plot in Fig. 5.3, the amplitude of the IPSCs was reduced slightly by 3 µM PS. This effect did not appear to be strongly concentration-dependent, as the average amplitude reached 0.91 ± 0.13 of control at 30 nM PS ($p = 0.127$, $n = 6$), 0.62 ± 0.14 at 1 µM ($p = 0.0252$, $n = 6$), 0.69 ± 0.10 at 3 µM ($p = 0.0113$, $n = 8$) and 0.65 ± 0.10 at 10 µM PS ($p = 0.0125$, $n = 8$) (Fig. 5.5B). The lack of concentration-dependent inhibition of IPSC peak amplitudes may be due to a large increase in small events caused by the surge in GABA release in the presence of PS, potentially combined with direct postsynaptic inhibition of IPSC peak amplitudes.

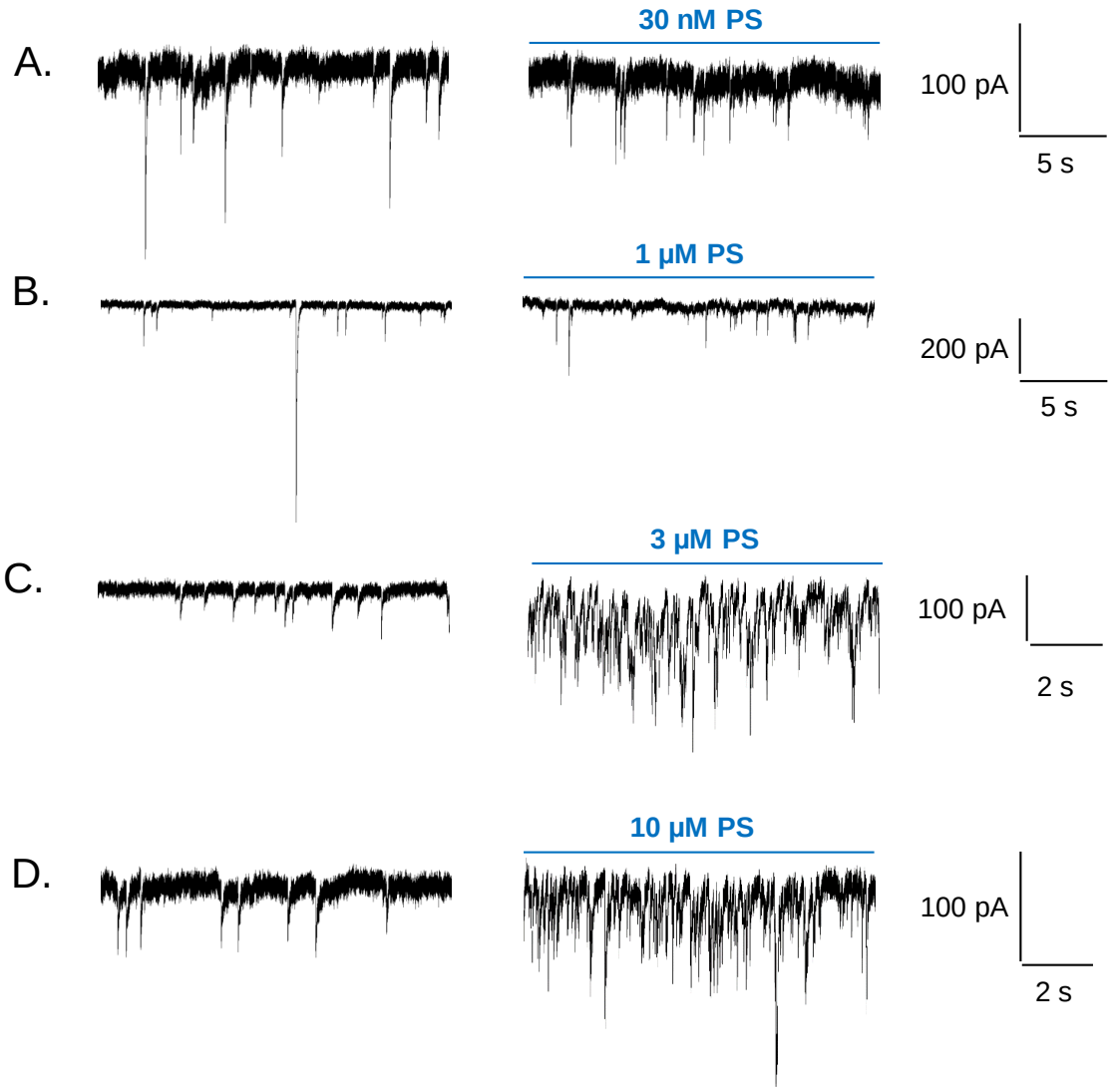

Figure 5.4 – Effect of 30 nM - 10 µM PS on IPSC frequency.

The current traces show a control recording (left) and the effect of PS on IPSC frequency (right) in one individual cell for several concentrations of PS as indicated in A-D.

To further investigate whether PS affects the amplitude of IPSCs, or if the decrease in the average peak amplitude in PS is due to an increased frequency of smaller IPSCs, amplitude distributions were generated (Fig. 5.6). In neurones treated with 3 µM PS, the distribution of IPSC amplitudes was similar in control and PS as two Gaussian fits best described the populations of events in each condition; whereas the bell curves had means (± standard deviation) of -26.9 ± 0.2 pA and -54.3 ± 3.1 pA in control, the means were -24.3 ± 0.5 pA and -52.6 ± 7.2 pA in 3 µM PS (Fig. 5.6A and B). This suggests that there is little effect of PS

on the peak amplitude of the IPSCs, though more small events (< -30 pA) are present in 3 μM PS than in control.

When neurones were treated with 10 μM PS, only one population of amplitudes was present as the data were best described by a single Gaussian fit (Fig. 5.6C and D). This had a mean of -29.5 ± 0.4 pA, whereas the two populations in control had means of -30.0 ± 0.2 pA and -62.6 ± 5.0 pA. This shows that the population of events of larger amplitudes (> -50 pA) had mostly been ablated in 10 μM PS. These histograms show that the distribution of events according to peak amplitude is changed by PS, as larger events are mostly absent and the number of smaller events has increased. This reduction or absence of large events may be due to direct inhibition of postsynaptic $GABA_A$ receptors by PS.

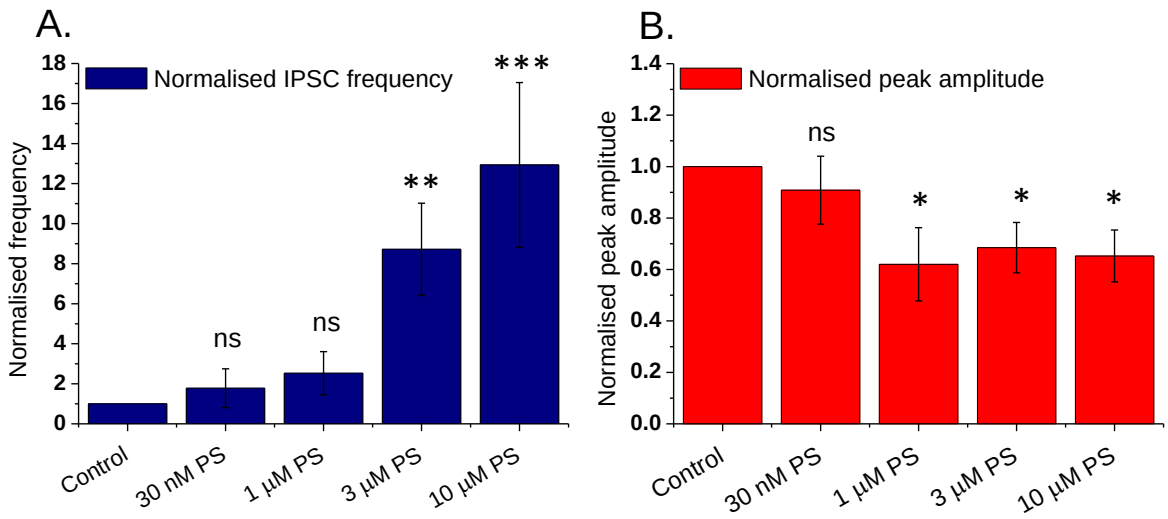

Figure 5.5 – The effect of PS on IPSC frequency and amplitude.

A. Normalised frequency of IPSCs in control conditions and in the presence of 30 nM - 10 μM PS. The cells had been exposed to PS for at least 1 min before the frequency was calculated over a time period of at least 2 mins (n = 6-8). Frequencies are normalised to the frequency measured in control in each cell. **B**. Normalised peak amplitudes of IPSCs in control conditions and in the presence of 30 nM - 10 μM PS (n = 6-8). The mean peak amplitude was calculated over a time period of at least 2 min for each condition. Peak amplitudes are normalised to the mean peak amplitude in control in each cell. Data are expressed as mean ± SEM. ns denotes not statistically significant, * $p < 0.05$, ** $p < 0.01$ and *** $p < 0.001$ (compared to control).

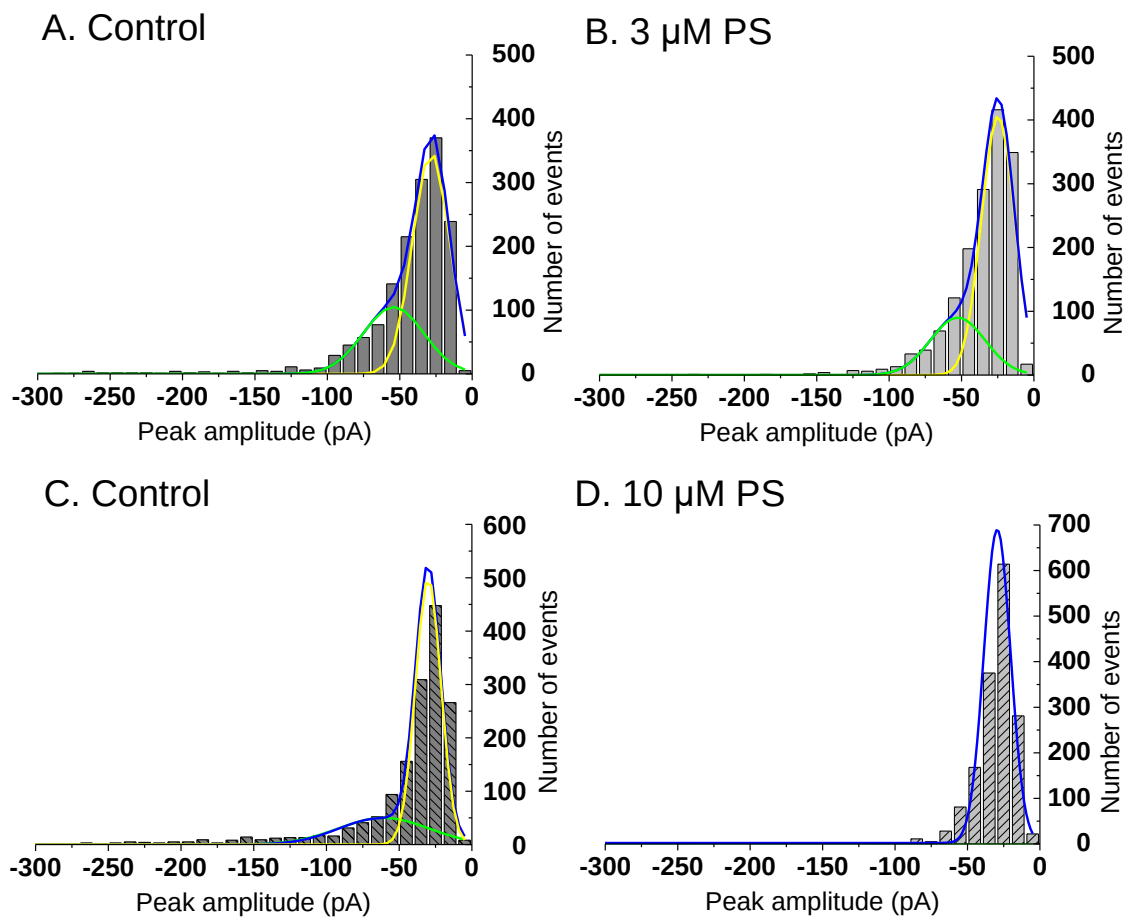

Figure 5.6 – IPSC amplitude distributions in control and at 3 and 10 µM PS.

A-D. The histograms with Gaussian fits show the distribution of events according to IPSC amplitude in control (on the left) and PS (right). 200 events from each recording were chosen in the control and after 2 min in 3 µM PS (**A** and **B**; n = 8) and 10 µM PS (**C** and **D**; n = 7). The curves in green and yellow show the two different distributions in each condition, and the curve in blue shows the sum of the two.

As PS appears to promote desensitisation of recombinant $GABA_A$ receptors in HEK cells, it is plausible that PS has a similar effect on the decay phase of IPSCs through modulating native $GABA_A$ receptors in the postsynaptic membrane. To determine if this is the case, a minimum of 50 'clean', non-overlapping events were selected in control, 1 µM and 3 µM PS. Events were averaged and the weighted tau (τ_w) was determined by fitting a biexponential curve to the mean waveform (Fig. 5.7). At 10 µM PS the frequency was too high to find enough clean events. Weighted τ_w was 26.9 ± 3.2 ms in 1 µM PS, compared to 32.0 ± 3.3 ms in control ($p = 0.00194$, $n = 5$). At 3 µM PS, weighted τ_w was 21.6 ± 1.2 ms, compared to 34.7 ± 2.0 ms in control ($p < 0.0001$, $n = 8$). This means that 1 µM

and 3 µM PS reduced the τ_w by 16.3 ± 2.6% and 37.5 ± 2.6%, respectively, indicating that PS increases the rate of IPSC decay in hippocampal neurones.

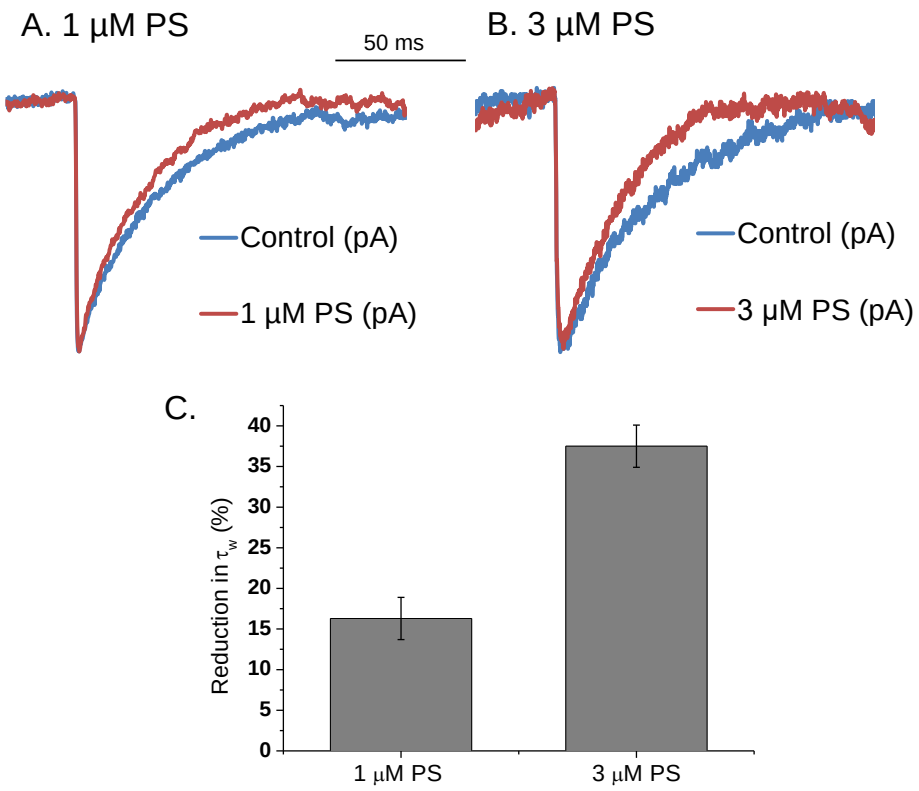

Figure 5.7 – Mean IPSC waveforms with and without 1 and 3 µM PS.

A. Mean IPSC waveforms for control (blue) and 1 µM PS (red) from a single cell. **B**. Mean IPSC waveforms for control (blue) and 3 µM PS (red) from one cell. Mean waveforms were calculated from at least 50 clean, non-overlapping events in each condition, and are normalised to the peak value in the mean waveform. **C**. The bar chart shows the percentage reduction in τ_w caused by 1 µM and 3 µM PS compared to control (n = 5-8). Data are expressed as mean ± SEM.

As PS is an inhibitory neurosteroid at $GABA_A$ receptors, and negatively modulates the receptors, one would expect PS to be excitatory at the synapse by diminishing inhibition. However, as PS also acts presynaptically and increases GABA release, the increased frequency of IPSCs could lead to an increased influx of Cl^- ions across the postsynaptic membrane, meaning the net effect of PS could be to reduce excitability of the postsynaptic cell. To determine if this is the case, charge transfer in control, 1 µM and 3 µM PS was calculated by multiplying the area under the mean IPSC waveform by the frequency of IPSCs in each condition (Fig. 5.8). In 1 µM PS, the average charge transfer was -3.8 ± 1.2 pC/s,

which was not different from -4.7 ± 1.2 pC/s in control (p = 0.2410, n = 8; Fig. 5.8A). When the concentration of PS was increased to 3 µM, the charge transfer was -3.4 ± 0.9 pC/s, which was higher than in control (1.2 ± 0.1 pC/s, p = 0.0233, n = 7; Fig. 5.8B). This represents a 2.8-fold increase in the influx of Cl^- ions across the postsynaptic membrane in the presence of 3 µM PS, suggesting that PS at 3 µM is likely to reduce rather than increase the excitability of the hippocampal neurone.

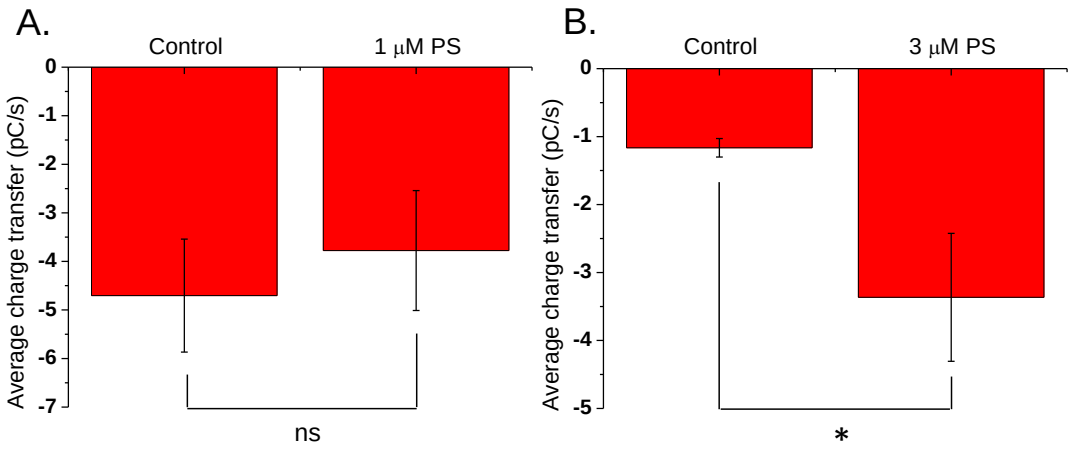

Figure 5.8 – Charge transfer is increased in neurones at 3 µM but not 1 µM PS.

The bar chart shows the charge transfer in control and in 1 µM PS (**A**; n = 8) and 3 µM PS (**B**; n = 7). Charge transfer was calculated by multiplying the frequency of IPSCs by the area under the mean IPSC waveform in each recording condition. The mean waveform was found by averaging at least 50 clean events in each condition. Data are expressed as mean ± SEM. ns denotes not statistically significant, * $p < 0.05$.

5.2.3. PS increases presynaptic GABA release in TTX and increases the rate of IPSC decay

Various ion channels and receptors are potential presynaptic targets of PS. To increase GABA release, PS must be acting to either increase the excitability of the presynaptic neurone or to locally increase the Ca^{2+} concentration in the synaptic terminal. Alternatively, it might also interfere directly with the machinery involved in vesicular neurotransmitter release, increasing the probability of vesicle release.

It is unclear whether PS acts to increase GABA release by increasing action potential (APs) firing in the presynaptic neurone, or if release is increased via an AP-independent mechanism. To assess whether PS increases presynaptic GABA release via a mechanisms that makes the presynaptic neurone more likely to fire APs, neurones were kept in 500 nM TTX before and after exposure to 1-10 µM PS. PS has, however, previously been described to inhibit voltage-gated Na^+ channels (Na_Vs) (Horishita et al., 2012), which would reduce excitability and GABA release. Nevertheless, blocking Na_Vs removes AP-dependent sIPSCs, allowing us to study the effect of PS on mIPSCs. If the frequency of IPSCs still goes up when APs are blocked, this suggests that PS acts on a presynaptic target to increase GABA release rather than increasing presynaptic interneurone excitability. The postsynaptic effect of PS may also be easier to study when the baseline frequency of IPSCs is lower.

Similar to the results obtained in the absence of TTX, PS evoked a concentration-dependent increase in mIPSC frequency (Fig. 5.9A-D), showing that the increase in GABA release is not due to PS stimulating AP firing in presynaptic interneurones. At 1 µM PS the frequency did not go up (1.1 ± 0.1 of control, p = 0.406, n = 8), but at 3 µM, the fold increase in frequency was 3.0 ± 0.6 (n = 0.0071, n = 8), and 20.6 ± 5.3 at 10 µM PS (p = 0.0013, n = 6).

PS did not reduce mIPSC peak amplitudes in TTX. At 1 µM PS the peak amplitude was 0.95 ± 0.47 of control (p = 0.2750, n = 8), at 3 µM it was 0.89 ± 0.62 (p = 0.05, n = 8) of control, and at 10 µM PS, the peak amplitude was 0.98

± 0.12 of control (p = 0.2757, n = 6; Fig. 5.9E). This indicates that PS does not modulate the amplitude of mIPSCs.

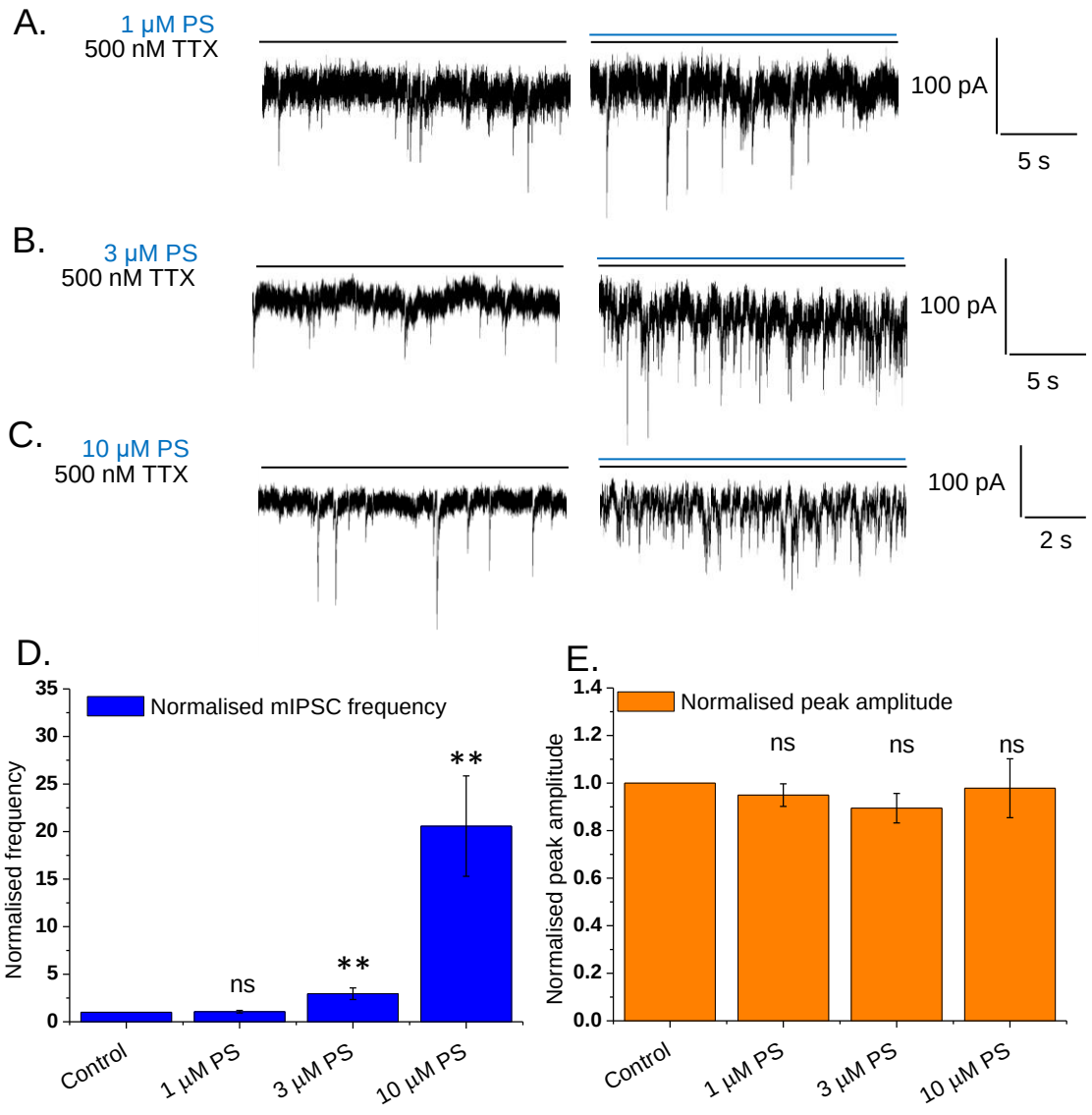

Figure 5.9 – PS increases IPSCs frequency in the presence of TTX.

A-C. Representative traces for the effect of 500 nM TTX (left) and TTX with PS (right) at 1 µM (**A**), 3 µM (**B**) and 10 µM PS (**C**). **D**. A bar chart demonstrating the effect of PS (1 – 10 µM) on IPSC frequency. **E**. A bar chart showing the effect of PS on IPSC peak amplitude. Data are normalised to control (TTX only) and expressed as mean ± SEM (n = 6-8). ns denotes not statistically significant, ** p < 0.01 (compared to control).

To determine if PS also increased the rate of mIPSC decay in TTX, the mean mIPSC waveform was calculated in control and with 1-10 µM PS by selecting at

least 50 clean, non-overlapping events in each condition. τ_w was determined by fitting a biexponential curve to the decay phase of each waveform (Fig. 5.10).

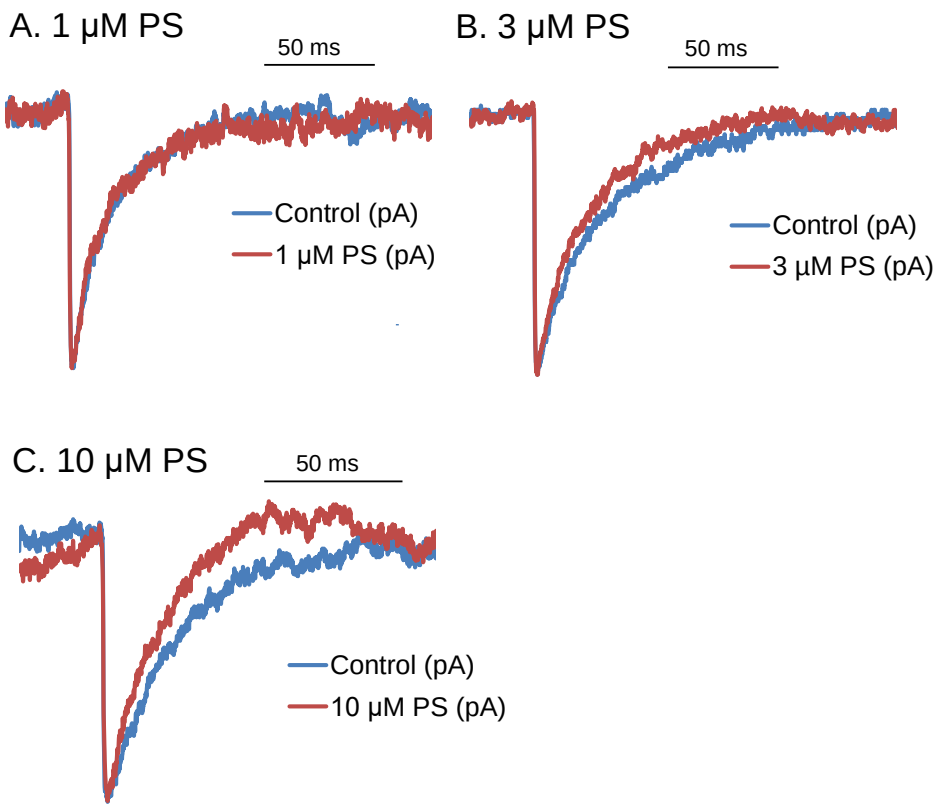

Figure 5.10 – Mean mIPSC waveforms with and without 1, 3 and 10 µM PS in TTX.

A-C. Mean mIPSC waveforms from one cell for control (blue) and PS (red) at 1 µM (**A**), 3 µM (**B**) and 10 µM (**C**). Mean waveforms were calculated from at least 50 clean, non-overlapping events in each condition, and are normalised to the peak value in the mean waveform.

At 1 µM PS, τ_w was 26.4 ± 2.8 ms, compared to 28.4 ± 3.2 ms in control, representing a change in τ_w of 3.8 ± 10.1% ($p = 0.2727$, $n = 8$; Fig. 5.11). The reduction in τ_w was greater at 3 µM PS, having reached 24.6 ± 1.3 ms compared to 32.6 ± 1.7 ms in control ($p < 0.0005$, $n = 7$), representing a change of 24.4 ± 2.3%. At 10 µM PS, τ_w was reduced by 50.5 ± 8.0%, being 16.6 ± 1.3 ms in PS, compared to 37.0 ± 5.0 ms in control ($p = 0.0041$, $n = 6$). Thus, PS had a concentration-dependent effect on the rate of decay. TTX did not itself have any

effect on decay; comparing τ_w in 13 cells with and without 500 nM TTX, showed that τ_w is 33.2 ± 1.7 ms in control and 34.6 ± 2.4 ms in TTX (n = 13, p = 0.6337).

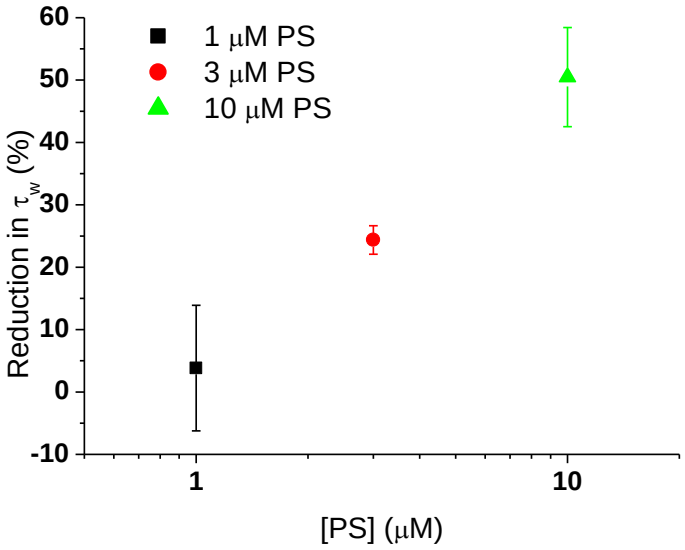

Figure 5.11 – PS has a concentration-dependent effect on mIPSC decay.

τ_w was calculated by fitting a biexponential curve to the mean waveform of the mIPSCs in 1 μM (black; n = 8), 3 μM (red; n = 7) and 10 μM PS (green; n = 6). Recordings were carried out in the presence of 500 nM TTX. The mean waveform was based on at least 50 clean events in each condition. Data are shown as a percentage reduction in τ_w compared to control in each recording and are expressed as mean ± SEM.

To determine if charge transfer is increased by PS also in the presence of TTX, charge transfer in control and 1-10 μM PS was calculated by multiplying the area under the mean waveform by the frequency of mIPSCs in each condition (Fig. 5.12). At 1 μM, PS did not increase the charge transfer across the membrane, being -1.35 ± 0.60 pC/s in control and -1.29 ± 0.56 pC/s in PS (p = 0.6975, n = 8). Charge transfer was almost doubled in 3 μM PS, as it went from -2.23 ± 0.38 pC/s in control to -4.35 ± 1.09 pC/s in PS (p = 0.0222, n = 8). The effect was even larger at 10 μM PS, as the average charge transfer went from -1.23 ± 0.93 pC/s in control to -4.16 ± 1.28 pC/s in PS (p = 0.0009, n = 6), representing a 3.4-fold increase. Thus, the effect of PS on increasing charge transfer was concentration-dependent in 500 nM TTX.

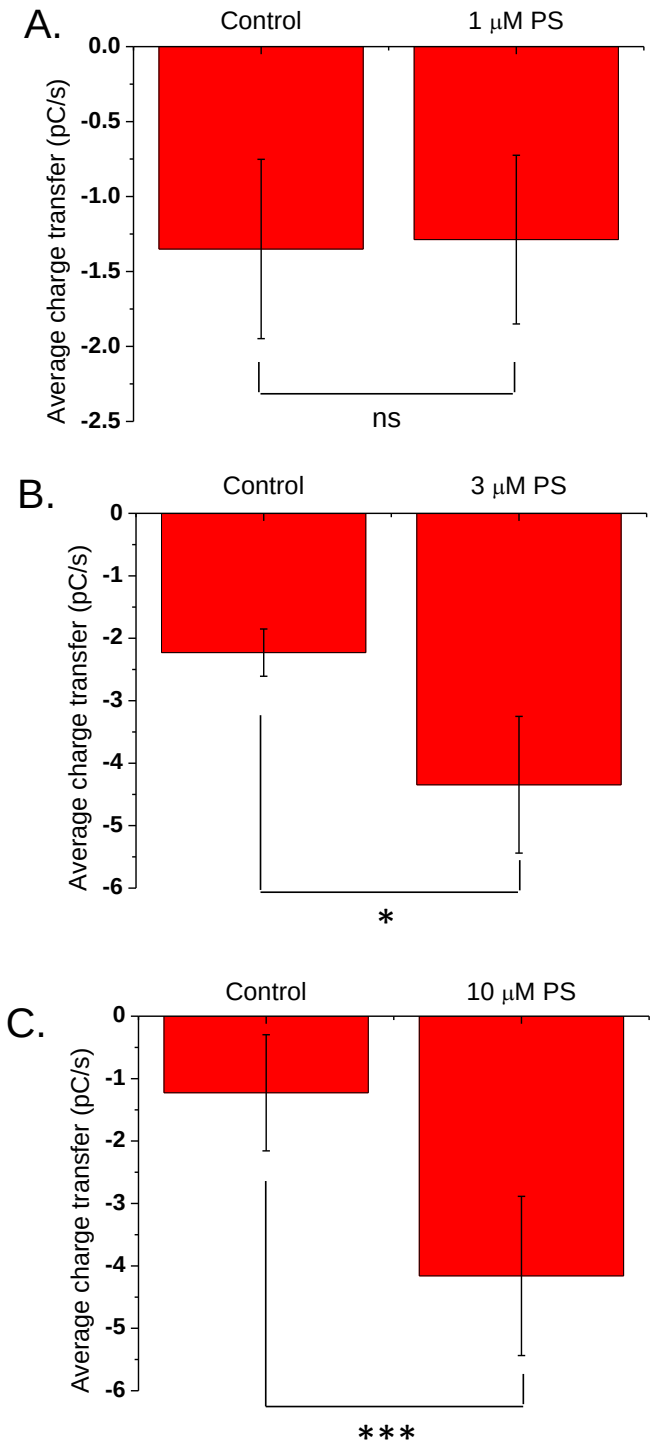

Figure 5.12 – Charge transfer in 1-10 μM PS in the presence of TTX.

A-C. The bar charts show the average charge transfer (pC/s) in control and 1 μM (**A**), 3 μM (**B**) and 10 μM (**C**) PS (n = 6-8). Charge transfer was calculated by multiplying the frequency of IPSCs by the area under the mean mIPSC waveform in each recording condition. The mean waveform was found by averaging at least 50 clean events in each condition. Data are expressed as mean ± SEM. ns denotes not statistically significant, * $p < 0.05$, *** $p < 0.001$.

5.2.4. Cd^{2+} does not block the presynaptic effect of PS

Another potential cause of the increase in GABA release could be increased flux of Ca^{2+} through voltage-gated Ca^{2+} channels (Ca_Vs) in the presynaptic membrane. PS has previously been shown to enhance glutamatergic transmission, most likely via direct modulation of Ca_Vs (Hige et al., 2006). To examine this possibility, Ca_Vs were blocked by 200 µM Cd^{2+}, which should produce a full block of the channels (Lansman et al., 1986). As can be discerned from the traces in Fig. 5.13, Cd^{2+} caused a large reduction in the frequency of IPSCs, showing that the block of the Ca_Vs significantly reduced GABA release. Furthermore, Cd^{2+} has also been shown to be an antagonist of $GABA_A$ receptors with an IC_{50} >100 µM (Kumamoto and Murata, 1995). It may also inhibit extrasynaptic $GABA_A$Rs (Fisher and Macdonald, 1998), and in accord with this produced a prominent block of the GABA-mediated tonic current. This went back to baseline upon wash-out of Cd^{2+} (Fig. 5.13B).

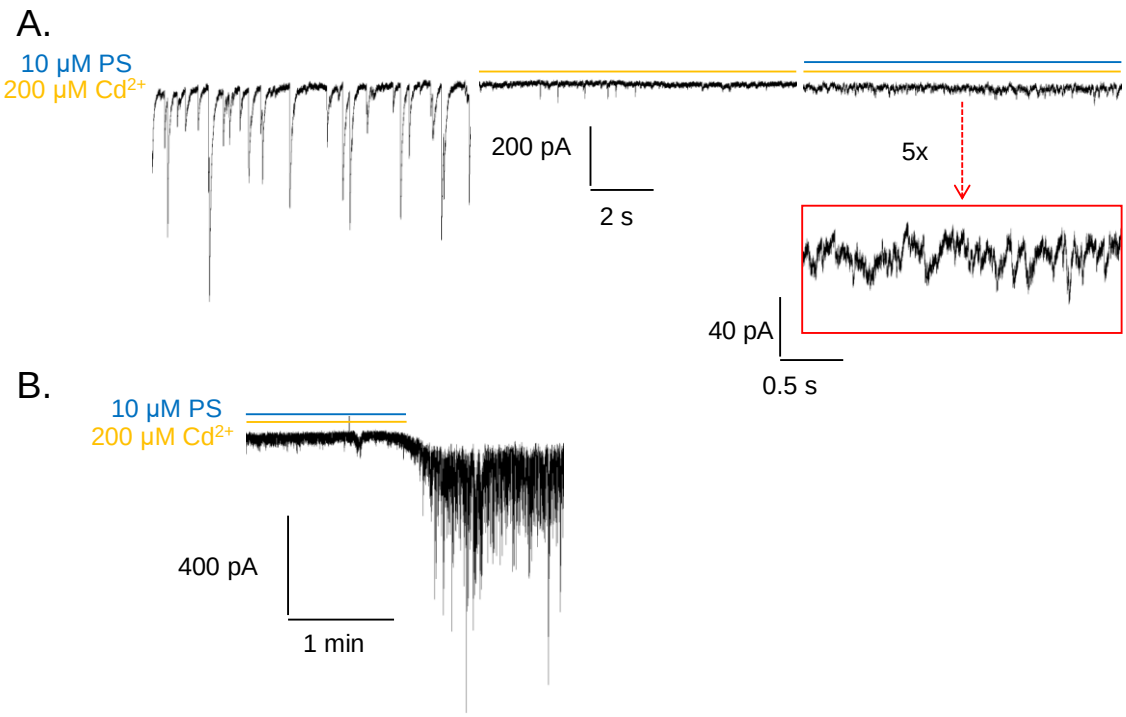

Figure 5.13 – The effect of Cd^{2+} and PS on IPSC frequency and amplitude.

A. Representative traces showing control (no drug; trace on the left), the effect of 200 µM Cd^{2+} (middle trace) and the effect of 10 µM PS on IPSCs in the presence of Cd^{2+}. The trace in the box gives a closer view of the effect of PS on the baseline. **B**. The trace demonstrates the increase in IPSC amplitude upon Cd^{2+} and PS wash-out, and the inhibitory effect of Cd^{2+} on the tonic GABA current.

PS (10 µM) caused a pronounced increase in the normalised frequency of IPSCs also in the presence of Cd^{2+}, which went up from 0.39 ± 0.09 of control in Cd^{2+} to 13.15 ± 6.29 in Cd^{2+} and PS, an almost 33-fold increase in frequency ($p = 0.0156$, $n = 6$; Fig. 5.14A). This suggests that presynaptic Ca_Vs are not a target for PS.

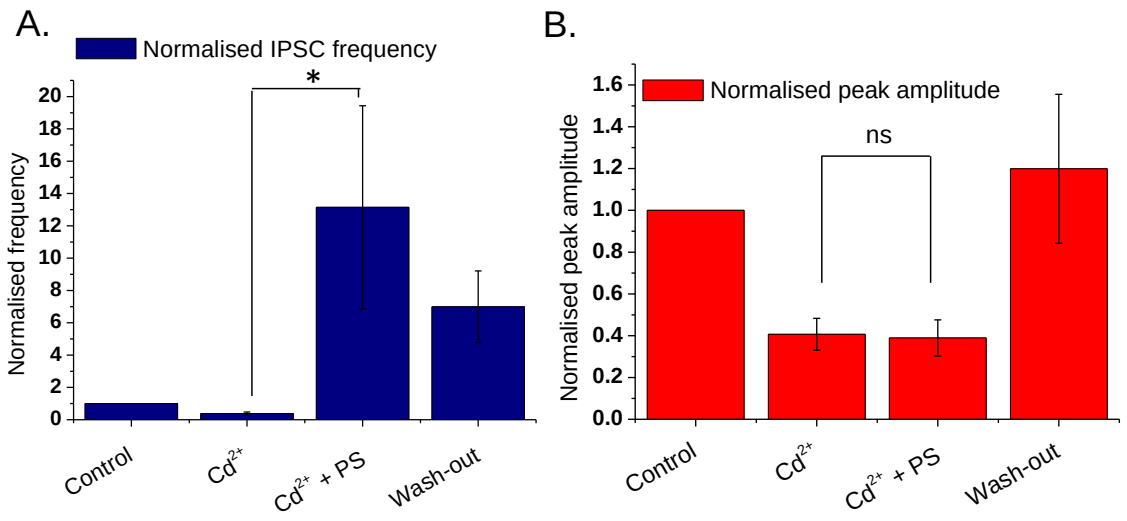

Figure 5.14 – The effect of Cd^{2+} and PS on IPSC frequency and amplitude.

The bar charts show the effect of 200 µM Cd^{2+} with and without 10 µM PS on IPSC frequency (**A**) and peak amplitude (**B)**. Data are normalised to control and expressed as mean ± SEM (n = 6). ns denotes not statistically significant, * $p < 0.05$.

The peak amplitude of the IPSCs was reduced by about 60% in the presence of 200 µM Cd^{2+} (Fig. 5.14B), to 0.41 ± 0.08 of control ($p = 0.0150$, n = 6). Furthermore, 10 µM PS did not add to this inhibition (0.39 ± 0.09 of control; $p = 0.2159$, n = 6).

5.2.5. TRPM3 channel blockers mefenamic acid and ononetin block PS-mediated presynaptic GABA release

The TRPM3 receptor is a well-documented target of PS (Wagner et al., 2008; Vriens et al., 2011), and is widely expressed in the human and rodent brain (Lee et al., 2003; Fonfria et al., 2006; Kunert-Keil et al., 2006; Zamudio-Bulcock and Valenzuela, 2011; Held et al., 2015). Acting as an agonist, PS increases the flux of cations through the TRMP3 channel, increasing the excitability of the cell. Furthermore, the TRPM3 channel shows up to 10 times higher permeability for Ca^{2+} than monovalent cations (Held et al., 2015).

Mefenamic acid (MFA) is a blocker of the TRPM3 receptor (Klose et al., 2011), but can also inhibit, potentiate and directly activate $GABA_A$ receptors *in vitro*

(Halliwell et al., 1999; Coyne et al., 2007). Whereas the IC_{50} of MFA is below 10 µM at TRPM3, the IC_{50} for other studied TRP channels is over 300 µM, making MFA a selective TRPM3 blocker relative to the other members of the receptor family (Klose et al., 2011). If PS increases GABA release by activating presynaptic TRPM3 receptors, a reduced or even zero increase in IPSC frequency would be expected when PS and MFA are co-applied.

At 10 µM, which is just above its IC_{50} (7 µM) (Klose et al., 2011), MFA caused a large increase in the tonic GABA conductance of hippocampal neurones, and this was inhibited to some extent by 10 µM PS (Fig. 5.15A). The normalised IPSC frequency was 0.81 ± 0.17 of control in the presence of 10 µM MFA ($p = 0.1603$, $n = 7$). When 10 µM PS was applied with MFA, the normalised frequency went down to 0.30 ± 0.11 of control, which was significantly lower than in MFA alone ($p = 0.0093$, $n = 7$; Fig. 5.13B and C). Thus, PS reduced rather than increased the frequency of IPSCs in the presence of MFA. Blocking presynaptic TRPM3 receptors with MFA was expected to prevent the increase in GABA release upon PS application. The finding that the effect of PS is reversed, and that it actually acted to reduce GABA release, could indicate that an additional presynaptic receptor or ion channel is targeted by PS. Blocking TRPM3 might have prevented PS-induced GABA release, and unmasked the ability of PS to also reduce GABA release.

In contrast to the results seen with Cd^{2+}, IPSC peak amplitudes were reduced by PS in the presence of MFA (Fig. 5.15D). IPSC amplitudes were also reduced in MFA alone compared to control (to 0.71 ± 0.10 of control; $p = 0.0131$, $n = 7$). Upon application of 10 µM PS with MFA, the average peak amplitude went down to 0.38 ± 0.03 of control, which was significantly lower than in MFA only ($p = 0.0060$, $n = 7$). This could either mean that PS directly modulates postsynaptic $GABA_A$ receptors and inhibits their activity, or that because the frequency is so low (0.30 ± 0.11 of control), and larger IPSCs are absent (see traces in Fig. 5.15B), the average peak amplitude is lowered.

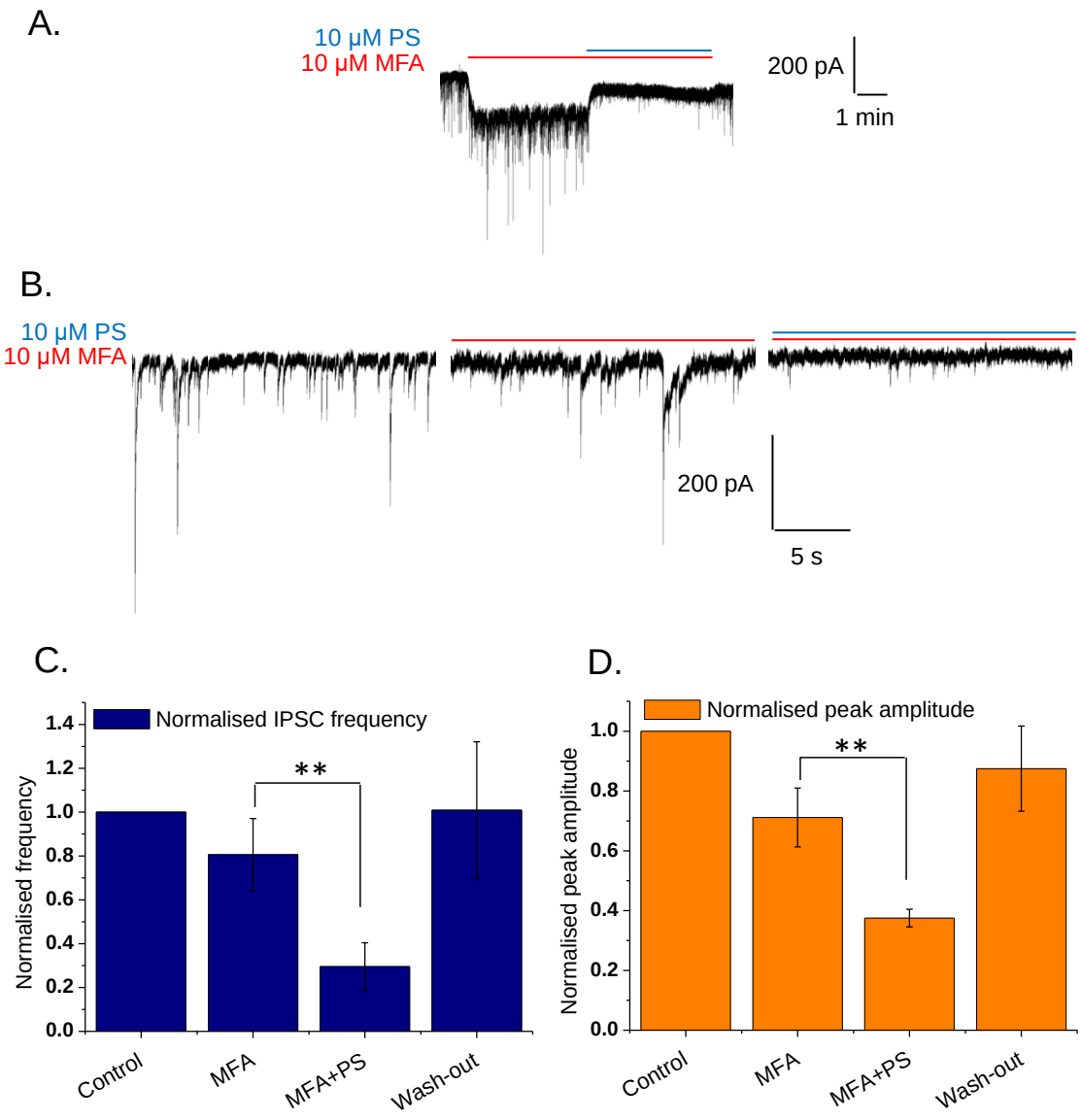

Figure 5.15 – Blocking the presynaptic effect of PS with MFA.

A. A trace showing the effect of both MFA and PS (both 10 μM) on the tonic GABA current in a hippocampal neurone. **B**. Representative traces for control (left), the effect of MFA only (middle) and MFA with PS (right) on IPSCs. **C-D**. Bar charts showing the effect of MFA with and without PS on IPSC frequency (**C**) and peak amplitude (**D**). Data are normalised to control and expressed as mean ± SEM (n = 7), ** $p < 0.01$.

Ononetin is a more selective antagonist at the TRPM3 receptor (IC_{50} = 0.3 μM) (Straub et al., 2013; Held et al., 2015) and does not show any activity at $GABA_A$ receptors (Fig. 5.24). To corroborate my findings that PS can increase GABA release by acting as an agonist at presynaptic TRPM3 receptors, ononetin was

used at 10 µM, a concentration that should produce a complete block of the TRPM3 receptor (Straub et al., 2013).

The results were similar to those obtained using MFA, except ononetin caused no increase in tonic GABA current and did not reduce the IPSC peak amplitude (Fig. 5.16A, B and D). The average peak amplitude was 1.19 ± 0.21 of control in 10 µM ononetin, which was not different from control ($p = 0.3647$, $n = 7$). When 10 µM PS was applied, the peak amplitude went down to 0.67 ± 0.10 of control, which was significantly lower than in the presence of ononetin only ($p = 0.0064$, $n = 7$).

Ononetin did not by itself affect the frequency of IPSCs (0.81 ± 0.20 of control; $p = 0.1010$, $n = 8$; Fig. 5.16B and C). When co-applied with 10 µM PS, the normalised frequency went down to 0.40 ± 0.12, which was significantly lower than in ononetin only ($p = 0.0243$, $n = 8$). Together with the MFA data, these results suggest that blocking TRPM3 with MFA or ononetin prevents the PS-induced increase in GABA release, and that PS must also act at an additional presynaptic target to reduce GABA release, an effect that can only be observed when TRPM3 is blocked. This also strongly supports that TRPM3 is a target of PS, and that PS acts as an agonist to increase cation influx across the presynaptic membrane. The additional presynaptic target of PS involved in reducing GABA release will be explored further in the next part of this chapter.

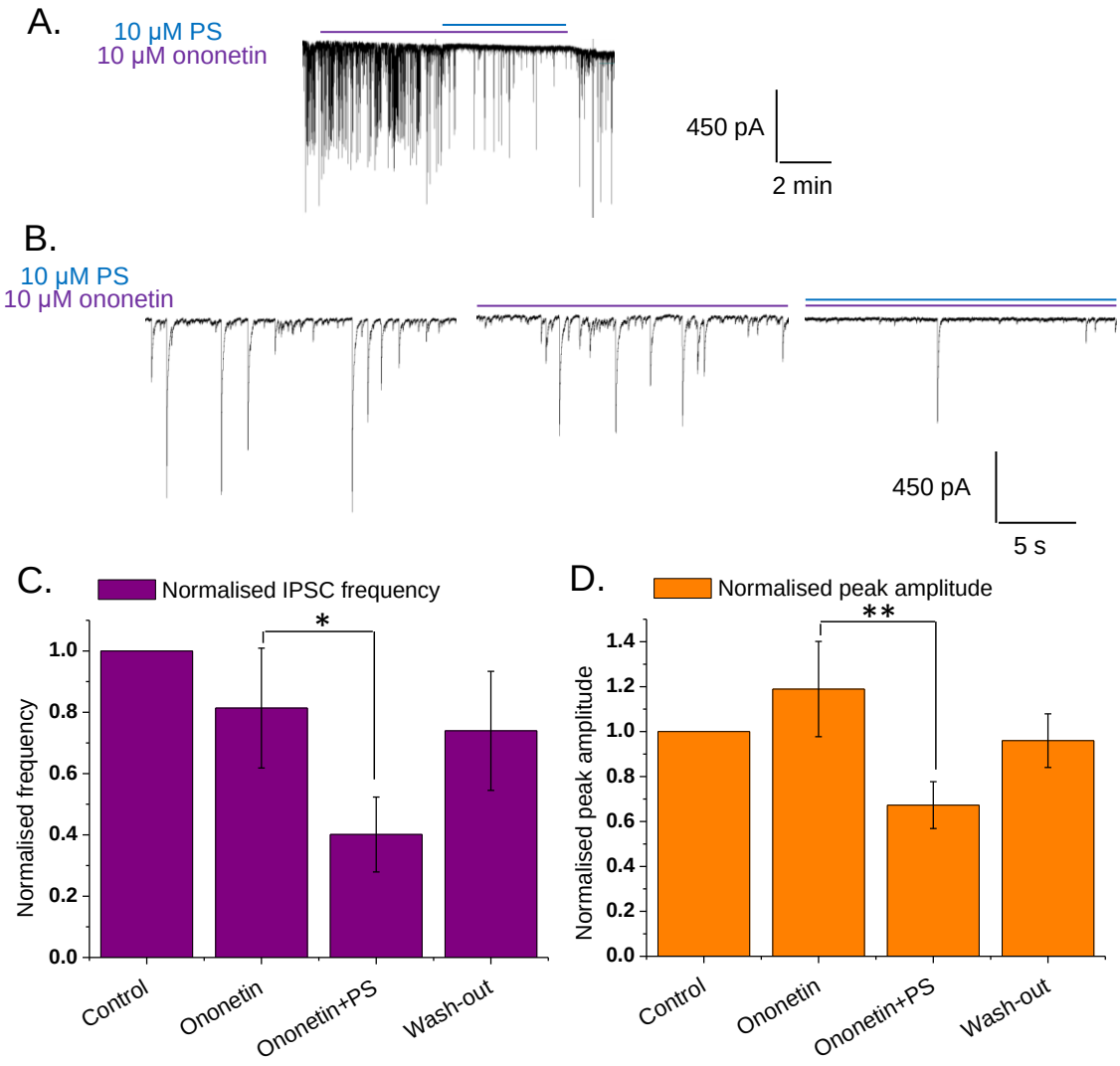

Figure 5.16 – Blocking the presynaptic effect of PS with ononetin.

A. A trace showing the effect of ononetin and PS (both 10 μM) on the GABA tonic current in a hippocampal neurone. **B**. Representative traces for control, the effect of ononetin and ononetin with PS in a hippocampal neurone. **C-D**. Bar charts showing the effect of ononetin and ononetin with PS on IPSC frequency (**C**) and peak amplitude (**D**). Data were normalised to control and expressed as mean ± SEM (n = 8), * $p < 0.05$, ** $p < 0.01$.

5.2.6. PS does not reduce presynaptic GABA release via presynaptic σ1 receptors in hippocampal neurones

PS has previously been reported to reduce GABA release in hippocampal neurones (Teschemacher et al., 1997; Mtchedlishvili and Kapur, 2003). This was thought to occur through the agonism of the σ1 receptor that exists in the presynaptic membrane. To determine whether this can be a mechanism by which PS reduces GABA release when TRPM3 receptors are blocked, haloperidol (50 µM) was used to antagonise σ1 receptors. Haloperidol has previously been used at this concentration to block the presynaptic effect of PS at the σ1 receptor (Mtchedlishvili and Kapur, 2003), and is a potent blocker of the receptor (Walker et al., 1990). By applying PS in the presence of haloperidol and ononetin, it can be discerned whether PS can reduce the frequency of IPSCs when the TPRM3 and σ1 receptors are blocked.

The effect of haloperidol was ambiguous, with the IPSC frequency going up in some cells (3/7) and down (2/7) in others (Fig. 5.17A and B). Haloperidol is active at an array of different receptor types, including dopamine $D_{1\text{-}4}$ receptors, σ receptors, muscarinic, histamine H_1, serotonin 5-HT_{1A} and 5-HT_2 receptors and α1 adrenoceptors (Tam and Cook, 1984; Borda et al., 1999; Kroeze et al., 2003), which may explain this inconsistency. The normalised frequency was 1.60 ± 0.62 in 50 µM haloperidol, which was not different from the baseline frequency due to the high variability ($p = 0.8392$, $n = 7$; Fig. 5.17C). When 10 µM PS was applied in the presence of haloperidol and 10 µM ononetin, the normalised frequency was 1.66 ± 0.7, which was not different from the frequency in haloperidol only ($p = 0.8200$, $n = 7$). The frequency did not recover upon wash-out of the drugs, and went down to 0.43 ± 0.12 of control.

This could mean that blocking presynaptic TRPM3 receptors with ononetin and σ1 receptors with haloperidol ablates the effect of PS on IPSC frequency. The variability in the cellular response is however somewhat confounding, and made it necessary to use a more selective blocker of the σ1 receptor.

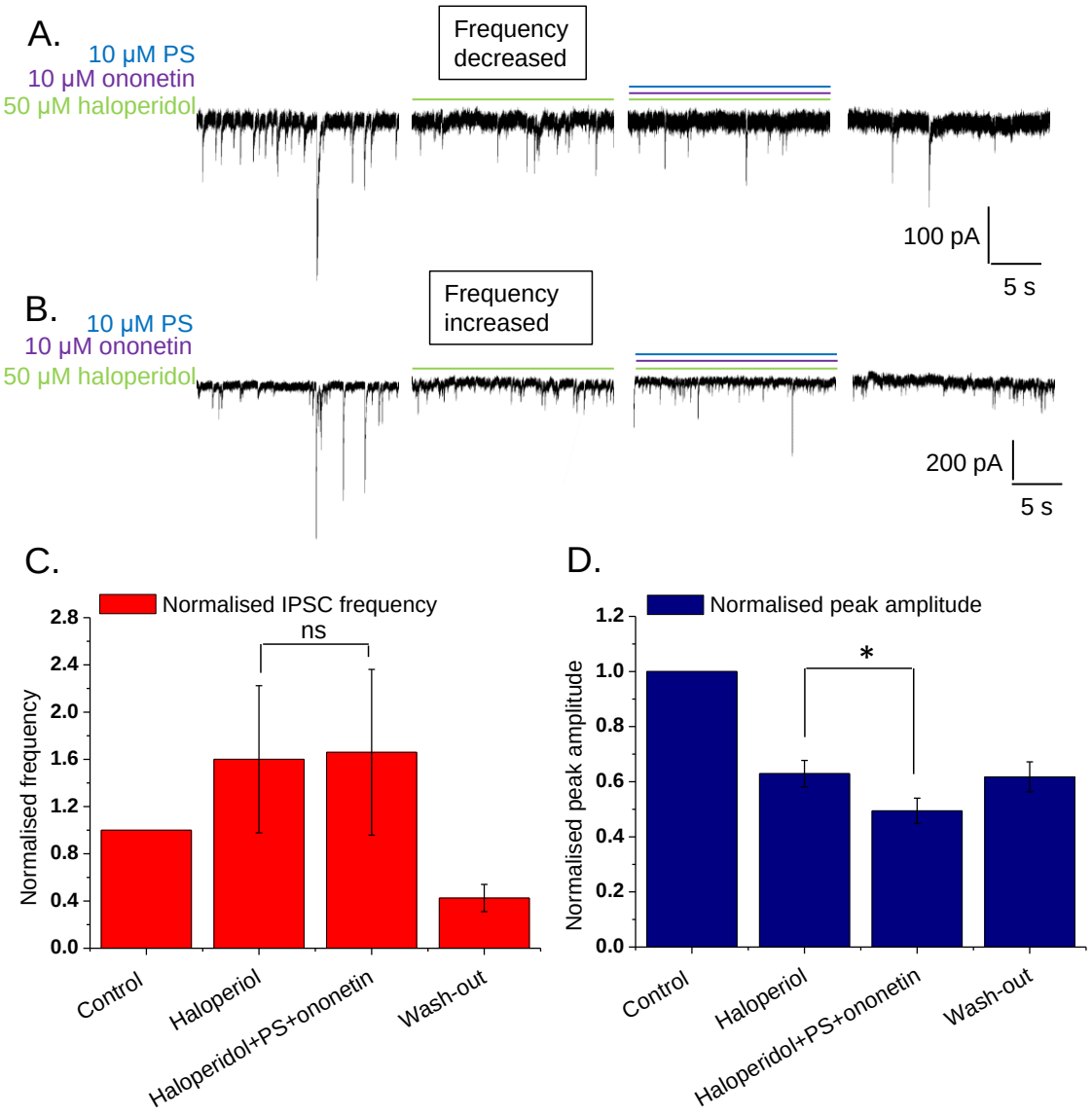

Figure 5.17 – Blocking the presynaptic effect of PS with haloperidol and ononetin.

A. Representative traces showing how haloperidol (50 μM; second trace from the left) can reduce the frequency of IPSCs compared to control (trace on the left), and the effect of PS (10 μM) in the presence of both haloperidol and ononetin (10 μM; second trace from the right). The frequency does not recover upon wash-out (trace on the right). **B**. Representative traces as in A, showing how the frequency of IPSCs went up in the presence of haloperidol in some cells. **C**. The bar chart shows the effect of haloperidol and haloperidol co-applied with PS and ononetin on the frequency of IPSCs. **D**. The bar chart shows the effect of haloperidol and haloperidol co-applied with PS and ononetin on IPSC amplitudes. Data are normalised to control and expressed as mean ± SEM (n = 7). ns denotes not statistically significant, * $p < 0.05$.

Haloperidol greatly reduced the IPSC amplitude (Fig. 5.17D). The normalised amplitude was 0.63 ± 0.05, which is significantly lower than in control ($p = 0.0014$,

n = 7). In the presence of haloperidol, ononetin and PS, the peak amplitude was reduced to 0.49 ± 0.05 of control, which is lower than in haloperidol only (p = 0.0237, n = 7). The effect of haloperidol on peak amplitude did not wash out (0.62 ± 0.05 of control, p = 0.0037, n = 7). This suggests that haloperidol also inhibits $GABA_A$ receptors, although no effect was observed on the recombinant α1β2γ2L receptor in HEK cells (Fig. 5.24).

As haloperidol produced disparate effects in different cells, BD-1063 was also used as this is a more selective blocker of σ1 receptors. The K_i (affinity) of BD-1063 at the rat σ1 receptor is below 10 nM (Matsumoto et al., 1995), and it has a 50-fold greater affinity for σ1 than for σ2 receptors. BD-1063 was first used at 300 nM, as described previously (Mtchedlishvili and Kapur, 2003). It was also used at 10 µM to ensure full block of the σ1 receptor is achieved. At the higher concentration, block of σ2 receptor and other neurotransmitter receptors is however more likely to occur, as the compound has a 100-fold or higher affinity for σ receptors compared to other neurotransmitter receptors (opioid, NMDA, muscarinic and dopamine receptors, α- and β-adrenoceptors and $5\text{-}HT_{1/2}$ receptors) (Matsumoto et al., 1995; McCracken et al., 1999).

At 300 nM BD-1063, the fold frequency of IPSCs was not changed from baseline as it was 1.17 ± 0.26 relative to control (p = 0.6694, n = 8; Fig. 5.18A and C). In the presence of 300 nM BD-1063, 10 µM ononetin and 10 µM PS, the normalised frequency went down to 0.45 ± 0.07, which is lower than in 300 nM BD-1063 only (p = 0.0125, n = 8). This would suggest that blocking σ1 receptors with BD-1063 does not prevent the PS-mediated reduction in GABA release when TRPM3 receptors are blocked with ononetin. The reduction in normalised IPSC frequency in the presence of 300 nM BD-1063, ononetin and PS was similar to that achieved by PS and ononetin only (0.40 ± 0.12 relative to control), which can mean one of two things: the concentration of BD-1063 may be too low to block σ1 receptors in the presynaptic membrane, or the receptors are blocked but PS modulates a different receptor to reduce GABA release.

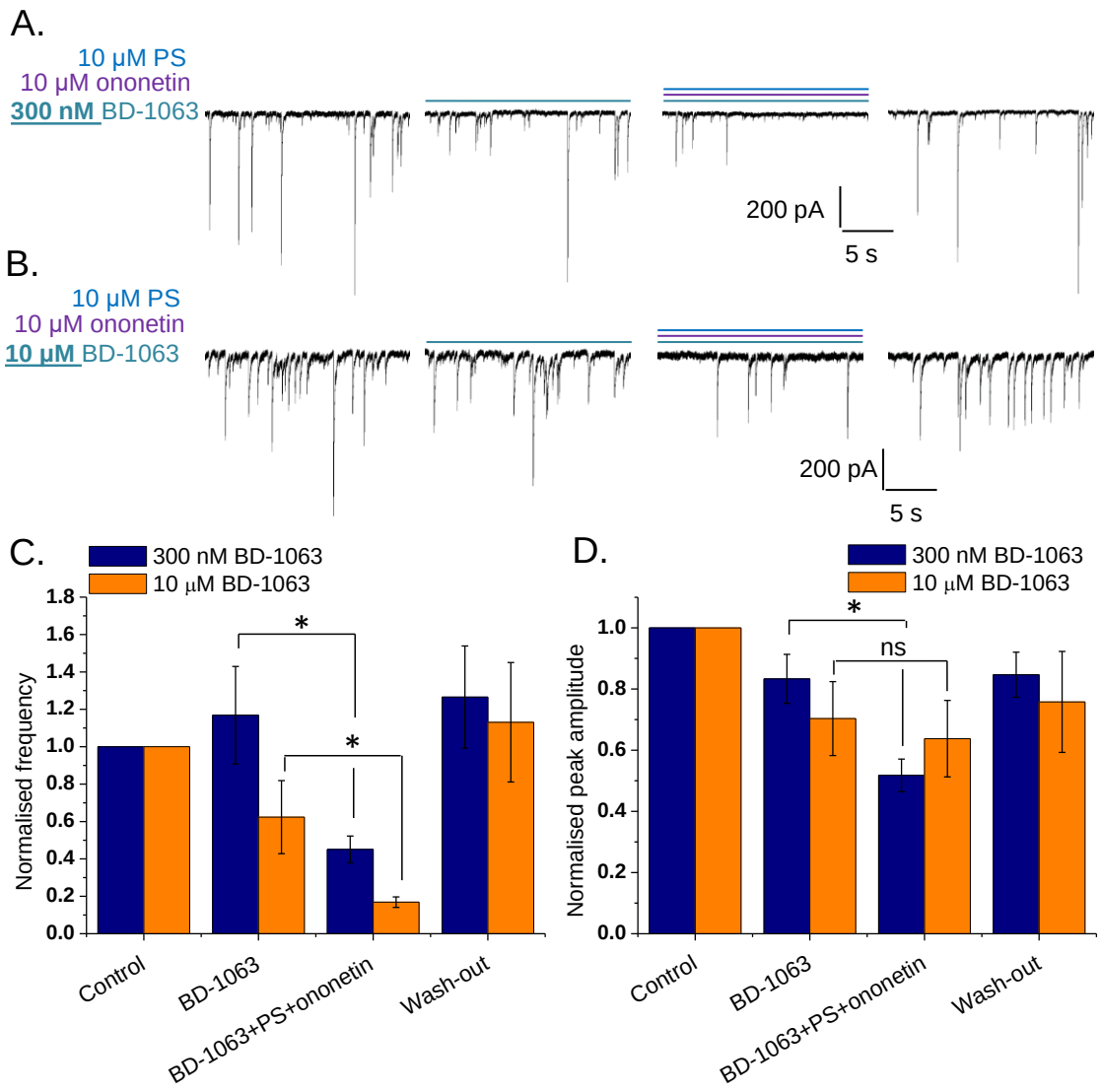

Figure 5.18 – BD-1063 does not block the presynaptic effect of PS.

A-B. Representative traces showing the effect of low (300 nM; **A**) and high (10 µM; **B**) concentrations of BD-1063 on IPSC frequency and amplitude (second trace from the left) and BD-1063 co-applied with PS (10 µM) and ononetin (10 µM) (second trace from the right). **C-D**. The bar charts show the effect of 300 nM (blue) and 10 µM (orange) BD-1063 on the frequency (**C**) and peak amplitude (**D**) of IPSCs with and without PS and ononetin. Data are normalised to control and expressed as mean ± SEM (n = 6-8). ns denotes not statistically significant, * $p < 0.05$.

Consequently, BD-1063 was applied at 10 µM to examine if this would prevent the PS-induced reduction in GABA release in the presence of ononetin. The frequency of IPSCs did not go down significantly relative to baseline in the presence of 10 µM BD-1063 alone (0.62 ± 0.20 of control; $p = 0.1302$, n = 6; Fig. 5.18B and C). When PS and ononetin were also applied, the normalised

frequency was reduced to 0.17 ± 0.03, which was significantly lower than in 10 µM BD-1063 only (p = 0.0271, n = 6). This reduction in IPSC frequency suggests it is unlikely that PS reduces GABA release by acting as an agonist at presynaptic σ1 receptors.

BD-1063 caused some inhibition of IPSC amplitudes at 10 µM (0.70 ± 0.12 of control, p = 0.0361, n = 6) but not at 300 nM (0.83 ± 0.08 of control; p = 0.0622, n = 8), which confirms that BD-1063 is less selective at higher concentrations (Fig. 5.18D). Compared to IPSC amplitudes measured in 300 nM BD-1063, IPSC amplitudes were lower when ononetin and PS were also applied (0.52 ± 0.05 of control; p = 0.0174, n = 8). PS did not add to the inhibition by 10 µM BD-1063, as amplitudes were 0.64 ± 0.13 of control in PS, ononetin and BD-1063 (p = 0.7014, n = 6).

5.2.7. PS does not reduce GABA release by negatively modulating Na_V channels

A plausible explanation for the inhibitory effect of PS on GABA release when TRPM3 channels are blocked, could be that PS inhibits voltage-gated sodium channels in the presynaptic membrane. PS has previously been shown to act as an inhibitor at Na_Vs at concentrations between 3 and 100 µM (Horishita et al., 2012). To test this hypothesis, neurones were kept in 500 nM TTX and 10 µM ononetin, the latter of which had already been shown not to have an effect on the baseline frequency of IPSCs (Fig. 5.16C). PS (10 µM) was then applied to determine if the frequency was still reduced when Na_Vs and TRPM3 are blocked (Fig. 5.19).

The mIPSC frequency went down to 0.65 ± 0.11 of control (TTX and ononetin) when PS was applied (p = 0.0314, n = 7), indicative of PS reducing GABA release and thus mIPSC frequency when Na_Vs were blocked (Fig. 5.19A and B). This demonstrates that PS does not reduce GABA release by causing less presynaptic AP firing. The mIPSC amplitude was also diminished in 10 µM PS, the fractional response being 0.68 ± 0.04 of the average amplitude in TTX and ononetin (p = 0.0012, n = 7). This is surprising, as 10 µM PS did not reduce the mIPSC

amplitude in TTX only (Fig. 5.9E). However, this may also show that the direct modulatory effect of PS on postsynaptic $GABA_AR$s is only visible when TRPM3 receptors are blocked, i.e. when the frequency of IPSCs is not increased by PS.

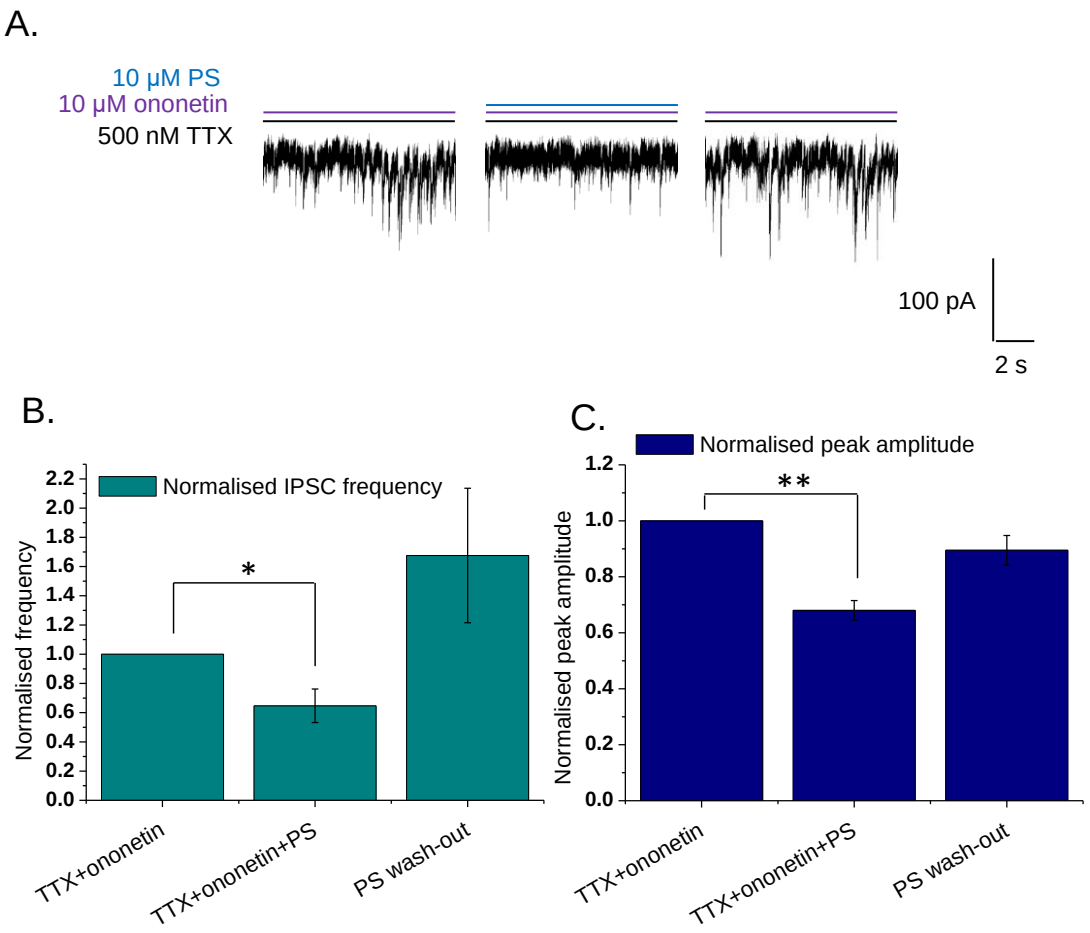

Figure 5.19 – TTX does not block the presynaptic effect of PS.

A. Representative traces showing that applying PS (10 µM; middle trace) leads to a reduction in the frequency of IPSCs when TTX (500 nM) and ononetin (10 µM) are present. **B-C**. The bar charts show the effects of PS on mIPSC frequency (**B**) and amplitude (**C**) in the presence of TTX and ononetin. Data are normalised to control (TTX + ononetin) and expressed as mean ± SEM (n = 7), * $p < 0.05$, ** $p < 0.01$.

5.2.8. PS reduces GABA release from the presynaptic membrane by potentiating Kir2 channels

It has previously been described that PS can potentiate inwardly-rectifying K^+ channels. In particular, the homomeric Kir2.3 channel and Kir2.3-containing heteromeric channels are greatly potentiated by PS in the micromolar range (Kobayashi et al., 2009). Although inwardly-rectifying K^+ channels pass more current in the inward than the outward direction, inward movement does not occur physiologically. Nevertheless, application of PS at potentials positive to the Kir2.3 channel's equilibrium potential could potentiate an outward K^+ current, which would lead to hyperpolarisation of presynaptic terminals. Indeed, activation of the Kir2.3 channel has previously been shown to produce membrane hyperpolarisation (Liu et al., 2002).

Ba^{2+} is an effective blocker of Kir channels (Dascal et al., 1993; Tanemoto et al., 2002; Kobayashi et al., 2009), and produces a full block of Kir2.3 currents at 3 mM (Kobayashi et al., 2009). To determine if PS potentiates Kir2.3 channels (or another Kir channel not previously found to be modulated by PS) to reduce synaptic GABA release, PS was applied with 3 mM Ba^{2+} and 10 µM ononetin. If the observed reduction in IPSC frequency upon TRPM3 block is removed when Ba^{2+} is present, this would imply that PS modulates an inwardly-rectifying K^+ channel in the presynaptic membrane.

To test this hypothesis, neurones were first exposed to 3 mM Ba^{2+} to determine the effect of this blocker on baseline activity, then Ba^{2+} was co-applied with 10 µM ononetin and 10 µM PS. Applying Ba^{2+} alone produced a large increase in the frequency of IPSCs compared to baseline activity (14.29 ± 3.72-fold; $p = 0.0078$, $n = 7$; Fig. 5.20A and B). Interestingly, the IPSC frequency did not change greatly when Ba^{2+} was co-applied with ononetin and PS, the fold increase being 20.84 ± 6.26 ($p = 0.1801$, $n = 7$). This finding supports a role for Kir2.3 currents in mediating the PS-induced decrease in GABA release.

IPSC amplitudes decreased to 0.62 ± 0.08 of control in Ba^{2+} ($p = 0.0104$, $n = 7$). When PS and ononetin were applied, this was further reduced to 0.34 ± 0.05,

which is significantly lower than in Ba^{2+} only (p = 0.0022, n = 7). This again suggests that PS directly modulates postsynaptic $GABA_A$ receptors to decrease IPSC amplitudes when the presynaptic effect of PS is absent.

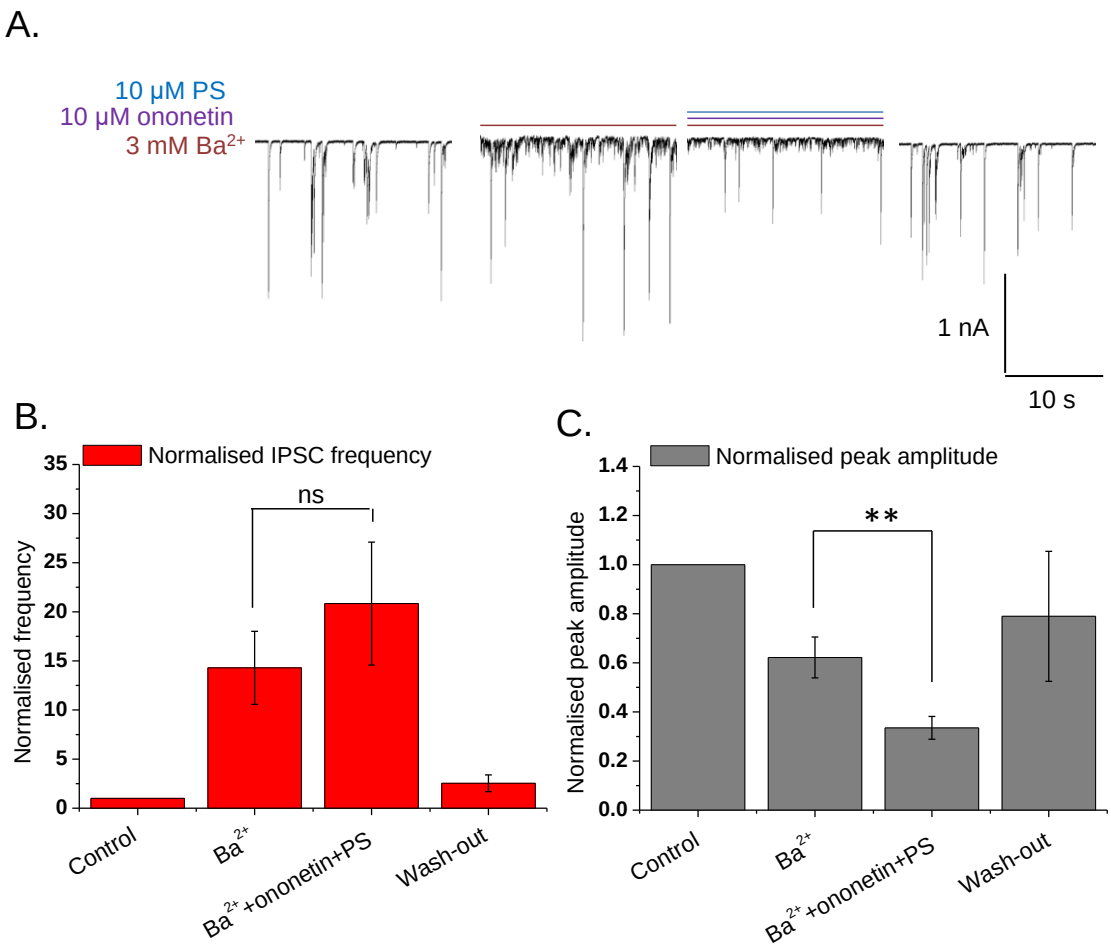

Figure 5.20 – Presynaptic effects of PS are blocked by ononetin and Ba^{2+}.

A. Representative traces showing the effect of 3 mM Ba^{2+} (second from the left) and Ba^{2+} co-applied with ononetin and PS (both 10 µM; second from the right) on IPSC frequency and peak amplitude. **B-C**. The bar charts demonstrate the effects of Ba^{2+} and Ba^{2+} with PS and ononetin on the frequency (**B**) and peak amplitude (**C**) of IPSCs in hippocampal neurones. Data are normalised to control and expressed as mean ± SEM (n = 6). ns denotes not statistically significant, ** p < 0.01.

Although effective, Ba^{2+} lacks potency and selectivity in blocking inward-rectifying K channels. However, ML133 is a selective blocker of Kir2 channels, including Kir2.1, Kir2.2, Kir2.3 and Kir2.6 (Wu et al., 2010; Wang et al., 2011). The IC_{50} for block of Kir2.3 channels is 4 µM, and ML133 was therefore applied at 100 µM to produce a complete block of the channel. To see if the results obtained using

Ba^{2+} could be reproduced using ML133 as a Kir2 channel blocker, neurones were kept in 10 µM ononetin throughout the experiment, and 100 µM ML133 was applied to assess whether it affected the baseline activity. ML133 was then co-applied with 10 µM ononetin and 10 µM PS to determine if the frequency of IPSCs is reduced by PS in the presence of ML133.

ML133 produced a large increase in the frequency of IPSCs (12.74 ± 1.79-fold) compared to the ononetin control ($p = 0.0013$, $n = 8$; Fig. 5.21A and B). When ononetin, ML133 and PS were co-applied, the fold increase in IPSC frequency was 11.88 ± 1.92, which was only slightly lower than the frequency in the presence of ononetin and ML133 ($p = 0.0161$, $p = 8$). A much larger reduction in IPSC frequency would have been expected if ML133 did not block the presynaptic target of PS that mediates the decrease in GABA release. Therefore, these results suggest that PS is likely to decrease GABA release from the presynaptic terminal by potentiating Kir2 channels, most probably the Kir2.3 channel. This effect is only visible when the TRPM3 receptor is blocked.

IPSC amplitudes in the presence of ML133 were 0.81 ± 0.14 compared to the ononetin control ($p = 0.1151$, $n = 8$; Fig. 5.21C). The peak amplitude was reduced further by PS, as the mean IPSC amplitude in the presence of PS, ML133 and ononetin was 0.68 ± 0.12 ($p = 0.0003$, $n = 8$), again suggesting that the postsynaptic effect of PS might be more clear when its presynaptic targets are blocked.

To determine if PS increases the rate of IPSC decay when TRPM3 and Kir2.3 channels are blocked (and the effect of PS on IPSC frequency removed), τ_w was calculated in the presence of ML133 and ononetin with and without PS. In ML133 and ononetin, τ_w was 19.4 ± 1.7 ms. When PS was added, this went down to 16.1 ± 0.9 ms, representing a reduction of 19.3 ± 1.6% in the presence of PS ($p = 0.0069$, $n = 7$; data not shown).

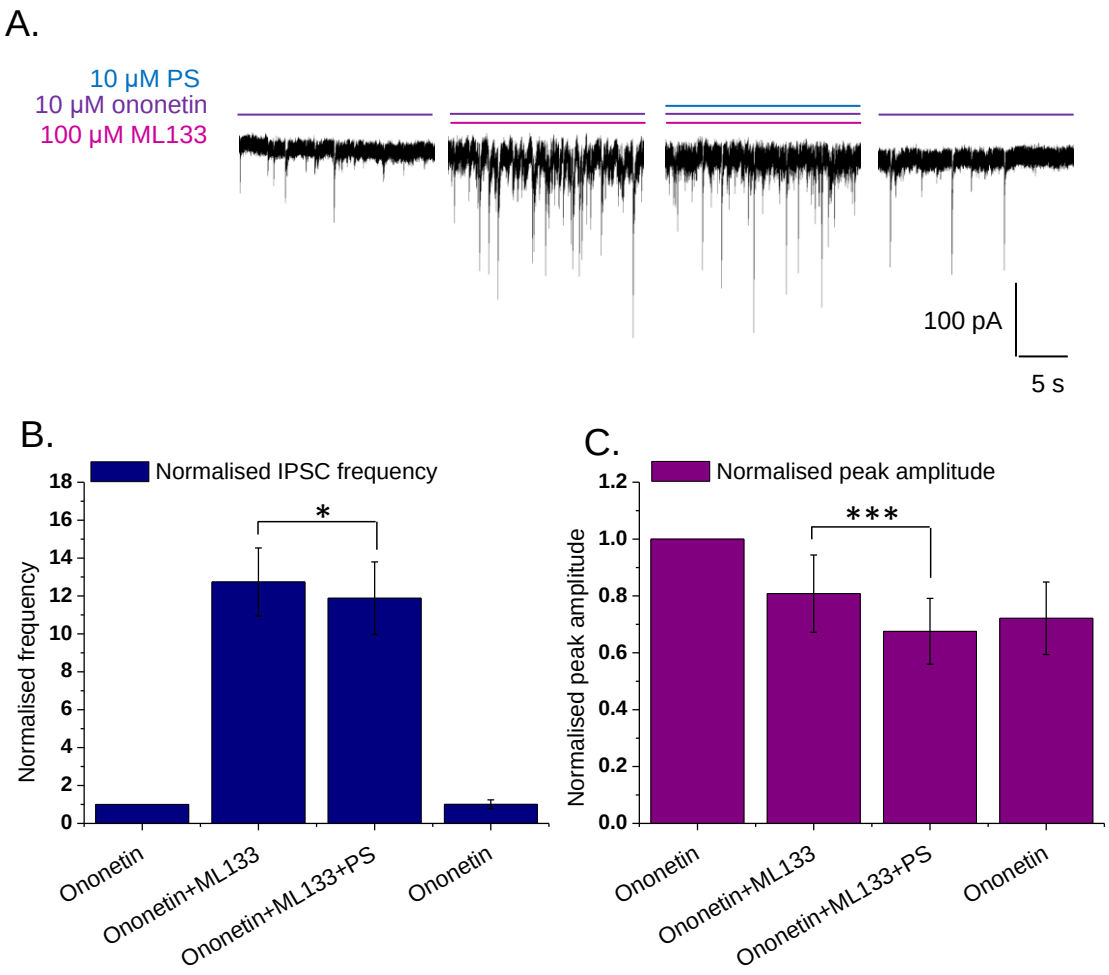

Figure 5.21 – Ononetin and ML133 block the presynaptic effects of PS.

A. Representative traces showing the effect of ML133 (100 µM; second trace from the left) and ML133 co-applied with PS (10 µM; second trace from the right) on the frequency and peak amplitude of IPSCs in the presence of ononetin (10 µM). **B-C**. The bar charts show the effects of ML133 and ML133 with PS on the frequency (**C**) and peak amplitude (**D**) of IPSCs in the presence of ononetin. Data are normalised to control (ononetin only) and expressed as mean ± SEM, * $p < 0.05$, *** $p < 0.001$.

5.2.9. PS increases presynaptic GABA release also in CNQX and AP5

Other studies have reported that PS acts to reduce GABA release in hippocampal neurones (Teschemacher et al., 1997; Mtchedlishvili and Kapur, 2003), whereas this work shows that PS increases GABA release by activating presynaptic TRPM3 receptors. Only when TRPM3 receptors are blocked, does PS reduce GABA release by potentiating Kir2 channels. Similar to the present study, Mtchedlishvili and Kapur (2003) used E18 hippocampal neurones after 2-3 weeks in culture. However, they used PS at concentrations between 10 and 30 nM, far lower than the concentration of PS used here for studying the presynaptic effect of PS. At lower concentrations, 30 nM PS was found to have no effect on presynaptic GABA release as the frequency of IPSCs did not change from baseline (Fig. 5.5A). By contrast, Teschemacher et al. (1997) used older animals (postnatal day 1 + 3-9 weeks in culture) and higher concentrations of PS (1-50 µM), but still reported a reduction in GABA release. What these two studies have in common, is that instead of using kynurenic acid to block glutamatergic transmission, they used 6-cyano-7-nitroquinoxaline-2,3-dione (CNQX) and (2*R*)-amino-5-phosphonovaleric acid (AP5). Consequently, whether these compounds can influence whether PS increases or decreases GABA release from the synaptic terminal was investigated. CNQX is considered a less suitable blocker of α-amino-3-hydroxy-5-methyl-4-isoxazolepropionic acid (AMPA) receptors due to its partial agonist activity at AMPA receptors co-expressed with transmembrane AMPA receptor regulatory proteins (TARPs) (Menuz et al., 2007). This partial agonist activity of CNQX is associated with increased GABA release (Brickley et al., 2001).

CNQX (5 µM) and AP5 (10 µM) were added to the Krebs solution instead of kynurenic acid, and PS (10 µM) was applied to assess its effect on the frequency of IPSCs (Fig. 5.22A and B). The frequency of IPSCs was still increased by PS, and the increase relative to control was up to 27.18 ± 14.19-fold ($p = 0.0250$, $n = 6$). This confirms that the glutamatergic blockers do not interact with the presynaptic targets of PS. The fold increase in IPSC frequency in the presence of 10 µM PS in 1 mM kynurenic acid was 12.93 ± 4.11, which was not significantly different from the frequency in CNQX and AP5 ($p = 0.4259$, $n = 6$-8; Fig. 5.22C).

In conclusion, the choice of glutamate receptor blocker does not affect the outcome of the experiments investigating the effect of PS on GABAergic transmission in hippocampal neurones.

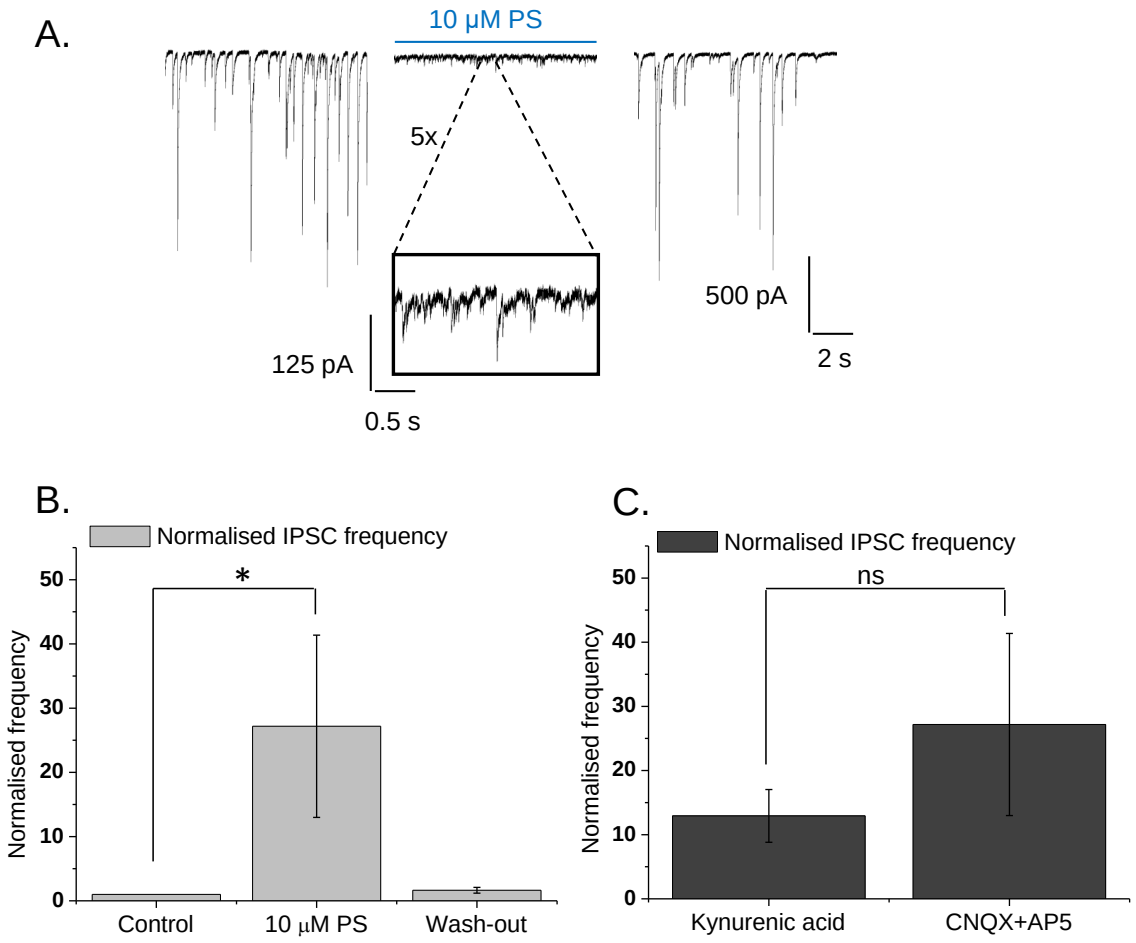

Figure 5.22 – PS increases the frequency of IPSCs in CNQX and AP5.

A. Representative traces showing how the frequency of IPSCs is increased by 10 µM PS when glutamatergic transmission is blocked by 5 µM CNQX and 10 µM AP5. **B**. The bar chart shows the increase in IPSC frequency caused by PS in the presence of CNQX and AP5 (n = 6). **C**. The bar chart shows the increase in IPSC frequency caused by 10 µM PS in 1 mM kynurenic acid or CNQX with AP5. Data are normalised to control and expressed as mean ± SEM (n = 6-8). ns denotes not statistically significant, * $p < 0.05$.

5.2.10. Can PS inhibit tonic $GABA_A$ receptor currents?

As discussed in Chapter 3, PS can inhibit receptors containing the $GABA_AR$ δ subunit in HEK cells when GABA is present at a low concentration (100 nM). These are receptors that typically reside outside the synapse in neurones, and generate a tonic GABA current (Farrant and Nusser, 2005). The ability of PS to inhibit 100 nM GABA currents in HEK cells suggests that the steroid should also be able to inhibit neuronal tonic GABA currents. However, the increase in GABA release that is induced by the presynaptic action of PS at TRPM3 receptors might confound this by increasing tonic current instead.

To investigate whether PS can inhibit tonic GABA currents, hippocampal neurones were exposed to PS for up to 30 s at concentrations ranging between 0.01 and 100 μM. Bicuculline (50 μM; BIC) was used to block the tonic current and enable its amplitude to be determined.

PS did not have any effect at 1 μM or lower concentrations (results not shown). At 10-100 μM, the effects of PS were mixed. In some cells (n = 4/8), the frequency of IPSCs went up immediately, which also led to an increase in tonic current (Fig. 5.23B). In other cells (n = 4/8), PS depressed the tonic current, but upon wash-out, presynaptic GABA release went up, causing an increase in the tonic current (Fig. 5.23A). Surprisingly, 100 μM PS was found to add to the block induced by 50 μM BIC when the two antagonists were co-applied. This suggests that PS acts at a postsynaptic target that is not a $GABA_A$ receptor, as all $GABA_A$ receptor currents should be blocked by 50 μM BIC (Krishek et al., 1996a). This also fits with the observations that PS can cause a greater block (or outward current) than PTX (see section 3.2.7.) and produce an outward current in untransfected HEK cells (section 3.2.8.). Although 100 μM PS appears capable of blocking the tonic GABA current and ablating IPSCs, it is likely that PS will mainly cause increased GABA release and hence an increase in the tonic current at lower concentrations. It is therefore unlikely to inhibit tonic GABA currents under physiological conditions.

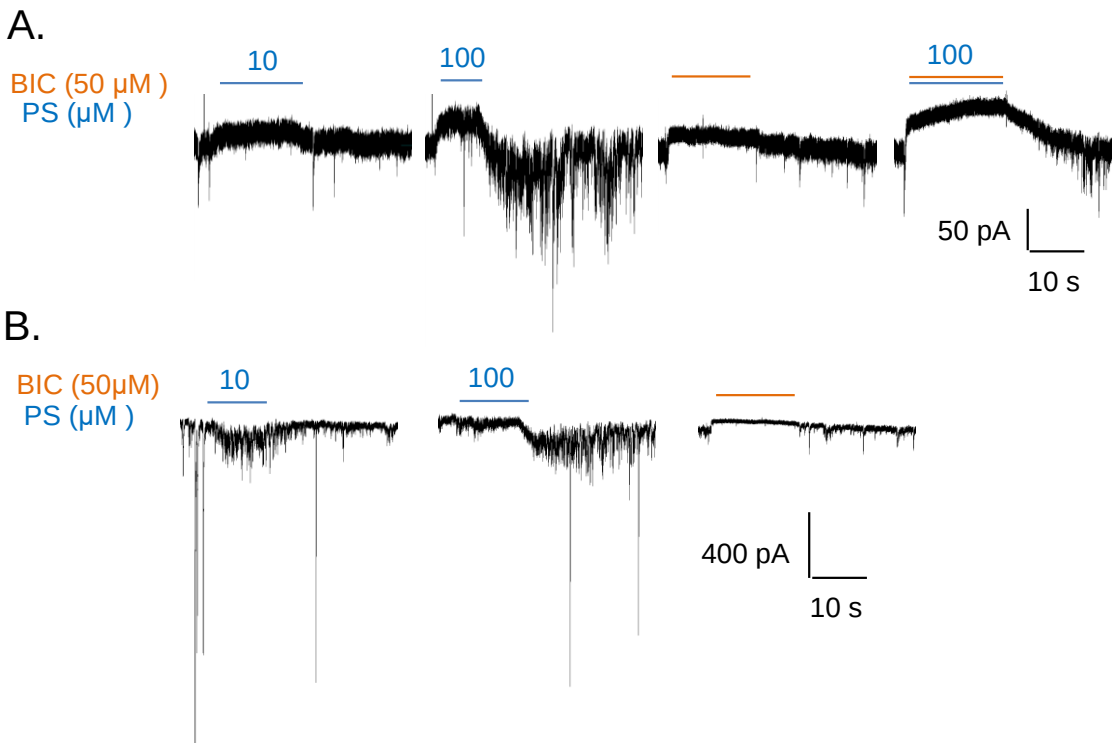

Figure 5.23 – The effect of PS on tonic GABA currents.

A. Traces showing the inhibitory response of a hippocampal neurone tonic GABA current to 10 and 100 µM PS, inhibition by 50 µM BIC and the additive inhibition caused by PS and BIC. **B**. Traces showing the increase in GABA release and tonic current in response to 10 µM PS and upon wash-out of 100 µM PS, and inhibition of the tonic GABA current by 50 µM BIC.

5.2.11. The presynaptic channel blockers used in this study do not modulate $GABA_A$ receptors in HEK cells

Not all of the blockers used in these experiments to determine how PS affects GABA release have been fully characterised and screened for activity at $GABA_A$ receptors. Therefore, whole-cell electrophysiology was carried out in HEK cells to determine if these compounds modulated the GABA EC_{50} (10 µM) response of recombinant α1β2γ2L receptors (Fig. 5.24). GABA was applied at EC_{50} so that the compounds may cause both potentiation and inhibition of the currents. Both peak and steady-state state currents at 10 s were measured. For the peak currents, all measured responses were within 100 ± 10% of the control GABA response (Fig. 5.24A). Steady-state current responses were also similar to the control response (100 ± 10%), except in the presence of 10 µM MFA which was 122.2 ± 11.3% of the control response (Fig. 5.24B). This suggests that MFA modulates the decay phase of the whole-cell GABA current, possibly by affecting the desensitisation kinetics of the receptor.

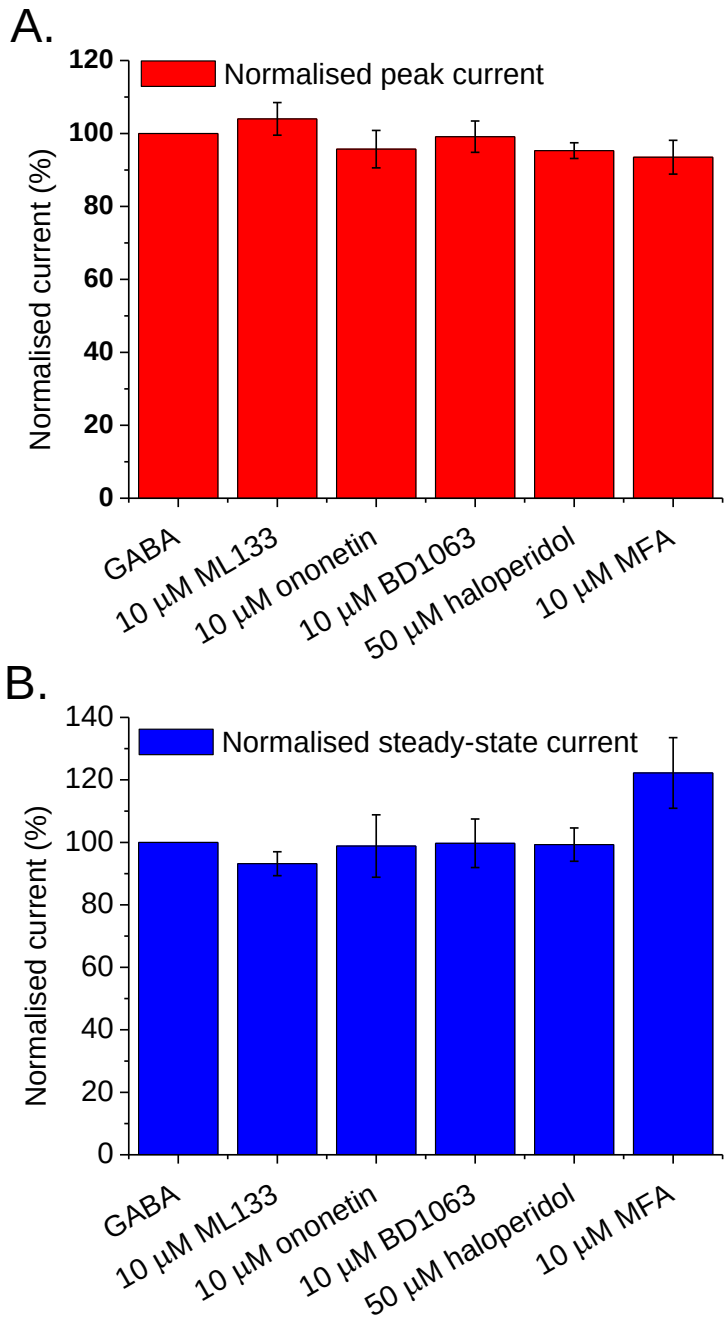

Figure 5.24 – The effect of the pharmacological agents on GABA whole-cell currents in HEK cells.

ML133, ononetin, BD-1063, haloperidol and MFA at the concentrations shown (and used previously in this study) have no effect on peak (**A**) and steady-state currents (**B**) in HEK cells. Data were normalised to the GABA EC_{50} response and are expressed as mean ± SEM (n = 4).

5.3. Discussion

This chapter has explored the modulation of GABAergic transmission by PS in hippocampal neurones in culture. PS inhibited whole-cell GABA currents in a concentration-dependent manner, with the concentration-response curve shifted to the right compared to inhibition of recombinant αβγ/δ receptors expressed in HEK cells. At synaptic level, PS had a concentration-dependent effect on GABA release, with the frequency of IPSCs increasing at 1 μM and higher concentrations of PS. Inhibition of IPSC amplitudes was not concentration-dependent, the mean amplitudes being reduced by 30-40% at 1-10 μM PS, an effect that might be due to an increased frequency of IPSCs of smaller amplitude. PS did however seem to directly modulate postsynaptic $GABA_A$ receptors, as the rate of IPSC decay was increased in a concentration-dependent manner, an effect that was also present in TTX.

The increase in GABA release was also apparent when PS was applied in the presence of TTX, showing that the effect was AP-independent and unlikely to depend on neural network activity. The presynaptic mechanism by which PS increases GABA release is likely to be via the activation of cationic TRPM3 receptors located in the presynaptic membrane. Interestingly, blocking this receptor reversed the action of PS with the IPSC frequency now reduced below baseline activity. The use of Kir channel blockers implicated the role of Kir2 channels in downregulating GABA release, an effect that was only evident when TRPM3 receptors were blocked. Although PS is considered an antagonist of $GABA_A$ receptors, this study has shown that the steroid might potentiate GABAergic transmission under physiological conditions, as PS increased the inhibitory charge transfer in hippocampal neurones in a concentration-dependent manner.

5.3.1. PS increases neurotransmitter release in hippocampal neurones

The most prominent effect of PS in hippocampal neurones was to increase GABA release. Despite previous studies having reported a decrease in GABA release

mediated by PS in hippocampal neurones (Teschemacher et al., 1997; Mtchedlishvili and Kapur, 2003), PS has also been reported to increase neurotransmitter release via different mechanisms in the hippocampus and other regions of the brain. In hippocampal slices from rats, PS has been shown to increase glutamate release by potentiating presynaptic GluN2D-containing NMDA receptors (Mameli, 2005). This effect could not be observed in rats older than postnatal day 5, and it was thought to be involved in long-term enhancement of AMPA receptor function and synaptic strengthening in development. Interestingly, this study showed that PS or a PS-like compound can be released from the postsynaptic membrane upon depolarisation, and that the effect of this depolarisation could be blocked by an anti-PS antibody scavenger. This was the first study to suggest that PS can act like a retrograde messenger that is released in an activity-dependent manner. Moreover, the effect of postsynaptic neurone depolarisation could be mimicked by applying 17 μM PS exogenously. This finding indicates that ambient levels of PS can exist at micromolar concentrations, sufficient for direct modulation of $GABA_A$ receptors.

In a later study, PS (25 μM) was found to induce a 30-fold increase in the frequency of AMPA receptor-mediated miniature excitatory postsynaptic currents (mEPSCs) in cerebellar Purkinje cells in acute cerebellar slices from neonatal rats (Zamudio-Bulcock and Valenzuela, 2011). The frequency of GABA-mediated mIPSCs was also increased in cerebellar Purkinje cells, but to a lesser extent (< 2-fold) than the mEPSCs. The increase in glutamate release onto neonatal Purkinje cells was later shown to be mediated by presynaptic TRPM3 receptors, as the effect was mimicked by TRPM3 receptor agonists nifedipine and epipregnanolone sulphate, and blocked by MFA (GABA release was not investigated further) (Zamudio-Bulcock et al. 2011). PS has also been found to increase glutamate release onto acutely isolated dentate gyrus hilar neurones via a Ca^{2+}-induced Ca^{2+} release mechanism involving a presynaptic TRP channel and intracellular ryanodine receptors (Lee et al., 2010). These three studies demonstrate that TRPM3 channels, and possibly other members of the TRP family, are likely to have a role in modulating neurotransmitter release in various parts of the brain, and corroborates the hypothesis that PS can act to increase GABA release via these receptors in hippocampal neurones. High expression

levels of TRPM3 mRNA has been shown with *in situ* hybridisation and quantitative PCR studies in mouse and human brain, including the basal ganglia, cerebellum, forebrain and hippocampus (Fonfria et al., 2006; Kunert-Keil et al., 2006; Hawrylycz et al., 2012), and may thus exist in inhibitory terminals. It would be interesting to further establish the role of TRPM3 in regulating GABA release by chelating intracellular Ca^{2+} with BAPTA-AM to determine if Ca^{2+}-induced Ca^{2+} release is also involved. Immunocytochemistry can also be used to co-localise TRPM3 receptors with synaptic markers like glutamate decarboxylase 65 (GAD65). However, the lack of commercially available high-quality anti-TRPM3 antibodies has made this difficult. It would also be interesting to investigate whether the frequency of GABA-mediated IPSCs can be increased in response to CA1 pyramidal cell depolarisation-induced PS release in hippocampal slices, as described for EPSCs (Mameli, 2005).

It is uncertain why studies by others have found that PS reduces GABA release from hippocampal neurones (Teschemacher et al., 1997; Mtchedlishvili and Kapur, 2003). The IPSC frequency went up almost 30-fold when CNQX and AP5 were used as blockers of glutamatergic transmission instead of kynurenic acid, showing that the use of particular glutamate receptor blockers did not affect the action of PS, despite this being the clearest difference between the experimental protocols used in the present study and that by Mtchedlishvili and Kapur (2003) and Teschemacher at al. 1997. The reason for this discrepancy therefore remains unclear.

A surprising result was that IPSC frequency was reduced by 50% by 10 μM PS when TRPM3 receptors were blocked by ononetin. Although PS has been shown to potentiate Kir2.3 channel currents in *Xenopus* oocytes (Kobayashi et al., 2009), the channel has not previously been shown to be involved in regulating neurotransmitter release. The blockers used in the present study are not specific for Kir2.3: Ba^{2+} shows antagonist activity at an array of inwardly-rectifying K^+ channels (for extensive list, see http://www.guidetopharmacology.org/GRAC), whereas ML133 is also active at other members of the Kir2 family (Wang et al. 2011; Wu et al. 2010). However, this evidence for modulation of a Kir2 channel together with the previously described role of PS in modulating Kir2.3 channels (Kobayashi et al., 2009), a new role for Kir2.3-containing channels in regulating

neurotransmitter release in response to PS may therefore have been identified. Kir2 channels are widely expressed in neurones but not in glia, and are expressed throughout the brain (Prüss et al., 2005). Immunohistochemical studies have demonstrated that Kir2.3 shows high levels of expression in the olfactory bulb, basal ganglia, cortex, cerebellar Purkinje cells and the dentate gyrus, and shows moderate levels of expression in CA1 and CA2 neurones of the hippocampus. *In situ* hybridisation also confirms the presence of Kir2.3 mRNA in the hippocampus (Hawrylycz et al., 2012). To further explore the potential role of Kir2.3 in regulating GABA release at inhibitory terminals, immunocytochemical staining needs to be performed to confirm the channel's presence in the presynaptic membrane.

5.3.2. Evidence for direct modulation of native $GABA_A$ receptors by PS

Whereas PS mediated clear concentration-dependent inhibition of whole-cell steady-state GABA currents in HEK cells and neurones, no concentration-dependent inhibition of GABA-mediated IPSC amplitudes was observed. The average IPSC amplitude was reduced by 30-40% at 1, 3 and 10 μM PS, which suggests that the reduction in amplitude may not be due to direct modulation of postsynaptic $GABA_A$ receptors. Previous studies have also suggested that PS does not affect the peak amplitude of GABA-induced IPSCs (Teschemacher et al., 1997; Mtchedlishvili and Kapur, 2003; Haage et al., 2005). The large increase in the frequency of IPSCs in the presence of PS also makes it difficult to interpret effects of PS on amplitude. The histograms show that a larger number of IPSCs of smaller peak amplitudes are present in PS than in control, and that larger events are absent at a high concentration (10 μM) of PS as the data are best described by one rather than two Gaussian fits. Whether the presence of many smaller events and the absence of larger events demonstrate that PS is directly inhibiting the postsynaptic $GABA_A$ receptors, or if IPSCs of smaller amplitude reflect the large increase in GABA release, is uncertain. Alternatively, the larger amplitude IPSCs may provide an increased opportunity for block by PS by virtue of their increased number of open channels/activated receptors. Direct inhibition of postsynaptic $GABA_A$Rs may also have been revealed in the conditions where the presynaptic effects of PS were blocked, as inhibition of IPSC amplitudes by

PS was present when co-applied with ononetin and ML133 as well as Ba^{2+} and ononetin.

PS reduced the decay time constant (τ_w) in a concentration-dependent manner, both for mIPSCs and sIPSCs. The decay time constant of mIPSCs was reduced by as much as 50% at 10 μM PS, which suggests that PS had a profound effect on the desensitisation/deactivation kinetics of the postsynaptic $GABA_A$ receptors. Given the activation-dependence and slow onset of PS inhibition of GABA whole-cell currents in HEK cells, the condition of increased GABA release and spillover caused by the presynaptic action of PS might promote this type of inhibition by causing prolonged and repeated receptor activation. Although some studies have reported no effect of PS on the decay kinetics of IPSCs (Mtchedlishvili and Kapur, 2003; Haage et al., 2005), PS can reduce the prolongation of decay induced by allopregnanolone in a concentration-dependent manner in neurones of the medial preoptic nucleus (Haage et al., 2005).

At autaptic synapses formed by hippocampal neurones in culture, PS had a greater effect on both the peak amplitude and the decay of IPSCs when GABA release was elevated by using a high external concentration of Ca^{2+} (4 mM compared to 1 mM) (Eisenman et al., 2003). However, under conditions of elevated GABA release (4 mM external Ca^{2+}), IPSCs were also found to decay 55 ± 38% slower than in conditions of lower GABA release (1 mM external Ca^{2+}), possibly due to the increased lifetime of GABA in the synaptic cleft when synaptic release is increased. This idea is consistent with the activity and open probability of $GABA_A$ receptors needing to be high for inhibition to occur. In the present study, PS did however also increase the rate of decay when the presynaptic effects of PS were blocked.

5.3.3. Can PS inhibit tonic GABA currents?

Although PS could inhibit simulated tonic GABA currents in HEK cells, it is less certain whether this will occur under physiological conditions in which PS increases synaptic GABA release. As elevated GABA release is likely to lead to increased spillover, PS may indirectly cause increased activation of extrasynaptic

$GABA_A$ receptors and thus potentiate rather than inhibit the tonic GABA current. In neurones from the medial preoptic nucleus, PS (10 μM) inhibited a baseline current evoked by 1 μM allopregnanolone, but did not cause a shift in the baseline when applied on its own (Haage et al., 2005). It should be noted that no appropriate control was made to check if a tonic GABA current was present.

5.4. Conclusion

This chapter has investigated the pharmacological action of PS on dissociated hippocampal neurones. It has been shown that although PS can inhibit GABA whole-cell currents in these neurones in a concentration-dependent manner, the level of inhibition of IPSC amplitudes was similar at 1,3 and 10 μM PS. On the other hand, PS caused a concentration-dependent increase in the presynaptic release of GABA, and hence IPSC frequency. This led to a high frequency of IPSCs of small amplitude, mediated by activation of the presynaptic TRPM3 receptor. Upon block of the TRPM3 receptor, PS supressed GABA release, most likely by potentiating presynaptic Kir2.3-containing channels. Under conditions of increased synaptic activity, PS also increased the rate of IPSC decay, as the decay time constant τ_w was reduced for both mIPSCs and sIPSCs. This effect on the rate of decay was also present when the presynaptic effects of PS were blocked. Under these conditions, some inhibition of IPSC amplitudes by PS was also present. Furthermore, PS increased inhibitory charge transfer in hippocampal neurones in a concentration-dependent manner.

Chapter 6: General discussion

6.1. Discussion

The main aims of this thesis were to characterise the mode of inhibition by PS at the $GABA_ARs$, determine whether PS exhibits $GABA_AR$ subtype selectivity in

recombinant expression systems and hippocampal neurones, probe potential binding sites for the inhibitory neurosteroid and establish its effects on fast GABAergic neurotransmission in hippocampal neurones.

As discussed in Chapter 3, PS is a state-dependent negative allosteric modulator at $GABA_AR$s incorporating any of the α1-6 subunits, with the potency differing only marginally between different receptor subtypes. Although PS is a more potent inhibitor at higher agonist concentrations when the channel open probability is high (Eisenman et al., 2003), the block elicited by PS developed only slowly, suggesting it could be more effective at blocking tonically-active extrasynaptic receptors. Pre-applying PS prior to $GABA_AR$ activation in HEK cells did not increase GABA peak current inhibition by the steroid, indicating that inhibition occurs after the binding of and activation by GABA, a finding that is consistent with the block being state-dependent.

In hippocampal pyramidal neurones, the most prominent effect of PS was on presynaptic GABA release (Fig. 6.1). PS caused an increase in GABA release by activating presynaptic TRPM3 channels, leading to increased influx of cations at the nerve terminal and subsequently, increased GABA release. Surprisingly, when TRPM3 was blocked with ononetin, the effect of PS on GABA release was reversed; the frequency of IPSCs fell below baseline, suggesting that PS acted at a different channel or receptor to reduce GABA release. This later effect was blocked by Kir2 channel blockers, Ba^{2+} and ML133, indicating that PS acts as a positive modulator at this channel, leading to increased K^+ efflux and less GABA release. This Kir2 channel is most likely to be Kir2.3, as PS is known to be more potent at this channel than other members of the Kir2 subfamily (Kobayashi et al., 2009).

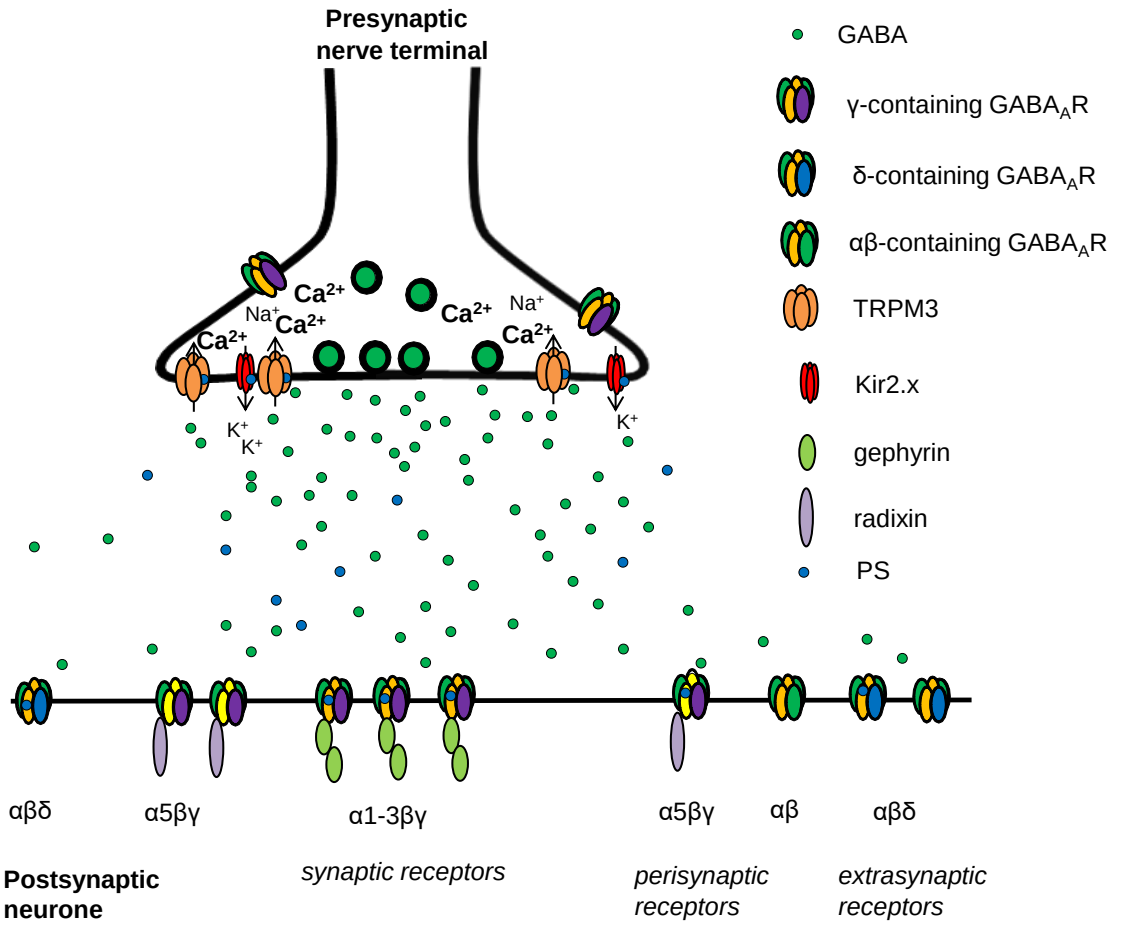

Figure 6.1 – Suggested effects of PS in a GABAergic synapse.

The figure depicts how PS activates TRPM3 receptors to increase the flux of cations (Ca^{2+} and Na^{+}) across the membrane of the presynaptic neurone, leading to membrane depolarisation and vesicular GABA release. PS also acts at a Kir2.x channel (most likely Kir2.3), letting K^{+} out of the cell. This effect is masked by TRPM3 activation; only upon block of TRPM3 does the efflux of K^{+} reduce GABA release to levels below baseline.

Although the most prominent effect of PS at inhibitory synapses in cultured hippocampal neurones was to increase GABA release, evidence was also presented demonstrating that PS directly modulates postsynaptic $GABA_AR$s. In HEK cells expressing recombinant $GABA_AR$s, PS produced a slowly developing block that manifested as an increased apparent rate of desensitisation. Thus, it was not surprising to find that PS also increased the rate of IPSC decay in hippocampal neurones, both for mIPSCs and sIPSCs. However, although PS increased IPSC decay rates, the average inhibitory charge transfer was actually increased by PS due to its prominent presynaptic effect on increasing GABA release and thus IPSC frequency. Although the large increase in IPSC frequency

made it difficult to establish whether PS directly negatively modulated postsynaptic $GABA_AR$s, IPSC peak amplitudes were reduced when the presynaptic targets of PS were blocked with ononetin and ML133, suggesting that direct $GABA_AR$ inhibition was present.

As removal of released GABA from the synapse is fast, the decay phase of IPSCs is dominated by ion channel closure (deactivation) that follows agonist dissociation from the receptor (Farrant and Nusser, 2005). This phase is also determined by the entry into and exit from agonist-bound desensitised states of the receptor. Furthermore, the decay kinetics also differ between different receptor subtypes, and differences in IPSC decay kinetics can be observed at different stages of development and in different cell types (Okada et al., 2000; Bacci et al., 2003; Ramadan et al., 2003). Assuming the receptor subtypes stay constant during the recordings, the rate of IPSC decay is likely to be influenced only by rates of deactivation and desensitisation in these hippocampal neurones. Although individual rate constants were not determined, the increase in the rate of IPSC decay that is observed when PS is applied is more likely to reflect an increase in the rate of desensitisation rather than deactivation, which is in accord with the increased apparent rate of desensitisation of GABA whole-cell currents that was observed in HEK cells. Furthermore, when the potency of PS was assessed in HEK cells expressing $GABA_AR$s that desensitised faster ($\alpha1\beta2\gamma2L^{V262F}$) or slower ($\alpha1\beta2^{L296V}\gamma2L$) than wild-type α1β2γ2L, lower levels of inhibition were observed for the faster-desensitising mutant. This is interpreted as faster-desensitising receptors limiting the scope for inhibition by PS if it acts to promote entry of receptors into a desensitised state. Taken together, these findings suggest that PS may act by promoting entry of receptors into a desensitised state, or prevent exit from this state to the open state, thereby reducing the open probability for GABA channels.

Due to the observation that inhibition by PS develops slowly and manifests as an increase in the apparent rate of $GABA_AR$ desensitisation in HEK cells, the possibility that PS might be more potent as an inhibitor of tonic GABA currents was considered. PS did inhibit a simulated tonic current using low GABA concentrations (100 nM; EC_{10}) in HEK cells expressing α4β2δ, but was less potent than at higher GABA concentrations. In hippocampal neurones, the effect

of PS on the tonic current was mixed. Due to the increase in GABA release mediated by PS, the tonic current increased in most cells during PS exposure rather than decreased, possibly due to GABA overspill. In neurones where the tonic current was potentiated (*e.g*. by MFA; see Chapter 5, Fig. 5.15A), PS did however produce inhibition of the tonic current, demonstrating that there are conditions in which this may occur. Similarly, PS has been shown to abolish the increased tonic GABA current produced by allopregnanolone in neurones of the rat medial preoptic nucleus (Haage et al., 2005).

Investigating the mode of inhibition by PS of recombinant $GABA_AR$ has provided an indication as to where this inhibitory neurosteroid might bind. Experiments with PTX showed that PS does not compete with the open-channel blocker for binding, making the ion channel an unlikely binding site for PS. Furthermore, inhibition by PS is only weakly voltage-dependent, a finding that has also been made by others (Majewska et al., 1988; Eisenman et al., 2003). As PS carries a negatively charged sulphate group, greater block would be expected at depolarised membrane potentials if the neurosteroid binds in the channel pore. The α1 subunit 2' residue ($\alpha1^{V256}$) situated near the intracellular end of the M2 helix is also, for these reasons, unlikely to be involved in the binding of PS, but appears to be an important signal transduction residue. The lack of $GABA_AR$ inhibition following application of PS through the intracellular solution demonstrates that the binding site can only be accessed from the extracellular side of the receptor. Taken together, the binding site for PS is likely to exist around the extracellular face of the receptor, and is largely unaffected by the membrane electric field.

Experiments with recombinant β3 homomers and ρ1 chimeras showed that the binding site for PS is likely to exist on multiple subunits, including α1, β2, γ2 and ρ1. As PS is active at all recombinant αβγ/δ receptors studied in this project, incorporating any of the α1-6 subunits, it is likely that one or more binding site(s) for PS exist at all of the $GABA_AR$ subunits. This also corroborates the hypothesis that PS does not share a binding site with the potentiating neurosteroids, which only exists on the α subunits (Hosie et al., 2006, 2009).

PS exhibits no appreciable diasteroselectivity in chick spinal cord and rat hippocampal neurones, as the steroid is almost equally active when the sulphate

group is in the 3α or 3β configuration (Park-Chung et al., 1999). The sulphate group is also not essential for inhibition, but does confer increased potency. In rat hippocampal neurones, PS shows little enantioselectivity (Nilsson et al., 1998). Enantioselectivity is often used as evidence for a specific ligand binding site at a receptor, and lack thereof can be indicative of indirect interactions between the ligand and the membrane (Akk et al., 2009; Seljeset et al., 2015). Sulphated steroids, including PS, increase the membrane capacitance of cells at a concentration range similar to that causing inhibition of $GABA_AR$ currents (Mennerick et al., 2008). In contrast, the potentiating neurosteroids, e.g. allopregnanolone, produce no change in membrane capacitance. Capacitive currents caused by PS do not show voltage-dependence, suggesting that PS alters the membrane capacitance without physical movement of the molecule through the electric field. Thus, sulphated steroids are likely to partition into the membrane without translocating across the lipid bilayer, likely with the sulphate group pointing outwards to the extracellular environment, possibly interacting with the polar head groups of lipid molecules.

Lipid modulation of $GABA_ARs$ is not a new concept. Docosahexaenoic acid (DHA) and other polyunsaturated fatty acids (PUFAs) have been shown to promote [^{3}H]-muscimol binding at $GABA_ARs$ and increase the rate of desensitisation (Søgaard et al., 2006). Cholesterol depletion, which reduces lipid bilayer stiffness, was also shown to promote [^{3}H]-muscimol binding at $GABA_ARs$ (Søgaard et al., 2006), and enhanced the effect of PS, pregnenolone and alphaxalone in hippocampal neurones (Sooksawate and Simmonds, 2001). Cholesterol enrichment diminished the effect of these steroids on $GABA_AR$ function and might argue for cholesterol competing with neurosteroids at their binding sites. For other non-steroidal potentiators, e.g. propofol and flunitrazepam, cholesterol depletion had no effect on their potency whilst enrichment increased it. Furthermore, hydrophobic anions and structurally diverse amphiphiles can act as non-competitive antagonists at $GABA_ARs$, most probably by partitioning into the lipid membrane, and are, like PS, sensitive to the 2' mutation $\alpha1^{V256S}$ (Chisari et al., 2010, 2011). Notably, these molecules also appear to increase the apparent rate of desensitisation in a manner similar to that by PS. The mechanisms behind this type of modulation of $GABA_AR$ function are not completely understood, but

changes in lipid bilayer elasticity have been implicated. Changes in membrane elasticity have however been shown to have no effect on $GABA_AR$ function, and were also originally hypothesised (erroneously) to underlie the anaesthetic action of GAs like pentobarbitone (Franks and Lieb, 1982). There is, however, still some uncertainty as to whether PS interacts with a chiral binding site at $GABA_ARs$, or if modulation occurs through non-specific interactions due to PS partitioning into the membrane.

There is evidence to suggest that PS does interact with a binding site on $GABA_ARs$ and other receptors. PS does not exclusively act as a negative modulator, as it negatively modulates NMDA receptors comprised of GluN1 with GluN2C or GluN2D subunits and conversely acts as a potentiator at those comprising GluN1 with GluN2A or GluN2B subunits (Malayev et al., 2002; Jang et al., 2004; Kostakis et al., 2011). Furthermore, potentiation of NMDA receptors by PS depends on their phosphorylation state, as it is reduced by kinase inhibitors and recovered by a PKA activator, arguing for direct interaction between the steroid and the receptor subunits (Petrovic et al., 2009). Some specificity in engaging with a binding site is also suggested from the structure-activity studies of PS at native $GABA_ARs$ (Park-Chung et al., 1999; Seljeset et al., 2015). One could also argue that if membrane perturbation by PS is sufficient to cause inhibition of $GABA_ARs$, then some inhibition would also be present when PS is applied inside the cell, a feature that was not observed in this project. It is possible that PS-receptor interactions are not very specific, and PS could potentially access an intra-subunit binding site from within the lipid membrane.

It is also conceivable that other lipid molecules might compete with PS for such a position in the lipid bilayer that could be adjacent to, or part of, the $GABA_A$ receptor. In this regard, the structural determination of the *apo* state of the GluCl channel in the presence of 1-palmitoyl-2-oleoyl-*sn*-glycero-3-phosphocholine (POPC) reveals close packing of several molecules of POPC around the transmembrane domain, particularly M1 and M3 (Althoff et al., 2014). POPC can compete with the partial agonist at GluCl, ivermectin. This therefore demonstrates that a lipophilic molecule (POPC) can partition into the plasma membrane, and act as an antagonist of a pLGIC (GluCl). A similar type of interaction may exist between PS and the mammalian $GABA_ARs$.

6.2. Remaining questions and future work

6.2.1. Do TRPM3 and Kir2.3 exist in the terminals of hippocampal interneurones?

In the present study, PS was found to increase GABA release by acting at TRPM3 receptors located at the terminals of hippocampal interneurones. Upon block of TRPM3, PS reduced the frequency of IPSCs, most likely by acting as a positive modulator at Kir2.3-containing channels in the presynaptic membrane, causing a reduction in GABA release. To confirm that these receptors and channels exist in the presynaptic membrane of GABAergic neurones, immunocytochemistry would be helpful. To localise their presence to inhibitory synapses, antibodies for synaptic markers like the vesicular GABA transporter (vGAT) or the enzyme for synaptic synthesis of GABA, glutamic acid decarboxylase 65 (GAD65) (Kaufman et al., 1991), can be used. If the staining for these markers co-localised with similar staining for TRPM3 and Kir2.3, this would confirm their presence at presynaptic terminals. Alternatively, *in situ* hybridisation can also be performed to confirm the presence of TRPM3 and Kir2.3 mRNA, though this would only confirm that the respective cDNAs are transcribed, and not that the proteins are expressed in the presynaptic terminals.

6.2.2. Determining the effect of PS on excitability in hippocampal neurones and other brain regions at different stages of development

As demonstrated in Chapter 5, PS increased the rate of IPSC decay in cultured hippocampal neurones, demonstrating direct modulation of postsynaptic $GABA_AR$s. PS also caused a large increase in GABA release and IPSC frequency. As a result, charge transfer was increased, raising the question as to whether PS might act to reduce the excitability of hippocampal neurones rather than increase it, despite being considered a negative modulator of $GABA_AR$s. However, to unequivocally identify IPSCs, fast glutamatergic transmission was blocked by kynurenic acid. Knowing that PS can also positively modulate NMDA receptors (Kostakis et al., 2011), and increase glutamate release from

presynaptic terminals (Lee et al., 2010; Zamudio-Bulcock and Valenzuela, 2011; Zamudio-Bulcock et al., 2011), PS will under physiological conditions also increase excitatory glutamatergic transmission. In neonatal cerebellar Purkinje cells, 25 μM PS increased the frequency of AMPA receptor-mediated mEPSCs by ~30-fold, whereas the increase in $GABA_AR$-mediated mIPSCs was less than 2-fold (Zamudio-Bulcock and Valenzuela, 2011). This suggests that the overall effect of PS might be to increase the excitability of cerebellar Purkinje cells in neonatal rats. However, as Purkinje cells are GABAergic neurones (Najac and Raman, 2015), they will in turn release GABA, leading to inhibition.

Whether PS acts to increase or decrease neuronal excitability will depend on the receptors present in the presynaptic terminal and the type of transmitter released, something that may differ between types of neurones, brain regions and stages of development. Previous studies suggest that PS is synthesised and released from postsynaptic membranes up until postnatal day 5 in hippocampal slice preparations, as anti-PS antibodies prevented the NMDA receptor-mediated increase in glutamate release during this period (Mameli, 2005; Mameli and Valenzuela, 2006). It may also be that the GluN2D-containing receptors in the presynaptic membrane that mediated the PS-induced increase in glutamate release are only expressed until postnatal day 5. As the gestation period for rats is about three weeks, the neurones used in the present study are older than those used by the Valenzuela group. In the present study, increased GABA release was mediated by TRPM3 channels, which have also been found to mediate PS-induced GABA and glutamate release in the developing cerebellum (Zamudio-Bulcock and Valenzuela, 2011; Zamudio-Bulcock et al., 2011).

To further characterise differences between the effect of PS in different regions of the brain and stages of development, recordings could target different parts of the brain from animals of various ages. Furthermore, to determine if the overall effect of PS is to increase the excitability of the postsynaptic neurone, current clamp recordings can be performed under physiological conditions when neither fast GABAergic nor glutamatergic blockers are present to assess how PS affects the input-output relationship of the neurone. Although PS increased the mean inhibitory charge transfer in hippocampal neurones in the present study, the effect

of PS on glutamate release might result in a net increase in postsynaptic excitability in the absence of kynurenic acid.

As TRPM3 is heat-sensitive, and increasing the temperature from room temperature to 37 °C has been shown to sensitise the channel to PS (Held et al., 2015), it would be interesting to determine if increasing the ambient temperature during recordings can shift the concentration-response relationship of PS at TRPM3 to the left. If this is the case, a lower concentration of PS may induce GABA release in hippocampal neurones under physiological conditions, and an ever larger increase in IPSC frequency in response to 10 µM PS may be observed.

6.2.3. Is PS synthesised and released from hippocampal neurones?

Postsynaptic depolarisation can cause the retrograde release of PS in hippocampal slices from neonatal rats to increase AMPA receptor-mediated mEPSCs in CA1 pyramidal neurones during a restricted developmental period (Mameli, 2005). The increase in glutamate release was thought to be mediated by GluN2D-containing NMDA receptors in presynaptic terminals. In a later study, the frequency of EPSCs was shown to be increased in hippocampal slices following 5 min exposure to the sulphatase blocker DU-14 (Mameli and Valenzuela, 2006). This increase in EPSCs was prevented by an anti-PS antibody, and by blocking PS synthesis using aminogluthetimide to block the conversion of cholesterol into pregnenolone. It would be interesting to determine if pyramidal neurone depolarisation can also cause retrograde PS release that evokes GABA release via a TRPM3-dependent mechanism from hippocampal interneurones in slices, and whether this occurs during the same developmental time period (postnatal days 3-5).

6.2.4. Determining whether PS-$GABA_AR$ interaction is specific and localising the PS binding site(s)

One of the aims of this project was to localise the binding site for PS and the other inhibitory neurosteroids at $GABA_ARs$. The chimera approach using the ρ1 subunit

and other $GABA_AR$ subunits suggests that the potential binding site for PS is likely to exist in the transmembrane domain, but that ρ1 also contains this binding site. These chimera studies therefore do not exclude the possibility that PS interacts with the receptor via a binding site that is not very specific after partitioning into the membrane, as discussed in section 6.1.

If insertion of PS into the lipid membrane is necessary for inhibition of $GABA_ARs$, it might be possible to manipulate this using surface charge screening. The rationale here is to prevent PS from binding to the membrane by increasing the screening of surface charge using increased extracellular concentrations of divalent cations (Hille, 1992). This may prevent PS from partitioning into the membrane, leaving relatively unaffected any effects caused by direct binding of PS to the receptor. It might then be possible to determine whether insertion into the membrane by PS is a necessary pre-requisite for it to inhibit $GABA_AR$.

As mentioned in section 6.1, POPC can partition into the membrane around the GluCl receptor and compete with the partial agonist ivermectin (Althoff et al., 2014). Another line of enquiry would be to examine if POPC and related phosphocholines can prevent or reduce the inhibition of PS at $GABA_ARs$.

As the enantioselectivity of PS at $GABA_ARs$ has only been studied at native receptors in hippocampal neurones and the *C. elegans* UNC-49B/C receptor (Nilsson et al., 1998; Twede et al., 2007), the activity of the PS enantiomer should also be assessed at recombinant $GABA_ARs$ in HEK cells. If PS is found to be enantioselective, this would increase the likelihood of PS interacting with a chiral binding site at $GABA_ARs$.

Another line of enquiry to consider is whether PS binds to any binding sites that have been identified for other modulators with known pharmacological activity at the $GABA_A$ receptor. Binding sites of interest include intra- and an intersubunit modulatory sites for general anaesthetics (Nury et al., 2011; Corringer et al., 2012; Sauguet et al., 2014), as described in Chapter 1, section 1.1.4. The intrasubunit binding pocket, first described in the Cys-loop receptor bacterial ortholog, GLIC (Nury et al., 2011), is found in the upper half of the transmembrane domain, forming a cavity that is accessible from the lipid bilayer. The intersubunit

binding cavity was identified when GluCl was crystallised in complex with ivermectin (Hibbs and Gouaux, 2011). This pocket is formed in the upper part of the transmembrane domain at each subunit interface, comprising residues from M2 and M3 of one subunit, and M1 from the adjacent subunit. These inter- and intrasubunit binding pockets may accommodate various ligands and modulators at pLGICs, including general anaesthetics and ivermectin (Mihic et al., 1997; Li et al., 2006; Nury et al., 2011). Some of the residues identified in the GLIC and the GluCl crystal structures could potentially contribute to accommodate PS in an inter- or intrasubunit binding site. This can be explored by performing docking studies with PS at the $GABA_A$ receptor at these cavities. This could tentatively identify residues that could be involved in the binding of PS. Their potential involvement can further be explored by site-directed mutagenesis of the identified residues.

Another more challenging method that can be used to directly identify the binding site(s) for PS, is X-ray crystallography. If PS is co-crystallised with a $GABA_AR$ or another pLGIC, this could provide insight into which residue(s) contribute to the binding site(s) for the neurosteroid. This can then be further explored by using molecular biology and electrophysiological techniques.

References

Abramian, A.M., Comenencia-Ortiz, E., Vithlani, M., Tretter, E.V., Sieghart, W., Davies, P.A., et al. (2010). Protein kinase C phosphorylation regulates membrane insertion of $GABA_A$ receptor subtypes that mediate tonic inhibition. J. Biol. Chem. *285*: 41795–805.

Adams, J.M., Thomas, P., and Smart, T.G. (2015). Modulation of neurosteroid potentiation by protein kinases at synaptic- and extrasynaptic-type $GABA_A$ receptors. Neuropharmacology *88*: 63–73.

Akk, G., Bracamontes, J., and Steinbach, J.H. (2001). Pregnenolone sulfate block of $GABA_A$ receptors: Mechanism and involvement of a residue in the M2 region of the α subunit. J. Physiol. *532*: 673–684.

Akk, G., Covey, D.F., Evers, A.S., Steinbach, J.H., Zorumski, C.F., and Mennerick, S. (2007). Mechanisms of neurosteroid interactions with $GABA_A$ receptors. Pharmacol. Ther. *116*: 35–57.

Akk, G., Covey, D.F., Evers, A.S., Steinbach, J.H., Zorumski, C.F., and Mennerick, S. (2009). The influence of the membrane on neurosteroid actions at $GABA_A$ receptors. Psychoneuroendocrinology *34*: S59–S66.

Akk, G., Li, P., Bracamontes, J., Reichert, D.E., Covey, D.F., and Steinbach, J.H. (2008). Mutations of the $GABA_A$ receptor α1 subunit M1 domain reveal unexpected complexity for modulation by neuroactive steroids. Mol. Pharmacol. *74*: 614–627.

Akk, G., Shu, H., Wang, C., Steinbach, J.H., Zorumski, C.F., Covey, D.F., et al. (2005). Neurosteroid access to the $GABA_A$ receptor. J. Neurosci. *25*: 11605–11613.

Althoff, T., Hibbs, R.E., Banerjee, S., and Gouaux, E. (2014). X-ray structures of GluCl in apo states reveal a gating mechanism of Cys-loop receptors. Nature

512: 333–337.

Andrews, P.R., and Johnston, G.A. (1979). GABA agonists and antagonists. Biochem. Pharmacol. *28*: 2697–2702.

Augustine, G.J., and Kasai, H. (2007). Bernard Katz, quantal transmitter release and the foundations of presynaptic physiology. J. Physiol. *578*: 623–5.

Bacci, A., Rudolph, U., Huguenard, J.R., and Prince, D.A. (2003). Major differences in inhibitory synaptic transmission onto two neocortical interneuron subclasses. J. Neurosci. *23*: 9664–9674.

Baker, C., Sturt, B.L., and Bamber, B.A. (2010). Multiple roles for the first transmembrane domain of $GABA_A$ receptor subunits in neurosteroid modulation and spontaneous channel activity. Neurosci. Lett. *473*: 242–247.

Bamber, B.A., Beg, A.A., Twyman, R.E., and Jorgensen, E.M. (1999). The *Caenorhabditis elegans* UNC-49 locus encodes multiple subunits of a heteromultimeric GABA receptor. J. Neurosci. *19*: 5348–5359.

Bamber, B.A., Richmond, J.E., Otto, J.F., and Jorgensen, E.M. (2005). The composition of the GABA receptor at the *Caenorhabditis elegans* neuromuscular junction. Br. J. Pharmacol. *144*: 502–509.

Bamber, B.A., Twyman, R.E., and Jorgensen, E.M. (2003). Pharmacological characterization of the homomeric and heteromeric UNC-49 GABA receptors in *C. elegans*. Br. J. Pharmacol. *138*: 883–893.

Barbour, B., and Häusser, M. (1997). Intersynaptic diffusion of neurotransmitter. Trends Neurosci. *20*: 377–84.

Baulieu, E.E. (1981). Steroid hormones in the brain: several mechanisms? In Steroid Hormone Regulation of the Brain, Elsevier, pp 3–14.

Baulieu, E.E., and Robel, P. (1990). Neurosteroids: a new brain function? J. Steroid Biochem. Mol. Biol. *37*: 395–403.

Bedford, F.K., Kittler, J.T., Muller, E., Thomas, P., Uren, J.M., Merlo, D., et al. (2001). $GABA_A$ receptor cell surface number and subunit stability are regulated by the ubiquitin-like protein Plic-1. Nat. Neurosci. *4*: 908–916.

Belelli, D., Casula, A., Ling, A., and Lambert, J.J. (2002). The influence of subunit composition on the interaction of neurosteroids with $GABA_A$ receptors. Neuropharmacology *43*: 651–661.

Belelli, D., Lambert, J.J., Peters, J.A., Wafford, K., and Whiting, P.J. (1997). The interaction of the general anesthetic etomidate with the γ-aminobutyric acid type A receptor is influenced by a single amino acid. Proc. Natl. Acad. Sci. U. S. A. *94*: 11031–11036.

Belelli, D., Pistis, M., Peters, J.A., and Lambert, J.J. (1999). The interaction of general anaesthetics and neurosteroids with $GABA_A$ and glycine receptors. Neurochem. Int. *34*: 447–452.

Ben-Ari, Y., Khalilov, I., Kahle, K.T., and Cherubini, E. (2012). The GABA excitatory/inhibitory shift in brain maturation and neurological disorders. Neuroscientist *18*: 467–486.

Bernardi, F., Salvestroni, C., Casarosa, E., Nappi, R.E., Lanzone, A., Luisi, S., et al. (1998). Aging is associated with changes in allopregnanolone concentrations in brain, endocrine glands and serum in male rats. Eur. J. Endocrinol. *138*: 316–321.

Bettler, B., Kaupmann, K., Mosbacher, J., and Gassmann, M. (2004). Molecular Structure and Physiological Functions of $GABA_B$ Receptors. Physiol. Rev. *84*: 835–867.

Bianchi, M.T., and Macdonald, R.L. (2002). Slow phases of $GABA_A$ receptor desensitization: structural determinants and possible relevance for synaptic function. J. Physiol. *544*: 3–18.

Bocquet, N., Nury, H., Baaden, M., Poupon, C. Le, Changeux, J.-P., Delarue, M.,

et al. (2009). X-ray structure of a pentameric ligand-gated ion channel in an apparently open conformation. Nature *457*: 111–114.

Bogdanov, Y., Michels, G., Armstrong-Gold, C., Haydon, P.G., Lindstrom, J., Pangalos, M., et al. (2006). Synaptic $GABA_A$ receptors are directly recruited from their extrasynaptic counterparts. EMBO J. *25*: 4381–9.

Bonnert, T.P., McKernan, R.M., Farrar, S., Bourdellès, B. le, Heavens, R.P., Smith, D.W., et al. (1999). θ, a novel gamma-aminobutyric acid type A receptor subunit. Proc. Natl. Acad. Sci. U. S. A. *96*: 9891–6.

Borda, T., Genaro, A.M., and Cremaschi, G. (1999). Haloperidol Effect on Intracellular Signals System Coupled to α1-Adrenergic Receptor in Rat Cerebral Frontal Cortex. Cell. Signal. *11*: 293–300.

Bormann, J., Hamill, O.P., and Sakmann, B. (1987). Mechanism of anion permeation through channels gated by glycine and γ-aminobutyric acid in mouse cultured spinal neurones. J. Physiol. *385*: 243–286.

Bowery, N.G., Bettler, B., Froestl, W., Gallagher, J.P., Marshall, F., Raiteri, M., et al. (2002). International Union of Pharmacology. XXXIII. Mammalian γ-aminobutyric acidB receptors: structure and function. Pharmacol. Rev. *54*: 247–264.

Bowery, N.G., and Smart, T.G. (2006). GABA and glycine as neurotransmitters: a brief history. Br. J. Pharmacol. *147*: S109–S119.

Bracamontes, J.R., Li, P., Akk, G., and Steinbach, J.H. (2012). A neurosteroid potentiation site can be moved among $GABA_A$ receptor subunits. J. Physiol. *590*: 5739–5747.

Breitinger, H.-G., and Becker, C.-M. (2002). The inhibitory glycine receptor - simple views of a complicated channel. ChemBioChem *3*: 1042–1052.

Brejc, K., Dijk, W.J. van, Klaassen, R. V, Schuurmans, M., Oost, J. van Der, Smit,

A.B., et al. (2001). Crystal structure of an ACh-binding protein reveals the ligand-binding domain of nicotinic receptors. Nature *411*: 269–276.

Brickley, S.G., Cull-Candy, S.G., and Farrant, M. (1996). Development of a tonic form of synaptic inhibition in rat cerebellar granule cells resulting from persistent activation of $GABA_A$ receptors. J. Physiol. 753–759.

Brickley, S.G., Farrant, M., Swanson, G.T., and Cull-Candy, S.G. (2001). CNQX increases GABA-mediated synaptic transmission in the cerebellum by an AMPA/kainate receptor-independent mechanism. Neuropharmacology *41*: 730–736.

Bright, D.P., Aller, M.I., and Brickley, S.G. (2007). Synaptic release generates a tonic $GABA_A$ receptor-mediated conductance that modulates burst precision in thalamic relay neurons. J. Neurosci. *27*: 2560–2569.

Bright, D.P., and Smart, T.G. (2013). Protein kinase C regulates tonic $GABA_A$ receptor-mediated inhibition in the hippocampus and thalamus. Eur. J. Neurosci. *38*: 3408–3423.

Brown, N., Kerby, J., Bonnert, T.P., Whiting, P.J., and Wafford, K.A. (2002). Pharmacological characterization of a novel cell line expressing human α4β3δ $GABA_A$ receptors. Br. J. Pharmacol. *136*: 965–974.

Brünig, I., Scotti, E., Sidler, C., and Fritschy, J.-M. (2002). Intact sorting, targeting, and clustering of γ-aminobutyric acid A receptor subtypes in hippocampal neurons in vitro. J. Comp. Neurol. *443*: 43–55.

Castillo, J. Del, and Katz, B. (1954). Quantal components of the end-plate potential. J. Physiol. *124*: 560–73.

Chavas, J., and Marty, A. (2003). Coexistence of excitatory and inhibitory GABA synapses in the cerebellar interneuron network. J. Neurosci. *23*: 2019–2031.

Che Has, A.T., Absalom, N., Nieuwenhuijzen, P.S. van, Clarkson, A.N., Ahring,

P.K., and Chebib, M. (2016). Zolpidem is a potent stoichiometry-selective modulator of α1β3 $GABA_A$ receptors: evidence of a novel benzodiazepine site in the α1-α1 interface. Sci. Rep. *6*: 1–12.

Chen, L., and Sokabe, M. (2005). Presynaptic Modulation of Synaptic Transmission by Pregnenolone Sulfate as Studied by Optical Recordings. J. Neurophysiol. *94*: 4131–4144.

Chen, N.H., Reith, M.E.A., and Quick, M.W. (2004). Synaptic uptake and beyond: the sodium- and chloride-dependent neurotransmitter transporter family SLC6. Pflügers Arch. Eur. J. Physiol. *447*: 519–31.

Chiara, D.C., Jayakar, S.S., Zhou, X., Zhang, X., Savechenkov, P.Y., Bruzik, K.S., et al. (2013). Specificity of intersubunit general anesthetic-binding sites in the transmembrane domain of the human α1β3γ2 γ-aminobutyric acid type A ($GABA_A$) receptor. J. Biol. Chem. *288*: 19343–19357.

Chisari, M., Shu, H.J., Taylor, A., Steinbach, J.H., Zorumski, C.F., and Mennerick, S. (2010). Structurally diverse amphiphiles exhibit biphasic modulation of $GABA_A$ receptors: Similarities and differences with neurosteroid actions. Br. J. Pharmacol. *160*: 130–141.

Chisari, M., Wu, K., Zorumski, C.F., and Mennerick, S. (2011). Hydrophobic anions potently and uncompetitively antagonize $GABA_A$ receptor function in the absence of a conventional binding site. Br. J. Pharmacol. *164*: 667–680.

Christian, C.A., Herbert, A.G., Holt, R.L., Peng, K., Sherwood, K.D., Pangratz-Fuehrer, S., et al. (2013). Endogenous positive allosteric modulation of $GABA_A$ receptors by diazepam binding inhibitor. Neuron *78*: 1063–74.

Collinson, N., Kuenzi, F.M., Jarolimek, W., Maubach, K.A., Cothliff, R., Sur, C., et al. (2002). Enhanced Learning and Memory and Altered GABAergic Synaptic Transmission in Mice Lacking the α5 Subunit of the $GABA_A$ Receptor. J. Neurosci. *22*: 5572–5580.

Colquhoun, D. (1998). Binding, gating, affinity and efficacy: the interpretation of structure-activity relationships for agonists and of the effects of mutating receptors. Br. J. Pharmacol. *125*: 924–47.

Compagnone, N.A., and Mellon, S.H. (2000). Neurosteroids: Biosynthesis and Function of These Novel Neuromodulators. Front. Neuroendocrinol. *21*: 1–56.

Concas, A., Mostallino, M.C., Porcu, P., Follesa, P., Barbaccia, M.L., Trabucchi, M., et al. (1998). Role of brain allopregnanolone in the plasticity of gamma-aminobutyric acid type A receptor in rat brain during pregnancy and after delivery. Proc. Natl. Acad. Sci. U. S. A. *95*: 13284–13289.

Corpéchot, C., Robel, P., Axelson, M., Sjövall, J., and Baulieu, E.E. (1981). Characterization and measurement of dehydroepiandrosterone sulfate in rat brain. Proc. Natl. Acad. Sci. U. S. A. *78*: 4704–4707.

Corpéchot, C., Synguelakis, M., Talha, S., Axelson, M., Sjövall, J., Vihko, R., et al. (1983). Pregnenolone and its sulfate ester in the rat brain. Brain Res. *270*: 119–125.

Corringer, P.J., Novère, N. Le, and Changeux, J.P. (2000). Nicotinic Receptors at the Amino Acid Level. Annu. Rev. Pharmacol. Toxicol. *40*: 431–458.

Corringer, P.J., Bertrand, S., Bohler, S., Edelstein, S.J., Changeux, J.P., and Bertrand, D. (1998). Critical elements determining diversity in agonist binding and desensitization of neuronal nicotinic acetylcholine receptors. J. Neurosci. *18*: 648–657.

Corringer, P.J., Poitevin, F., Prevost, M.S., Sauguet, L., Delarue, M., and Changeux, J.P. (2012). Structure and pharmacology of pentameric receptor channels: From bacteria to brain. Structure *20*: 941–956.

Coyne, L., Su, J., Patten, D., and Halliwell, R.F. (2007). Characterization of the interaction between fenamates and hippocampal neuron $GABA_A$ receptors. Neurochem. Int. *51*: 440–446.

Craig, A.M., Blackstone, C.D., Huganir, R.L., and Banker, G. (1994). Selective clustering of glutamate and γ-aminobutyric acid receptors opposite terminals releasing the corresponding neurotransmitters. Proc. Natl. Acad. Sci. U. S. A. *91*: 12373–12377.

Crestani, F., Keist, R., Fritschy, J.-M., Benke, D., Vogt, K., Prut, L., et al. (2002). Trace fear conditioning involves hippocampal α5 $GABA_A$ receptors. Proc. Natl. Acad. Sci. U. S. A. *99*: 8980–8985.

Crestani, F., Löw, K., Keist, R., Mandelli, M., Möhler, H., and Rudolph, U. (2001). Molecular targets for the myorelaxant action of diazepam. Mol. Pharmacol. *59*: 442–445.

Cui, C., Xu, M., and Atzori, M. (2006). Voltage-Dependent Block of N-Methyl-D-aspartate Receptors by Dopamine D1 Receptor Ligands. Mol. Pharmacol. *70*: 1761–1770.

Darnaudéry, M., Koehl, M., Piazza, P. V, Moal, M. Le, and Mayo, W. (2000). Pregnenolone sulfate increases hippocampal acetylcholine release and spatial recognition. Brain Res. *852*: 173–179.

Darnaudéry, M., Pallarès, M., Piazza, P.-V., Moal, M. Le, and Mayo, W. (2002). The neurosteroid pregnenolone sulfate infused into the medial septum nucleus increases hippocampal acetylcholine and spatial memory in rats. Brain Res. *951*: 237–242.

Dascal, N., Schreibmayer, W., Lim, N.F., Wang, W., Chavkin, C., DiMagno, L., et al. (1993). Atrial G protein-activated K^+ channel: expression cloning and molecular properties. Proc. Natl. Acad. Sci. U. S. A. *90*: 10235–10239.

Davies, P.A., Hoffmann, E.B., Carlisle, H.J., Tyndale, R.F., and Hales, T.G. (2000). The influence of an endogenous β3 subunit on recombinant $GABA_A$ receptor assembly and pharmacology in WSS-1 cells and transiently transfected HEK293 cells. Neuropharmacology *39*: 611–620.

Davies, P.A., Pistis, M., Hanna, M.C., Peters, J.A., Lambert, J.J., Hales, T.G., et al. (1999). The 5-HT_3B subunit is a major determinant of serotonin-receptor function. Nature *397*: 359–363.

Davies, P.A., Wang, W., Hales, T.G., and Kirkness, E.F. (2003). A Novel Class of Ligand-gated Ion Channel Is Activated by Zn^{2+}. J. Biol. Chem. *278*: 712–717.

Du, J., Lü, W., Wu, S., Cheng, Y., and Gouaux, E. (2015). Glycine receptor mechanism elucidated by electron cryo-microscopy. Nature *526*: 224–229.

Edwards, F.A., Konnerth, A., and Sakmann, B. (1990). Quantal analysis of inhibitory synaptic transmission in the dentate gyrus of rat hippocampal slices: a patch-clamp study. J. Physiol. *430*: 213–49.

Eisenman, L.N., He, Y., Fields, C., Zorumski, C.F., and Mennerick, S. (2003). Activation-dependent properties of pregnenolone sulfate inhibition of $GABA_A$ receptor-mediated current. J. Physiol. *550*: 679–691.

Enz, R., and Cutting, G.R. (1999). $GABA_C$ receptor ρ subunits are heterogeneously expressed in the human CNS and form homo- and heterooligomers with distinct physical properties. Eur. J. Neurosci. *11*: 41–50.

Erkkila, B.E., Sedelnikova, A. V., and Weiss, D.S. (2008). Stoichiometric Pore Mutations of the $GABA_AR$ Reveal a Pattern of Hydrogen Bonding with Picrotoxin. Biophys. J. *94*: 4299–4306.

Fang, F., Christian, W. V, Gorman, S.G., Cui, M., Huang, J., Tieu, K., et al. (2010). Neurosteroid transport by the organic solute transporter OSTα-OSTβ. J. Neurochem. *115*: 220–233.

Farrant, M., and Kaila, K. (2007). The cellular, molecular and ionic basis of $GABA_A$ receptor signalling. Prog. Brain Res. *160*: 59–87.

Farrant, M., and Nusser, Z. (2005). Variations on an inhibitory theme: phasic and tonic activation of $GABA_A$ receptors. Nat. Rev. Neurosci. *6*: 215–229.

Ffrench-Constant, R.H., Rocheleau, T.A., Steichen, J.C., and Chalmers, A.E. (1993). A point mutation in a Drosophila GABA receptor confers insecticide resistance. Nature *363*: 449–451.

Fisher, J.L., and Macdonald, R.L. (1998). The role of an α subtype M2-M3 His in regulating inhibition of $GABA_A$ receptor current by zinc and other divalent cations. J. Neurosci. *18*: 2944–2953.

Flood, J.F., Morley, J.E., and Roberts, E. (1995). Pregnenolone sulfate enhances post-training memory processes when injected in very low doses into limbic system structures: the amygdala is by far the most sensitive. Proc. Natl. Acad. Sci. U. S. A. *92*: 10806–10810.

Fonfria, E., Murdock, P.R., Cusdin, F.S., Benham, C.D., Kelsell, R.E., and McNulty, S. (2006). Tissue distribution profiles of the human TRPM cation channel family. J. Recept. Signal Transduct. Res. *26*: 159–78.

Franks, N.P., and Lieb, W.R. (1982). Molecular mechanisms of general anaesthesia. Nature *300*: 487–493.

Fritschy, J.M., and Mohler, H. (1995). $GABA_A$-receptor heterogeneity in the adult rat brain: differential regional and cellular distribution of seven major subunits. J. Comp. Neurol. *359*: 154–194.

Fritschy, J.M., and Panzanelli, P. (2014). $GABA_A$ receptors and plasticity of inhibitory neurotransmission in the central nervous system. Eur. J. Neurosci. *39*: 1845–1865.

Fritschy, J.M., Panzanelli, P., and Tyagarajan, S.K. (2012). Molecular and functional heterogeneity of GABAergic synapses. Cell. Mol. Life Sci. *69*: 2485–2499.

Gao, Y., and Heldt, S.A. (2016). Enrichment of $GABA_A$ Receptor α-Subunits on the Axonal Initial Segment Shows Regional Differences. Front. Cell. Neurosci. *10*: 1–17.

Geiger, T., Wehner, A., Schaab, C., Cox, J., and Mann, M. (2012). Comparative proteomic analysis of eleven common cell lines reveals ubiquitous but varying expression of most proteins. Mol. Cell. Proteomics *11*: M111.014050.

Gibbs, T.T., Russek, S.J., and Farb, D.H. (2006). Sulfated steroids as endogenous neuromodulators. Pharmacol. Biochem. Behav. *84*: 555–567.

Gielen, M., Thomas, P., and Smart, T.G. (2015). The desensitization gate of inhibitory Cys-loop receptors. Nat. Commun. *6*: 1–10.

Glykys, J., Mann, E.O., and Mody, I. (2008). Which $GABA_A$ Receptor Subunits Are Necessary for Tonic Inhibition in the Hippocampus? J. Neurosci. *28*: 1421–1426.

Glykys, J., and Mody, I. (2007a). Activation of $GABA_A$ receptors: views from outside the synaptic cleft. Neuron *56*: 763–770.

Glykys, J., and Mody, I. (2007b). The main source of ambient GABA responsible for tonic inhibition in the mouse hippocampus. J. Physiol. *582*: 1163–1178.

Goldin, A.L. (2006). Expression of Ion Channels in Xenopus Oocytes. In Expression and Analysis of Recombinant Ion Channels: From Structural Studies to Pharmacological Screening, J.J.. Clare, and D.J. Trezise, eds. Wiley-VCH Verlag GmbH & Co. KGaA, Weinheim, FRG, pp 1–25.

Greka, A., Lipton, S.A., and Zhang, D. (2000). Expression of $GABA_C$ receptor ρ1 and ρ2 subunits during development of the mouse retina. Eur. J. Neurosci. *12*: 3575–3582.

Haage, D., Bäckström, T., and Johansson, S. (2005). Interaction between allopregnanolone and pregnenolone sulfate in modulating GABA-mediated synaptic currents in neurons from the rat medial preoptic nucleus. Brain Res. *1033*: 58–67.

Hadingham, K.L., Wingrove, P.B., Wafford, K.A., Bain, C., Kemp, J.A., Palmer,

K.J., et al. (1993). Role of the β subunit in determining the pharmacology of human γ-aminobutyric acid type A receptors. Mol. Pharmacol. *44*: 1211–1218.

Halliwell, R.F., Thomas, P., Patten, D., James, C.H., Miledi, R., and Smart, T.G. (1999). Subunit-selective modulation of $GABA_A$ receptors by the non-steroidal anti-inflammatory agent , mefenamic acid. Neuroscience *11*: 2897–2905.

Hassaine, G., Deluz, C., Grasso, L., Wyss, R., Tol, M.B., Hovius, R., et al. (2014). X-ray structure of the mouse serotonin 5-HT_3 receptor. Nature *512*: 276–281.

Hausrat, T.J., Muhia, M., Gerrow, K., Thomas, P., Hirdes, W., Tsukita, S., et al. (2015). Radixin regulates synaptic $GABA_A$ receptor density and is essential for reversal learning and short-term memory. Nat. Commun. *6*: 1–17.

Hawrylycz, M.J., Lein, E.S., Guillozet-Bongaarts, A.L., Shen, E.H., Ng, L., Miller, J.A., et al. (2012). An anatomically comprehensive atlas of the adult human brain transcriptome. Nature *489*: 391–399.

Held, K., Voets, T., and Vriens, J. (2015). TRPM3 in temperature sensing and beyond. Temp. Austin, Tex. *2*: 201–213.

Hibbs, R.E., and Gouaux, E. (2011). Principles of activation and permeation in an anion-selective Cys-loop receptor. Nature *474*: 54–60.

Higashi, T., Sugitani, H., Yagi, T., and Shimada, K. (2003). Studies on neurosteroids XVI. Levels of pregnenolone sulfate in rat brains determined by enzyme-linked immunosorbent assay not requiring solvolysis. Biol. Pharm. Bull. *26*: 709–711.

Hige, T., Fujiyoshi, Y., and Takahashi, T. (2006). Neurosteroid pregnenolone sulfate enhances glutamatergic synaptic transmission by facilitating presynaptic calcium currents at the calyx of Held of immature rats. Eur. J. Neurosci. *24*: 1955–1966.

Hilf, R.J.C., and Dutzler, R. (2008). X-ray structure of a prokaryotic pentameric

ligand-gated ion channel. Nature *452*: 375–379.

Hille, B. (1992). Ionic Channels of Excitable Membranes. Sinauer, pp 445–471.

Hong, J.S., Cho, J.H., Choi, I.-S., Lee, M.G., and Jang, I.S. (2013). Pregnenolone sulfate modulates glycinergic transmission in rat medullary dorsal horn neurons. Eur. J. Pharmacol. *712*: 30–38.

Horishita, T., Ueno, S., Yanagihara, N., Sudo, Y., Uezono, Y., Okura, D., et al. (2012). Inhibition by pregnenolone sulphate, a metabolite of the neurosteroid pregnenolone, of voltage-gated sodium channels expressed in *Xenopus* oocytes. J Pharmacol Sci *120*: 54–58.

Hörtnagl, H., Tasan, R.O., Wieselthaler, A., Kirchmair, E., Sieghart, W., and Sperk, G. (2013). Patterns of mRNA and protein expression for 12 $GABA_A$ receptor subunits in the mouse brain. Neuroscience *236*: 345–372.

Hosie, A.M., Clarke, L., Silva, H. da, and Smart, T.G. (2009). Conserved site for neurosteroid modulation of $GABA_A$ receptors. Neuropharmacology *56*: 149–154.

Hosie, A.M., Dunne, E.L., Harvey, R.J., and Smart, T.G. (2003). Zinc-mediated inhibition of $GABA_A$ receptors: discrete binding sites underlie subtype specificity. Nat. Neurosci. *6*: 362–369.

Hosie, A.M., Wilkins, M.E., Silva, H.M.A. da, and Smart, T.G. (2006). Endogenous neurosteroids regulate $GABA_A$ receptors through two discrete transmembrane sites. Nature *444*: 486–489.

Hosie, A.M., Wilkins, M.E., and Smart, T.G. (2007). Neurosteroid binding sites on $GABA_A$ receptors. Pharmacol. Ther. *116*: 7–19.

Houston, C.M., He, Q., and Smart, T.G. (2009). CaMKII phosphorylation of the $GABA_A$ receptor: receptor subtype- and synapse-specific modulation. J. Physiol. *587*: 2115–2125.

Houston, C.M., and Smart, T.G. (2006). CaMK-II modulation of $GABA_A$ receptors

expressed in HEK293, NG108-15 and rat cerebellar granule neurons. Eur. J. Neurosci. *24*: 2504–2514.

Huang, X., Chen, H., Michelsen, K., Schneider, S., and Shaffer, P.L. (2015). Crystal structure of human glycine receptor-α3 bound to antagonist strychnine. Nature *526*: 277–280.

Jang, M.K., Mierke, D.F., Russek, S.J., and Farb, D.H. (2004). A steroid modulatory domain on NR2B controls N-methyl-D-aspartate receptor proton sensitivity. Proc. Natl. Acad. Sci. U. S. A. *101*: 8198–8203.

Johnston, G.A. (2013). Advantages of an antagonist: bicuculline and other GABA antagonists. Br. J. Pharmacol. *169*: 328–336.

Kaila, K. (1994). Ionic basis of $GABA_A$ receptor channel function in the nervous system. Prog. Neurobiol. *42*: 489–537.

Kaufman, D.L., Houser, C.R., and Tobin, A.J. (1991). Two forms of the γ-aminobutyric acid synthetic enzyme glutamate decarboxylase have distinct intraneuronal distributions and cofactor interactions. J. Neurochem. *56*: 720–723.

Kimoto, T., Tsurugizawa, T., Ohta, Y., Makino, J., Tamura Ho, Hojo, Y., et al. (2001). Neurosteroid synthesis by cytochrome p450-containing systems localized in the rat brain hippocampal neurons: N-methyl-D-aspartate and calcium-dependent synthesis. Endocrinology *142*: 3578–3589.

Kittler, J.T., Chen, G., Honing, S., Bogdanov, Y., McAinsh, K., Arancibia-Carcamo, I.L., et al. (2005). Phospho-dependent binding of the clathrin AP2 adaptor complex to $GABA_A$ receptors regulates the efficacy of inhibitory synaptic transmission. Proc. Natl. Acad. Sci. U. S. A. *102*: 14871–14876.

Kittler, J.T., and Moss, S.J. (2003). Modulation of $GABA_A$ receptor activity by phosphorylation and receptor trafficking: implications for the efficacy of synaptic inhibition. Curr. Opin. Neurobiol. *13*: 341–347.

Kittler, J.T., Rostaing, P., Schiavo, G., Fritschy, J.M., Olsen, R., Triller, A., et al. (2001). The subcellular distribution of GABARAP and its ability to interact with NSF suggest a role for this protein in the intracellular transport of $GABA_A$ receptors. Mol. Cell. Neurosci. *18*: 13–25.

Klose, C., Straub, I., Riehle, M., Ranta, F., Krautwurst, D., Ullrich, S., et al. (2011). Fenamates as TRP channel blockers: mefenamic acid selectively blocks TRPM3. Br. J. Pharmacol. *162*: 1757–1769.

Kobayashi, T., Washiyama, K., and Ikeda, K. (2009). Pregnenolone sulfate potentiates the inwardly rectifying K^+ channel Kir2.3. PLoS One *4*: 1–8.

Kostakis, E., Jang, M.K., Russek, S.J., Gibbs, T.T., and Farb, D.H. (2011). A steroid modulatory domain in NR2A collaborates with NR1 exon-5 to control NMDAR modulation by pregnenolone sulfate and protons. J. Neurochem. *119*: 486–496.

Kozlov, A.S., Angulo, M.C., Audinat, E., and Charpak, S. (2006). Target cell-specific modulation of neuronal activity by astrocytes. Proc. Natl. Acad. Sci. U. S. A. *103*: 10058–63.

Krasowski, M.D., Nishikawa, K., Nikolaeva, N., Lin, A., and Harrison, N.L. (2001). Methionine 286 in transmembrane domain 3 of the $GABA_A$ receptor β subunit controls a binding cavity for propofol and other alkylphenol general anesthetics. Neuropharmacology *41*: 952–64.

Kreinin, A., Bawakny, N., and Ritsner, M.S. (2014). Adjunctive pregnenolone ameliorates the cognitive deficits in recent-onset schizophrenia. Clin. Schizophr. Relat. Psychoses 1–31.

Krishek, B.J., Moss, S.J., and Smart, T.G. (1996a). A functional comparison of the antagonists bicuculline and picrotoxin at recombinant $GABA_A$ receptors. Neuropharmacology *35*: 1289–1298.

Krishek, B.J., Moss, S.J., and Smart, T.G. (1996b). Homomeric β1 γ-aminobutyric

acid A receptor-ion channels: evaluation of pharmacological and physiological properties. Mol. Pharmacol. *49*: 494–504.

Krivov, G.G., Shapovalov, M. V, and Dunbrack, R.L. (2009). Improved prediction of protein side-chain conformations with SCWRL4. Proteins *77*: 778–795.

Kroeze, W.K., Hufeisen, S.J., Popadak, B.A., Renock, S.M., Steinberg, S., Ernsberger, P., et al. (2003). H1-histamine receptor affinity predicts short-term weight gain for typical and atypical antipsychotic drugs. Neuropsychopharmacology *28*: 519–526.

Kudo, K., Tachikawa, E., and Kashimoto, T. (2002). Inhibition by pregnenolone sulfate of nicotinic acetylcholine response in adrenal chromaffin cells. Eur. J. Pharmacol. *456*: 19–27.

Kullmann, D.M. (2000). Spillover and synaptic cross talk mediated by glutamate and GABA in the mammalian brain. Prog. Brain Res. *125*: 339–351.

Kullmann, D.M., Ruiz, A., Rusakov, D.M., Scott, R., Semyanov, A., and Walker, M.C. (2005). Presynaptic, extrasynaptic and axonal $GABA_A$ receptors in the CNS: where and why? Prog. Biophys. Mol. Biol. *87*: 33–46.

Kumamoto, E., and Murata, Y. (1995). Characterization of GABA current in rat septal cholinergic neurons in culture and its modulation by metal cations. J. Neurophysiol. *74*: 2012–2027.

Kunert-Keil, C., Bisping, F., Krüger, J., Brinkmeier, H., Montell, C., Montell, C., et al. (2006). Tissue-specific expression of TRP channel genes in the mouse and its variation in three different mouse strains. BMC Genomics *7*: 1–14.

Kvist, T., Hansen, K.B., and Bräuner-Osborne, H. (2011). The use of *Xenopus* oocytes in drug screening. Expert Opin. Drug Discov. *6*: 141–153.

Lambert, J.J., Belelli, D., Peden, D.R., Vardy, A.W., and Peters, J.A. (2003). Neurosteroid modulation of $GABA_A$ receptors. Prog. Neurobiol. *71*: 67–80.

Lansman, J.B., Hess, P., and Tsien, R.W. (1986). Blockade of current through single calcium channels by Cd^{2+}, Mg^{2+}, and Ca^{2+}. Voltage and concentration dependence of calcium entry into the pore. J. Gen. Physiol. *88*: 321–347.

Laurie, D.J., Seeburg, P.H., and Wisden, W. (1992a). The distribution of 13 $GABA_A$ receptor subunit mRNAs in the rat brain. II. Olfactory bulb and cerebellum. J. Neurosci. *12*: 1063–1076.

Laurie, D.J., Wisden, W., and Seeburg, P.H. (1992b). The distribution of thirteen $GABA_A$ receptor subunit mRNAs in the rat brain. III. Embryonic and postnatal development. J. Neurosci. *12*: 4151–4172.

Lee, K.H., Cho, J.H., Choi, I.S., Park, H.M., Lee, M.G., Choi, B.J., et al. (2010). Pregnenolone sulfate enhances spontaneous glutamate release by inducing presynaptic Ca^{2+}-induced Ca^{2+} release. Neuroscience *171*: 106–116.

Lee, N., Chen, J., Sun, L., Wu, S., Gray, K.R., Rich, A., et al. (2003). Expression and characterization of human transient receptor potential melastatin 3 (hTRPM3). J. Biol. Chem. *278*: 20890–20897.

Leil, T.A., Chen, Z.W., Chang, C.S.S., and Olsen, R.W. (2004). $GABA_A$ receptor-associated protein traffics $GABA_A$ receptors to the plasma membrane in neurons. J. Neurosci. Off. J. Soc. Neurosci. *24*: 11429–11438.

Lerma, J., Herranz, A.S., Herreras, O., Abraira, V., and Martín del Río, R. (1986). In vivo determination of extracellular concentration of amino acids in the rat hippocampus. A method based on brain dialysis and computerized analysis. Brain Res. *384*: 145–155.

Li, G.D., Chiara, D.C., Sawyer, G.W., Husain, S.S., Olsen, R.W., and Cohen, J.B. (2006). Identification of a $GABA_A$ Receptor Anesthetic Binding Site at Subunit Interfaces by Photolabeling with an Etomidate Analog. J. Neurosci. *26*: 11599–11605.

Li, W., Jin, X., Covey, D.F., and Steinbach, J.H. (2007). Neuroactive steroids and

human recombinant ρ1 $GABA_C$ receptors. J. Pharmacol. Exp. Ther. *323*: 236–247.

Liere, P., Pianos, A., Eychenne, B., Cambourg, A., Liu, S., Griffiths, W., et al. (2004). Novel lipoidal derivatives of pregnenolone and dehydroepiandrosterone and absence of their sulfated counterparts in rodent brain. J. Lipid Res. *45*: 2287–2302.

Liu, Q.Y., Schaffner, A.E., Chang, Y.H., Maric, D., and Barker, J.L. (2000). Persistent activation of $GABA_A$ receptor/Cl^- channels by astrocyte-derived GABA in cultured embryonic rat hippocampal neurons. J. Neurophysiol. *84*: 1392–1403.

Liu, Y., Liu, D., Printzenhoff, D., Coghlan, M.J., Harris, R., and Krafte, D.S. (2002). Tenidap, a novel anti-inflammatory agent, is an opener of the inwardly rectifying K^+ channel hKir2.3. Eur. J. Pharmacol. *435*: 153–160.

Löw, K., Crestani, F., Keist, R., Benke, D., Brünig, I., Benson, J.A., et al. (2000). Molecular and neuronal substrate for the selective attenuation of anxiety. Science *290*: 131–134.

Luscher, B., Fuchs, T., and Kilpatrick, C.L. (2011). $GABA_A$ receptor trafficking-mediated plasticity of inhibitory synapses. Neuron *70*: 385–409.

Majewska, M.D., Dermirgoren, S., and London, E.D. (1990). Binding of pregnenolone sulfate to rat brain membranes suggests multiple sites of steroid action at the $GABA_A$ receptor. Eur. J. Pharmacol. Mol. Pharmacol. *189*: 307–315.

Majewska, M.D., Harrison, N.L., Schwartz, R.D., Barker, J.L., and Paul, S.M. (1986). Steroid hormone metabolites are barbiturate-like modulators of the GABA receptor. Science *232*: 1004–1007.

Majewska, M.D., Mienville, J.M., and Vicini, S. (1988). Neurosteroid pregnenolone sulfate antagonizes electrophysiological responses to GABA in neurons. Neurosci. Lett. *90*: 279–284.

Majewska, M.D., and Schwartz, R.D. (1987). Pregnenolone-sulfate: an endogenous antagonist of the γ-aminobutyric acid receptor complex in brain? Brain Res *404*: 355–360.

Maksay, G., Laube, B., and Betz, H. (2001). Subunit-specific modulation of glycine receptors by neurosteroids. Neuropharmacology *41*: 369–376.

Malayev, A., Gibbs, T.T., and Farb, D.H. (2002). Inhibition of the NMDA response by pregnenolone sulphate reveals subtype selective modulation of NMDA receptors by sulphated steroids. Br. J. Pharmacol. *135*: 901–909.

Mameli, M. (2005). Neurosteroid-induced plasticity of immature synapses via retrograde modulation of presynaptic NMDA receptors. J. Neurosci. *25*: 2285–2294.

Mameli, M., and Valenzuela, C.F. (2006). Alcohol increases efficacy of immature synapses in a neurosteroid-dependent manner. Eur. J. Neurosci. *23*: 835–839.

Marx, C.E., Lee, J., Subramaniam, M., Rapisarda, A., Bautista, D.C.T., Chan, E., et al. (2014). Proof-of-concept randomized controlled trial of pregnenolone in schizophrenia. Psychopharmacology (Berl). *231*: 3647–3662.

Matsumoto, R.R., Bowen, W.D., Tom, M.A., Vo, V.N., Truong, D.D., and Costa, B.R. De (1995). Characterization of two novel σ receptor ligands: antidystonic effects in rats suggest σ receptor antagonism. Eur. J. Pharmacol. *280*: 301–310.

Mayo, W., Dellu, F., Robel, P., Cherkaoui, J., Moal, M. Le, Baulieu, E.E., et al. (1993). Infusion of neurosteroids into the nucleus basalis magnocellularis affects cognitive processes in the rat. Brain Res. *607*: 324–328.

McCracken, K.A., Bowen, W.D., and Matsumoto, R.R. (1999). Novel σ receptor ligands attenuate the locomotor stimulatory effects of cocaine. Eur. J. Pharmacol. *365*: 35–38.

McDonald, B.J., Amato, A., Connolly, C.N., Benke, D., Moss, S.J., and Smart,

T.G. (1998). Adjacent phosphorylation sites on GABAA receptor β subunits determine regulation by cAMP-dependent protein kinase. Nat. Neurosci. *1*: 23–28.

McKernan, R., and Whiting, P. (1996). Which GABAA-receptor subtypes really occur in the brain? Trends Neurosci. *19*: 139–143.

McKernan, R.M., Rosahl, T.W., Reynolds, D.S., Sur, C., Wafford, K.A., Atack, J.R., et al. (2000). Sedative but not anxiolytic properties of benzodiazepines are mediated by the GABA(A) receptor α1 subtype. Nat. Neurosci. *3*: 587–592.

Melchior, C.L., and Ritzmann, R.F. (1994). Pregnenolone and pregnenolone sulfate, alone and with ethanol, in mice on the plus-maze. Pharmacol. Biochem. Behav. *48*: 893–897.

Mellon, S.H., and Griffin, L.D. (2002). Neurosteroids: biochemistry and clinical significance. Trends Endocrinol. Metab. *13*: 35–43.

Mennerick, S., Lamberta, M., Shu, H.-J., Hogins, J., Wang, C., Covey, D.F., et al. (2008). Effects on membrane capacitance of steroids with antagonist properties at $GABA_A$ receptors. Biophys. J. *95*: 176–185.

Menuz, K., Stroud, R.M., Nicoll, R.A., and Hays, F.A. (2007). TARP auxiliary subunits switch AMPA receptor antagonists into partial agonists. Science *318*: 815–7.

Mihic, S.J., Ye, Q., Wick, M.J., Koltchine, V. V., Krasowski, M.D., Finn, S.E., et al. (1997). Sites of alcohol and volatile anaesthetic action on $GABA_A$ and glycine receptors. Nature *389*: 385–389.

Miller, P.S., and Aricescu, A.R. (2015). Crystal structure of a human $GABA_A$ receptor. Nature *512*: 270–275.

Miyazawa, A., Fujiyoshi, Y., and Unwin, N. (2003). Structure and gating mechanism of the acetylcholine receptor pore. Nature *423*: 949–55.

Mody, I., Koninck, Y. De, Otis, T.S., and Soltesz, I. (1994). Bridging the cleft at GABA synapses in the brain. Trends Neurosci. *17*: 517–25.

Morales-Perez, C.L., Noviello, C.M., and Hibbs, R.E. (2016). X-ray structure of the human α4β2 nicotinic receptor. Nature *538*: 411–415.

Morris, K.D., Moorefield, C.N., and Amin, J. (1999). Differential modulation of the γ-aminobutyric acid type C receptor by neuroactive steroids. Mol. Pharmacol. *56*: 752–7529.

Mortensen, M., Ebert, B., Wafford, K., and Smart, T.G. (2010). Distinct activities of GABA agonists at synaptic- and extrasynaptic-type $GABA_A$ receptors. J. Physiol. *588*: 1251–1268.

Mortensen, M., Kristiansen, U., Ebert, B., Frølund, B., Krogsgaard-Larsen, P., and Smart, T.G. (2004). Activation of single heteromeric $GABA_A$ receptor ion channels by full and partial agonists. J. Physiol. *557*: 389–413.

Mortensen, M., Patel, B., and Smart, T.G. (2012). GABA potency at $GABA_A$ receptors found in synaptic and extrasynaptic zones. Front. Cell. Neurosci. *6*: 1–10.

Mortensen, M., and Smart, T.G. (2006). Extrasynaptic αβ subunit $GABA_A$ receptors on rat hippocampal pyramidal neurons. J. Physiol. *577*: 841–856.

Moss, S.J., and Smart, T.G. (1996). Modulation of amino acid-gated ion channels by protein phosphorylation. Int. Rev. Neurobiol. *39*: 1–52.

Mtchedlishvili, Z., and Kapur, J. (2003). A presynaptic action of the neurosteroid pregnenolone sulfate on GABAergic synaptic transmission. Mol. Pharmacol. *64*: 857–864.

Mukherjee, J., Kretschmannova, K., Gouzer, G., Maric, H.M., Ramsden, S., Tretter, V., et al. (2011). The residence time of $GABA_A$Rs at inhibitory synapses is determined by direct binding of the receptor α1 subunit to gephyrin. J. Neurosci.

31: 14677–14687.

Najac, M., and Raman, I.M. (2015). Integration of Purkinje cell inhibition by cerebellar nucleo-olivary neurons. J. Neurosci. *35*: 544–549.

Neelands, T.R., and Macdonald, R.L. (1999). Incorporation of the π subunit into functional gamma-aminobutyric Acid A receptors. Mol. Pharmacol. *56*: 598–610.

Newland, C.F., and Cull-Candy, S.G. (1992). On the mechanism of action of picrotoxin on GABA receptor channels in dissociated sympathetic neurones of the rat. J. Physiol. *447*: 191–213.

Nilsson, K.R., Zorumski, C.F., and Covey, D.F. (1998). Neurosteroid analogues. 6. The synthesis and $GABA_A$ receptor pharmacology of enantiomers of dehydroepiandrosterone sulfate, pregnenolone sulfate, and (3α,5β)-3-hydroxypregnan-20-one sulfate. J. Med. Chem. *41*: 2604–2613.

Nury, H., Renterghem, C. Van, Weng, Y., Tran, A., Baaden, M., Dufresne, V., et al. (2011). X-ray structures of general anaesthetics bound to a pentameric ligand-gated ion channel. Nature *469*: 428–431.

Nusser, Z., Ahmad, Z., Tretter, V., Fuchs, K., Wisden, W., Sieghart, W., et al. (1999). Alterations in the expression of $GABA_A$ receptor subunits in cerebellar granule cells after the disruption of the α6 subunit gene. Eur. J. Neurosci. *11*: 1685–1697.

Nusser, Z., Cull-Candy, S., and Farrant, M. (1997). Differences in synaptic $GABA_A$ receptor number underlie variation in GABA mini amplitude. Neuron *19*: 697–709.

Nusser, Z., Roberts, J.D., Baude, A., Richards, J.G., and Somogyi, P. (1995). Relative densities of synaptic and extrasynaptic $GABA_A$ receptors on cerebellar granule cells as determined by a quantitative immunogold method. J. Neurosci. *15*: 2948–2960.

Nusser, Z., Sieghart, W., Benke, D., Fritschy, J.M., and Somogyi, P. (1996). Differential synaptic localization of two major γ-aminobutyric acid type A receptor α subunits on hippocampal pyramidal cells. Proc. Natl. Acad. Sci. U. S. A. *93*: 11939–11944.

Nusser, Z., Sieghart, W., and Somogyi, P. (1998). Segregation of different $GABA_A$ receptors to synaptic and extrasynaptic membranes of cerebellar granule cells. J. Neurosci. *18*: 1693–1703.

Okada, M., Onodera, K., Renterghem, C. Van, Sieghart, W., and Takahashi, T. (2000). Functional correlation of $GABA_A$ receptor α subunits expression with the properties of IPSCs in the developing thalamus. J. Neurosci. *20*: 2202–2208.

Olsen, R.W. (2015). Allosteric ligands and their binding sites define γ-aminobutyric acid (GABA) type A receptor subtypes. Adv. Pharmacol. *73*: 167–202.

Olsen, R.W., and Sieghart, W. (2008). International Union of Pharmacology. LXX. Subtypes of γ-aminobutyric acidA receptors: Classification on the basis of subunit composition, pharmacology, and function. Update. Pharmacol. Rev. *60*: 243–260.

Olsen, R.W., and Tobin, A.J. (1990). Molecular biology of $GABA_A$ receptors. FASEB J. *4*: 1469–1480.

Osuji, I.J., Vera-Bolaños, E., Carmody, T.J., and Brown, E.S. (2010). Pregnenolone for cognition and mood in dual diagnosis patients. Psychiatry Res. *178*: 309–312.

Pan, J., Chen, Q., Willenbring, D., Yoshida, K., Tillman, T., Kashlan, O.B., et al. (2012). Structure of the pentameric ligand-gated ion channel ELIC cocrystallized with its competitive antagonist acetylcholine. Nat. Commun. *3*: 714.

Panzanelli, P., Gunn, B.G., Schlatter, M.C., Benke, D., Tyagarajan, S.K., Scheiffele, P., et al. (2011). Distinct mechanisms regulate $GABA_A$ receptor and

gephyrin clustering at perisomatic and axo-axonic synapses on CA1 pyramidal cells. J. Physiol. *589*: 4959–4980.

Park-Chung, M., Malayev, A., Purdy, R.H., Gibbs, T.T., and Farb, D.H. (1999). Sulfated and unsulfated steroids modulate γ-aminobutyric acid A receptor function through distinct sites. Brain Res *830*: 72−87.

Patel, B., Mortensen, M., and Smart, T.G. (2014). Stoichiometry of δ subunit containing $GABA_A$ receptors. Br. J. Pharmacol. *171*: 985–994.

Pavlov, I., Savtchenko, L.P., Song, I., Koo, J., Pimashkin, A., Rusakov, D.A., et al. (2014). Tonic $GABA_A$ conductance bidirectionally controls interneuron firing pattern and synchronization in the CA3 hippocampal network. Proc. Natl. Acad. Sci. U. S. A. *111*: 504–509.

Petrovic, M., Sedlacek, M., Cais, O., Horak, M., Chodounska, H., and Vyklicky, L. (2009). Pregnenolone sulfate modulation of *N*-methyl-*D*-aspartate receptors is phosphorylation dependent. Neuroscience *160*: 616–628.

Pirker, S., Schwarzer, C., Wieselthaler, A., Sieghart, W., and Sperk, G. (2000). $GABA_A$ receptors: immunocytochemical distribution of 13 subunits in the adult rat brain. Neuroscience *101*: 815–850.

Pistis, M., Belelli, D., Peters, J.A., and Lambert, J.J. (1997). The interaction of general anaesthetics with recombinant $GABA_A$ and glycine receptors expressed in *Xenopus* laevis oocytes: a comparative study. Br. J. Pharmacol. *122*: 1707–1719.

Pollard, S., Thompson, C.L., and Stephenson, F.A. (1995). Quantitative characterization of α6 and α1α6 subunit-containing native γ-aminobutyric acid A receptors of adult rat cerebellum demonstrates two α subunits per receptor oligomer. J. Biol. Chem. *270*: 21285–21290.

Pritchett, D.B., Sontheimer, H., Shivers, B.D., Ymer, S., Kettenmann, H., Schofield, P.R., et al. (1989). Importance of a novel $GABA_A$ receptor subunit for

benzodiazepine pharmacology. Nature *338*: 582–585.

Prüss, H., Derst, C., Lommel, R., and Veh, R.W. (2005). Differential distribution of individual subunits of strongly inwardly rectifying potassium channels (Kir2 family) in rat brain. Brain Res. Mol. Brain Res. *139*: 63–79.

Quiram, P.A., and Sine, S.M. (1998). Identification of residues in the neuronal α7 acetylcholine receptor that confer selectivity for conotoxin ImI. J. Biol. Chem. *273*: 11001–11006.

Rahman, M., Lindblad, C., Johansson, I.M., Bäckström, T., and Wang, M.D. (2006). Neurosteroid modulation of recombinant rat α5β2γ2L and α1β2γ2L $GABA_A$ receptors in *Xenopus* oocyte. Eur. J. Pharmacol. *547*: 37–44.

Ramadan, E., Fu, Z., Losi, G., Homanics, G.E., Neale, J.H., and Vicini, S. (2003). $GABA_A$ receptor β3 subunit deletion decreases α2/3 subunits and IPSC duration. J. Neurophysiol. *89*: 128–134.

Ramerstorfer, J., Furtmüller, R., Sarto-Jackson, I., Varagic, Z., Sieghart, W., and Ernst, M. (2011). The $GABA_A$ receptor $\alpha^+\beta^-$ interface: a novel target for subtype selective drugs. J. Neurosci. *31*: 870–877.

Reddy, D.S. (2003). Pharmacology of endogenous neuroactive steroids. Crit. Rev. Neurobiol. *15*: 197–234.

Reddy, D.S., and Estes, W.A. (2016). Clinical potential of neurosteroids for CNS disorders. Trends Pharmacol. Sci. *37*: 543–561.

Reddy, D.S., Kaur, G., and Kulkarni, S.K. (1998). σ (σ1) receptor mediated anti-depressant-like effects of neurosteroids in the Porsolt forced swim test. Neuroreport *9*: 3069–3073.

Reddy, D.S., and Kulkarni, S.K. (1997). Differential anxiolytic effects of neurosteroids in the mirrored chamber behavior test in mice. Brain Res. *752*: 61–71.

Reddy, D.S., and Kulkarni, S.K. (1998). Proconvulsant effects of neurosteroids pregnenolone sulfate and dehydroepiandrosterone sulfate in mice. Eur. J. Pharmacol. *345*: 55–59.

Richerson, G.B., and Wu, Y. (2003). Dynamic equilibrium of neurotransmitter transporters: not just for reuptake anymore. J. Neurophysiol. *90*: 1363–1374.

Rijnsoever, C. van, Täuber, M., Choulli, M.K., Keist, R., Rudolph, U., Mohler, H., et al. (2004). Requirement of α5-$GABA_A$ receptors for the development of tolerance to the sedative action of diazepam in mice. J. Neurosci. *24*: 6785–6790.

Ritsner, M.S., Bawakny, H., and Kreinin, A. (2014). Pregnenolone treatment reduces severity of negative symptoms in recent-onset schizophrenia: an 8-week, double-blind, randomized add-on two-center trial. Psychiatry Clin. Neurosci. *68*: 432–440.

Rudolph, U., Crestani, F., Benke, D., Brünig, I., Benson, J.A., Fritschy, J.M., et al. (1999). Benzodiazepine actions mediated by specific γ-aminobutyric acid A receptor subtypes. Nature *401*: 796–800.

Rudolph, U., and Knoflach, F. (2011). Beyond classical benzodiazepines: novel therapeutic potential of $GABA_A$ receptor subtypes. Nat. Rev. Drug Discov. *10*: 685–697.

Rustichelli, C., Pinetti, D., Lucchi, C., Ravazzini, F., and Puia, G. (2013). Simultaneous determination of pregnenolone sulphate, dehydroepiandrosterone and allopregnanolone in rat brain areas by liquid chromatography-electrospray tandem mass spectrometry. J. Chromatogr. B Anal. Technol. Biomed. Life Sci. *930*: 62–69.

Sali, A., and Blundell, T.L. (1993). Comparative protein modelling by satisfaction of spatial restraints. J. Mol. Biol. *234*: 779–815.

Sauguet, L., Shahsavar, A., Poitevin, F., Huon, C., Menny, A., Nemecz, À., et al. (2014). Crystal structures of a pentameric ligand-gated ion channel provide a

mechanism for activation. Proc. Natl. Acad. Sci. U. S. A. *111*: 966–971.

Saxena, N.C., and Macdonald, R.L. (1994). Assembly of $GABA_A$ receptor subunits: role of the δ subunit. J. Neurosci. *14*: 7077–7086.

Schumacher, M., Akwa, Y., Guennoun, R., Robert, F., Labombarda, F., Desarnaud, F., et al. (2000). Steroid synthesis and metabolism in the nervous system: trophic and protective effects. J. Neurocytol. *29*: 307–326.

Schumacher, M., Liere, P., Akwa, Y., Rajkowski, K., Griffiths, W., Bodin, K., et al. (2008). Pregnenolone sulfate in the brain: A controversial neurosteroid. Neurochem. Int. *52*: 522–540.

Scimemi, A., Semyanov, A., Sperk, G., Kullmann, D.M., and Walker, M.C. (2005). Multiple and plastic receptors mediate tonic $GABA_A$ receptor currents in the hippocampus. J. Neurosci. *25*: 10016–24.

Seljeset, S., Laverty, D., and Smart, T.G. (2015). Inhibitory neurosteroids and the $GABA_A$ receptor. Adv. Pharmacol. *72*: 165–187.

Shen, W., Mennerick, S., Covey, D.F., and Zorumski, C.F. (2000). Pregnenolone sulfate modulates inhibitory synaptic transmission by enhancing $GABA_A$ receptor desensitization. J. Neurosci. *20*: 3571–3579.

Shimada, M., Yoshinari, K., Tanabe, E., Shimakawa, E., Kobashi, M., Nagata, K., et al. (2001). Identification of ST2A1 as a rat brain neurosteroid sulfotransferase mRNA. Brain Res. *920*: 222–225.

Sieghart, W. (2015). Allosteric modulation of $GABA_A$ receptors via multiple drug-binding sites. Adv. Pharmacol. *72*: 53–96.

Sieghart, W., and Sperk, G. (2002). Subunit composition, distribution and function of $GABA_A$ receptor subtypes. Curr. Top. Med. Chem. *2*: 795–816.

Sigel, E. (2002). Mapping of the benzodiazepine recognition site on $GABA_A$ receptors. Curr. Top. Med. Chem. *2*: 833–839.

Sigel, E., Baur, R., Kellenberger, S., and Malherbe, P. (1992). Point mutations affecting antagonist affinity and agonist dependent gating of $GABA_A$ receptor channels. EMBO J. *11*: 2017–2023.

Sigel, E., Baur, R., Rácz, I., Marazzi, J., Smart, T.G., Zimmer, A., et al. (2011). The major central endocannabinoid directly acts at $GABA_A$ receptors. Proc. Natl. Acad. Sci. U. S. A. *108*: 18150–18155.

Sigel, E., and Buhr, A. (1997). The benzodiazepine binding site of $GABA_A$ receptors. Trends Pharmacol. Sci. *18*: 425–429.

Simon, J., Wakimoto, H., Fujita, N., Lalande, M., and Barnard, E.A. (2004). Analysis of the set of $GABA_A$ receptor genes in the human genome. J. Biol. Chem. *279*: 41422–41435.

Sliwinski, A., Monnet, F.P., Schumacher, M., and Morin-Surun, M.P. (2004). Pregnenolone sulfate enhances long-term potentiation in CA1 in rat hippocampus slices through the modulation of *N*-methyl-*D*-aspartate receptors. J. Neurosci. Res. *78*: 691–701.

Smart, T.G. (2015). $GABA_A$ receptors. In Handbook of Ion Channels, J. Zheng, and M.C. Trudeau, eds. CRC Press, pp 345–354.

Smart, T.G., and Paoletti, P. (2012). Synaptic neurotransmitter-gated receptors. Cold Spring Harb. Perspect. Biol. *4*: a009662.

Smart, T.G., Xie, X., and Krishek, B.J. (1994). Modulation of inhibitory and excitatory amino acid receptor ion channels by zinc. Prog. Neurobiol. *42*: 393–441.

Smith, C.C., Gibbs, T.T., and Farb, D.H. (2014). Pregnenolone sulfate as a modulator of synaptic plasticity. Psychopharmacology (Berl). *231*: 3537–3556.

Smith, G.B., and Olsen, R.W. (1994). Identification of a [^{3}H]muscimol photoaffinity substrate in the bovine γ-aminobutyric acid A receptor α subunit. J. Biol. Chem.

269: 20380–20387.

Smith, G.B., and Olsen, R.W. (1995). Functional domains of $GABA_A$ receptors. Trends Pharmacol. Sci. *16*: 162–168.

Søgaard, R., Werge, T.M., Bertelsen, C., Lundbye, C., Madsen, K.L., Nielsen, C.H., et al. (2006). $GABA_A$ receptor function is regulated by lipid bilayer elasticity. Biochemistry *45*: 13118–13129.

Sooksawate, T., and Simmonds, M. (2001). Influence of membrane cholesterol on modulation of the $GABA_A$ receptor by neuroactive steroids and other potentiators. Br. J. Pharmacol. *134*: 1303–1311.

Steckelbroeck, S., Nassen, A., Ugele, B., Ludwig, M., Watzka, M., Reissinger, A., et al. (2004). Steroid sulfatase (STS) expression in the human temporal lobe: enzyme activity, mRNA expression and immunohistochemistry study. J. Neurochem. *89*: 403–417.

Stoffel-Wagner, B. (2003). Neurosteroid biosynthesis in the human brain and its clinical implications. Ann. N. Y. Acad. Sci. *1007*: 64–78.

Straub, I., Mohr, F., Stab, J., Konrad, M., Philipp, S.E., Oberwinkler, J., et al. (2013). Citrus fruit and fabacea secondary metabolites potently and selectively block TRPM3. Br. J. Pharmacol. *168*: 1835–1850.

Strous, R.D., Maayan, R., and Weizman, A. (2006). The relevance of neurosteroids to clinical psychiatry: from the laboratory to the bedside. Eur. Neuropsychopharmacol. *16*: 155–169.

Tam, S.W., and Cook, L. (1984). σ opiates and certain antipsychotic drugs mutually inhibit $(^+)$-[^{3}H] SKF 10,047 and [^{3}H]haloperidol binding in guinea pig brain membranes. Proc. Natl. Acad. Sci. U. S. A. *81*: 5618–5621.

Tan, K.R., Brown, M., Labouèbe, G., Yvon, C., Creton, C., Fritschy, J.M., et al. (2010). Neural bases for addictive properties of benzodiazepines. Nature *463*:

769–774.

Tanemoto, M., Fujita, A., Higashi, K., and Kurachi, Y. (2002). PSD-95 mediates formation of a functional homomeric Kir5.1 channel in the brain. Neuron *34*: 387–397.

Teschemacher, A., Kasparov, S., Kravitz, E.A., and Rahamimoff, R. (1997). Presynaptic action of the neurosteroid pregnenolone sulfate on inhibitory transmitter release in cultured hippocampal neurons. Brain Res. *772*: 226–232.

Thomas, P., Mortensen, M., Hosie, A.M., and Smart, T.G. (2005). Dynamic mobility of functional $GABA_A$ receptors at inhibitory synapses. Nat. Neurosci. *8*: 889–897.

Thomas, P., and Smart, T.G. (2005). HEK293 cell line: A vehicle for the expression of recombinant proteins. J. Pharmacol. Toxicol. Methods *51*: 187–200.

Thompson, A.J., and Lummis, S.C.R. (2006). $5\text{-}HT_3$ Receptors. Curr. Pharm. Des. *12*: 3615–3630.

Tossman, U., Jonsson, G., and Ungerstedt, U. (1986). Regional distribution and extracellular levels of amino acids in rat central nervous system. Acta Physiol. Scand. *127*: 533–545.

Tretter, V., Ehya, N., Fuchs, K., and Werner, S. (1997). Stoichiometry and assembly of a recombinant $GABA_A$ receptor subtype. J. Neurosci. *17*: 2728–2737.

Twede, V., Tartaglia, A.L., Covey, D.F., and Bamber, B.A. (2007). The neurosteroids dehydroepiandrosterone sulfate and pregnenolone sulfate inhibit the UNC-49 GABA receptor through a common set of residues. Mol. Pharmacol. *72*: 1322–1329.

Twelvetrees, A.E., Yuen, E.Y., Arancibia-Carcamo, I.L., MacAskill, A.F.,

Rostaing, P., Lumb, M.J., et al. (2010). Delivery of $GABA_A$Rs to synapses is mediated by HAP1-KIF5 and disrupted by mutant huntingtin. Neuron *65*: 53–65.

Tyagarajan, S.K., and Fritschy, J.M. (2014). Gephyrin: a master regulator of neuronal function? Nat. Rev. Neurosci. *15*: 141–156.

Ueno, S., Bracamontes, J., Zorumski, C., Weiss, D.S., and Steinbach, J.H. (1997). Bicuculline and gabazine are allosteric inhibitors of channel opening of the $GABA_A$ receptor. J. Neurosci. *17*: 625–634.

Ueno, S., Lin, A., Nikolaeva, N., Trudell, J.R., Mihic, S.J., Harris, R.A., et al. (2000). Tryptophan scanning mutagenesis in TM2 of the $GABA_A$ receptor α subunit: effects on channel gating and regulation by ethanol. Br J Pharmacol *131*: 296–302.

Ueno, S., Zorumski, C., Bracamontes, J., and Steinbach, J.H. (1996). Endogenous subunits can cause ambiguities in the pharmacology of exogenous γ-aminobutyric acid A receptors expressed in human embryonic kidney 293 cells. Mol. Pharmacol. *50*: 931–938.

Ulens, C., Spurny, R., Thompson, A.J., Alqazzaz, M., Debaveye, S., Han, L., et al. (2014). The Prokaryote Ligand-Gated Ion Channel ELIC Captured in a Pore Blocker-Bound Conformation by the Alzheimer's Disease Drug Memantine. Structure *22*: 1399–1407.

Unwin, N. (2005). Refined structure of the nicotinic acetylcholine receptor at 4Å resolution. J. Mol. Biol. *346*: 967–989.

Uzunov, D.P., Cooper, T.B., Costa, E., and Guidotti, A. (1996). Fluoxetine-elicited changes in brain neurosteroid content measured by negative ion mass fragmentography. Proc. Natl. Acad. Sci. U. S. A. *93*: 12599–12604.

Vallée, M., Mayo, W., Darnaudéry, M., Corpéchot, C., Young, J., Koehl, M., et al. (1997). Neurosteroids: Deficient cognitive performance in aged rats depends on low pregnenolone sulfate levels in the hippocampus. Neurobiology *94*: 14865–

14870.

Vallée, M., Mayo, W., and Moal, M. Le (2001a). Role of pregnenolone, dehydroepiandrosterone and their sulfate esters on learning and memory in cognitive aging. Brain Res. Rev. *37*: 301–312.

Vallée, M., Shen, W., Heinrichs, S.C., Zorumski, C.F., Covey, D.F., Koob, G.F., et al. (2001b). Steroid structure and pharmacological properties determine the anti-amnesic effects of pregnenolone sulphate in the passive avoidance task in rats. Eur. J. Neurosci. *14*: 2003–2010.

Vaňková, M., Hill, M., Velíková, M., Včelák, J., Vacínová, G., Lukášová, P., et al. (2015). Reduced sulfotransferase SULT2A1 activity in patients with Alzheimer's disease. Physiol. Res. *64 Suppl 2*: S265-273.

Vithlani, M., Terunuma, M., and Moss, S.J. (2011). The dynamic modulation of $GABA_A$ receptor trafficking and its role in regulating the plasticity of inhibitory synapses. Physiol. Rev. *91*: 1009–1022.

Vriens, J., Owsianik, G., Hofmann, T., Philipp, S.E., Stab, J., Chen, X., et al. (2011). TRPM3 is a nociceptor channel involved in the detection of noxious heat. Neuron *70*: 482–494.

Wagner, T.F.J., Loch, S., Lambert, S., Straub, I., Mannebach, S., Mathar, I., et al. (2008). Transient receptor potential M3 channels are ionotropic steroid receptors in pancreatic β cells. Nat. Cell Biol. *10*: 1421–1430.

Wagoner, K.R., and Czajkowski, C. (2010). Stoichiometry of expressed α4β2δ γ-aminobutyric acid type A receptors depends on the ratio of subunit cDNA transfected. J. Biol. Chem. *285*: 14187–14194.

Walker, J.M., Bowen, W.D., Walker, F.O., Matsumoto, R.R., Costa, B. De, and Rice, K.C. (1990). Sigma receptors: biology and function. Pharmacol. Rev. *42*: 355–402.

Wang, H.R., Wu, M., Yu, H., Long, S., Stevens, A., Engers, D.W., et al. (2011). Selective inhibition of the Kir2 family of inward rectifier potassium channels by a small molecule probe: the discovery, SAR, and pharmacological characterization of ML133. ACS Chem. Biol. *6*: 845–856.

Wang, M. (2011). Neurosteroids and $GABA_A$ receptor function. Front. Endocrinol. (Lausanne). *2*: 1–23.

Wang, M. De, Rahman, M., Zhu, D., Johansson, I.M., and Bäckström, T. (2007). 3β-hydroxysteroids and pregnenolone sulfate inhibit recombinant rat $GABA_A$ receptor through different channel property. Eur. J. Pharmacol. *557*: 124–131.

Wang, M., He, Y., Eisenman, L.N., Fields, C., Zeng, C.-M., Mathews, J., et al. (2002). 3β-Hydroxypregnane steroids are pregnenolone sulfate-like $GABA_A$ receptor antagonists. J. Neurosci. *22*: 3366–3375.

Wang, M.D., Rahman, M., Zhu, D., and Bäckström, T. (2006). Pregnenolone sulphate and Zn^{2+} inhibit recombinant rat $GABA_A$ receptor through different channel property. Acta Physiol. *188*: 153–162.

Wang, M.D., Wahlström, G., and Bäckström, T. (1997). The regional brain distribution of the neurosteroids pregnenolone and pregnenolone sulfate following intravenous infusion. J. Steroid Biochem. Mol. Biol. *62*: 299–306.

Wang, Q., Liu, L., Pei, L., Ju, W., Ahmadian, G., Lu, J., et al. (2003). Control of synaptic strength, a novel function of Akt. Neuron *38*: 915–928.

Wang, T.L., Hackam, A.S., Guggino, W.B., and Cutting, G.R. (1995). A single amino acid in γ-aminobutyric acid ρ1 receptors affects competitive and noncompetitive components of picrotoxin inhibition. Proc. Natl. Acad. Sci. U. S. A. *92*: 11751–11755.

Wardell, B., Marik, P.S., Piper, D., Rutar, T., Jorgensen, E.M., and Bamber, B.A. (2006). Residues in the first transmembrane domain of the *Caenorhabditis elegans* $GABA_A$ receptor confer sensitivity to the neurosteroid pregnenolone

sulfate. Br. J. Pharmacol. *148*: 162–172.

Wei, W., Zhang, N., Peng, Z., Houser, C.R., and Mody, I. (2003). Perisynaptic localization of δ subunit-containing $GABA_A$ receptors and their activation by GABA spillover in the mouse dentate gyrus. J. Neurosci. *23*: 10650–10661.

Weill-Engerer, S., David, J.P., Sazdovitch, V., Liere, P., Eychenne, B., Pianos, A., et al. (2002). Neurosteroid quantification in human brain regions: comparison between Alzheimer's and nondemented patients. J. Clin. Endocrinol. Metab. *87*: 5138–5143.

Weir, C.J., Ling, A.T.Y., Belelli, D., Wildsmith, J.A.W., Peters, J.A., and Lambert, J.J. (2004). The interaction of anaesthetic steroids with recombinant glycine and $GABA_A$ receptors. Br. J. Anaesth. *92*: 704–711.

Whiting, P., McKernan, R.M., and Iversen, L.L. (1990). Another mechanism for creating diversity in γ-aminobutyrate type A receptors: RNA splicing directs expression of two forms of γ2 phosphorylation site. Proc. Natl. Acad. Sci. U. S. A. *87*: 9966–9970.

Wieland, H.A., Lüddens, H., and Seeburg, P.H. (1992). A single histidine in $GABA_A$ receptors is essential for benzodiazepine agonist binding. J. Biol. Chem. *267*: 1426–1429.

Wilkins, M.E., Hosie, A.M., and Smart, T.G. (2002). Identification of a β subunit TM2 residue mediating proton modulation of GABA type A receptors. J. Neurosci. *22*: 5328–5333.

Wilkins, M.E., Hosie, A.M., and Smart, T.G. (2005). Proton modulation of recombinant $GABA_A$ receptors: influence of GABA concentration and the β subunit TM2-TM3 domain. J. Physiol. *567*: 365–377.

Wisden, W., Laurie, D.J., Monyer, H., and Seeburg, P.H. (1992). The distribution of 13 $GABA_A$ receptor subunit mRNAs in the rat brain. I. Telencephalon, diencephalon, mesencephalon. J. Neurosci. *12*: 1040–1062.

Wlodarczyk, A.I., Sylantyev, S., Herd, M.B., Kersanté, F., Lambert, J.J., Rusakov, D.A., et al. (2013). GABA-independent $GABA_A$ receptor openings maintain tonic currents. J. Neurosci. *33*: 3905–3914.

Wohlfarth, K.M., Bianchi, M.T., and Macdonald, R.L. (2002). Enhanced neurosteroid potentiation of ternary $GABA_A$ receptors containing the σ subunit. J. Neurosci. *22*: 1541–1549.

Wong, P., Sze, Y., Chang, C.C.R., Lee, J., and Zhang, X. (2015). Pregnenolone sulfate normalizes schizophrenia-like behaviors in dopamine transporter knockout mice through the AKT/GSK3β pathway. Transl. Psychiatry *5*: e528.

Wood, C.E., Gridley, K.E., and Keller-Wood, M. (2003). Biological activity of 17β-estradiol-3-sulfate in ovine fetal plasma and uptake in fetal brain. Endocrinology *144*: 599–604.

Woodward, R.M., Polenzani, L., and Miledi, R. (1992). Effects of hexachlorocyclohexanes on γ-aminobutyric acid receptors expressed in *Xenopus* oocytes by RNA from mammalian brain and retina. Mol.Pharmacol. *41*: 1107–1115.

Wooltorton, J.R., Moss, S.J., and Smart, T.G. (1997). Pharmacological and physiological characterization of murine homomeric β3 $GABA_A$ receptors. Eur. J. Neurosci. *9*: 2225–2235.

Wu, F.S., Chen, S.C., and Tsai, J.J. (1997). Competitive inhibition of the glycine-induced current by pregnenolone sulfate in cultured chick spinal cord neurons. Brain Res. *750*: 318–320.

Wu, F.S., Gibbs, T.T., and Farb, D.H. (1991). Pregnenolone sulfate: a positive allosteric modulator at the *N*-methyl-*D*-aspartate receptor. Mol. Pharmacol. *40*: 333–336.

Wu, M., Wang, H., Yu, H., Makhina, E., Xu, J., Dawson, E.S., et al. (2010). A potent and selective small molecule Kir2.1 inhibitor. Probe Reports from NIH Mol.

Libr. Progr.

Wu, Y., Wang, W., Díez-Sampedro, A., and Richerson, G.B. (2007). Nonvesicular inhibitory neurotransmission via reversal of the GABA transporter GAT-1. Neuron *56*: 851–865.

Xu, M., Covey, D.F., and Akabas, M.H. (1995). Interaction of picrotoxin with $GABA_A$ receptor channel-lining residues probed in cysteine mutants. Biophys. J. *69*: 1858–1867.

Yaghoubi, N., Malayev, A., Russek, S.J., Gibbs, T.T., and Farb, D.H. (1998). Neurosteroid modulation of recombinant ionotropic glutamate receptors. Brain Res. *803*: 153–160.

Yang, J., Cheng, Q., Takahashi, A., and Goubaeva, F. (2006). Kinetic Properties of GABA ρ1 Homomeric Receptors Expressed in HEK293 Cells. Biophys. J. *91*: 2155–2162.

Yang, R., Chen, L., Wang, H., Xu, B., Tomimoto, H., and Chen, L. (2012). Anti-amnesic effect of neurosteroid PREGS in Aβ25-35-injected mice through σ1 receptor- and α7 nAChR-mediated neuroprotection. Neuropharmacology *63*: 1042–50.

Yee, B.K., Hauser, J., Dolgov, V. V, Keist, R., Möhler, H., Rudolph, U., et al. (2004). GABA receptors containing the α5 subunit mediate the trace effect in aversive and appetitive conditioning and extinction of conditioned fear. Eur. J. Neurosci. *20*: 1928–1936.

Yoon, K.W., Covey, D.F., and Rothman, S.M. (1993). Multiple mechanisms of picrotoxin block of GABA-induced currents in rat hippocampal neurons. J. Physiol. *464*: 423–439.

Zaman, S.H., Shingai, R., Harvey, R.J., Darlison, M.G., and Barnard, E.A. (1992). Effects of subunit types of the recombinant $GABA_A$ receptor on the response to a neurosteroid. Eur. J. Pharmacol. *225*: 321–330.

Zamudio-Bulcock, P.A., Everett, J., Harteneck, C., and Valenzuela, C.F. (2011). Activation of steroid-sensitive TRPM3 channels potentiates glutamatergic transmission at cerebellar Purkinje neurons from developing rats. J. Neurochem. *119*: 474–485.

Zamudio-Bulcock, P.A., and Valenzuela, C.F. (2011). Pregnenolone sulfate increases glutamate release at neonatal climbing fiber-to-Purkinje cell synapses. Neuroscience *175*: 24–36.

Zhang, H.G., Ffrench-Constant, R.H., and Jackson, M.B. (1994). A unique amino acid of the Drosophila GABA receptor with influence on drug sensitivity by two mechanisms. J. Physiol. *479*: 65–75.

Zhu, W.J., Wang, J.F., Krueger, K.E., and Vicini, S. (1996). δ subunit inhibits neurosteroid modulation of $GABA_A$ receptors. J. Neurosci. *16*: 6648–6656.